Université de Montréal

Écologie et évolution des syndromes de pollinisation des Gesneriaceae Antillaises

par

Marion Leménager

Département des Sciences Biologiques
Faculté des arts et des sciences

Thèse présentée en vue de l'obtention du grade de
Philosophiæ Doctor (Ph.D.)
en Sciences Biologiques

Le 24 Avril 2024

Université de Montréal

Faculté des arts et des sciences

Cette thèse intitulée

Écologie et évolution des syndromes de pollinisation des Gesneriaceae Antillaises

présentée par

Marion Leménager

a été évaluée par un jury composé des personnes suivantes :

Étienne Léveillé-Bourret

(président-rapporteur)

Simon Joly

(directeur de recherche)

Anne Bruneau

(membre du jury)

Mathieu Perret

(examinateur externe)

Étienne Léveillé-Bourret

(représentant du doyen de la FESP)

Résumé

Les pollinisateurs ont un impact direct sur le succès reproductif de la majorité des angiospermes et influencent l'évolution des caractéristiques florales, en particulier leur morphologie. À travers la grande diversité de formes florales chez les angiospermes, les plantes ont développé des adaptations distinctes aux différents vecteurs de pollinisation, définissant ainsi la notion de syndrome de pollinisation. En particulier, le degré de spécialisation de la pollinisation peut influencer la morphologie florale et sa variation. Les stratégies spécialisées, adaptées à un type fonctionnel de pollinisateurs spécifique, sont parfois caractérisées par des adaptations extrêmes, tandis que les stratégies plus généralistes offrent généralement un certain degré d'adaptabilité et de résilience, notamment dans des environnements dépourvus de pollinisateurs tels que les milieux insulaires. La complexité des interactions entre les plantes et les pollinisateurs sous-tend ainsi la complexité de l'évolution et de la diversification florale. Cette thèse examine la relation complexe entre la morphologie florale, la spécialisation et généralisation des systèmes de pollinisation, et les patrons macroévolutifs au sein des Gesneriaceae antillaises.

L'hypothèse de la variation de niche propose que les espèces généralistes présentent une plus grande variation morphologique entre individus en raison de leur niche écologique plus large. En utilisant la morphométrie géométrique, j'ai analysé la morphologie florale des spécialistes et des généralistes, révélant des modèles nuancés de variation de forme. Nos résultats soutiennent partiellement l'hypothèse de la variation de niche, indiquant que si les généralistes pollinisateurs présentent une plus grande variation intraspécifique dans certains aspects de la morphologie de la corolle, la décomposition de la forme générale en composantes principales révèle des schémas différentiels entre les traits.

Pour explorer la forme et la couleur en 3D, j'ai mis au point un nouveau protocole de photogrammétrie pour reconstruire des modèles de fleurs en 3D, ce qui permet d'étudier efficacement la morphologie des fleurs en trois dimensions. Basé sur un équipement facilement disponible, ce protocole constitue une alternative abordable au micro-CT et facilite la recherche sur le terrain concernant l'évolution et l'écologie des fleurs.

J'ai également étudié l'impact des stratégies spécialistes pour les colibris, pour les chauves souris, et généralistes sur les taux de diversification, en particulier dans les environnements insulaires tels que les Antilles. En reconstruisant la phylogénie extensive des Gesneriinae et en

appliquant des modèles de spéciation et d'extinction, contrairement aux attentes, nos analyses suggèrent que la spécialisation n'est pas nécessairement une impasse évolutive dans les archipels ; au contraire, les spécialistes peuvent se diversifier à des taux similaires à ceux des généralistes. Notre étude met en lumière les interactions complexes entre les stratégies écologiques et la dynamique évolutive chez les Gesneriaceae des Antilles, un groupe qui a connu des transitions répétées entre la spécialisation et la généralisation des stratégies de pollinisation.

Dans l'ensemble, cette recherche souligne l'importance de prendre en compte le contexte écologique pour comprendre les variations morphologiques florales et leurs implications pour la biodiversité à des échelles macroévolutives. Elle met en évidence l'influence réciproque des plantes et de leurs pollinisateurs sur la morphologie florale et souligne la nécessité d'adopter des approches nuancées pour étudier les mécanismes évolutifs qui sous-tendent la spécialisation et la diversification de la biodiversité dans les systèmes insulaires.

Mots clefs : Gesneriaceae Antillaises, stratégies de pollinisation, syndromes de pollinisation, morphologie florale, généraliste-spécialiste, variation intraspécifique, macroévolution, hypothèse de variation de niche, photogrammétrie, diversification.

Abstract

Pollinators directly impact the reproductive success of the majority of angiosperms and influence the evolution of floral characteristics, particularly their morphology. Among the great diversity of floral forms in angiosperms, plants have developed distinct adaptations to different pollination vectors, thus defining the notion of pollination syndrome. Specialised strategies, adapted to specific pollinators, demonstrate extreme adaptations, while more generalist strategies offer a degree of adaptability and resilience, particularly in pollinator-deprived environments such as insular habitats. The complex interaction between plants and pollinators highlights the complexity of floral evolution and diversification. This thesis examines the complex relationship between floral morphology, specialisation and generalisation of pollination strategies, and macroevolutionary patterns within Antillean Gesneriaceae.

The niche variation hypothesis proposes that generalist species exhibit greater morphological variation among individuals due to their wider ecological niche. Using geometric morphometrics, I analysed the floral morphology of specialists and generalists, revealing nuanced patterns of shape variation. Our results partially support the niche variation hypothesis, indicating that while pollinating generalists exhibit greater intraspecific variation in certain aspects of corolla morphology, the decomposition of the general shape into principal components reveals differential patterns across traits.

To explore shape and color in 3D, I have developed a novel photogrammetry protocol for reconstructing 3D flower models, allowing the efficient study of flower morphology in three dimensions. Based on readily available equipment, this protocol provides an affordable alternative to micro-CT scanning and facilitates field-based research on flower evolution and ecology.

I also investigated the impact of specialist strategies for hummingbirds, bats and generalists on diversification rates, particularly in insular environments such as the Antilles. By reconstructing the extensive phylogeny of the Gesneriinae and applying speciation and extinction models, contrary to expectations, our analyses suggest that specialisation is not necessarily an evolutionary dead end in archipelagos; instead, specialists can diversify at comparable rates to generalists. Our study sheds light on the complex interactions between ecological strategies and evolutionary dynamics in the Antillean Gesneriaceae, a group that has undergone repeated transitions between specialisation and generalisation in pollination strategies. By reconstructing the phylogeny of Gesneriinae and

applying state speciation and extinction models, I elucidate the correlation between pollination syndromes and speciation/extinction rates.

Overall, this research highlights the importance of considering ecological context in understanding floral morphological variation and its implications for biodiversity at macroevolutionary scales. It highlights the reciprocal influence between plants and their pollinators on floral morphology and emphasises the need for nuanced approaches to studying the evolutionary mechanisms underlying ecological specialisation and diversification of biodiversity in insular systems.

Key words : Antillean Gesneriaceae, pollination strategies, pollination syndromes, floral morphology, generalists-specialists, intraspecific variation, macroevolution, niche variation hypothesis, photogrammetry, diversification.

Table des matières

Liste des tableaux

Table des figures

Liste des sigles et des abréviations

AIC   Critère d'information d'Akaike, indice de sélection de modèle, de l'anglais *Akaike Information Criterion*.

AICc   Critère d'information d'Akaike corrigé pour la taille de l'échantillon, indice de sélection de modèle, de l'anglais *Akaike Information Criterion corrected for sample size*.

BF   Facteurs Bayésiens, indice de sélection de modèles, de l'anglais *Bayes Factors*.

BM   Mouvement Brownien, modèle d'évolution, de l'anglais *Brownian Motion*.

CPU   Unité centrale de traitement,composant électronique, de l'anglais *central processing unit*.

DNA   Acide désoxyribonucléique (ADN), macromolécule biologique, de l'anglais *Desoxyribonucleic acid*.

DNG   Négatif numérique Adobe, format de fichier, de l'anglais *Adobe Digital Negative*.

DSLR   Reflex numérique mono-objectif, caméra numérique, de l'anglais *Digital single-lens reflex*.

GBIF   Système mondial d'information sur la biodiversité, base de données, de l'anglais *Global Biodiversity Information Facility*.

GBS   Génotypage par séquençage, méthode de séquençage, de l'anglais *Genotyping By Sequencing*.

GM   Morphométrie gémoétrique, méthode d'analyse, de l'anglais *Geometric Morphometrics*.

GPA   Analyses de Procrustes généralisée, méthode d'analyse, de l'anglais *Generalised Procrustes analysis*.

ISO   Sensibilité à la lumière, paramètre de caméra, de l'anglais *International Organization for Standardization*.

JPG   Groupe mixte d'experts en photographie, format de fichier, de l'anglais *Joint Photographic Experts Group*.

JIVE Évolution conjointe de la variance inter- et intraspécifique, méthode d'analyse, de l'anglais *Joint inter- and intraspecific Variance Evolution*.

MCMC Monte Carlo par chaînes de Markov, classe de méthodes d'échantillonnage, de l'anglais *Markov Chain Monte Carlo*.

micro-CT Tomodensitométrie, méthode de modélisation 3D, de l'anglais *micro-computed tomography*. Aussi sous le nom de *high-resolution CT* (HRCT).

NVH Hypothèse de variation de niche, théorie, de l'anglais *Niche Variation Hypothesis*.

OU Ornstein-Uhlenbeck, modèle d'évolution.

OUM Ornstein-Uhlenbeck Multivariate, modèle d'évolution multivarié

PC Composante principale, direction des données qui expliquent le plus de variation,de l'anglais *Principal component*.

PCA Analyse en composantes principales, analyse de données, de l'anglais *Principal Component Analysis*.

PGLS Les moindres carrés généralisés phylogénétiques, analyse de données, de l'anglais *Phylogenetic Generalized Least Squares*.

PROTEUS Base de données de traits phénotypiques.

RAM Accès à la mémoire aléatoire, paramètre informatique, de l'anglais *Random access memory*.

REML Maximum de vraissemblance restreint, méthode d'ajustement des modèles linéaires mixtes, de l'anglais *restricted maximum likelihood*.

SIMMAP Simulation stochastique de caractères discrets le long de la phylogénie, méthode de simulation de données, de l'anglais *simmulated Stochastic character map*.

SNP Polymorphisme à nucléotide unique, variation génétique, de l'anglais *Single Nucleotide Polymorphism*.

TIB Théorie de la Biogéographie Insulaire, théorie, de l'anglais *Theory of Insular Biogeography*.

TRY Base de données de traits phénotypiques.

Remerciements

Faire une thèse aura été une aventure, un périple avec ses hauts et ses bas, une collection d'obstacles qu'on pense insurmontables, mais qui finissent par être surmontés. Cet aboutissement, il n'aurait jamais été possible sans Simon Joly. Je m'estime incroyablement chanceuse d'avoir pu être sous sa supervision pour mon doctorat. Sa disponibilité, son enthousiasme et sa passion pour les sujets d'études que j'ai abordé au cours de ma thèse m'ont permis de persévérer, et d'aller même plus loin que ce que j'aurais imaginé.

Merci Daniel Schoen, Anne Bruneau et Colin Favret pour m'avoir conseillée et m'avoir fait approfondir mes thèmes de recherche lors de mes comités conseils et examen de synthèse. Merci à mes co-auteurs, John, Silvana, Dan, Jérôme, et Abel, pour leur confiance, leur passion pour les plantes et leurs fleurs, et leur partage. Merci à Jérôme, Samy, Maryane, Diana, et Mila, pour leur curiosité et pour avoir exploré avec moi des bouts de ma thèse pendant leurs stages de recherche. Je remercie aussi les personnes qui m'ont entourée tout au long de mon doctorat à l'IRBV, au Centre sur la Biodiversité et au Jardin Botanique de Montréal. Un merci tout particulier à Carole et Jeff, pour m'avoir partagé leur passion pour l'herbier. Merci aussi à Martin pour son efficacité incroyable au Centre, ainsi que Dave et Nicolas, pour leur aide logistique. Merci à Janique pour s'être occupée de la collection vivante des Gesneriaceae, et de m'avoir permis de me sentir comme faisant partie de son équipe au Jardin Botanique. Je remercie également Josianne, Anne-Caroline et leurs collègues pour s'être occupé de cette collection unique.

Pouvoir partager ma recherche dans des conférences et participer à des ateliers et sorties terrain ont été des très beaux moments pendant ma thèse. Tout cela n'aurait bien entendu pas pu être possible sans le soutient financier de l'IRBV, du CSBQ, et de la Faculté des Arts et Sciences de l'Université de Montréal, du Département des Sciences Biologiques, et des fonds de recherche de mon directeur (NSERC).

Pendant ma thèse, j'ai eu l'occasion d'explorer la vulgarisation de la Science de bien des façons. Merci mille fois à Marika pour sa confiance et complicité, de m'avoir fait participer à la Nuit des Chercheuses set Chercheurs, et aussi de m'avoir proposé d'être un de ses bras droits pour l'organisation de la plus belle nuit de l'année, chaque année. Merci aussi à la fine équipe de la Nuit, qui me permet de participer à cette fabuleuse ébullition d'idées alliant la vulgarisation de la science et l'art. Merci à la brillantissime Geneviève pour son aide, pour ses élans créatifs,

et pour être une chercheuse modèle inspirante pour les femmes en sciences. Merci à l'ACFAS et aux Lucioles pour leur élans dans le partage de la science, et de m'avoir offert une plateforme pour partager mes propres sujets. Je renouvelle aussi mes remerciements à Anne que je considère également comme un rôle modèle en sciences, pour ses encouragements, mais aussi pour m'avoir soutenue dans mes explorations artistiques et muséales.

Je remercie aussi Julie pour nos discussions sur la pollinisation lorsqu'elle faisait partie du labo, mais aussi après. Pour sa belle amitié, et les nombreux fou rires. Merci aussi à Simon pour sa complicité tout au long de mon doctorat et notre symbiose en tant que représentants étudiants de l'IRBV. Un grand merci aussi à Florence et sa belle détermination pour l'organisation d'activités et d'événements et son coeur en or, j'ai adoré notre beau duo. Merci aussi à Justine pour ses encouragements, ses discussions constructives et motivantes, son soutient moral, et de nous avoir métamorphosées en bergères et athlètes médaillées. Un énorme merci aussi à Eszter, mon binôme d'objectif éclipse, pour ses talents de planificatrice et de soutient inconditionnel lors de notre dernière ligne droite de rédaction de thèse. Merci aussi à Alfonso et Eric de m'avoir fait découvrir la collection Ware de fleurs de verre d'Harvard, et à nouveau à Anne pour m'avoir accueillie dans son cours de muséologie. Avoir pu maintenir à travers mon doctorat cet aspect de la mise en valeur de l'histoire naturelle dans les musées tient une place particulière dans mon coeur.

Et enfin, je remercie les amies et amis, que ce soit au Canada, en France, aux États-Unis, au Royaume-Uni ou en Australie. Pour m'avoir motivée dans mes idées scientifiques et artistiques, avoir partagé une passion pour les plantes ou les méthodes que j'ai utilisées, les randonnées en forêt, les marches à la plage, les plongeons dans les lacs, rivières, ou dans la mer (avec ou sans phoque), les glissades sur la neige, les belles et longues sorties en vélo, les randonnées en raquettes, le camping au printemps, été, automne, et presque hiver, les longues soirées autour du feu (avec ou sans grenouilles qui chantent), les soirées cocktails, les après-midi matcha, les brunchs très tôt ou très tard, et les évasions dans les musées. C'est aussi tout ça qui m'a permis d'avancer.

Et merci à ma famille, mes parents, grands-parents, Paul, et Tosca, sans qui je ne serais probablement pas qui je suis aujourd'hui. Enfin, je ne remercierai jamais assez Maxence, qui a partagé ce beau périple avec moi. Être entourée d'aussi belles personnes est un vrai privilège.

J'ai vu fleurir bien des amitiés au cours de mon doctorat, qui ne sont pas prêtes de faner.

Avant propos

Cette thèse est rédigée sous forme d'articles scientifiques, qui forment le cœur du document, tandis que l'introduction et la conclusion générales viennent compléter l'histoire. Deux des articles sont déjà publiés ou acceptés à des revues avec comité de lecture, et un article reste en préparation pour soumission.

(1) Leménager, M., Clark, J. L., Martén-Rodríguez, S., Almarales-Castro, A., & Joly, S. (2024). Evolution of intraspecific floral variation in a generalist–specialist pollination system. Journal of Evolutionary Biology, voae028. https ://doi.org/10.1093/jeb/voae028

(2) Leménager, M., Burkiewicz, J., Schoen, D. J., & Joly, S. (2023). Studying flowers in 3D using photogrammetry. New Phytologist, 237(5), 1922-1933. https ://doi.org/10.1111/nph.18553

(3) Leménager, M., Clark, J. L., Martén-Rodríguez, S., & Joly, S. Impact of pollination syndromes on diversification rates in a neotropical insular system. (En préparation).

J'ai développé les idées derrière les trois chapitres de cette thèse, collecté les données, effectué les analyses et rédigé les manuscrits. Mon directeur Simon Joly a aussi participé à chacune de ces étapes et a contribué à l'amélioration des manuscrits. Tout au long de ma thèse, j'ai eu le plaisir de collaborer avec plusieurs co-auteurs, John L. Clark, Silvana Martén-Rodríguez, Daniel Schoen, Jérôme Burkiewicz, Abel Almarales-Castro. Celleux-ci ont participé à la récolte de données, notamment sur le terrain, à initier des idées, et à la révision des manuscrits. Pour le troisième chapitre de cette thèse, je tiens également à remercier les herbiers qui m'ont partagé des échantillons de Gesneriaceae, The William & Lynda Steere Herbarium (NY), et The United States National Herbarium (US).

Accessibilité et reproductibilité de mes travaux

Les données et les scripts associés au premier article sont disponibles sur Dryad : https ://doi.org/10.5061/dryad.hqbzkh1nh. La base de données de modèles 3D, textures, et les images brutes utilisées pour créer les modèles 3D du deuxième article sont disponible sur MorphoSource : https ://www.morphosource.org/, ID : 000369440.

Introduction

Introduction générale

Les relations plantes-pollinisateurs représentent l'une des classes d'interactions écologiques les plus importantes des écosystèmes terrestres, et peuvent être considérées comme l'un des principaux moteurs de la biodiversité (Ollerton, 2017). Les pollinisateurs auraient favorisé il y a près de 170 million d'années l'émergence et la rapide diversification des angiospermes qui sont aujourd'hui majoritairement (87.5%) pollinisés par des vecteurs animaux (Ollerton et al., 2011; Ollerton, 2017).

En constante évolution, les angiospermes subissent les pressions de sélection imposées par les pollinisateurs et leurs préférences, qui varient dans le temps et dans l'espace. Grâce au lien étroit entre les pollinisateurs et les plantes qu'ils pollinisent, les entités complexes que représentent les fleurs sont d'une incroyable diversité phénotypique, soulignant ainsi une variété de stratégies de pollinisation. Lorsque pollinisées par des vecteurs biotiques du même type fonctionnel, les fleurs de taxons sans liens de parenté étroits subissent des pressions de sélection semblables et peuvent ainsi être menées à évoluer vers des ensembles de traits floraux similaires. Ce mécanisme de convergence évolutive n'est pas un phénomène hors du commun malgré l'apparente diversité des fleurs qu'il existe à l'échelle des angiospermes (Losos, 2017).

La notion de syndrome de pollinisation permet de caractériser ces ensembles de traits floraux convergents qui, ensemble, sont associés à l'attraction et l'utilisation efficace de groupes fonctionnels spécifiques de pollinisateurs pour assurer la transmission de pollen (Delpino, 1874; Vogel, 1954; Faegri and Van Der Pijl, 2013; Johnson and Steiner, 2000; Fenster et al., 2004; Martén-Rodríguez and Fenster, 2008; Thomson and Wilson, 2008; Ollerton et al., 2009; Lagomarsino et al., 2017; Dellinger, 2020). Les syndromes de pollinisation ont ainsi servi ces dernières décennies à simplifier et organiser la diversité florale d'un point de vue fonctionnel et écologique (Dellinger, 2020). Pour catégoriser les syndromes de pollinisation, sont utilisés les traits floraux qui sont impliqués dans la sélection par les pollinisateurs tels que la phénologie, les types de signaux, type de récompense, morphologie florale, et le comportement des pollinisateurs (Fenster et al., 2004; Schiestl and Johnson, 2013).

La validité de ce concept de syndrome de pollinisation a été remise en question du fait que des fleurs conformes à un syndrome de pollinisation donné puissent être pollinisées par d'autres pollinisateurs que ceux attendus, et que tous les pollinisateurs ne puissent être inférés à partir d'un syndrome donné, montrant ainsi que les systèmes de pollinisation sont souvent plus généralisés et dynamiques que initialement supposé (Ollerton et al., 2009; Waser et al., 1996). Plutôt que de subir des pressions de sélection imposées par un seul type fonctionnel de pollinisateur, les généralistes subissent un ensemble de pressions de sélection dont la force et la direction peuvent varier, voire être antagonistes selon la composition et l'abondance des types fonctionnels des visiteurs des fleurs au sein des guildes de pollinisateurs (Gómez et al., 2014; Gómez et al., 2014).

Bien que le principe de syndrome de pollinisation reste une simplification des interactions complexes entre plantes et pollinisateurs, des ensembles de traits permettent tout de même d'inférer correctement des syndromes pour des espèces sans observation de pollinisation, mettant en lumière les différentes efficacités des différents types de pollinisateurs (Martén-Rodríguez et al., 2009; Rosas-Guerrero et al., 2014). En particulier, cette inférence est d'autant plus prévisible pour les plantes qui dépendent de leurs pollinisateurs pour se reproduire, et pour les espèces qui proviennent des régions tropicales (Rosas-Guerrero et al., 2014).

Les syndromes de pollinisation : une palette de stratégies et de morphologies

Les stratégies spécialistes et les généralistes

On peut considérer une stratégie de pollinisation spécialisée lorsque les pressions de sélection imposées sur les traits floraux se font par la pollinisation effectuée par un groupe fonctionnel de pollinisateurs particulier, ou autrement dit pour un groupe d'organismes rassemblés par leurs caractéristiques communes. Différents syndromes ont été proposés pour des vecteurs biotiques appartenant à des grands groupes d'animaux (Ollerton et al., 2009). Ce sont en tout 11 groupes fonctionnels qui sont classiquement utilisées pour définir les syndromes de pollinisation : abeille, oiseau, chauve-souris, mouche, guêpe, papillon, mouche à longue langue, coléoptère, mouche charognarde et mammifères non volant (Ollerton et al., 2009; Dellinger, 2020).

Il a longtemps été pensé que les plantes tendaient à se spécialiser pour le pollinisateur le plus efficace lorsque celui-ci est disponible de façon fiable (Stebbins, 1970). L'efficacité d'un pollinisateur peut être représentée par le nombre de graines produites par la visite d'un pollinisateur, et ainsi le dépôt de pollen sur le stigmate d'une plante ou exportation de pollen depuis les anthères sur le stigma d'autres plantes conspécifiques (Johnson and Steiner, 2000; Armbruster, 2014). Cette notion de spécialisation pour le pollinisateur le plus efficace a pu être vérifiée empiriquement (Rosas-Guerrero et al., 2014), mais les différences d'efficacité des pollinisateurs ne sont

toutefois ni nécessaires ni suffisantes pour prédire une spécialisation (Aigner, 2001). Une apparente spécialisation pour un pollinisateur particulier peut se cacher derrière une stratégie plus généraliste, et ainsi des patrons de visites par des pollinisateurs plus variés que ceux attendus (Aigner, 2001), faisant des généralistes des débouchés évolutifs au moins aussi importants que les stratégies spécialistes (Waser et al., 1996). Bien que les syndromes de spécialisation florale aient particulièrement attiré l'attention, la stratégie généraliste semble ainsi être représentée par une grande proportion des plantes à fleurs (Waser et al., 1996; Johnson and Steiner, 2000). Il a même été démontré qu'en réalité ce sont très peu de plantes et pollinisateurs qui ont une stratégies spécialisée (Olesen and Jordano, 2002).

Les différentes façons d'être généraliste

Le long du gradient écologique spécialiste-généraliste, une stratégie généraliste est associée à une niche écologique plus large, soit en termes de ressources (niche Grinnellienne), soit en termes de fonctions qu'une espèce remplit dans l'écosystème (niche Eltonienne) (Devictor et al., 2010). Une espèce spécialiste exploite ainsi moins de ressources qu'une espèce généraliste, ou contribue à une fonction très spécifique dans l'écosystème.

L'exploitation de ressources plus variées peut se faire lors d'une relâche écologique. Cette notion reflète l'expansion et le déplacement des niches lorsqu'une interaction interspécifique contraignante est réduite ou supprimée (Herrmann et al., 2021). Cette relâche peut ainsi avoir lieu lors de la colonisation d'un nouvel environnement, tel qu'il est le cas lors de l'immigration d'une espèce non native sur une île. La relâche écologique, et donc l'augmentation de la taille de la niche écologique, peut être en principe atteinte de deux façons (voir Bolnick et al., 2007). D'une part, les espèces généralistes peuvent être constituées d'individus spécialisés qui occupent différentes niches écologiques. D'autre part, les espèces généralistes peuvent être constituées d'individus qui sont intrinsèquement généralistes, ce qui implique qu'ils sont tous capables d'exploiter un large éventail de ressources.

Impacts des stratégies spécialistes et généralistes sur la morphologie florale

L'importance de la variation intraspécifique

La variation intra-spécifique de traits fonctionnels (dont morphologiques) est importante à prendre en compte pour aborder des questions sur l'évolution des plantes, le fonctionnement des écosystèmes et l'assemblage des communautés végétales (Violle et al., 2012; Siefert et al., 2015). La variation intra-spécifique est à la fois le reflet de la part de variation génétique héritable, de la plasticité phénotypique et de la variation ontogénique. C'est cette variation qui permet aux organismes de répondre aux facteurs environnementaux biotiques et abiotiques (Siefert et al.,

2015). Bien que de moindre ampleur que la variation inter-spécifique, la variation intra-spécifique représente une part importante de la variation totale des phénotypes des organismes (Siefert et al., 2015), et est l'unité de base de l'évolution par sélection naturelle.

L'hypothèse de la variation de la niche

Sur le plan morphologique, selon l'hypothèse de la variation de la niche (NVH), les espèces ayant une niche écologique plus large devraient présenter une plus grande variation morphologique (Van Valen, 1965). Bien que l'hypothèse de la variation de la niche écologique ait reçu un soutien mitigé par le passé (Patterson, 1983; Grant and Price, 1981), les généralistes ont tendance à présenter une plus grande variation morphologique intraspécifique (Futuyma and Peterson, 1985).

L'hypothèse de la variation de niche écologique sous-tend également que la variation peut être elle-même adaptative, et donc sélectionnée (Van Valen, 1965; Bolnick et al., 2007). Le maintient de la variation morphologique peut ainsi se faire grâce à la coexistence de différents phénotypes morphologiques ou physiologiques et de plus de diversité comportementale ou micro-géographique, et ainsi exploiter des ressources plus diversifiée (Van Valen, 1965). Ces notions peuvent ainsi s'appliquer au concept de stratégie spécialiste et généraliste en considérant les guildes de pollinisateurs en tant que ressource limitante (Aigner, 2001; Sahli and Conner, 2011).

L'hypothèse du compromis phénotypique

D'autre part, du fait de pressions sélectives qui peuvent être antagonistes, l'amélioration d'un aspect du phénotype d'un organisme peut réduire l'aptitude ou la performance d'un autre aspect phénotypique. Selon cette hypothèse du compromis phénotypique on s'attend à ce que les généralistes évoluent vers un phénotype intermédiaire aux espèces spécialistes par des compromis évolutifs suffisamment faibles ou asymétriques (Aigner, 2001). En raison de ce compromis phénotypique, il est attendu que les espèces généralistes présentent une plus grande variation morphologique que les spécialistes. Au contraire, plutôt que d'avoir une simple forme intermédiaire, les espèces généralistes peuvent également occuper une région bien distincte de l'espace morphologique des possibilités de formes florales, et ne pas varier plus que les spécialistes (Joly et al., 2018).

Cependant, ces deux processus ne permettent toutefois pas de mieux savoir si les processus à l'échelle intraspécifique sont les mêmes qu'à l'échelle interspécifique. L'étude de l'évolution de la variation intraspécifiques des formes de fleurs en lien avec leur stratégie de pollinisation et leur impact à l'échelle macroévolutive n'a pas encore été explorée. Les patrons de spécialisation et généralisation des systèmes de pollinisation observés à large échelle peuvent ainsi refléter des mécanismes complexes à l'échelle des individus.

La variation phénotypique à l'échelle tridimensionnelle

À plus grande échelle phénotypique cette fois, du fait que les pollinisateurs interagissent avec les fleurs dans un espace en trois dimensions, il est ainsi important de prendre en compte leur complexité tridimensionnelle pour mieux en comprendre les patrons évolutifs (van der Niet et al., 2010; Dellinger et al., 2019). Il existe cependant un réel paradoxe entre cette importance morphologique et fonctionnelle des fleurs en trois dimensions, et le manque d'études qui prennent en compte les aspects tridimensionnels de la morphologie florale. Depuis que plusieurs outils de caractérisation des structures en trois dimensions existent (voir van der Niet et al., 2010; Bardua et al., 2019; Dellinger et al., 2019), ainsi que les outils analytiques pour faciliter l'utilisation de ces données complexes dans un contexte phylogénétique (Clavel et al., 2018), la vraie limitation semble être l'obtention des modèles tridimensionnels de fleurs.

Impacts des stratégies spécialistes et généralistes sur les taux de diversification

Les syndromes de pollinisation impactent directement la diversification des espèces

La diversité des organismes peut être attribuée à l'accélération de la diversification, accompagnée de la radiation écologique adaptative ou l'acquisition d'innovation clés. Les interactions entre espèces sont aussi des éléments important qui affectent les patrons d'évolution des traits, ainsi que les taux de spéciation et d'extinction (révisé par Harmon et al., 2019). En plus d'avoir un impact sur la forme et la variation florale, les pollinisateurs peuvent ainsi avoir un rôle direct sur le succès de la reproduction des angiospermes, leur isolation reproductive, et ainsi sur leur succès à large échelle évolutive.

La fascination et la frustration de Darwin face à l'émergence et la diversification rapide des angiospermes du milieu du Crétacé l'ont amené à décrire l'origine des angiospermes comme un abominable mystère (Friedman, 2009). Il supposa également que cette rapide diversification puisse être liée à d'étroits liens plantes-pollinisateurs, en particulier un processus de coévolution entre des plantes et insectes. Aujourd'hui on sait que des liens très étroits existent entre certains groupes de plantes et leurs pollinisateurs. Par exemple, la spécialisation est observée typiquement chez certaines familles de plantes telles que les Orchidaceae, Asclepiadaceae, et Polemoniaceae, tandis que les généralistes sont retrouvés surtout dans d'autre familles comme les Asteraceae et Ranunculaceae (Johnson and Steiner, 2000). La convergence des traits est limitée par les contraintes phylogénétiques de design floral (Johnson and Steiner, 2000) ce qui pourrait influencer une tendance phylogénétique de la spécialisation et généralisation.

Les adaptations florales qui permettent d'occuper une nouvelle zone adaptative peuvent ainsi faciliter la spéciation ou limiter l'extinction des plantes. Les syndromes de pollinisation peuvent ainsi avoir un rôle important pour la diversification des plantes. Par exemple, la spécialisation des fleurs pour la pollinisation par les colibris a conduit à une diversification rapide des Gesneriaceae (Serrano-Serrano et al., 2017) et chez les Campanules des Andes (Lagomarsino et al., 2016). Au contraire, l'adaptation à la pollinisation par les colibris est associée à une diversification réduite chez les espèces de *Penstemon* en Amérique du Nord (Wessinger et al., 2019).

Le cas particulier des îles

La particularité des îles est qu'elles sont de petite taille avec une diversité et une immigration limitées en terme d'espèces, et qu'elles possèdent des limites distinctes permettant des réplicas évolutifs facilitant l'observation et l'étude des patrons d'évolution (Losos and Ricklefs, 2009). De part leur isolation, que ce soit dans les îles océaniques, les lacs, et les montagnes, les espèces colonisant des îles ont le potentiel d'explorer des niches écologiques encore inexploitées et de se diversifier dans de nouvelles directions, d'autant plus sur des îles de grandes taille qui offrent plus de niche écologique et donc plus de potentiel de coexistence pour les espèces (Losos and Ricklefs, 2009). L'étude récente de l'évolution dans les îles a pu démontrer notamment l'importance de l'isolation géographique (allopatrie) dans les premières étapes de la formation des espèces et le rôle des interactions entre les espèces dans la radiation adaptative (Losos and Ricklefs, 2009). Par exemple, les pinçons de Darwin dans les îles des Galapagos (Grant, 1981), les sabres d'argent dans les îles d'Hawaii (Baldwin and Sanderson, 1998), les lézards anoles dans les îles des Antilles (Mahler et al., 2010), les poissons Cichlidés dans les lacs d'Afrique (Salzburger, 2018), et les campanules des Andes dans les forêts de nuages d'Amérique du Sud (Lagomarsino et al., 2016) sont devenus des modèles iconiques pour étudier les processus de radiation adaptative dans les îles. La diversification phénotypique rapide des espèces peut être issue de radiation adaptative, mais aussi d'autres processus comme la sélection sexuelle, et des événements fondateurs ou de dérive génétique. Par exemple, la dérive génétique est un mécanisme évolutif dominant à l'origine de la divergence entre les populations de renards insulaires (*Urocyon littoralis*) (Funk et al., 2016).

Les interactions biotiques constituent un filtre environnemental primaire pour l'établissement des espèces dans les habitats insulaires (Taylor et al., 2019). Le filtrage de l'environnement peut même exercer une pression plus importante sur la dispersion des espèces vers les îles que la capacité à migrer sur de longues distances (Taylor et al., 2019). Cela inclue l'environnement de pollinisation, le fait que la présence d'un pollinisateur associé sur une nouvelle île peut également limiter la colonisation des plantes. Pour expliquer les patrons de diversité sur les îles, il faut donc prendre en compte les interactions biotiques, telles que les interactions de pollinisation. Les caractéristiques des plantes associées aux systèmes de pollinisation peuvent donc être à l'origine des processus de colonisation des îles. Par exemple, les espèces insulaires présentent généralement des changements

dans leurs traits fonctionnels, passant de spécialistes à généralistes pour surmonter la limitation des pollinisateurs en raison des faunes de pollinisateurs dépaupérisées sur les îles (Taylor et al., 2019; Barrett, 1996).

Les pollinisateurs des plantes spécialisées peuvent être moins abondants, présenter une variabilité temporelle plus élevée, ou ne pas correspondre de la même manière sur le plan spécifique par rapport à leur environnement d'origine des plantes immigrées. Le fait de dépendre d'une seule espèce ou d'un seul type fonctionnel de pollinisateur pourrait augmenter les risques d'extinction des espèces avec un syndrome de pollinisation spécialisé, et ainsi réduire leur taux de diversification dans les îles (Barrett, 1996).

Les espèces qui sont pollinisées par une diversité plus large de pollinisateurs pourraient ainsi avoir plus de chances de s'établir avec succès dans les îles océaniques. Les espèces généralistes sont généralement moins sujettes à l'extinction (McKinney, 1997; Colles et al., 2009), mais dans le contexte des îles cela s'explique en partie par le fait que ces espèces généralistes peuvent bénéficier de leur capacité à être pollinisées par différents types de pollinisateurs, ce qui peut réduire leur risque d'extinction par rapport à des espèces spécialisées plus susceptibles de souffrir de la limitation des pollinisateurs (McKinney, 1997; Colles et al., 2009).

Le paradoxe spécialistes-généralistes et îles-continent

Il y aurait une tendance à trouver une augmentation de la spécialisation des plantes dans les îles, du fait qu'il y ait moins d'animaux pollinisateurs dans les îles que sur le continent (Olesen and Jordano, 2002). Mais il a aussi été observé que les plantes dans les îles sont généralement plus généralistes (Barrett, 1996), notamment du fait que la relâche écologique entraîne une transition de spécialiste à généraliste. La dispersion du continent vers les îles peut entraîner le passage d'une spécialisation extrême à une généralisation du système de pollinisation du fait de l'absence des pollinisateurs spécifiques sur les îles (Armbruster and Baldwin, 1998). Les exigences en terme de pollinisateurs des plantes spécialistes peuvent ainsi être un frein à leur établissement dans les îles. Le succès de l'adaptation subséquente de ces plantes pour ce nouveau système de pollinisation peut aussi résulter en une diversification secondaire dans les îles (Armbruster and Baldwin, 1998).

Bien que cela semble paradoxal, les deux phénomènes ne sont pas exclusifs. La raison de ce paradoxe serait qu'il existe une différence entre la spécialisation absolue et relative (Petanidou and Potts, 2006) : les plantes des îles sont spécialisées du fait qu'il y ait peu de pollinisateurs potentiels par rapport au continent, et sont généralistes (non-sélectifs) du fait qu'ils utilisent plus de types fonctionnels de pollinisateurs.

Bien que de nombreuses études se soient penchées sur le sujet, le succès relatif des spécialistes et généralistes dans le contexte particulier des îles ne semble pas être éclairci.

Modèle d'étude : Les Gesneriaceae Antillaises

Le contexte particulier insulaire des Antilles offre des conditions uniques d'habitats, de communautés, et d'isolation génétique des populations (Ricklefs and Bermingham, 2008) pour aborder des questions sur l'évolution des syndromes de pollinisation. En particulier, dans les Antilles, le groupe des Gesneriacées Antillaises représente un modèle d'étude intéressant du fait que des syndromes de pollinisation spécialistes ainsi que généralistes y ont été identifiés.

Les Antilles comme laboratoire d'évolution

Les archipels, dont les Antilles, représentent un laboratoire d'écologie et d'évolution grâce à la nature discrète des îles qui les composent (Ricklefs and Bermingham, 2008). Ces regroupements d'îles ont notamment eu un rôle important pour initier l'élaboration de théories fondatrices en biogéographie, mais aussi en évolution et écologie, permettant ainsi de mieux comprendre les processus d'immigration, de diversification et d'extinction des espèces (MacArthur and Wilson, 1963; Ricklefs and Bermingham, 2008; Warren et al., 2015).

La complexité historique et géographique des îles des Antilles offre un contexte propice pour étudier ces processus (Ricklefs and Bermingham, 2008). Les Antilles sont composées d'un ensemble d'îles d'origine, d'âge et de taille différentes qui ont été propices pour développer des hypothèses sur l'histoire biogéographique de la biodiversité dans les îles (Ricklefs and Bermingham, 2008; Warren et al., 2015; Regalado et al., 2018; Roncal et al., 2020), et pour lesquelles l'origine et l'âge sont détaillés par Iturralde-Vinent (2006). Les Grandes Antilles sont les plus anciennes et proviennent de fragments continentaux, possiblement au dessus du niveau de la mer depuis l'Éocène moyen (il y a environ 40 millions d'années). La plus grande île est celle de Cuba, avec ses 2000km de long et 105 000 km^2, et la deuxième plus grande île (76000km^2), Hispaniola, offre le plus haut relief avec un sommet à plus de 3000m d'altitude. Pour l'ensemble des îles les plus anciennes des Antilles, l'âge des territoires émergés en permanence date de 40 million d'années. Plus récemment les 22 îles des Petites Antilles se sont formées à partir d'un arc volcanique pendant l'Oligocène (-34 à -23 millions d'années), et leur géographie actuelle date du Pliocène ($-5,332 \pm 0,005$ à $-2,588 \pm 0,005$ millions d'années). Enfin, les Bahamas sont un regroupement de près de 700 îles, cayes et îlots d'origine marine (plus précisément de la remontée relativement récente à la surface de récifs coralliens en eau peu profonde) datant du Miocène (-23 à $-5,3$ millions d'années). Dans le scénario paléogéographique de la formation des Antilles, une des particularités est la présence d'une grande extension péninsulaire de l'Amérique du Sud reliant les Antilles au nord de l'Amérique du Sud (sous le nom de Gaarlandia), au début de l'Oligocène (-35 à -33 million d'années), facilitant ainsi les migrations entre ces deux régions pendant une courte période (< 3 millions d'années) (voir également Roncal et al., 2020).

En lien avec leur origine géologique complexe, les îles des Antilles ont une une diversité d'élévation, d'habitats, d'exposition aux ouragans, d'isolation géographique, et de source de colonisation

au niveau de ces îles. Ces facteurs favorisent l'isolation reproductive des plantes et ainsi, permettent un terreau fertile pour des patrons complexes de richesse spécifique et d'endémisme dans les îles des Antilles (Iturralde-Vinent, 2006).

Les Antilles regroupent une diversité biotique et un endémisme importantes, ce qui les classe parmi les 8 points chauds de diversité les plus riches au monde : sur les $\sim$12000 espèces de plantes, plus de la moitié ($\sim$7000) sont endémiques dans les Antilles (représentant 23.5 espèces endémiques/100km^2) (Myers et al., 2000). Parmi les facteurs qui pourraient expliquer cette flore unique dans les Antilles, la géologie complexe des îles, l'histoire écologique, et des évènements tectoniques et climatiques importants peuvent être mis en cause (Fritsch and McDowell, 2003).

Diversité et répartition des Gesneriinae

Les Gesneriaceae sont un groupe d'herbacées pérennes, d'arbustes, ou petits arbres majoritairement d'origine sub-tropicale, dont le premier point chaud de diversité se situe dans les Andes, et le second dans les Antilles (Perret et al., 2013). Du fait de la grande diversification morphologique des fleurs et du haut taux de convergence au sein de ce groupe, l'établissement des liens entre espèces et de leur taxonomie a historiquement généré beaucoup de confusion (Clark et al., 2012). Ce groupe comprend près de 3200 espèces réparties dans 140-160 genres et 3 principales sous-familles (Weber et al., 2013; Perret et al., 2013) dont les *Gesneriinae*, que l'on retrouve majoritairement dans les Antilles avec quelques espèces présentes au nord de l'Amérique du Sud, qui sont représentées par 4 genres : *Bellonia* L., *Gesneria* Plum. ex L., *Pheidonocarpa* L.E.Skog, et *Rhytidophllum* Mart. (Acevedo-Rodríguez and Strong, 2012). Le groupe des Gesneriaceae, et plus particulièrement le clade Antillais des *Gesneriinae*, présente une grande diversité de morphologies florales qui sous-tend un panel de stratégies de pollinisation, de spécialiste à généraliste pour plusieurs types fonctionnels de pollinisateurs.

Syndromes de pollinisation des Gesneriinae

Plusieurs études ont permis de distinguer différents syndromes de pollinisation pour ces différentes stratégies reproductives (Martén-Rodríguez and Fenster, 2008; Martén-Rodríguez et al., 2009; Martén-Rodríguez et al., 2010; Martén-Rodríguez et al., 2015). Cette caractéristique en fait un groupe idéal pour étudier l'évolution des stratégies spécialistes et généralistes. Les Gesneriaceae insulaires seraient notamment les seules ayant un syndrome généraliste (Martén-Rodríguez et al., 2015) parmi les représentants du nouveau monde. L'ancêtre commun des espèces de Gesneriaceae Antillaises semble avoir eu un syndrome spécialisé pour la pollinisation par les colibris (Martén-Rodríguez et al., 2010). L'évolution des syndromes de pollinisation vers une stratégie plus généraliste a ensuite eu lieu de façon récurrente, et on retrouve désormais cette stratégie sur plusieurs îles des Antilles. Le contexte insulaire de ce groupe est donc propice pour l'étude de la répétabilité de l'évolution des stratégies convergentes de pollinisation.
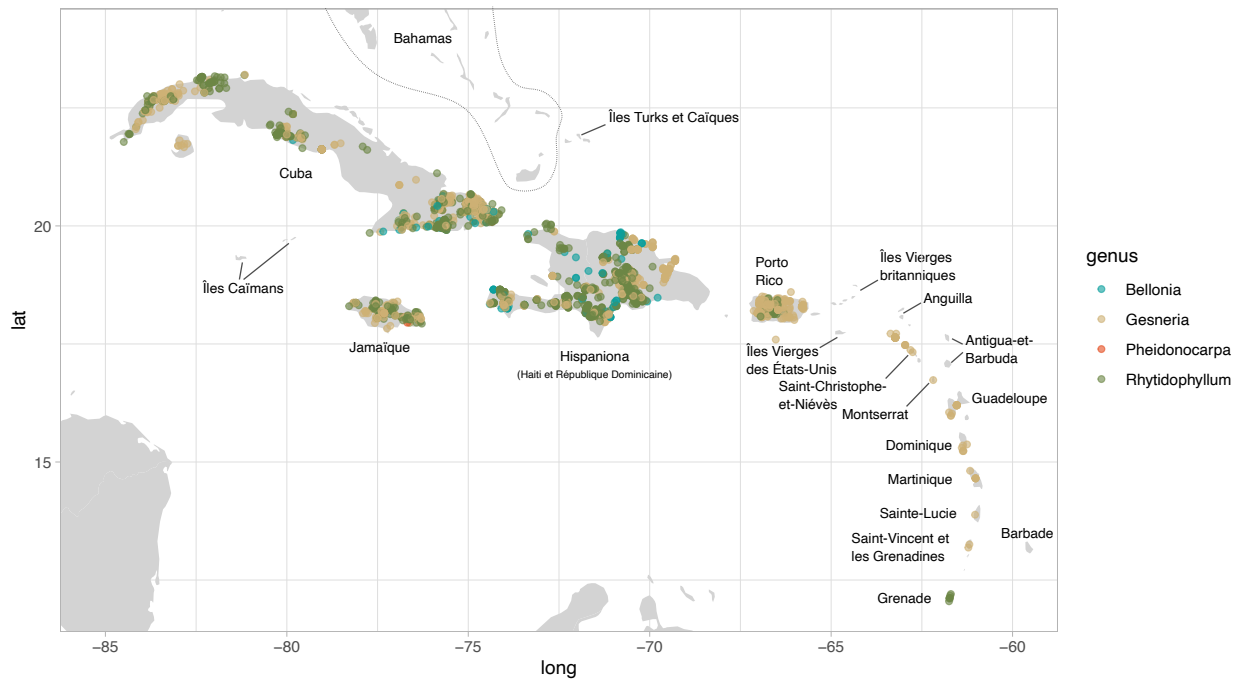
Figure 1. Carte de la distribution des Gesneriinae dans les Antilles à partir des données d'occurrences de la base de données de la Global Biodiversity Information Facility pour les genres *Gesneria*, *Rhytidophyllum*, *Bellonia* et *Pheidonocarpa* (GBIF.org (17 Avril 2024) téléchargement d'occurrences GBIF https ://doi.org/10.15468/dl.fbj64c). Parmi ces observations, 39 espèces ont été récoltées moins de 10 fois, dont 6 espèces qui ne possèdent que deux occurrences, et 6 autres qui n'ont qu'une seule occurrence. Les espèces les plus observées (plus de 100 fois chacune) sont *Rhytidophyllum auriculatum*, *Rhytidophyllum exsertum*, *Rhytidophyllum grandiflorum*, *Gesneria humilis*, *Gesneria duchartreoides*, et *Gesneria pedunculosa*.

Les observations de Martén-Rodríguez et al. (2009) apportent un soutien aux syndromes classiques de pollinisation par les colibris et les chauves-souris, ainsi que des preuves d'un syndrome généraliste caractérisé par une constriction de la corolle. Ces observations démontrent l'importance de la sélection médiée par les pollinisateurs dans la diversification florale des Gesnerieae antillaises, et que les morphologies florales au sein de ce groupe ont évolué sous la pression de sélection de plusieurs types fonctionnels de pollinisateurs différents.

Les espèces spécialistes pour la pollinisation par les colibris ont une corolle tubulaire, une couleur vive (rouge et jaune) et ont une anthèse diurne, et produisent également de grandes quantités de nectar dilué (Martén-Rodríguez et al., 2009). Cet ensemble de caractères qui correspondent à l'ornithophylie est un des cas de convergence de traits floraux les plus répandus (dans 65 familles de plantes) et acceptés (voir Cronk and Ojeda, 2008). Du fait que les colibris fassent du vol stationnaire, les plantes spécialisées pour les colibris n'ont pas besoin de fournir de perchoir pour leur pollinisateurs, et ont généralement de longues fleurs pendantes (Cronk and Ojeda, 2008),

ce qui se retrouve chez les Gesneriinae. L'inclinaison de la corolle tubulaire vers le bas permet également de limiter la dilution du nectar et de limiter la pollinisation par les insectes, qui vont difficilement manipuler de telles fleurs tandis qu'elles restent accessibles par les colibris (Cronk and Ojeda, 2008). La plupart des colibris sélectionne des fleurs de couleur rouge vif, non pas parce que leur vision des couleurs est particulièrement adaptée aux grandes longueurs d'onde, mais parce qu'elles sont moins visitées par les abeilles qui ne détectent pas la couleur rouge (Altshuler and Wylie, 2020). Les colibris peuvent ainsi optimiser leur stratégies de recherche de nourriture et favoriser les fleurs rouges qui sont moins visitées par les insectes, et donc souvent plus associées à de grandes quantités de nectar (voir Skog, 1976). La combinaison de ces traits floraux caractéristiques des spécialistes pour la pollinisation par les colibris servent ainsi à exclure d'autres compétiteurs potentiels pour le pollen et le nectar (Skog, 1976).

Plusieurs espèces de colibris (n=14) ont été supposées pollinisatrices des *Gesneria* dans les Antilles par Skog (1976) d'après la morphologie de leur bec et la longueur des tubes des corolles des espèces avec un syndrome spécialisé pour la pollinisation par les colibris dans les Grandes et Petites Antilles. Parmi les quatorze espèces mentionnées, six de ces espèces ont pu être observées entrer en interaction avec des Gesneriinae sur le terrain par Martén-Rodríguez and Fenster (2008), Martén-Rodríguez et al. (2009), ainsi que Martén-Rodríguez et al. (2015). Les colibris ont également effectivement pu être observés entrer en contact avec les organes reproducteurs de fleurs de *Gesneria*, *Rhytidophyllum* et *Pheidonocarpa corymbosa*. Les espèces de Trochilidae observées sont détaillées pour chacune des espèces de Gesneriinae et impliquent *Chlorostilbon maugaeus* (Puerto Rican emerald) comme pollinisateur le plus dominant (dans les trois publications), *Chlorostilbon swainsonii* (aussi plusieurs fois observé pour plusieurs espèces de *Gesneria* et *Rhytidophyllum*, tant spécialistes que généralistes), *Chlorostilbon ricordii*, et un peu plus rarement les espèces *Anthracothorax dominicus*, *Anthracocorax viridis* (green mango), *Anthracothorax mango*, *Eulampis jugularis*, *Eulampis sp.*, *Trochilus polytmus* et une autre espèce non identifiée du genre *Trochilus*.

Les espèces spécialistes des chauve-souris ont une corolle courte campanulée (en cloche) de coloration relativement terne (couleur pâle, jaunâtre, verdâtre, ou pourpre) avec des tâches brunes ou pourpre, à anthèse nocturne ou crépusculaire. Le nectar est produit en abondance comme ressource pour les chauve-souris, et les fleurs pollinisées par les chauve-souris ont typiquement une augmentation de la production de nectar pendant la nuit, et une forte odeur. Les chauves-souris des continents américains qui se nourrissent de nectar et de pollen appartiennent au sous-ordre des microchiroptères de l'ordre des chiroptères et représentent deux sous-familles, Glossophaginae et Phyllonycterinae, de la famille des Phyllostomidae (les chauves-souris à nez de feuille) (Skog, 1976). L'olfaction est utilisée par de nombreuses espèces de chauves-souris, notamment lorsqu'elles se nourrissent de nectar, d'autant plus que l'écho-localisation peut être un mécanisme inefficace pour détecter les objets lorsqu'il y a beaucoup de bruit de fond (i.e. de la végétation dense), même à courte distance (voir Brokaw and Smotherman, 2020). Une des particularités des fleurs de Gesneriinae pollinisées spécifiquement par les chauves souris est que les fleurs sont érigées

ou pendantes sur de long pédoncules, telles que *Rhytidophyllum grande* (Swartz) Mart. et *G. pedunculosa* (DC.) Fritsch (Skog, 1976), ce qui semble permettre aux chauve-souris de les détecter plus facilement en les détachant du reste du feuillage. Lors du contact entre les chauve-souris et les anthères, les étamines touchent le dessus de la tête, le rostre, ou le nez de ces pollinisateurs, avec un contact facilité par la taille des étamines et leur grande production de pollen par les espèces spécialistes pour ce type de pollinisation. Par exemple, Skog (1976) mentionne qu'une ou deux anthères de *G. calycosa* (pollinisée par les chauve-souris) produit autant de pollen que 50 anthères de *G. acaulis* (pollinisée par les colibris). Peu d'interactions plantes-pollinisateurs ont été recensées dans les Antilles pour les chauve-souris nectarivores, mais les principales espèces observées sont *Monophyllus redmani* (24%), *Erophylla sezekorni* (15%), *Leptonycteris curasoae* (10%), *Glossophaga longirostris* (10%), and *Brachyphylla cavernarum* (8%) (Gonzalez-Gutierrez et al., 2022). Seule l'espèce *Monophyllus redmanii* a pu être observée et identifiée par Martén-Rodríguez and Fenster (2008) comme étant pollinisatrice de plusieurs espèces de *Gesneria*, et une quinzaines d'espèces de Phyllostomidae en tout ont été supposées pollinisatrices des Gesneriinae par Skog (1976) en comparant l'adéquation entre les mesures des tubes des corolles et les tailles des têtes et rostres des chauves-souris.

Plus rares, des espèces sont aussi spécialisées pour les papillons de nuits et les abeilles respectivement. Une espèce de *Gesneriinae* possède un syndrome de pollinisation par des Hétérocères (papillons de nuit) avec une corolle tubulaire blanche-jaunâtre (*Gesneria humilis* L.) (Martén-Rodríguez et al., 2015), qu'on retrouve essentiellement sur l'île de Cuba, mais dont l'identification des pollinisateurs n'a pas pu être faite (Martén-Rodríguez et al., 2015). Également, *Bellonia spinosa* Swartz et *Bellonia aspera* L., les deux seules espèces de ce genre, présentes uniquement sur les îles de Cuba et Hispaniola (Haiti et la République Dominicaine) sont distinctes des autres espèces de Gesneriinae de part l'absence de corolle tubulaire prononcée. Ce sont les seules à présenter un syndrome spécialisé pour la pollinisation par les abeilles. Les corolles sont blanches, avec un tube très court, à face plate et actinomorphes avec des lobes elliptiques et arrondis et libère le pollen par un cône de d'anthères à déhiscence poricidale (jusqu'à 6 à 8 étamines), et ne produisent pas de nectar comme les autres espèces du group de par l'absence de nectaires (Zhaoran and Skog, 1990).

Enfin, les espèces à stratégie de pollinisation mixte ont une corolle campanulée avec une constriction relativement importante à la base, de différentes couleurs et différents motifs tachetés, à anthèse tant diurne que nocturne, et produisent du nectar (Martén-Rodríguez et al., 2009; Joly et al., 2018). La corolle des généralistes présentent des colorations très variables, jaunes, oranges, rouges, et souvent tachetées de rouge (Martén-Rodríguez et al., 2009). La constriction de la corolle au dessus de la chambre a nectar est le caractéristique principale qui a amené à la description de ce syndrome généraliste chez les Gesneriinae et les distingue des spécialistes pour les chauve-souris (Martén-Rodríguez et al., 2009). Cette constriction chez *Gesneria* et *Rhytidophyllum* permettrait de faciliter l'accès au nectar pour les chauve-souris tout en maintenant la dualité de l'efficacité

de la pollinisation par les colibris et chauve-souris (Martén-Rodríguez et al., 2009). Cette forme de fleur permet ainsi de diriger les colibris dans la fleur pour contraindre un contact direct entre les étamines et le pistil avec le colibris, ainsi que de créer un réservoir à nectar pour le rendre plus accessible. En plus des espèces de colibris et chauve-souris mentionnées précédemment, ce sont aussi des espèces de papillons de nuit (espèce non-identifiée), de fourmis (*Solenopsis invicta* et des espèces non-identifiées), de cafards (non-identifié), des abeilles domestiques (*Apis mellifera*), et des mouches (Syrphidae) qui ont pu être observées visitant les espèces de *Gesneria* et *Rhytidophyllum* (Martén-Rodríguez et al., 2015).
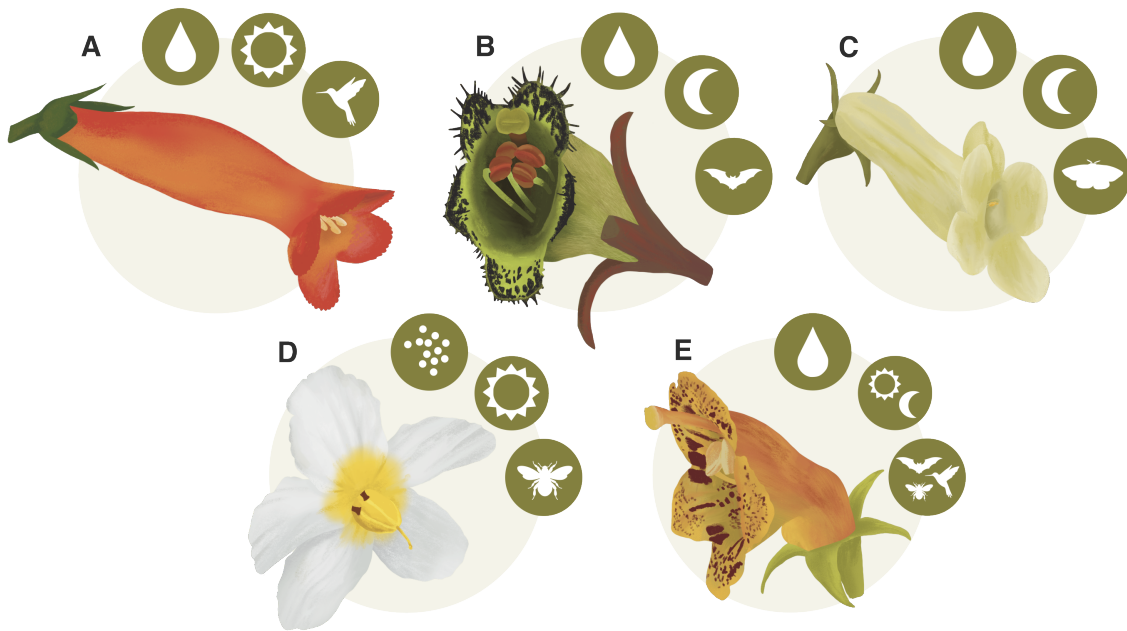
Figure 2. Illustration des syndromes de pollinisation retrouvés chez les Gesneriaceae Antillaises (Gesneriinae), (A) spécialistes des colibris (fleurs tubulaires rouges ou jaunes, anthèse diurne et production de nectar comme récompense), (B) spécialistes des chauve-souris (fleurs vertes ou banches, en cloche, à anthèse nocturne, et production de nectar comme récompense, parfum fort), (C) spécialistes des papillons de nuit (fleurs pâles verts ou roses, production de nectar comme récompense et parfum fort), (D) spécialistes des abeilles (fleurs actinomorphes pâles, oligandres et pollinisation par vibration pour libérer le pollen récompense, à anthèse diurne), (E) généralistes pour la pollinisation par les chauve-souris, colibris et insectes (fleurs à jaunes à oranges à ornementation orange à rouge en cloche avec une constriction médiane, anthèse diurne et/ou nocturne, et production de nectar).

Objectifs de la thèse

Dans le but de mieux comprendre les forces sélectives qui influencent l'évolution des stratégies de pollinisation des Gesneriaceae Antillaises (Gesneriinae), les objectifs principaux de cette thèse sont les suivants :

Le premier objectif de cette thèse est de mieux comprendre le rôle des stratégies de pollinisation spécialistes et généralistes sur l'évolution de la variation intraspécifique, et si l'hypothèse de variation de niche est vérifiée à échelle microévolutive. À l'échelle interspécifique, la comparaison des formes de fleurs moyenne par espèce chez les Gesneriinae n'a pas permis de confirmer la présence de plus de variation florale chez les généralistes que chez les spécialistes (Joly et al., 2018). Le syndrome généraliste semble ainsi occuper une zone distincte dans l'espace phénotypique, avec une morphologie adaptée spécifiquement pour attirer des pollinisateurs distincts, sans pour autant avoir plus de variation morphologique inter-spécifique.

Cette question peut ainsi être abordée à l'échelle intra-spécifique, car les mécanismes à échelle macroévolutive pourraient ne pas être représentatifs des mécanismes opérant au sein des populations pour chaque espèce. Dans un premier chapitre, on tente de vérifier si les espèces généralistes suivent l'hypothèse de variation de niche, c'est à dire si les généralistes ont une valeur optimale de variance plus élevée que les spécialistes.

D'autre part, malgré la complexité tridimensionnelle des fleurs et des interactions plantes-pollinisateurs, les traits morphologiques le plus à disposition pour explorer la forme des fleurs et leur évolution restent des traits de morphologie en deux dimensions. Le deuxième objectif de cette thèse vise à démontrer la pertinence de l'approche de la photogrammétrie pour détecter les patrons de variation morphologiques floraux en 3D. Le second chapitre présenté dans cette thèse est une démonstration de l'utilité de la photogrammétrie et la présentation d'un protocole généralisé pour stimuler l'étude de la forme et de la couleur des fleurs en trois dimensions. La mise en avant de la photogrammétrie devrait permettre de stimuler l'étude de l'évolution de la morphologie florale en rendant accessible la quantification de la morphologie florale en 3D.

Il a plusieurs fois été observé des changements morphologiques et écologiques rapides liés à la radiation adaptative de plantes suite à leur colonisation d'îles océanique (voir les exemples dans Barrett, 1996). Les stratégies généralistes pourraient être plus avantagées que les spécialistes dans un environnement où les populations de pollinisateurs ne sont pas présentes de façon constante (voir Waser et al., 1996; Johnson and Steiner, 2000), et où les pollinisateurs alternatifs sont sous-exploités (Givnish, 2015). Par exemple, les généralistes sont pollinisés par des guildes de pollinisateurs qui peuvent varier en abondance selon une mosaïque spatiale et selon le temps (Gómez et al., 2014).

Sachant que chez les Gesneriaceae Antillaises (Gesneriinae) le syndrome généraliste a été identifié comme un syndrome *de novo* sur les îles (Martén-Rodríguez et al., 2010), on peut se

demander si il représente une innovation adaptative suite à la colonisation des Antilles qui aurait permis de générer un taux de diversification plus important chez les généralistes que chez les spécialistes. L'objectif du troisième chapitre est de déterminer la dynamique de la diversification des Gesneriaceae dans un contexte insulaire, au cours du temps, selon les stratégies de pollinisation.

Bibliographie

Acevedo-Rodríguez, P. and Strong, M. T. (2012). Catalogue of seed plants of the west indies. *Smithsonian Contributions to Botany*, (98) :1–1192.

Aigner, P. A. (2001). Optimality modeling and fitness trade-offs : when should plants become pollinator specialists ? *Oikos*, 95(1) :177–184.

Altshuler, D. L. and Wylie, D. R. (2020). Hummingbird vision. *Current Biology*, 30(3) :R103–R105.

Armbruster, W. S. (2014). Floral specialization and angiosperm diversity : phenotypic divergence, fitness trade-offs and realized pollination accuracy. *AoB Plants*, 6.

Armbruster, W. S. and Baldwin, B. G. (1998). Switch from specialized to generalized pollination. *Nature*, 394(6694) :632–632.

Baldwin, B. G. and Sanderson, M. J. (1998). Age and rate of diversification of the hawaiian silversword alliance (compositae). *Proceedings of the National Academy of Sciences*, 95(16) :9402–9406.

Bardua, C., Felice, R. N., Watanabe, A., Fabre, A.-C., and Goswami, A. (2019). A practical guide to sliding and surface semilandmarks in morphometric analyses. *Integrative Organismal Biology*, 1(1) :obz016.

Barrett, S. C. H. (1996). The reproductive biology and genetics of island plants. *Philosophical Transactions of the Royal Society of London. Series B : Biological Sciences*, 351(1341) :725–733.

Bolnick, D. I., Svanbäck, R., Araújo, M. S., and Persson, L. (2007). Comparative support for the niche variation hypothesis that more generalized populations also are more heterogeneous. *Proceedings of the National Academy of Sciences*, 104(24) :10075–10079.

Brokaw, A. F. and Smotherman, M. (2020). Role of ecology in shaping external nasal morphology in bats and implications for olfactory tracking. *PLoS One*, 15(1) :e0226689.

Clark, J. L., Funke, M. M., Duffy, A. M., and Smith, J. F. (2012). Phylogeny of a neotropical clade in the gesneriaceae : more tales of convergent evolution. *International Journal of Plant Sciences*, 173(8) :894–916.

Clavel, J., Aristide, L., and Morlon, H. (2018). A penalized likelihood framework for high-dimensional phylogenetic comparative methods and an application to new-world monkeys brain evolution. *Systematic biology*, 68(1) :93–116.

Colles, A., Liow, L. H., and Prinzing, A. (2009). Are specialists at risk under environmental change ? neoecological, paleoecological and phylogenetic approaches. *Ecology letters*, 12(8) :849–863.

Cronk, Q. and Ojeda, I. (2008). Bird-pollinated flowers in an evolutionary and molecular context. *Journal of experimental botany*, 59(4) :715–727.

Dellinger, A. S. (2020). Pollination syndromes in the 21st century : where do we stand and where may we go ? *New Phytologist*, 228(4) :1193–1213.

Dellinger, A. S., Artuso, S., Pamperl, S., Michelangeli, F. A., Penneys, D. S., Fernández-Fernández, D. M., Alvear, M., Almeda, F., Scott Armbruster, W., Staedler, Y., and Schönenberger, J. (2019). Modularity increases rate of floral evolution and adaptive success for functionally specialized pollination systems. *Communications Biology*, 2(1) :1–11.

Delpino, F. (1874). Ulteriori osservazioni e considerazioni sulla dicogamia nel regno vegetale. 2 (iv). delle piante zoidifile. *Atti della Societa Italiana Scientia Naturale*, 16 :151–349.

Devictor, V., Clavel, J., Julliard, R., Lavergne, S., Mouillot, D., Thuiller, W., Venail, P., Villeger, S., and Mouquet, N. (2010). Defining and measuring ecological specialization. *Journal of Applied Ecology*, 47(1) :15–25.

Faegri, K. and Van Der Pijl, L. (2013). *Principles of pollination ecology*. Elsevier.

Fenster, C. B., Armbruster, W. S., Wilson, P., Dudash, M. R., and Thomson, J. D. (2004). Pollination syndromes and floral specialization. *Annual Reviews of Ecology Evolution and Systematic*, 35 :375–403.

Friedman, W. E. (2009). The meaning of darwin's "abominable mystery". *American Journal of Botany*, 96(1) :5–21.

Fritsch, P. W. and McDowell, T. D. (2003). Biogeography and phylogeny of caribbean plants—introduction. *Systematic Botany*, 28(2) :376–378.

Funk, W. C., Lovich, R. E., Hohenlohe, P. A., Hofman, C. A., Morrison, S. A., Sillett, T. S., Ghalambor, C. K., Maldonado, J. E., Rick, T. C., Day, M. D., et al. (2016). Adaptive divergence despite strong genetic drift : genomic analysis of the evolutionary mechanisms causing genetic differentiation in the island fox (urocyon littoralis). *Molecular ecology*, 25(10) :2176–2194.

Futuyma, D. J. and Peterson, S. C. (1985). Genetic variation in the use of resources by insects. *Annual review of entomology*, 30(1) :217–238.

Givnish, T. J. (2015). Adaptive radiation versus 'radiation'and 'explosive diversification' : why conceptual distinctions are fundamental to understanding evolution. *New Phytologist*, 207(2) :297–303.

Gómez, J. M., Perfectti, F., and Klingenberg, C. P. (2014). The role of pollinator diversity in the evolution of corolla-shape integration in a pollination-generalist plant clade. *Philosophical Transactions of the Royal Society B : Biological Sciences*, 369(1649) :20130257.

Gonzalez-Gutierrez, K., Castaño, J. H., Perez-Torres, J., and Mosquera-Mosquera, H. R. (2022). Structure and roles in pollination networks between phyllostomid bats and flowers : a systematic

review for the americas. *Mammalian Biology*, 102(1) :21–49.

Grant, P. and Price, T. (1981). Population variation in continuously varying traits as an ecological genetics problem. *American Zoologist*, 21(4) :795–811.

Grant, P. R. (1981). Speciation and the adaptive radiation of darwin's finches : The complex diversity of darwin's finches may provide a key to the mystery of how intraspecific variation is transformed into interspecific variation. *American Scientist*, 69(6) :653–663.

Gómez, J. M., Perfectti, F., Abdelaziz, M., Lorite, J., and Muñoz-Pajares, A. J. (2014). Evolution of pollination niches in a generalist plant clade. *New Phytologist*, 205(1) :440–453.

Harmon, L. J., Andreazzi, C. S., Débarre, F., Drury, J., Goldberg, E. E., Martins, A. B., Melián, C. J., Narwani, A., Nuismer, S. L., Pennell, M. W., et al. (2019). Detecting the macroevolutionary signal of species interactions. *Journal of evolutionary biology*, 32(8) :769–782.

Herrmann, N. C., Stroud, J. T., and Losos, J. B. (2021). The evolution of 'ecological release'into the 21st century. *Trends in Ecology & Evolution*, 36(3) :206–215.

Iturralde-Vinent, M. A. (2006). Meso-cenozoic caribbean paleogeography : implications for the historical biogeography of the region. *International Geology Review*, 48(9) :791–827.

Johnson, S. D. and Steiner, K. E. (2000). Generalization versus specialization in plant pollination systems. *Trends in ecology & evolution*, 15(4) :140–143.

Joly, S., Lambert, F., Alexandre, H., Clavel, J., Léveillé-Bourret, E., and Clark, J. L. (2018). Greater pollination generalization is not associated with reduced constraints on corolla shape in Antillean plants. *Evolution*.

Lagomarsino, L. P., Condamine, F. L., Antonelli, A., Mulch, A., and Davis, C. C. (2016). The abiotic and biotic drivers of rapid diversification in a ndean bellflowers (campanulaceae). *New Phytologist*, 210(4) :1430–1442.

Lagomarsino, L. P., Forrestel, E. J., Muchhala, N., and Davis, C. C. (2017). Repeated evolution of vertebrate pollination syndromes in a recently diverged andean plant clade. *Evolution*, 71(8) :1970–1985.

Losos, J. B. (2017). *Improbable destinies : Fate, chance, and the future of evolution*. Penguin.

Losos, J. B. and Ricklefs, R. E. (2009). Adaptation and diversification on islands. *Nature*, 457(7231) :830–836.

MacArthur, R. H. and Wilson, E. O. (1963). An equilibrium theory of insular zoogeography. *Evolution*, 17(4) :373–387.

Mahler, D. L., Revell, L. J., Glor, R. E., and Losos, J. B. (2010). Ecological opportunity and the rate of morphological evolution in the diversification of greater antillean anoles. *Evolution : International Journal of Organic Evolution*, 64(9) :2731–2745.

Martén-Rodríguez, S., Fenster, C. B., Agnarsson, I., Skog, L. E., and Zimmer, E. A. (2010). Evolutionary breakdown of pollination specialization in a caribbean plant radiation. *New Phytologist*, 188(2) :403–417.

Martén-Rodríguez, S., Almarales-Castro, A., and Fenster, C. B. (2009). Evaluation of pollination syndromes in Antillean Gesneriaceae : evidence for bat, hummingbird and generalized flowers. *Journal of Ecology*, 97(2) :348–359.

Martén-Rodríguez, S. and Fenster, C. B. (2008). Pollination Ecology and Breeding Systems of Five Gesneria Species from Puerto Rico. *Annals of Botany*, 102(1) :23–30.

Martén-Rodríguez, S., Quesada, M., Castro, A.-A., Lopezaraiza-Mikel, M., and Fenster, C. B. (2015). A comparison of reproductive strategies between island and mainland Caribbean Gesneriaceae. *Journal of Ecology*, 103(5) :1190–1204.

McKinney, M. L. (1997). Extinction vulnerability and selectivity : combining ecological and paleontological views. *Annual review of ecology and systematics*, 28(1) :495–516.

Myers, N., Mittermeier, R. A., Mittermeier, C. G., Da Fonseca, G. A., and Kent, J. (2000). Biodiversity hotspots for conservation priorities. *Nature*, 403(6772) :853.

Olesen, J. M. and Jordano, P. (2002). Geographic patterns in plant–pollinator mutualistic networks. *Ecology*, 83(9) :2416–2424.

Ollerton, J. (2017). Pollinator diversity : distribution, ecological function, and conservation. *Annual Review of Ecology, Evolution, and Systematics*, 48 :353–376.

Ollerton, J., Alarcón, R., Waser, N. M., Price, M. V., Watts, S., Cranmer, L., Hingston, A., Peter, C. I., and Rotenberry, J. (2009). A global test of the pollination syndrome hypothesis. *Annals of botany*, 103(9) :1471–1480.

Ollerton, J., Winfree, R., and Tarrant, S. (2011). How many flowering plants are pollinated by animals ? *Oikos*, 120(3) :321–326.

Patterson, B. D. (1983). Grasshopper mandibles and the niche variation hypothesis. *Evolution*, 37(2) :375–388.

Perret, M., Chautems, A., De Araujo, A. O., and Salamin, N. (2013). Temporal and spatial origin of gesneriaceae in the new world inferred from plastid dna sequences. *Botanical Journal of the Linnean Society*, 171(1) :61–79.

Petanidou, T. and Potts, S. G. (2006). Mutual use of resources in mediterranean plant–pollinator communities : how specialized are pollination webs. *Plant–pollinator interactions : from specialization to generalization*, pages 220–244.

Regalado, L., Lóriga, J., Bechteler, J., Beck, A., Schneider, H., and Heinrichs, J. (2018). Phylogenetic biogeography reveals the timing and source areas of the adiantum species (pteridaceae) in the west indies, with a special focus on cuba. *Journal of Biogeography*, 45(3) :541–551.

Ricklefs, R. and Bermingham, E. (2008). The west indies as a laboratory of biogeography and evolution. *Philosophical Transactions of the Royal Society B : Biological Sciences*, 363(1502) :2393–2413.

Roncal, J., Nieto-Blázquez, M. E., Cardona, A., and Bacon, C. D. (2020). Historical biogeography of caribbean plants revises regional paleogeography. *Neotropical diversification : Patterns and processes*, pages 521–546.

Rosas-Guerrero, V., Aguilar, R., Martén-Rodríguez, S., Ashworth, L., Lopezaraiza-Mikel, M., Bastida, J. M., and Quesada, M. (2014). A quantitative review of pollination syndromes : do floral traits predict effective pollinators ? *Ecology letters*, 17(3) :388–400.

Sahli, H. F. and Conner, J. K. (2011). Testing for conflicting and nonadditive selection : floral adaptation to multiple pollinators through male and female fitness. *Evolution : International Journal of Organic Evolution*, 65(5) :1457–1473.

Salzburger, W. (2018). Understanding explosive diversification through cichlid fish genomics. *Nature Reviews Genetics*, 19(11) :705–717.

Schiestl, F. P. and Johnson, S. D. (2013). Pollinator-mediated evolution of floral signals. *Trends in ecology & evolution*, 28(5) :307–315.

Serrano-Serrano, M. L., Rolland, J., Clark, J. L., Salamin, N., and Perret, M. (2017). Hummingbird pollination and the diversification of angiosperms : an old and successful association in gesneriaceae. *Proceedings of the Royal Society B : Biological Sciences*, 284(1852) :20162816.

Siefert, A., Violle, C., Chalmandrier, L., Albert, C. H., Taudiere, A., Fajardo, A., Aarssen, L. W., Baraloto, C., Carlucci, M. B., Cianciaruso, M. V., et al. (2015). A global meta-analysis of the relative extent of intraspecific trait variation in plant communities. *Ecology letters*, 18(12) :1406–1419.

Skog, L. E. (1976). *A study of the tribe Gesnerieae, with a revision of Gesneria (Gesneriaceae, Gesnerioideae)*, volume no.29 (1976). Washington Smithsonian Institution Press 1969-. https ://www.biodiversitylibrary.org/bibliography/100822.

Stebbins, G. L. (1970). Adaptive radiation of reproductive characteristics in angiosperms, i : pollination mechanisms. *Annual review of ecology and systematics*, 1(1) :307–326.

Taylor, A., Weigelt, P., König, C., Zotz, G., and Kreft, H. (2019). Island disharmony revisited using orchids as a model group. *New Phytologist*, 223(2) :597–606.

Thomson, J. D. and Wilson, P. (2008). Explaining evolutionary shifts between bee and hummingbird pollination : convergence, divergence, and directionality. *International Journal of Plant Sciences*, 169(1) :23–38.

van der Niet, T., Zollikofer, C. P., de León, M. S. P., Johnson, S. D., and Linder, H. P. (2010). Three-dimensional geometric morphometrics for studying floral shape variation. *Trends in plant science*, 15(8) :423–426.

Van Valen, L. (1965). Morphological variation and width of ecological niche. *The American Naturalist*, 99(908) :377–390.

Violle, C., Enquist, B. J., McGill, B. J., Jiang, L., Albert, C. H., Hulshof, C., Jung, V., and Messier, J. (2012). The return of the variance : intraspecific variability in community ecology. *Trends in ecology & evolution*, 27(4) :244–252.

Vogel, S. (1954). *Blütenbiologische typen als elemente der Sippengliederung*. Number 1. G. Fischer.

Warren, B. H., Simberloff, D., Ricklefs, R. E., Aguilée, R., Condamine, F. L., Gravel, D., Morlon, H., Mouquet, N., Rosindell, J., Casquet, J., et al. (2015). Islands as model systems in ecology and evolution : Prospects fifty years after macarthur-wilson. *Ecology Letters*, 18(2) :200–217.

Waser, N. M., Chittka, L., Price, M. V., Williams, N. M., and Ollerton, J. (1996). Generalization in pollination systems, and why it matters. *Ecology*, 77(4) :1043–1060.

Weber, A., Clark, J. L., and Möller, M. (2013). A new formal classification of Gesnericeae. *Selbyana Special Issue : Proceedings of the World Gesneriad Research Conference 2010 (2013)*, Vol. 31(No. 2) :28.

Wessinger, C. A., Rausher, M. D., and Hileman, L. C. (2019). Adaptation to hummingbird pollination is associated with reduced diversification in penstemon. *Evolution letters*, 3(5) :521–533.

Zhaoran, X. and Skog, L. (1990). A study of bellonia l. (gesneriacea).

Premier chapitre.

Evolution of intraspecific floral variation in a generalist-specialist pollination system

par

Marion Leménager[1], John L. Clark[2], Silvana
Martén-Rodríguez[3], Abel Almarales-Castro[4] et Simon Joly[5]

[1] Institut de recherche en biologie végétale, Département de Sciences Biologiques, Université de Montréal, 4101 Sherbrooke East, Montréal, QC H1X 2B2, Canada

[2] Marie Selby Botanical Gardens, 1534 Mound Street Sarasota, FL 34236

[3] Laboratorio Nacional de Análisis y Síntesis Ecológica, Escuela Nacional de Estudios Superiores–Morelia, Universidad Nacional Autónoma de México, Morelia, Michoacán C.P. 58190, México

[4] Centro Oriental de Ecosistemas y Biodiversidad (Bioeco). Museo de Historia Natural "Tomás Romay". José A. Saco #601, esq. a Barnada. Santiago de Cuba, C.P. 90100. Cuba.

[5] Institut de recherche en biologie végétale, Département de Sciences Biologiques, Université de Montréal, 4101 Sherbrooke East, Montréal, QC H1X 2B2, Canada
Jardin Botanique de Montréal, 4101 Sherbrooke East, Montréal, QC H1X 2B2, Canada

Résumé.

Les processus intraspécifiques ont un impact sur les schémas macroévolutifs par le biais de la variation individuelle, de la sélection et de la spécialisation écologique. Selon l'hypothèse de la variation de niche, la niche écologique plus large des espèces généralistes entraîne une variation morphologique accrue entre les individus, soit parce qu'ils sont constitués d'individus spécialisés diversifiés exploitant chacun une fraction de la niche de l'espèce, soit parce qu'ils sont constitués de véritables individus généralistes qui font l'objet d'une sélection assouplie. Pour tester cette hypothèse, nous avons étudié la morphologie florale individuelle d'espèces de Gesneriaceae antillaises, un groupe qui est passé de la spécialisation pour la pollinisation par les colibris à la généralisation à plusieurs reprises au cours de son histoire évolutive. Nous avons caractérisé les profils des corolles à l'aide de la morphométrie géométrique et comparé la variance de forme intraspécifique des spécialistes et des généralistes dans un contexte phylogénétique. Nous avons utilisé trois approches qui tiennent compte différemment de la haute dimensionnalité des traits morphologiques, de la reconstruction ancestrale des syndromes de pollinisation au fil du temps et de l'erreur associée à l'estimation de la variance intraspécifique. Nos résultats soutiennent partiellement l'hypothèse de la variation de niche. Si la prise en compte de l'ensemble de la forme dans l'analyse corrobore cette idée, la décomposition de la forme en composantes principales indique que tous les aspects de la corolle ne présentent pas le même schéma de variation. Plus précisément, les pollinisateurs généralistes ont tendance à présenter une plus grande variation intraspécifique que les spécialistes en termes de tubularité, mais pas de courbure. La prise en compte de l'erreur dans l'estimation de la variance a également réduit le soutien à l'hypothèse, ce qui suggère que des échantillons de plus grande taille pourraient être nécessaires pour parvenir à des conclusions plus solides. Cette étude souligne l'influence réciproque entre les plantes et leurs pollinisateurs sur la morphologie florale à différentes échelles de biodiversité, et suggère que les stratégies écologiques des espèces peuvent affecter les schémas de variation morphologique à des échelles macroévolutives.

Mots clés : Stratégies de pollinisation des plantes, généralistes de la pollinisation, spécialistes de la pollinisation, variation intraspécifique, morphologie florale, Gesneriaceae antillaises, macroévolution, hypothèse de variation de niche

ABSTRACT.

Intraspecific processes impact macroevolutionary patterns through individual variation, selection, and ecological specialisation. According to the niche variation hypothesis, the broader ecological niche of generalist species results in an increased morphological variation among individuals, either because they are constituted of diversified specialised individuals each exploiting a fraction of the species' niche, or because they are constituted of true generalist individuals that experience relaxed selection. To test this hypothesis, we surveyed the individual floral morphology of species of Antillean Gesneriaceae, a group that has transitioned between specialisation for hummingbird pollination and generalisation multiple times throughout its evolutionary history. We characterised the profiles of corollas using geometric morphometrics and compared the intraspecific shape variance of specialists and generalists in a phylogenetic context. We used three approaches that differently accounted for the high dimensionality of morphological traits, the ancestral reconstruction of pollination syndromes over time, and the error associated with the estimation of the intraspecific variance. Our findings provide partial support for the niche variation hypothesis. If considering the whole shape in the analysis corroborated this idea, decomposing the shape into principal components indicated that not all aspects of the corolla exhibit the same pattern of variation. Specifically, pollination generalists tend to display greater intraspecific variation than specialists in terms of tubularity, but not of curvature. Accounting for the error in the variance estimation also reduced the support for the hypothesis, suggesting that larger sample sizes may be required to reach stronger conclusions. This study emphasises the reciprocal influence between plants and their pollinators on floral morphology at different biodiversity scales, and suggests that ecological strategies of species can affect patterns of morphological variation at macroevolutionary scales.

Keywords: Plant pollination strategies, pollination generalists, pollination specialists, intraspecific variation, floral morphology, Antillean Gesneriaceae, macroevolution, niche variation hypothesis

49

1. Introduction

The patterns of morphological variation we observe at macroevolutionary scales have the potential to be influenced by processes occurring at the species level. For example, a higher degree of intraspecific trait variation may lead to a broader occupation of trait space at macroevolutionary scales. As a result, factors affecting intraspecific morphological variations, such as climate (Kuppler et al., 2020) or the ecological generalisation of species (Van Valen, 1965) can shape macroevolutionary trends. Furthermore, intraspecific morphological variation contributes substantially to the overall trait diversity in communities (Siefert et al., 2015) and plays a crucial role across scales in driving their assembly and functioning (Bolnick et al., 2011; Violle et al., 2012; Westerband et al., 2021).

The impact of the level of ecological generalisation on intraspecific variation has attracted much interest in the past. Along the ecological specialist-generalist gradient, increased generalisation is associated with a broader niche breadth, either in terms of resources (Grinnellian niche) or in terms of the functions a species performs in the ecosystem (Eltonian niche) (Devictor et al., 2010). A specialist thus exploits fewer resources than a generalist or contributes to a very specific function in the ecosystem. According to the ecological niche variation hypothesis (NVH), species with a broad ecological niche should have greater intraspecific morphological variation (Van Valen, 1965) (Figure 3a vs. b). This pattern can be caused by two distinct processes. On the one side, generalist species can be constituted of specialist individuals that occupy different ecological niches (Figure 3c). On the other hand, generalist species could be constituted of individuals that are intrinsically generalists, implying that they are all able to exploit a wide range of resources (Figure 3d).

Although there has been mixed support for the ecological niche variation hypothesis in the past (Patterson, 1983; Grant and Price, 1981), there is a tendency for generalists to display greater intraspecific morphological variation (Futuyma and Peterson, 1985). For instance, in hummingbird-pollinated plant species, long corolla tubes that are more ecologically specialised have lower intraspecific variation in corolla tube length (Fenster, 1991). However, there have been few tests of the niche variation hypothesis in a specific group by investigating simultaneously the intraspecific variation of multiple species while controlling for their evolutionary relationships. And despite the inherent importance of intraspecific variation across scales, few studies have incorporated it in macroevolutionary models.

In this study, we tested if differences in the degree of pollination generalisation affect macroevolutionary patterns of intraspecific floral variation in a group of Antillean Gesneriaceae. In this group, pollination specialists are pollinated by a smaller subset of the potential pollinators in their environment (i.e. a single or a few species belonging to a functional group of pollinators)

than pollination generalists (i.e., having more than one pollinator functional group). We hypothesise that floral traits of pollination generalists show greater intraspecific variation compared to specialists, as predicted by the niche variation hypothesis.

The Gesneriinae (Gesneriaceae) is a monophyletic group of ca. 80 species mostly endemic to the Antilles. In contrast to their relatives present on the American continent that are all pollination specialists (amongst those studied), several species of the insular group are pollination generalists (Martén-Rodríguez et al., 2015). Indeed, although a large proportion of the species are hummingbird specialists and a few are bat or moth specialists, many species have a mixed-pollination generalist strategy being effectively pollinated by hummingbirds, bats, and insects (Martén-Rodríguez et al., 2009; Martén-Rodríguez et al., 2010). Interestingly, the generalist pollination syndrome has evolved repeatedly in this group towards a convergent flower shape now found in all major islands of the Antilles (Martén-Rodríguez et al., 2010; Joly et al., 2018), making it an ideal group to study the impact of generalist pollination strategies on the macroevolutionary patterns of variation in the group.

Several studies have distinguished different pollination syndromes for these different reproductive strategies (Martén-Rodríguez and Fenster, 2008; Martén-Rodríguez et al., 2009; Martén-Rodríguez et al., 2010; Martén-Rodríguez et al., 2015). Species specialised for hummingbird pollination have a tubular corolla, a bright colour (red to yellow), and diurnal anthesis, and species specialised for bats have a campanulate (bell-shaped) corolla of pale colour (white to greenish) with nocturnal anthesis. Finally, species with a mixed pollination strategy have a campanulate corolla with a relatively large constriction at the base, of different colours and mottled patterns, with both diurnal and nocturnal anthesis (Martén-Rodríguez et al., 2009; Joly et al., 2018). One species of Gesneriinae also has a Heteroceran (moth) pollination syndrome with a yellowish tubular corolla.

A previous study of the group suggested that the flower shape of generalists is not an intermediate between the different specialist shapes (Joly et al., 2018) as might have been expected if the shape of generalists evolved under weak trade-offs (e.g., Aigner, 2001; Sahli and Conner, 2011). In contrast, the flower shapes of generalists occupy a completely distinct region of the floral morphospace, which was interpreted as their shapes being adapted specifically to be pollinated by distinct functional pollinators (Joly et al., 2018). At least at the inter-specific level, the corolla shapes of generalist species did not show more variation than that of specialist species (Joly et al., 2018). However, we do not know if the corolla shape of generalists is more variable than that of specialists intraspecifically across the group, as would be predicted by the niche variation hypothesis, or if it mirrors the interspecific pattern of variation. In this research, we studied 261 individual flowers of 30 species to test if generalists show greater intra-specific corolla shape variation. As there is currently no method capable of taking into account the complexity of multivariate geometric morphometric data, the stochastic nature of the evolutionary process and measurement error, we used three approaches, each with its advantages and disadvantages,

to test whether generalists have greater intraspecific variance in corolla shape than specialists in a clade of West Indian Gesneriaceae.
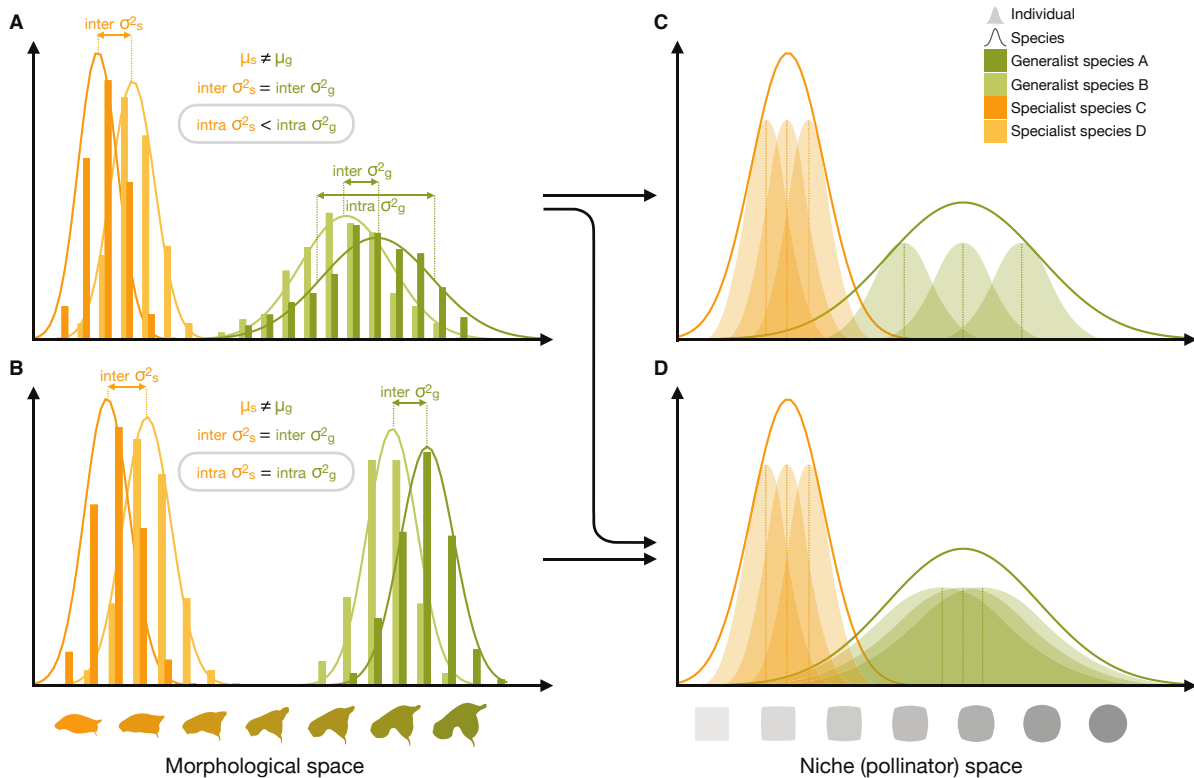
Figure 3. Illustration of the niche variation hypothesis (NVH) and three different ways (black arrows) that species can increase their ecological niche space (generalisation). Interspecific morphological variations in Antillean Gesneriaceae are similar among pollination syndromes of hummingbird specialists (orange) and generalists (green) (inter σ_s = inter σ_g) even though they do not have the same mean floral shape ($\mu_s \neq \mu_g$). However, we do not know if the transition from specialist to generalist conforms to the niche variation hypothesis (NVH) that predicts (a) higher intraspecific morphological variation for generalists than specialists (intra σ_s > inter σ_g) in contrast to (b) similar intraspecific morphological variation among pollination syndromes (intra σ_s = intra σ_g). On an ecological scale (niche space) generalisation (niche breadth expansion) can occur (c) if generalist species are constituted of specialist individuals that occupy distinct niches or (d) if generalist species are constituted of intrinsic generalist individuals.

2. Materials and methods

2.1. Floral data

We quantified the corolla shape of species from the Gesneriinae subtribe using geometric morphometrics from flower photographs in strict lateral view. The floral image data set was

compiled using the dataset used in Joly et al. (2018), to which we added new photographs mainly associated with herbarium vouchers or from the online database iNaturalist (Available from `https://www.inaturalist.org`).

Pollinator information was obtained from field-based information (Martén-Rodríguez and Fenster, 2008; Martén-Rodríguez et al., 2009; Martén-Rodríguez et al., 2010; Martén-Rodríguez et al., 2015; Faure and Joly, 2020), or inferred from flower characteristics for species with unstudied pollination biology in the field as previous studies have shown that flower traits are a very good predictor of the pollination strategies in this clade (see Martén-Rodríguez et al., 2009).

Species names of West Indian Gesneriaceae were used in accordance with the Catalogue of Seed plants of the West Indies (Acevedo-Rodríguez and Strong, 2012) and Joly et al. (2023).

2.2. Phylogenetic reconstruction

The phylogeny of the Gesneriinae subtribe (Gesneriaceae) species studied was reconstructed for taking evolutionary relationships into account when comparing the floral shape variance of generalist and specialist species. DNA sequences of 5 nuclear genes (*CYCLOIDEA*, *CHI*, *UFR3GT*, *F3H*, and *GAPDH*) were collected from previous studies (Joly et al., 2018, 2023) to which sequences from 10 additional species were added to the dataset following the protocol of Joly et al. (2018). *Kohleria sp.* Regel 'Trinidad' (Gesneriae) and *Codonoboea malayana* (Hook.f.) Kiew (Trichosporeae) were used as outgroups.

Sequences were aligned with MAFFT version 7 (Katoh and Standley, 2013) and the alignment was manually verified. A species tree was reconstructed with *BEAST in BEAST version 1.8.4 (Heled and Drummond, 2010). Site substitution, molecular clock, and relative substitution rate were assigned independently to each gene. The site substitution model used was the GTR+Γ+I model (Yang, 1994a,b) for each gene because over-parameterisation of nucleotide substitution models brings very little bias compared to the under-parameterisation of these models in Bayesian Markov Chain Monte Carlo (MCMC) analyses (Lemmon and Moriarty, 2004). An uncorrelated log-normal relaxed molecular clock was chosen for each gene. A birth-death prior was applied for the species tree and population sizes were allowed to vary along the branches linearly with a constant population size at the root of the tree. Two MCMC chains were run for 50 million generations, with a recording of the parameter values every 2000 generations, discarding the first 20 million generations as burn-in. The software Tracer (Rambaut et al., 2018) is used to verify the convergence of the chain for all parameters and the acquisition of good effective sample sizes. A maximum clade credibility (MCC) tree was then retrieved from the sampled trees.

2.3. Ancestral pollination regimes reconstruction

To test our hypothesis regarding the evolution of intraspecific variance, we used methods that require an explicit evolutionary scenario, specifically a phylogenetic tree with information about

the character states of the species (specialist or generalist) along the branches of the tree. We used stochastic character mapping (Huelsenbeck et al., 2003) to simulate these evolutionary scenarios along the branches of the phylogeny. We first tested the fit of symmetrical and asymmetrical models of character evolution using an extended Mk model (Lewis, 2001) for discrete character evolution using the function `fitMk` from the R package `phytools` (version 1.0-1) (Revell, 2012). The model with the smallest AIC (Akaike Information Criterion) (Akaike, 1987) was then selected to perform 100 character simulations using the function `make.simmap` of the `phytools` package. The resulting ancestral trait maps were then used in the multivariate analysis of continuous trait evolution as well as the Bayesian analysis of joint inter- and intraspecific morphological evolution.

2.4. Characterisation of corolla shape

To characterise the corolla shape of each individual floral profile, we used principles of geometric morphometrics. For each flower photograph, 32 landmarks were placed (6 landmarks and 26 semi-landmarks) (Joly et al., 2018) using the ImageJ software (version 1.5.3) (Schneider et al., 2012) and the PointPicker plugin ($http : //bigwww.epfl.ch/thevenaz/pointpicker/$). Two landmarks were positioned at the tips of the petal lobes, two at the base of the petal lobes, and two at the base of the corolla (see landmark placements in Figure S1). The 26 semi-landmarks were evenly distributed along the upper and lower curvature of the corolla tube (13 points for each curve) between the base of the corolla and the base of the lobes to capture the shape of the corolla. We did not evaluate the variation of landmark placement between independent pictures because the error in data acquisition was estimated as minimal following this technique (i.e. 0.15% of the total variation was attributed to landmark placement Joly et al., 2018).

The specimens were aligned using a generalised Procrustes analysis (GPA) (Gower, 1975; Rohlf and Slice, 1990) using the `geomorph` R package version 4.0.1 (Adams and Otárola-Castillo, 2013). The GPA translates all the shapes to the origin, scales them, and rotates them to align the shapes as closely as possible. Landmark optimisation during the Procrustes transformation was achieved by minimising the curvature energy (Bookstein, 1997) rather than by minimising the Procrustes distances (Rohlf, 2010), as recommended by Perez et al. (2006). For larger shape variations, as is the case with flower profiles of Gesneriaceae, the curvature energy minimisation approach generally achieves better optimisation of the displacement of the semi-landmarks and takes into account the local morphological deformation (Gunz and Mitteroecker, 2013; Perez et al., 2006). With curvature energy minimization, all landmarks and semi-landmarks are taken into account as well as the regularity of the analysed shape, while the points are taken independently with the Procrustes distance minimisation method. This can make a semi-landmark slip beyond the limit of the curvature of the studied shape or exceed another semi-landmark (Gunz and Mitteroecker, 2013), which was observed with our data set. The coordinates of the aligned landmarks resulting

from the Procrustes transformation (Kendall, 1984) were then used in the intra-specific floral shape variation analyses.

2.5. Floral morphospace

We used Principal Component Analysis (PCA) to summarise the morphological variation in a few variables representing a maximum of the total variation of the corolla shape. Using the results of the Procrustean generalised analysis (the aligned sets of points coordinates), individual flower morphology was projected in a morphospace representing the phenotypical variation between individuals. The morphospace was obtained by PCA of the covariance matrix of landmarks using the function `prcomp` from the R package `stats` version 4.1.2. Diagnostic graphs and scree plot for the eigenvalues of the main PCA axes were generated using the R package `factoextra` (Kassambara and Mundt, 2020). To account for the morphological variation in the whole subtribe, we included the morphological data for all species with either a hummingbird specialist or a generalist syndrome in the morphospace that have at least three images per species, even if the species was not in the phylogenetic tree. Coordinates of individuals in the phylogeny were then selected in downstream comparative analyses.

2.6. Phylogenetic generalised least squares analysis of variance

To test whether generalist species exhibit greater intraspecific corolla shape variation (variance) than hummingbird-pollinated species while accounting for the phylogenetic non-independence of observations, we first used a phylogenetic generalised least squares (PGLS) approach (Grafen, 1989). We calculated the corolla shape variance using the standard formula $\frac{1}{n-1}\sum_{i=1}^{n}(x_i - \bar{x})^2$, where $(x_i - \bar{x})$ is the Procrustes (euclidean) distance calculated from the landmarks between the corolla shape of individual i and the mean shape of that species ($\bar{x}$). This approach has the advantage of considering the entire multivariate space in which the morphological shape of the species varies. The relationship between the intraspecific corolla shape variance and pollination strategy (specialists vs. generalist) was tested with a PGLS analysis using the function `glm` from the R package `nlme` version 3.1-153 Pinheiro et al. (2021). We allowed the residuals of the model to be partly phylogenetically structured by using the `corPagel` correlation structure from the R package ape version 5.6-2 (Paradis and Schliep, 2019) and optimising the lambda parameter. Estimating the strength of the phylogenetic structure in the residuals results in better statistical behaviour (Revell, 2010). Model fitting was done using the restricted maximum likelihood (REML), and the effect of the pollination strategy was tested using a t-test. The normality of the residuals and a plot of the residuals vs. fitted values were inspected to ensure the adequacy of the model.

2.7. Multivariate evolution of continuous traits evolution

To further test if pollination specialists differ less in corolla shape variance than pollination generalists, we used Ornstein-Uhlenbeck (OU) evolutionary models that differ in whether specialists and generalists are allowed to have the same or different intraspecific variance, and verified in the case of two distinct variances if generalists had greater corolla shape variation than specialists. Two models were fitted, one that used the corolla shape variance calculated from the Procrustes aligned floral shapes and previously used in the PGLS approach, and another one using the variance estimated from the first three principal components (PC) of the morphospace. In both cases, the natural logarithm of the variance (ln-variance) was used in the analyses.

We fitted univariate and multivariate Ornstein-Uhlenbeck evolutionary models with a single optimum (OU1) or different optima (OUM) of intraspecific variance for each pollination strategy (specialists and generalists) using the `mvOU` function of the R package `mvMROPH` (Clavel et al., 2015). A random root variance-covariance matrix was used and the tree was scaled to unit length. These analyses were repeated on 100 stochastic mapping of the pollination strategies to consider the uncertainty associated with these reconstructions. To compare the model fit during each analysis, the Akaike Weights were calculated using the second-order information criterion (AICc) for each model and SIMMAP using the function `aicw` of the R package `mvMROPH`. The proportions of SIMMAPs supporting either the OU model with one optimum (OU1) or two optima (OUM) models of trait evolution were summarised.

2.8. Bayesian Analysis of intra- and interspecific morphological evolution

General approach

To test if both pollination strategies evolved towards distinct optimal values of intraspecific floral variation while taking into account the incertitude on the sample sizes of each species, we used a Joint inter- and intraspecific Variance Evolution (JIVE) model integrated into a hierarchical Bayesian framework (Kostikova et al., 2016; Gaboriau et al., 2020). This approach takes as input the individual trait values for individuals in several species, a phylogeny with the pollination strategies mapped on the tree (specialist or generalist), and models of evolution for the intraspecific trait variance and for the mean trait. It then estimates the intraspecific variances and the parameters of the evolutionary models using MCMC. By using evolutionary models that allow different species to evolve under different regimes, it is possible to test, for instance, if generalist species tend to evolve toward a greater intraspecific variance in corolla shape than specialist species (see Kostikova et al., 2016). This approach has the advantage of taking into account the uncertainty in the intra-specific variance while modelling both the evolution of the intraspecific shape variance and mean shape across species. One drawback, however, is that it is an univariate approach and that the whole floral shape space cannot be taken into account in one analysis. We thus decomposed

the global shape into principal components and we analysed the first 3 principal axes of the floral morphospace with this approach. Only species present in the phylogeny and represented by at least three photographs were included in this analysis.

Bayesian analysis of the tempo of phenotypic evolution
We determined a model of character evolution for mean corolla shape and intraspecific shape variance to use in the analysis. We used an OUM model for mean shape because this model was strongly supported in a previous study of corolla shape in West Indian Gesneriaceae (Joly et al., 2018). For the evolution of corolla shape variance, two models were considered. We fitted an OU1 model (Ornstein-Uhlenbeck process with one optimum) and an OUM model (Ornstein-Uhlenbeck process with one optimum per selective regime) that forces the specialists to have the same (OU) or different (OUM) optimal intra-specific variances. We used the R package `bite` (Bayesian Integrative Models of Trait Evolution) version 0.4 (Gaboriau et al., 2020) to fit these models.

JIVE objects are generated as input for the implementation of the Markov chain Monte Carlo sampling (MCMC) for trait evolution models. JIVE objects were created for each simulation with the function `make.jive` of the `bite` package : the two models were estimated for each of the first three principal components for all 100 ancestral character histories produced by stochastic character mapping, resulting in a total of 600 JIVE objects. We used the default proposal functions with the following proposal parameters : mean variance (likelihood) per species (0.02), prior mean ($\alpha : 4$, $\sigma^2 : 3$, $\theta : 0.2$), and prior ln-variance ($\alpha : 4$, $\sigma^2 : 4$, $\theta : 2$). We used a uniform hyperprior for the ln-variance bounded between -10 and -1.

The MCMC chains for all 600 analyses were run for 4 million generations, with a sampling frequency of 200 generations, a burn-in phase of 10000 generations, and 20 values of beta for the stepping-stone integration to allow for the estimation of the marginal likelihood for model selection (Xie et al., 2011) (see below). The sample size adjusted for auto-correlation (effective sample size, ESS) was estimated using the function `effectiveSize` from the R package `coda` version 0.19-4 (Plummer et al., 2006).Estimations plots (in particular the trace plot) were made using the functions ggmcmc and ggs from the R package ggmcmc (Fernández-i Marín, 2016). The individual trace plots were verified for MCMC chains that stalled between temperature changes for the stepping stone integration ; such analyses were repeated. The chains are then summarised per model and per principal component axes.

Model selection
To summarise the evidence provided by the data in favour of one statistical model over the other (OU or OUM), we used Bayes factors (Jeffreys, 1935; Kass and Raftery, 1995). The natural logarithms of the marginal likelihoods ($ln(p(D|M))$) required for Bayes Factor calculation were calculated by stepping stone integration (Xie et al., 2011) using the function `marginal_lik` from the R package `bite`. The Bayes Factor (BF_{10}) of model M_1 over the null (simpler) model M_0

is estimated as $BF_{10} = 2 \times (ln(p(D|M_1)) - ln(p(D|M_0)))$ and is interpreted following Kass and Raftery (1995); $BF_{10} > 2$ indicates positive evidence for M_1, $BF_{10} > 6$ indicates strong evidence for M_1, $BF_{10} > 10$ indicates very strong evidence for M_1. Here, model M_1 represents the model in which specialists and generalists have different variances.

Estimation of optimal variances for specialists and generalists

As another approach to test our hypothesis, we estimated the posterior probability that generalists have a greater intraspecific corolla shape variance than specialists ($\theta_g > \theta_s$) from the most complex model (mOUMvOUM). To calculate this posterior probability, we counted the number of generations from the post-burn-in chains with a temperature of 1 (no stepping stone integration) for which $\theta_g > \theta_s$. This was integrated over all stochastic mapping histories for each PC axis.

A summary of the approaches is present in Table 1 and a summarising flowchart of the methods used is present in the supplementary information (Figure S2).

	PGLS	mvMORPH	JIVE
Estimation of variance	On entire data set	On entire dataset or per principal component axis	Per principal component axis
Estimation of error (sample size)	no	no	yes
Multivariate	yes	yes	no
Consideration of ancestral trait estimation (pollination regimes)	no	yes	yes

Tableau 1. Details on the different approaches used in the intra-specific floral shape variation analyses.

3. Results

3.1. Floral morphology

Images of 261 distinct individuals representing 30 Gesneriinae species (at least 3 individuals per species) with an identified or inferred pollination syndrome for hummingbird pollination and mixed-pollination were retrieved (see table S1). Pollination system data and sources of images are presented in table S2 and table S3 respectively.

Corolla morphospace explained 86.8% of the total shape variance in the first three principal components (PC) (see Figs. 4 and S3); the other PC explained each less than 5% of the total variance. The first PC explained 64.4% of the total variance and characterised tubular-shaped flowers from campanulate flowers with a wider opening and a median ventral constriction of the corolla (Figure 4 (a) and Figure4 (b)). The first axis is the main one discriminating between

specialist and generalist species. The second PC axis accounted for 14.3% of the total variance and broadly characterises a change in corolla curvature, with more curved flowers showing more pronounced corolla constriction. The third PC axis accounted for 8.1% of the total variance and characterises a smaller difference in the shape of the corolla curvature. These floral variations along the axes are concordant with Joly et al. (2018).
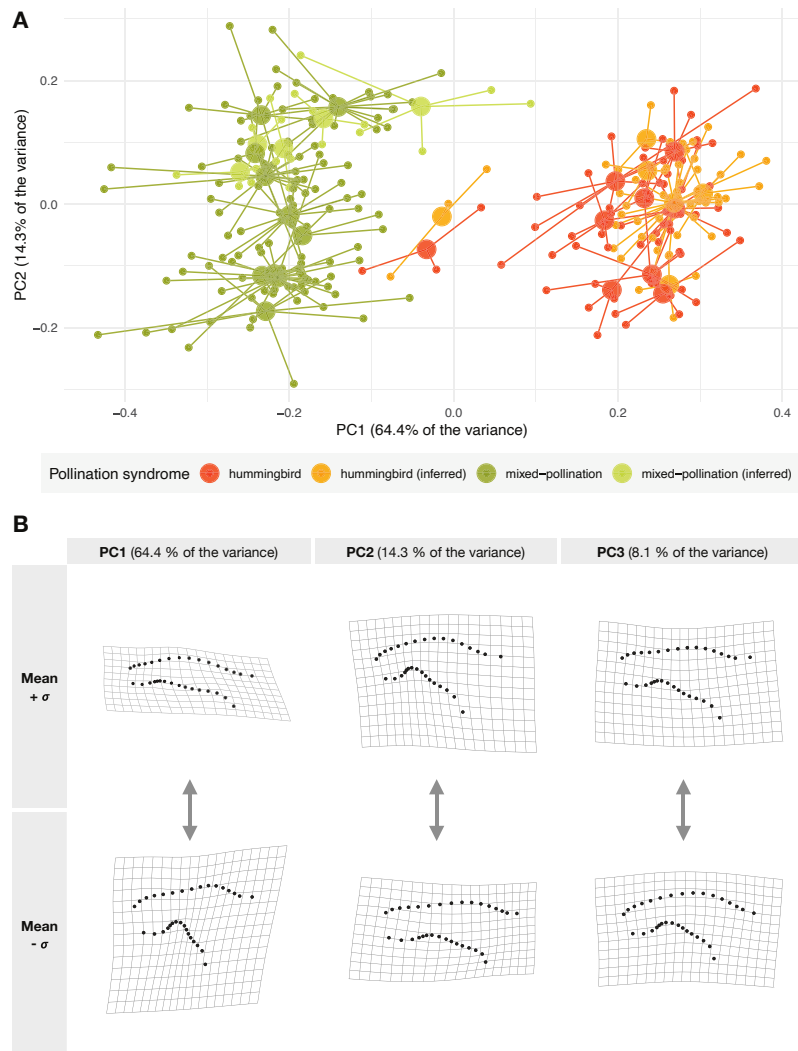
Figure 4. Corolla shape variation in Antillean Gesneriaceae. (a) Principal Component Analysis (PCA) of shape variation (morphospace). The arithmetic mean coordinate values for each species were calculated for each of the first three axes of the morphospace, and are represented by the larger symbols, linked to individual values. (b) Table of the morphological variation along the first three axes of the morphospace.

3.2. Phylogenetic reconstruction

We gathered sequence data from most of the five selected genes for 110 individuals representing 53 species of the Gesneriinae tribe (Table S4). In total, 23 individuals representing 15 species, including 10 additional species since the phylogeny presented in Joly et al. (2018) were added to the phylogenetic reconstruction of the subtribe Gesneriinae. The genus *Bellonia* L. is sister to the rest of the subtribe with branch support of pp=0.99. *Rhytidophyllum* Mart. and *Gesneria* L. formed distinct groups, with less support for the *Gesneria* genus (1.00 and 0.59 respectively). In comparison with the phylogeny from Joly et al. (2018), *Gesneria depressa* (Griseb.) Urb. and *Gesneria pulverulenta* Alain were not included in the phylogenetic analysis because they importantly decreased the tree resolution. Only two genes (*GCYC* and *F3H*) were sequenced for *G. depressa* and only one (*GCYC*) for *G. pulverulenta*, from one individual each. This phylogeny is overall congruent with the one from Joly et al. (2018). For the following analyses, the species tree (Figure S4) was pruned to remove all but the 24 hummingbird specialists and generalist species that had at least three profile images (11 specialists and 13 generalists) (Figure 5).

3.3. Ancestral character mapping of syndromes

For the ancestral reconstruction of pollination strategies, the equal (ER) model (AIC=68.03) was selected over the asymmetrical (ARD) model (AIC=70.03). Stochastic simulations on 100 trees suggest 6 changes between generalist and specialist strategies on average. The estimated number of transitions between states is higher from generalist to hummingbird specialists (3.75) than from hummingbird specialists to generalists (2.25). Hummingbird specialist was the most likely ancestral state for the ancestor of *Gesneria* and *Rhitidophyllum* with a probability of 0.6 (Figure 5). The proportion of time spent in the hummingbird specialist state is also greater than the proportion of time spent in the generalist state (51.7% and 48.3% respectively).

3.4. Phylogenetic generalised linear model

The species intra-specific variances of corolla shape (Figure 5) estimated from the Procrustes aligned corollas were used in a phylogenetic generalised linear regression to test if pollination generalists have a greater intra-specific corolla shape variance. Distribution of the normalised residuals and fitted values are available in the supplements (Figure S5). The results showed that pollination strategy significantly influences floral shape variation (p=0.0064; Table 2). The estimated variance of specialists was 0.0093 and generalists had a variance 0.0069 greater than that of specialists (Table 2). The strength of the phylogenetic signal of the residuals ($\lambda = -0.0266$) suggests that closely related species have more different intraspecific variances than would be expected under a neutral (i.e., Brownian) model of evolution.
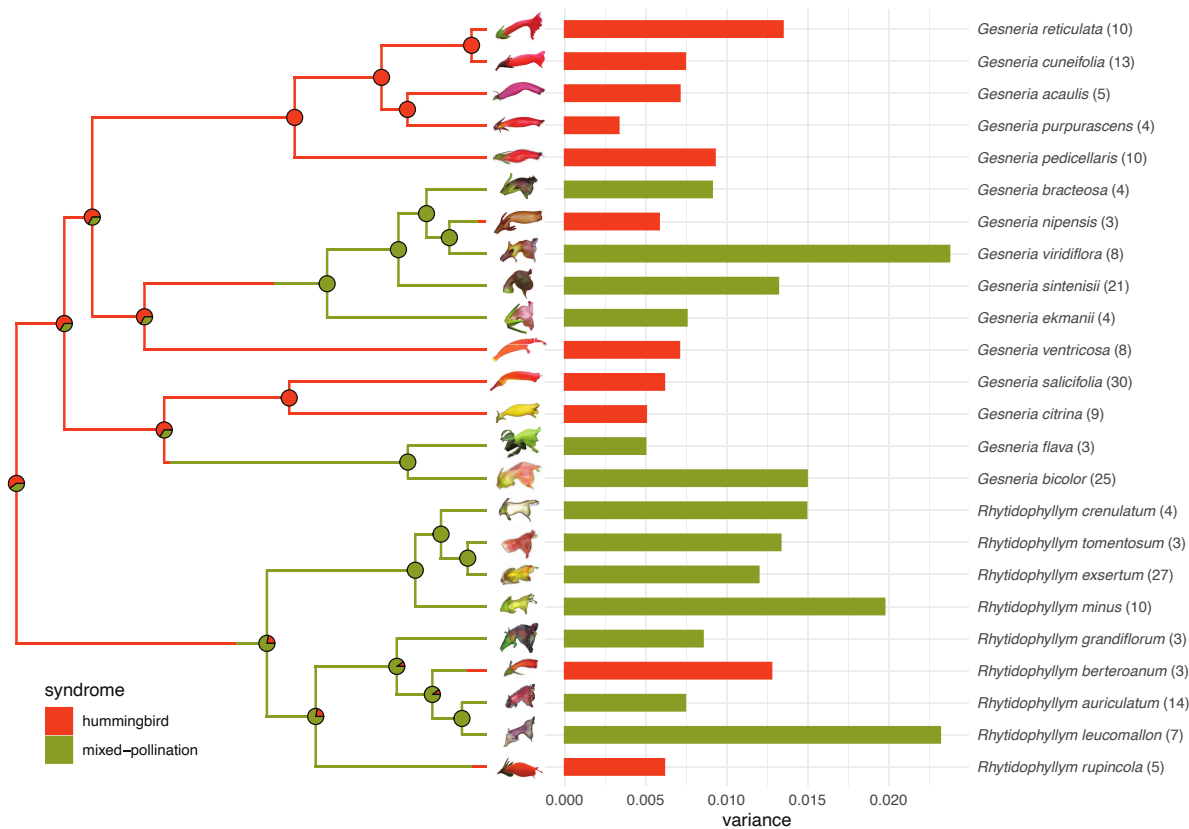
Figure 5. Phylogenetic tree and the total intraspecific corolla shape variance. The phylogenetic tree is a species tree (*BEAST) obtained from 5 nuclear genes. The pie charts at the nodes indicate the ancestral state probabilities of pollination strategies as estimated by stochastic mapping and the colour on the branch represents one stochastic simulation outcome. Sample sizes for each species are indicated in parentheses. Photo credit goes to John L. Clark, Abel Almarales-Castro, Silvana Martén-Rodrìguez, François Lambert, and Simon Joly.

Tableau 2. Phylogenetic Generalised Least Squares (PGLS) model results (n=24 species) for the effect of pollination syndrome on the whole corolla shape variation.

Coefficients	Value	Std. Error	T-value	P-value
Intercept	0.0093	0.0017	5.6091	0.0000
Generalist syndrome	0.0069	0.0023	3.0123	0.0064

3.5. Multivariate models of continuous traits evolution

Ornstein-Uhlenbeck models with one optimum (OU1) or two optima (OUM) of trait variance were fitted on the ln-variance of the first three principal components of the morphospace, the first three PCs combined, and on the Procrustes variance estimated from the whole dataset. The OUM

model was supported in the analysis of PC1 for the totality of the simulated maps of ancestral syndromes (AIC weights of the OUM model > 0.50; Figure 6 (a)). On the contrary, the model OU1 was the model with the best fit for the totality of the simulated maps when considering independently PC2 and PC3, as well as the three PCs analysed simultaneously in the multivariate approach (AIC weights of the OUM model < 0.50; Figure 6 (a)).

The OUM model is selected for PC1 (mean=0.577, sd=0.0281) and even more strongly for the variances calculated from aligned Procrustes shapes (mean=0.9241, sd=0.01923699) (see Figure 6 (a)). On the other hand, the OU1 model is increasingly selected for PC2 (mean=0.405, sd=0.0146), PC3 (mean=0.222, sd=0.0147), and the joint PC1+2+3 (mean=0.105, sd=0.0367). Even though the first principal component represents 64.5% of the total variation, the modelisation of the trait variance along the first principal component alone reveals the opposite model selection compared with the first three components taken into account simultaneously (Figure 6 (a)). The OU1 model best fitted the first three principal components taken simultaneously PC1+2+3, even more so than when the PC2 and PC3 were analysed independently.

Considering the OUM model, variance estimates (θ) revealed concordant values of variance for specialists (θ_s) and generalists (θ_g) across analyses as values of variances along the PC axes whether analysed independently(PC1, PC2, PC3) or jointly (PC1+2+3) are clustered together (Figure 6 (b)). The θ_s are lower than θ_g for the PC1, and PC3 (with the exception of 4 SIMMAPs for PC3) and θ_s are higher than θ_g along the PC2 (Figure 6 (b)). The multivariate approach that considers the variance calculated from the Procrustes aligned floral shapes however places the totality of the estimations using the 100 SIMMAPs above the $\theta_s = \theta_g$ limit (Figure 6 (b)). When using the overall shape variance as in the PGLS approach, the θ_s is also estimated lower than θ_g (Figure 6 (c)).
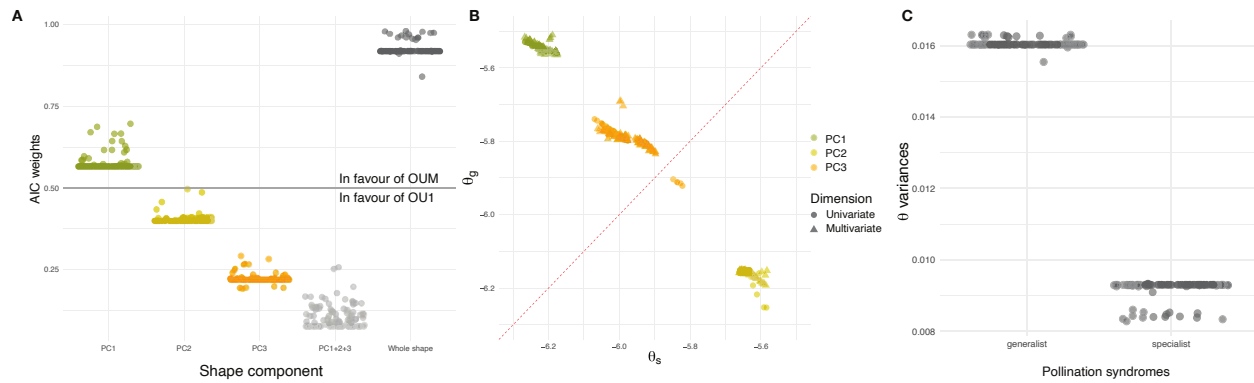
Figure 6. Results of the OU model selection and parameter estimation with mvMORPH. (a) AIC weights of the multivariate Ornstein-Uhlenbeck model of evolution using the first three components of the floral morphospace independently and jointly, using their calculated intraspecific variation on the total Procrustes aligned shapes. (b) Optimal values of variances (θ) estimated for generalists and specialists using their calculated intraspecific variation on the total Procrustes aligned shapes in the multivariate approach mvMORPH. (c) Optimal values of variances (θ) estimated for generalists and specialists using their calculated intraspecific variation on the total Procrustes aligned shapes in the multivariate approach mvMORPH. Each point represents one character simulation (SIMMAP).

3.6. Bayesian analysis of intra- and interspecific morphological evolution

We also used JIVE to compare OU1 and OUM models of evolution by modelling both intra- and inter-specific trait evolution. Bayes factors were calculated for each of the first three axes of the floral morphospace and for 100 simulated evolutionary scenarios of pollination strategies to account for the uncertainty in the ancestral states along the branches of the phylogeny. This resulted in 100 different BF values for each axis of the morphospace.

For each principal component of the morphospace, we found great variation in BF values, ranging from highly negative (suggesting a rejection of the model that specialists and generalists have different variances) to highly positive (selection of the most complex model) (Figure 7). Complete BF details for each SIMMAP are available in the supplementary information (Table S5). No distinct trend of evidence for one or the other model was found overall; each PC had character simulations that supported the simpler model, the more complex one, or non of them and PC1 and PC3 had sensibly the same amount of SIMMAPs in all categories (Table 3). In contrast, PC2 tended to support the simpler model (mOUMvOU) overall with a single optimal variance value in terms of corolla shape variance.

For the first axis, even though it represents a smaller proportion of the SIMMAPs, the OU1 model is supported by ancestral character maps that display a higher probability of the generalist syndrome at the root of the trees (upper left panel in Figure 8). On the contrary, the OUM model is supported by ancestral character maps that have a higher probability of a specialist at the base of the tree (bottom left panel in Figure 8). A more recent apparition of the generalist syndrome

suggests a multivariate model (OUM), whereas longer time spent as generalists suggests the simpler single optimum model (OU1). A clear pattern for PC2 and PC3 (two last columns in Figure 8) is however more difficult to distinguish.

Because the use and accuracy of model selection in Bayesian phylogenetic modeling have been debated (Lartillot, 2023), especially when none of the competing hypotheses may be true, it may be a good approach to use other evidence to test biological hypotheses. Here, we estimated the posterior probability that generalists have a higher intraspecific variance than specialists from the MCMC analysis in which the optimal variance for generalists and specialists was estimated (mOUMvOUM).

The probability that generalists have a higher intra-specific corolla shape variance than specialists $p(\theta_g > \theta_s)$ was 0.95 for PC1, 0.32 for PC2, and 0.92 for PC3 (Figure 9). The intra-specific variance for generalists was estimated to be 2.01 times that of specialists for PC1, 0.82 for PC2, and 1.49 for PC3. The summary of the estimated model parameters is provided in Table S6 and the effective sample sizes (ESS) of the parameters for the combined MCMC analyses are provided in Table S7.

Tableau 3. Number of SIMMAPs out of 100 following each BF category for each of the 3 first principal components of the morphospace : evidence in favour of OU1 (BF<-6), no evidence for either model (-6<BF<6) and evidence in favour of OUM (6<BF).

Principal axis of the morphospace	BF<-6	-6<BF<6	6<BF
PC1	2	84	14
PC2	35	58	4
PC3	12	76	10
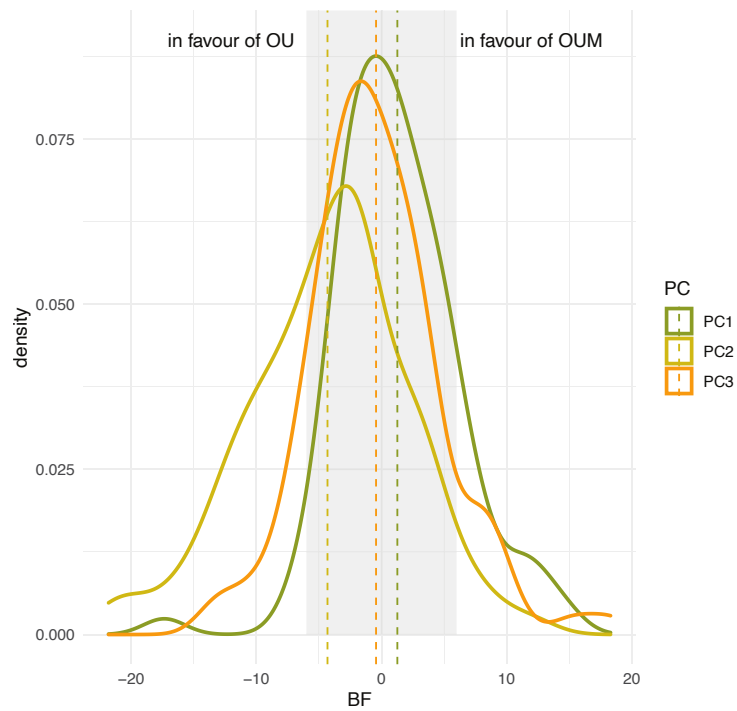
Figure 7. Density of Bayes Factor (BF) values for each principal component (PC) of the morphospace. The arithmetic mean of the BF for each PC is represented by a dashed vertical line. The BF confidence interval [-6,6] is indicated by a grey-shaded area. BF = 2 × (marginal likelihood mOUMvOUM - marginal likelihood mOUMvOU).
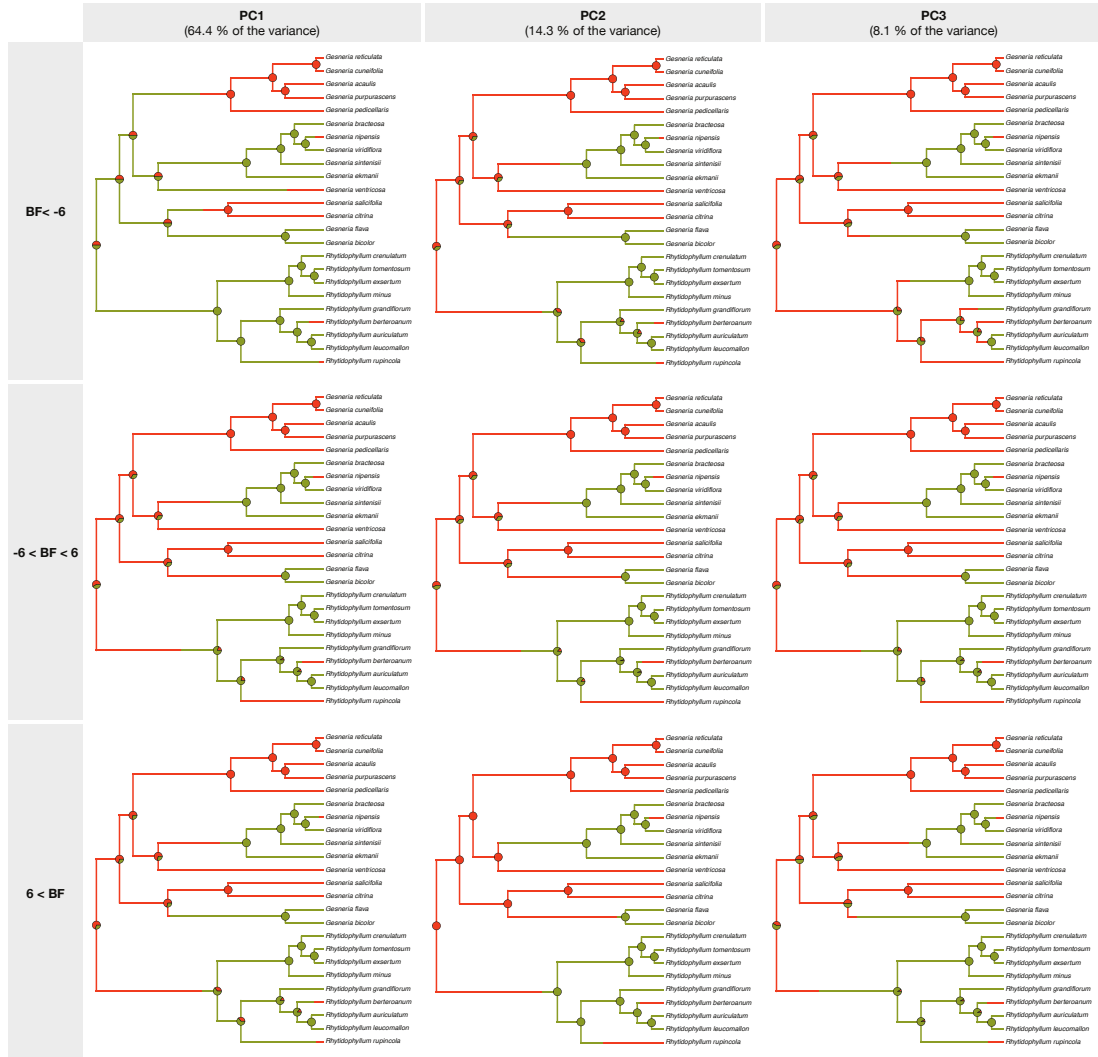
Figure 8. Summary of the simulated maps of ancestral syndromes (SIMMAPs) for specialists for hummingbird pollination (orange) and generalists (green) using the first principal components of the morphospace (PCA) and for the three Bayes factors categories : BF< -6 (in favour of OU), -6<BF<6 (no model favoured), and 6<BF (in favour of OUM).
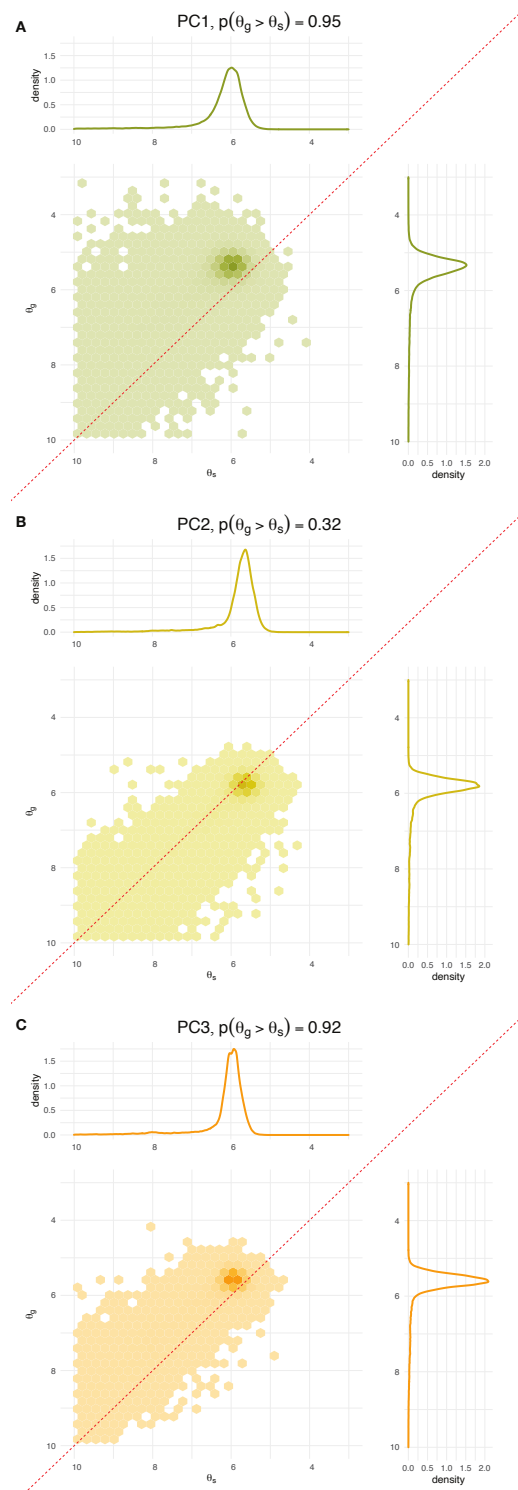
Figure 9. Distribution of the joint estimation of the optimal floral variance of specialists (θ_s) and generalists (θ_g). The densities of θ_s and θ_g are represented for the first three principal components PC1 (a), PC2 (b), and PC3 (c) and along both axes (top and left). The red dashed line indicates the limit of $\theta_s = \theta_g$.

4. Discussion

According to the niche variation hypothesis (NVH), a greater ecological niche is expected to lead to greater intraspecific morphological variation (Van Valen, 1965). We, therefore, hypothesised that pollination generalists should vary more in floral shape than specialists at the intraspecific level (Figure 3, a vs. b). Using floral morphologies of Antillean Gesneriaceae, we tested if generalists have greater intraspecific corolla shape variance than specialists.

We used three distinct approaches to test this hypothesis, each of which has different advantages and disadvantages. The simpler approach aimed at comparing the intraspecific variation in corolla shape among species while correcting for the phylogenetic correlations in the data using a phylogenetic generalised least square approach (PGLS). The PGLS approach considers the whole corolla shape but does not consider the error in the estimation of the variance and does not use explicit models of pollination strategy evolution. The other two approaches tested the hypothesis by comparing two Ornstein-Uhlenbeck stochastic models of evolution with explicit models of pollination strategy evolution, one with a single joint optimal value of trait variation for both pollination strategies (OU1) and one another with two distinct optima of trait variation for each syndrome respectively (OUM). The second approach (mvMORPH) takes into account the multi-dimensionality of the data but did not take into account the error involved in the estimation of the variance of the species. Lastly, the hierarchical Bayesian approach (JIVE) allowed accounting for the error in estimating species variances when estimating the optimal variances for the specialist and the generalists, but it cannot consider the whole corolla shape, which had to be simplified to principal components of variation.

Because inconclusive results were obtained with some of the different approaches, a strong conclusion could not be reached. Nevertheless, some trends are distinguishable. The PGLS and mvMORPH approaches support higher intraspecific corolla shape variation for generalists than specialists when the whole floral shape is considered. This was also the case for the first principal component of the morphospace when analysed with mvMORPH, which describes floral tubularity (64% of the total corolla shape variation). The JIVE approach also points toward increased variation for generalists for PC1 when the parameters of the OUM model are considered, but this more complex model is not supported statistically. In contrast to when the global shape or PC1 are considered, there is no support for greater variation in the corolla shape for generalists along the second principal component. Although the variation along PC3 points towards greater variation in generalists (multivariate mvMORPH), the result is not significant when analysed alone. This highlights that different axes of variation do not necessarily follow the global pattern of floral variance evolution.

A few things might explain the differences in results between the methods. First, there is more support for a greater variance for generalists when the whole corolla shape is considered compared to when the shape is reduced to principal components, even when the first three PCs are analysed

simultaneously. In this latter case, the lack of statistical support for the OUM model could be due to a lack of power because of the additional parameters that must be included in the multivariate model. Because JIVE does not allow us to analyse the whole corolla shape, the lack of statistical support with this approach could be partly due to this decomposition of shape. This said, we also observed that for the analysis of individual principal components, there was less support for the OUM model for JIVE than for mvMORPH. This is likely because the JIVE approach takes into account the uncertainty in the estimate of the intraspecific variance, which other methods do not. Because our sample sizes are relatively small, the absence of statistical results with JIVE might also point to low power. Ideally, future development of the JIVE model should include the possibility of assessing the variance from multidimensional data sets. This is even more relevant because it is known that analysis of only the first few principal axes of a multivariate dataset as independent traits with evolutionary models can lead to erroneous conclusions (Revell, 2009; Uyeda et al., 2015), which prompted the development of frameworks of high-dimensional phylogenetic comparative methods (Clavel et al., 2018).

It is interesting to note that character history simulations strongly impacted the JIVE results because some SIMMAPs supported one model and others rejected it for the same principal component of shape variation. For instance, the longer the generalist syndrome took to arise within Antillean Gesneriaceae, the higher their intraspecific morphological variation seems to be in comparison with specialists. Therefore, the lack of certainty in the ancestral evolution of the pollination strategies seems to affect the JIVE results and highlights the importance of considering this source of uncertainty in such evolutionary analysis because the reliance on a single SIMMAP could have completely biased our conclusions. Nevertheless, the impact of the SIMMAPS is much more minor for the mvMORPH analysis, although it affects the estimates of the parameter values and the support for the alternative models.

Although not conclusive, our results point towards the idea that generalist species have greater intraspecific morphological variation. The niche variation hypothesis was tested here using a group of closely related species that consist of several independent origins of a generalist strategy and we measured morphological variation on a key ecological trait : the corolla (Martén-Rodríguez et al., 2009). These results have interesting implications for this group. Indeed, because we know that variation among species in corolla shape is similar for specialists and generalists (see Joly et al., 2018), the greater intraspecific variation of generalists suggests a more complete filling of the corolla morphospace for generalists compared to specialists and/or a greater overlap in the corolla shape variation amongst generalist species. This illustrates how ecological strategies of species could affect macroevolutionary patterns of morphological variation.

Van Valen (1965) underlined that greater intraspecific morphological variation for generalists can occur either if generalists are constituted of specialist individuals (Figure 3c) or if the generalists are constituted of intrinsically generalist individuals (Figure 3d). Although we did not directly measure the niche of individuals in this study, previous pollination studies suggest that

individuals of generalist species are all pollinated by a variety of pollinators (e.g. Martén-Rodríguez et al., 2009, 2015). This suggests that in Antillean Gesneriaceae, the greater intraspecific corolla shape variation of generalists is due to more relaxed selective constraints than specialists (Rosas-Guerrero et al., 2011). One scenario that may lead to this pattern is if, for instance, different populations of generalist plants are pollinated by the same functional group of pollinators (e.g., hummingbirds, bats and bees), but in different proportions due to the environment (e.g., altitude). This could exert different selection pressures on the corolla in different populations, something not possible for pollination specialists pollinated by a single species.

The evolution of the generalist pollination strategy in the studied group occurs in an insular context. Islands are generally pollinator depauperate environments compared to the mainland (MacArthur and Wilson, 1967) where pollination specialists are more vulnerable to pollination inefficiency or failure (Armbruster, 2017). Moreover, temporal variation in pollinator communities, which may result from frequent storms and hurricanes in the Caribbean islands, may further favour the evolution of pollination generalists. Indeed, temporal variation offers fewer opportunities for specialist refuges, increasing their risk of extinction (Johnson, 2010). In Antillean Gesneriaceae, floral visitation rates are lower and pollen limitation of fruit set is greater in species with specialised compared to generalised pollination systems (Martén-Rodríguez and Fenster, 2010; Martén-Rodríguez et al., 2015). The generalist strategy, which evolved independently several times in Antillean Gesneriaceae (Martén-Rodríguez et al., 2010; Joly et al., 2018), can thus be considered as an alternative mechanism to assure their reproduction. At the same time, the paucity of pollinators can also reinforce specialisation as a result of a lack of alternative pollinators (Armbruster, 2017). In this context, the evolution of autonomous self-pollination could have allowed the maintenance of hummingbird specialists in Caribbean Gesneriaceae (Martén-Rodríguez et al., 2010). In addition, higher levels of self-pollination could reduce genetic variation, which could reduce floral trait variation and partly explain the results we observed.

The hummingbird specialist syndrome is not the only specialist strategy within the genera *Gesneria* and *Rhytidophyllum*. There are known moth and bat specialists in the group (Martén-Rodríguez et al., 2010), although there are very few species that fall in these categories (only *G. humilis* L. is specialised for moth pollination, and *G. quisqueyana* Alain, *G. pedunculosa* (DC.) Fritsch, *G. fruticosa* (L.) Kuntze, *G. shaferi* Urb. subsp. *depressa* (Griseb.) L.E. Skog and *G. clarensis* Britton & P. Wilson are bat specialists). Most of these species are narrowly distributed and occur in remote populations, hence, they could not be included in this study. Nevertheless, it would be interesting to include them in a future study to compare their corolla shape variation with those of hummingbird specialists and generalists pollinated by bats and hummingbirds.

In conclusion, our study sheds light on the evolutionary patterns of intraspecific variation in corolla shape in Antillean Gesneriaceae, revealing the crucial role of pollination strategies in shaping their floral morphology, both at the micro- and macroevolutionary levels. Although our findings are not conclusive, they suggest that pollination generalists tend to exhibit greater

intraspecific variation in corolla shape than pollination specialists, particularly in terms of general shape and tubularity, while they show similar variation in terms of curvature. These results support the niche variation hypothesis but also show that not all aspects of the corolla show the same pattern of variation. This increased variation in generalists is likely to be due to relaxed selective constraints on generalists that can be pollinated by various functional types of pollinators and has implications on the macroevolutionary pattern of variation in the group. As the Caribbean environment is rapidly changing due to anthropogenic and climatic impacts, understanding the impact of pollination strategies on floral diversity and evolution in this region is a timely and critical topic.

5. Conflict of interest statement

The authors have no conflict of interest to declare.

6. Acknowledgments

7. Open data and scripts

Scripts and data are available on Dryad (https ://doi.org/10.5061/dryad.hqbzkh1nh).

Bibliographie

Acevedo-Rodríguez, P. and Strong, M. T. (2012). Catalogue of seed plants of the west indies. *Smithsonian Contributions to Botany*, (98) :1–1192.

Adams, D. C. and Otárola-Castillo, E. (2013). geomorph : an r package for the collection and analysis of geometric morphometric shape data. *Methods in Ecology and Evolution*, 4(4) :393–399.

Aigner, P. A. (2001). Optimality modeling and fitness trade-offs : when should plants become pollinator specialists ? *Oikos*, 95(1) :177–184.

Akaike, H. (1987). Factor analysis and aic. In *Selected Papers of Hirotugu Akaike*, pages 371–386. Springer.

Armbruster, W. S. (2017). The specialization continuum in pollination systems : diversity of concepts and implications for ecology, evolution and conservation. *Functional Ecology*, 31(1) :88–100.

Bolnick, D. I., Amarasekare, P., Araújo, M. S., Bürger, R., Levine, J. M., Novak, M., Rudolf, V. H., Schreiber, S. J., Urban, M. C., and Vasseur, D. A. (2011). Why intraspecific trait variation matters in community ecology. *Trends in ecology & evolution*, 26(4) :183–192.

Bookstein, F. L. (1997). Shape and the information in medical images : A decade of the morphometric synthesis. *Computer Vision and Image Understanding*, 66(2) :97–118.

Clavel, J., Aristide, L., and Morlon, H. (2018). A penalized likelihood framework for high-dimensional phylogenetic comparative methods and an application to new-world monkeys brain evolution. *Systematic biology*, 68(1) :93–116.

Clavel, J., Escarguel, G., and Merceron, G. (2015). mvmorph : an r package for fitting multivariate evolutionary models to morphometric data. *Methods in Ecology and Evolution*, 6(11) :1311–1319.

Devictor, V., Clavel, J., Julliard, R., Lavergne, S., Mouillot, D., Thuiller, W., Venail, P., Villeger, S., and Mouquet, N. (2010). Defining and measuring ecological specialization. *Journal of Applied Ecology*, 47(1) :15–25.

Faure, J. and Joly, S. (2020). Pollinator performance of the pollination generalist rhytidophyllum bicolor (gesneriaceae) in haiti 15 months after the matthew hurricane. *Selbyana*, 33(3).

Fenster, C. B. (1991). Selection on floral morphology by hummingbirds. *Biotropica*, 23(1) :98–101.

Fernández-i Marín, X. (2016). ggmcmc : Analysis of MCMC samples and Bayesian inference. *Journal of Statistical Software*, 70(9) :1–20.

Futuyma, D. J. and Peterson, S. C. (1985). Genetic variation in the use of resources by insects. *Annual review of entomology*, 30(1) :217–238.

Gaboriau, T., Mendes, F. K., Joly, S., Silvestro, D., and Salamin, N. (2020). A multi-platform package for the analysis of intra-and interspecific trait evolution. *Methods in Ecology and*

Evolution, 11(11) :1439–1447.

Gower, J. C. (1975). Generalized procrustes analysis. *Psychometrika*, 40(1) :33–51.

Grafen, A. (1989). The phylogenetic regression. *Philosophical Transactions of the Royal Society of London. B, Biological Sciences*, 326(1233) :119–157.

Grant, P. and Price, T. (1981). Population variation in continuously varying traits as an ecological genetics problem. *American Zoologist*, 21(4) :795–811.

Gunz, P. and Mitteroecker, P. (2013). Semilandmarks : a method for quantifying curves and surfaces. *Hystrix, the Italian Journal of Mammalogy*, 24(1) :103–109.

Heled, J. and Drummond, A. J. (2010). Bayesian Inference of Species Trees from Multilocus Data. *Molecular Biology and Evolution*, 27(3) :570–580.

Huelsenbeck, J. P., Nielsen, R., and Bollback, J. P. (2003). Stochastic mapping of morphological characters. *Systematic Biology*, 52(2) :131–158.

Jeffreys, H. (1935). Some tests of significance, treated by the theory of probability. In *Mathematical proceedings of the Cambridge philosophical society*, volume 31, pages 203–222. Cambridge University Press.

Johnson, S. D. (2010). The pollination niche and its role in the diversification and maintenance of the southern african flora. *Philosophical Transactions of the Royal Society B : Biological Sciences*, 365(1539) :499–516.

Joly, S., Lambert, F., Alexandre, H., Clavel, J., Léveillé-Bourret, E., and Clark, J. L. (2018). Greater pollination generalization is not associated with reduced constraints on corolla shape in Antillean plants. *Evolution*.

Joly, S., Lambert, F., Cinea, W., and Clark, J. L. (2023). Three new gesneria species (gesneriaceae) support parc national pic macaya (haiti) as an important biodiversity hotspot. *Systematic Botany*, 48(1) :34–43.

Kass, R. E. and Raftery, A. E. (1995). Bayes factors. *Journal of the American Statistical Association*, 90(430) :773–795.

Kassambara, A. and Mundt, F. (2020). *factoextra : Extract and Visualize the Results of Multivariate Data Analyses*. R package version 1.0.7.

Katoh, K. and Standley, D. M. (2013). Mafft multiple sequence alignment software version 7 : improvements in performance and usability. *Molecular biology and evolution*, 30(4) :772–780.

Kendall, D. G. (1984). Shape manifolds, procrustean metrics, and complex projective spaces. *Bulletin of the London Mathematical Society*, 16(2) :81–121.

Kostikova, A., Silvestro, D., Pearman, P. B., and Salamin, N. (2016). Bridging inter-and intraspecific trait evolution with a hierarchical bayesian approach. *Systematic biology*, 65(3) :417–431.

Kuppler, J., Albert, C. H., Ames, G. M., Armbruster, W. S., Boenisch, G., Boucher, F. C., Campbell, D. R., Carneiro, L. T., Chacón-Madrigal, E., Enquist, B. J., et al. (2020). Global gradients in intraspecific variation in vegetative and floral traits are partially associated with climate and species richness. *Global Ecology and Biogeography*, 29(6) :992–1007.

Lartillot, N. (2023). Identifying the best approximating model in bayesian phylogenetics : Bayes factors, cross-validation or waic ? *Systematic Biology*, 72(3) :616–638.

Lemmon, A. R. and Moriarty, E. C. (2004). The importance of proper model assumption in bayesian phylogenetics. *Systematic Biology*, 53(2) :265–277.

Lewis, P. O. (2001). A likelihood approach to estimating phylogeny from discrete morphological character data. *Systematic biology*, 50(6) :913–925.

MacArthur, R. H. and Wilson, E. O. (1967). *Island biogeography*. Princeton.

Martén-Rodríguez, S. and Fenster, C. B. (2010). Pollen limitation and reproductive assurance in antillean gesnerieae : a specialists vs. generalist comparison. *Ecology*, 91(1) :155–165.

Martén-Rodríguez, S., Fenster, C. B., Agnarsson, I., Skog, L. E., and Zimmer, E. A. (2010). Evolutionary breakdown of pollination specialization in a caribbean plant radiation. *New Phytologist*, 188(2) :403–417.

Martén-Rodríguez, S., Almarales-Castro, A., and Fenster, C. B. (2009). Evaluation of pollination syndromes in Antillean Gesneriaceae : evidence for bat, hummingbird and generalized flowers. *Journal of Ecology*, 97(2) :348–359.

Martén-Rodríguez, S. and Fenster, C. B. (2008). Pollination Ecology and Breeding Systems of Five Gesneria Species from Puerto Rico. *Annals of Botany*, 102(1) :23–30.

Martén-Rodríguez, S., Quesada, M., Castro, A.-A., Lopezaraiza-Mikel, M., and Fenster, C. B. (2015). A comparison of reproductive strategies between island and mainland Caribbean Gesneriaceae. *Journal of Ecology*, 103(5) :1190–1204.

Paradis, E. and Schliep, K. (2019). ape 5.0 : an environment for modern phylogenetics and evolutionary analyses in R. *Bioinformatics*, 35 :526–528.

Patterson, B. D. (1983). Grasshopper mandibles and the niche variation hypothesis. *Evolution*, 37(2) :375–388.

Perez, S. I., Bernal, V., and Gonzalez, P. N. (2006). Differences between sliding semi-landmark methods in geometric morphometrics, with an application to human craniofacial and dental variation. *Journal of anatomy*, 208(6) :769–784.

Pinheiro, J., Bates, D., DebRoy, S., Sarkar, D., and R Core Team (2021). *nlme : Linear and Nonlinear Mixed Effects Models*. R package version 3.1-153.

Plummer, M., Best, N., Cowles, K., and Vines, K. (2006). Coda : Convergence diagnosis and output analysis for mcmc. *R News*, 6(1) :7–11.

Rambaut, A., Drummond, A. J., Xie, D., Baele, G., and M.A.Suchard (2018). Tracer v1.7. `http://beast.community/tracer`.

Revell, L. J. (2009). Size-correction and principal components for interspecific comparative studies. *Evolution*, 63(12) :3258–3268.

Revell, L. J. (2010). Phylogenetic signal and linear regression on species data. *Methods in Ecology and Evolution*, 1(4) :319–329.

Revell, L. J. (2012). phytools : an r package for phylogenetic comparative biology (and other things). *Methods in Ecology and Evolution*, 3(2) :217–223.

Rohlf, F. J. (2010). tpsrelw, relative warps analysis. *Department of Ecology and Evolution, State University of New York at Stony Brook, Stony Brook, NY.*

Rohlf, F. J. and Slice, D. (1990). Extensions of the procrustes method for the optimal superimposition of landmarks. *Systematic Biology*, 39(1) :40–59.

Rosas-Guerrero, V., Quesada, M., Armbruster, W. S., Pérez-Barrales, R., and Smith, S. D. (2011). Influence of pollination specialization and breeding system on floral integration and phenotypic variation in ipomoea. *Evolution*, 65(2) :350–364.

Sahli, H. F. and Conner, J. K. (2011). Testing for conflicting and nonadditive selection : floral adaptation to multiple pollinators through male and female fitness. *Evolution : International Journal of Organic Evolution*, 65(5) :1457–1473.

Schneider, C. A., Rasband, W. S., and Eliceiri, K. W. (2012). Nih image to imagej : 25 years of image analysis. *Nature methods*, 9(7) :671–675.

Siefert, A., Violle, C., Chalmandrier, L., Albert, C. H., Taudiere, A., Fajardo, A., Aarssen, L. W., Baraloto, C., Carlucci, M. B., Cianciaruso, M. V., et al. (2015). A global meta-analysis of the relative extent of intraspecific trait variation in plant communities. *Ecology letters*, 18(12) :1406–1419.

Uyeda, J. C., Caetano, D. S., and Pennell, M. W. (2015). Comparative analysis of principal components can be misleading. *Systematic Biology*, 64(4) :677–689.

Van Valen, L. (1965). Morphological variation and width of ecological niche. *The American Naturalist*, 99(908) :377–390.

Violle, C., Enquist, B. J., McGill, B. J., Jiang, L., Albert, C. H., Hulshof, C., Jung, V., and Messier, J. (2012). The return of the variance : intraspecific variability in community ecology. *Trends in ecology & evolution*, 27(4) :244–252.

Westerband, A., Funk, J., and Barton, K. (2021). Intraspecific trait variation in plants : a renewed focus on its role in ecological processes. *Annals of botany*, 127(4) :397–410.

Xie, W., Lewis, P. O., Fan, Y., Kuo, L., and Chen, M.-H. (2011). Improving marginal likelihood estimation for bayesian phylogenetic model selection. *Systematic biology*, 60(2) :150–160.

Yang, Z. (1994a). Estimating the pattern of nucleotide substitution. *Journal of molecular evolution*, 39(1) :105–111.

Yang, Z. (1994b). Maximum likelihood phylogenetic estimation from dna sequences with variable rates over sites : approximate methods. *Journal of Molecular evolution*, 39(3) :306–314.

Deuxième chapitre.

Studying flowers in 3D using photogrammetry

par

Marion Leménager[1], Jérome Burkiewicz[2], Daniel J. Schoen[3] et Simon Joly[4]

(¹) Institut de recherche en biologie végétale, Département de sciences biologiques, Université de Montréal, 4101 Rue Sherbrooke E, Montréal, QC H1X 2B2, Canada

(²) Institut de recherche en biologie végétale, Département de sciences biologiques, Université de Montréal, 4101 Rue Sherbrooke E, Montréal, QC H1X 2B2, Canada

(³) Biology department, McGill University, 205 Av. du Docteur-Penfield, Montréal, QC H3A 1B1, Canada

(⁴) Institut de recherche en biologie végétale, Département de sciences biologiques, Université de Montréal, 4101 Rue Sherbrooke E, Montréal, QC H1X 2B2, Canada
Jardin Botanique de Montréal, 4101 Rue Sherbrooke E, Montréal, QC H1X 2B2, Canada

Résumé.

— Les fleurs sont des structures tridimensionnelles complexes et intégrées, principalement étudiées en 2D en raison de la difficulté à caractériser quantitativement leur morphologie en 3D. Compte tenu du développement récent des méthodes d'analyse des données en haute dimension, la reconstruction des modèles de fleurs en trois dimensions représente le facteur limitant l'étude des fleurs en 3D.

— Nous avons développé un protocole de photogrammétrie florale pour reconstruire des modèles 3D de fleurs à partir d'images prises avec un appareil photo numérique à objectif unique, un plateau tournant et un caisson lumineux portable.

— Nous démontrons que la photogrammétrie permet une reconstruction rapide et précise de modèles 3D de fleurs à partir d'images 2D. Elle peut reconstruire toutes les parties visibles des fleurs et a l'avantage de conserver les informations de couleur. Nous avons illustré son utilisation en étudiant la forme et la couleur de 18 espèces de Gesneriaceae.

— La photogrammétrie est une alternative abordable à la tomographie micro-informatique (microCT) qui nécessite un investissement et un équipement minimaux, ce qui permet de l'utiliser directement sur le terrain. Elle a le potentiel de stimuler la recherche sur l'évolution et l'écologie des fleurs en fournissant un moyen simple d'accéder à des données morphologiques tridimensionnelles provenant d'une variété de types de fleurs.

Mots clés : Morphologie comparative, couleur de la fleur, forme de la fleur, morphométrie géométrique, photogrammétrie à très courte portée, modèles de fleurs en trois dimensions.

Abstract.

— Flowers are intricate and integrated three-dimensional structures predominantly studied in 2D due to the difficulty in quantitatively characterising their morphology in 3D. Given the recent development of analytical methods for high-dimensional data, the reconstruction of flower models in three dimensions represents the limiting factor to studying flowers in 3D.

— We developed a floral photogrammetry protocol to reconstruct 3D models of flowers based on images taken with a digital single-lens reflex camera, a turntable and a portable lightbox.

— We demonstrate that photogrammetry allows a rapid and accurate reconstruction of 3D models of flowers from 2D images. It can reconstruct all visible parts of flowers and has the advantage of keeping colour information. We illustrated its use by studying the shape and colour of 18 Gesneriaceae species.

— Photogrammetry is an affordable alternative to micro-computed tomography (microCT) that requires minimal investment and equipment, allowing it to be used directly in the field. It has the potential to stimulate research on the evolution and ecology of flowers by providing a simple way to access three-dimensional morphological data from a variety of flower types.

Keywords: Comparative morphology, flower colour, floral shape, geometric morphometrics, ultra close-range photogrammetry, three-dimensional flower models

1. Introduction

Flower shape, size and colour influence the attraction of pollinators, the way pollinators access floral rewards, and contingently the exchange of pollen between anthers and stigmas (Faegri and van der Pijl, 1979; Fenster et al., 2004; Willmer, 2011). Flower shape is also important in wind-pollinated species (anemophily) as it influences interactions with air flows and so determines efficient pollen release, dispersal and capture (Timerman and Barrett, 2019). Because flowers are three-dimensional structures that interact with a three-dimensional biotic and abiotic environment for conspecific exchange of pollen, characterising flower shape and colour in 3D is important to promote a comprehensive understanding of flower development and the role of flower shape in the ecology and evolution of species.

Only recently has it become feasible to study the variation of flower shape in three dimensions (3D) due to the development of methods to build 3D flower models. The first reconstruction of flowers in 3D used micro-computed tomography (microCT, or HRCT for high-resolution CT) to acquire and visually render digital three-dimensional shape data of both surfaces and internal structures (Stuppy et al., 2003). MicroCT helps to visualise minute plant structures and to study their external 3D morphology and internal structures qualitatively and quantitatively. The characterisation and comparison of these 3D flower models using geometric morphometrics (Rohlf and Marcus, 1993) has opened a vast array of possibilities for the study of flowers in 3D, which was deemed to represent a "revolution" for the study of flowers (van der Niet et al., 2010). Though other 3D modelling techniques are available such as laser-scanning and structured light that record surfaces, microCT scanning remains the most common 3D digitization technique applied to plant specimens (Mathys et al., 2013; Davies et al., 2017).

Despite the fact that several studies recently used 3D flowers models (Gamisch et al., 2013; Wang et al., 2015; Dellinger et al., 2019; Hsu et al., 2020; Reich et al., 2020; Artuso et al., 2021, 2022), the widespread analysis of 3D flowers has not occurred. Geometric morphometrics studies of flowers in 3D are still limited compared to the mass of literature in the fields of anthropology, zoology and paleontology. This could be due in part to the difficulties of using microCT on the soft tissues of flowers, even though solutions for optimising HRCT scanning of flowers have been proposed (e.g., Staedler et al., 2013; Dellinger et al., 2019). In addition, and perhaps more importantly, the high cost of microCT techniques (Mathys et al., 2013) contributes to reducing their accessibility. Lastly, the fact that flower colour is lost when reconstructing 3D models using X-ray scanning technologies (Mathys et al., 2013) limits the use of this technique for studies interested in colour or colour patterns.

Recently, research based on 3D imagery has evolved rapidly and has received considerable attention (e.g., Katz and Friess, 2014; Cunliffe et al., 2016; Evin et al., 2016; Ströbel et al., 2018; Christiansen et al., 2019; Giacomini et al., 2019; Florey and Moore, 2019; Iglhaut et al., 2019; Medina et al., 2020). A 3D technique of interest is photogrammetry (or structure from

motion), which uses a collection of digital images to reconstruct a 3D model (see Linder, 2009; Luhmann et al., 2013). Photogrammetry was originally used to reconstruct models of landscapes, buildings or large objects, but it can also be used for medium (close-range photogrammetry) or small objects (ultra-close-range photogrammetry). In short, photogrammetry begins by taking pictures of an object from all angles, ensuring that all aspects of the object are present in several overlapping photos. The sets of photos are then aligned using the relative position of homologous points in the overlapping pictures in a 3D space, and picture information is then used to reconstruct a 3D model with colour (see Floral photogrammetry protocol and Fig. **10** for more detailed information). Although used in many fields of biological sciences, photogrammetry has not yet been applied to the study of flowers.

The objective of this study is to demonstrate the potential of photogrammetry to reconstruct 3D models of flowers to facilitate studies of floral shape and colour. We describe an affordable and portable photogrammetric setup that could be used in the field, and outline a detailed protocol for reconstructing 3D photographic models of flowers of various shapes, colours and sizes. To illustrate the approach, we present an example of application in the study of the shape and colour of flowers from species of the Gesneriaceae.

2. Floral photogrammetry protocol

Here, we provide a summary of the photogrammetry protocol we developed. The full protocol is available from Github (`https://github.com/plantevolution/photogrammetry-protocol`) and details of the source and costs of materials, tools and software are provided as Supporting Information (Table **S1**). Specific terms in photography, 3D modelling and geometric morphometrics are defined in the glossary (Box **1**). Our objective is not to provide a unique and final protocol, but to provide guidelines for users to employ photogrammetry to 3D model flowers and guide them on how to adapt this approach for their own system.

2.1. Image acquisition

The first step of photogrammetry involves acquiring photos encapsulating flower details for later modelling in 3D. This step is perhaps the most important as high quality images are key to produce high quality 3D models. We capture images using a digital single-lens reflex (DSLR) camera and a fixed focal-length macro lens. We save images in RAW format using an aperture of F16 (highest field depth without deteriorating the image quality), lowest ISO (e.g. 100) to avoid image noise created by the sensor, and a shutter speed adjusted to allow the appropriate amount of light to reach the camera's sensor to result in a well-exposed image (see Supporting Information Table **S2** for a summary of the settings we used).

To facilitate the photo capture of the flower from all directions, we use a turntable and automated remote camera control (Fig. **10a,b**). To help later photo processing and mask the background in the pictures, we recommend using a uniform background. Good lighting conditions are also necessary for optimal picture quality. These conditions can be recreated in the field using a portable lightbox (see Supporting Information Table **S1**).

The flower to be photographed is fixed at the centre of the turntable using pins or clamps, or could be placed in a tube or a cut pipette tip depending on the structure and stiffness of the flower (see example Fig. **10c**). A scale should be placed so that it is visible in several photographs to allow scaling of the resulting model.

To capture the entire flower surface and details, we take a 360° series of photos of flowers placed in normal and inverted positions (e.g., ventrally and dorsally). Typically 20 photos per rotation were taken at 3 different camera heights and angles of approximately 0°, 30° and 60° for each side of a flower (see Fig.**10b**), for a total of 120 photos per flower. Depending on the flower complexity, the number of photos, camera angles and flower positions can be adjusted to capture all visible floral details. It is also possible to add close-ups photos to enhance the model and reveal concealed and minute parts (e.g., reproductive organs). If using a variable focal lens, it is preferable that the focal length is kept identical for all the pictures, and ideally at the minimum or maximum focal length possible to avoid optical deformations (Agisoft LLC, 2021).

2.2. Colour and exposure calibration

Photographs must be colour-calibrated to adjust the reflectance and colour of an object and allow accurate comparison between flowers (Troscianko and Stevens, 2015). To calibrate multiple photos with the same parameters, we use DNG (Digital Negative) colour profiles created from an additional RAW photo of a standardised colour chart, taken for each series of photos of a flower under the same light conditions and camera parameters. We convert the colour chart in a DNG profile (e.g. using Adobe Digital Negative converter) and standardise the series of photos corresponding to the colour chart (using e.g. Adobe Lightroom (Adobe Inc., San Jose, California, USA)), providing an accurate reproduction of the flower colour for subsequent analyses of pigmentation patterns. We also standardise the photo exposure using a 75% grey colour chip from the colour chart. Exposure calibration can also be performed at a later stage directly using the colour file (texture) of the 3D model. From the calibrated RAW photos, we export JPG images for the model reconstruction (Fig. **10c,d,e**).

2.3. 3D model reconstruction

The procedure we use to obtain a 3D model from photogrammetry includes photo alignment, which results in a sparse three-dimensional point cloud, surface generation through depth maps calculation, and texture generation using the projection of photos onto the surface of the model.

Our protocol uses the commercial software Agisoft Metashape Professional Edition version 1.7 (Agisoft LLC., St. Petersburg, Russia), but open-source photogrammetry software also exist (see Medina et al. (2020) for more details).

During photo alignment (also referred as camera alignment), source images are positioned by searching for common points in the photos (tie points) and by using the triangulation of the matching points. The alignment procedure can customarily be done in a single step, by attributing images from different flower positions to distinct camera groups, or by separating images from different flower positions into different chunks. Treating sets of images separately can be useful for merging models of different flower parts (e.g. for modelling a complete flower by merging the flower with and without its perianth). Chunks of images can also be treated separately during the alignment procedure when the overlap between pairs of images isn't optimal to facilitate the alignment calculation (Fig. **10f,g,h,i**, showing an example with two chunks of images). Prior to aligning images, masks can be captured manually or automatically to separate the flower from the background and restrict the searching of common points between images during the alignment procedure to the flower itself (Fig. **10g**). The picture alignment (Fig. **10h**) generates a three dimensional cloud of matching tie points for each set of images (Fig. **10i**). When different chunks of images are used separately, they need to be aligned together and then merged either automatically or by using manually-placed markers on distinctive features on the flowers on several images (e.g. tips of petals or sepals, anthers). If manual markers are used, a minimum of 3 markers spaced on the flower is required. The merging of images or groups of images results in a single tie point cloud (Fig. **10j**).

Once all the images are aligned around a single tie point cloud, the model (mesh) can be generated, using depth maps generated for each photo that represent the distance of the flower surface on the z axis for each camera positions (Fig. **10k**). The mesh is composed of vertices, edges and faces, together forming polygons (Fig. **10l**). During mesh reconstruction, the interpolated colour of the mesh polygons is calculated from images when using depth maps as source information (Fig. **10m**). The resulting mesh may need minor touch-ups, such as removing unwanted portions of the inflorescence or the pin used to attach the flower.

We then scale the model by manually positioning landmarks on the scale bar in the original images and defining these landmarks as being spaced by the length of the scale, which resizes the model accordingly. Finally we build the texture (detailed colour) of the model by using the 2D picture's information to generate a realistic visualisation of the flower surface in 3D (Fig. **10n,o**). The flower surface mesh can subsequently be used in geometric morphometric applications (Fig. **10p,q**) and the three-dimensional textured surface can be exported as a 2D layout of the 3D surface, used in quantification of flower colour using each pixel colour information (Fig. **10r,s**).
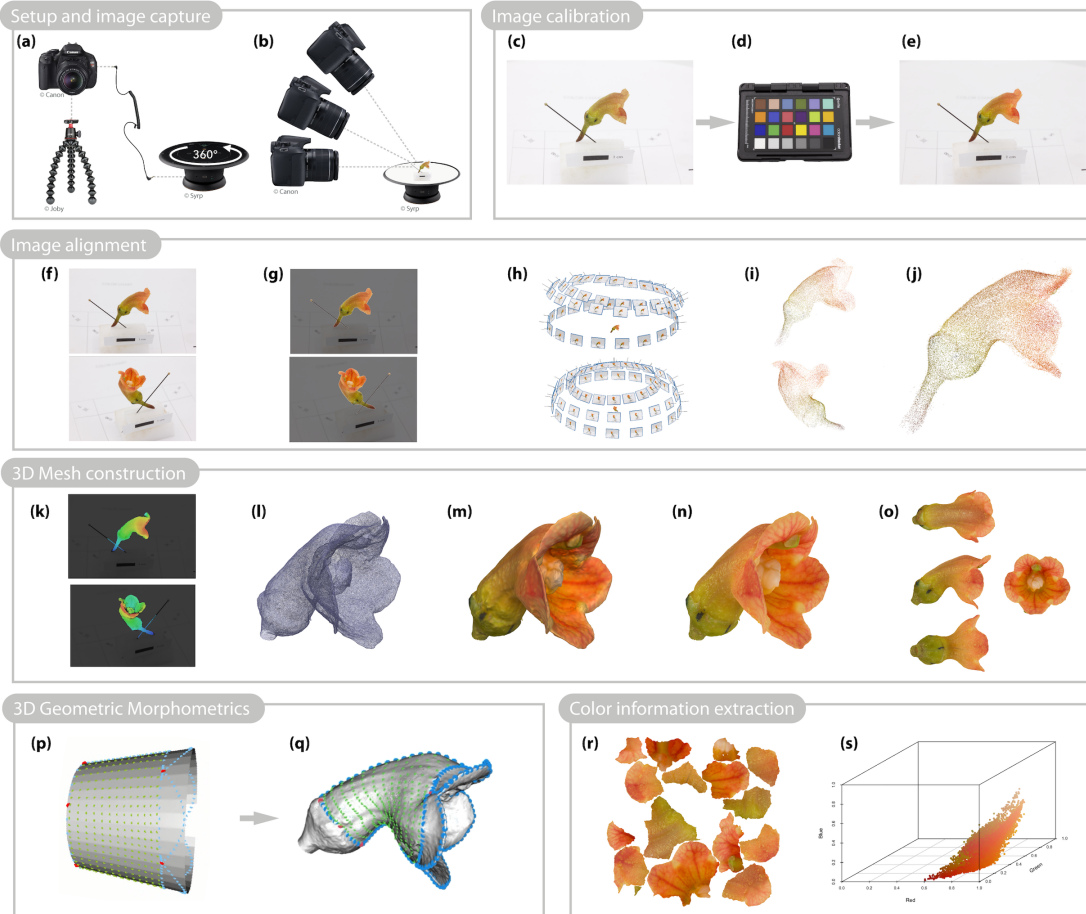
Figure 10. Graphical workflow of the photogrammetric approach used to study floral morphology and colour in three dimensions (3D). Flowers are attached to a 360° turntable that automatically triggers a camera as the turntable rotates in steps of a few degrees and are photographed using three camera angles for both ventral and dorsal view (a-b). All RAW images (c) are calibrated identically using a colour chart (d) to obtain realistic colour representation of flowers (e). Masks are applied to remove the background (f-g) before aligning the images (h), which results in a tie point cloud of homologous pixels detected in multiple photos (i). The separate sets of photos are then aligned and merged to give a unique tie points cloud (j). Using depth maps (k), a 3D mesh is reconstructed (l) and the interpolated colour of the mesh polygons is calculated from images (m). A more realistic 3D model is obtained by building the texture from the original photos (n), providing a finely detailed and coloured 3D model on the outer and inner surfaces of the flower (o). Landmarks (in red) and semi-landmarks are positioned on the flower model for curves (in blue) on the petal margin, petal base, dorsal and ventral corolla curvature, and the base of the sepals, as well as on the simplified truncated cone template. Surface semi-landmarks (in green) are automatically applied on flowers according to the template (p-q). The flower texture wrapping the model can be extracted as a 2D representation of the 3D surface (r) and used to analyse and quantify colour variation of the entire flower surface (s).

Box 1 - Glossary   83

Photography

Aperture: Size of the opening of a lens's diaphragm (or generically called shutter) through which light passes, noted f/N.

ISO: Camera sensor sensitivity to light.

Sensor: Part of the camera that detects and transforms light into information to produce an image.

Shutter speed: Time during which the shutter allows light to reach the sensor.

3D Modelling

3D Mesh (3D object): Structural tri-dimensional shape built of polygons along x,y and z axes to represent its height, width and depth.

Depth map: An image in which a colour gradient indicates the distance from the camera.

Edge: A connection between vertices.

Key point: A distinct feature recognised in a single image.

Mask: A delimited region of a photograph that is not the main subject.

Texture (or texture map): 2D object with details of the surface appearance, or information about the colours used to wrap a 3D object.

Tie points: Automatically detected or manually placed 3D points that are matched in multiple images and used to compute their 3D position.

Vertex: A position in a 3D space with three-dimensional x,y, and z coordinates.

Vertex colours: colours applied to each vertex according to the average colours of the corresponding areas on the images source.

Geometric morphometrics

Landmark: Fixed point at a particular position, usually on a distinguishable homologous feature.

Semi-landmark: Sliding point between landmarks or other semi-landmarks, describing curves or surfaces.

3. Performance of the photogrammetry approach

The above protocol was applied to diverse flowers selected to represent a variety of floral forms, colours and complexity. These were taken from species belonging to different Angiosperm families such as the Fabaceae (*Phaseolus coccineum*), Cactaceae (*Schlumbergera sp.*), Lamiaceae (*Salvia nemorosa*), as well as 19 Gesneriaceae species from the living collections of the Montreal Botanical Garden, mainly from the genera *Rhytidophyllum* and *Gesneria* (see example below for more information on these specimens). Flowers from 5 species modelled by photogrammetry were also scanned using microCT to compare models originating from both approaches.

3.1. 3D flower reconstruction

The overall 3D reconstruction process using photogrammetry took from 0.5 to 2h depending on the complexity of the project and the computer resources. The 3D models, the RAW photogrammetry image series to generate these models, and the corresponding colour charts and calibrated textures can be accessed from MorphoSource (https://www.morphosource.org/) under the project "Gesneriaceae of the Montreal Botanical Garden".

The photogrammetric approach generated models of high quality that accurately represent the shape and colour of flowers of different structures, sizes (2cm to 8cm), and symmetry (see Fig. **11** for a sample of flower models). The flower models presented in figure **11** were also deposited in SketchFab (sketchfab.com/plantevolution), an online platform for hosting and visualising 3D models with textures, to allow a closer inspection of the models. In many cases, very minute details could be modelled, such as the delicate petal margins of *Rhytidophyllum vernicosum* (Fig. **11g**) or the styles and stamens of several species (Fig. **11c, d, e, f**). Overall, the flower shape and colour of the models were very accurate and were essentially identical to the real flowers.

Some structures are more difficult to reconstruct, particularly those that are slender, translucent or reflective. Pillose organs were also challenging, in part due to the difficulty of applying masks. Structures that are very close to each other such as overlapping petals (*Schlumbergera sp.*; Fig. **11b**) or styles that very close to petals (Fig. **11f, h, i**) were also difficult to reconstruct independently from each other. Finally, very thin surfaces or parts that were party concealed depending on the camera angles may require more source images to be further improved such as below the basal petal surfaces on *Schlumbergera sp.*, the petal margins inside the corolla on *Phaseolus coccineum*, and the dorsal midrib of the sepal on *Salvia nemorosa*. Despite the occurrence of slight imperfections in some of the models, the global shape and colour of flowers reconstructed should allow most downstream applications.
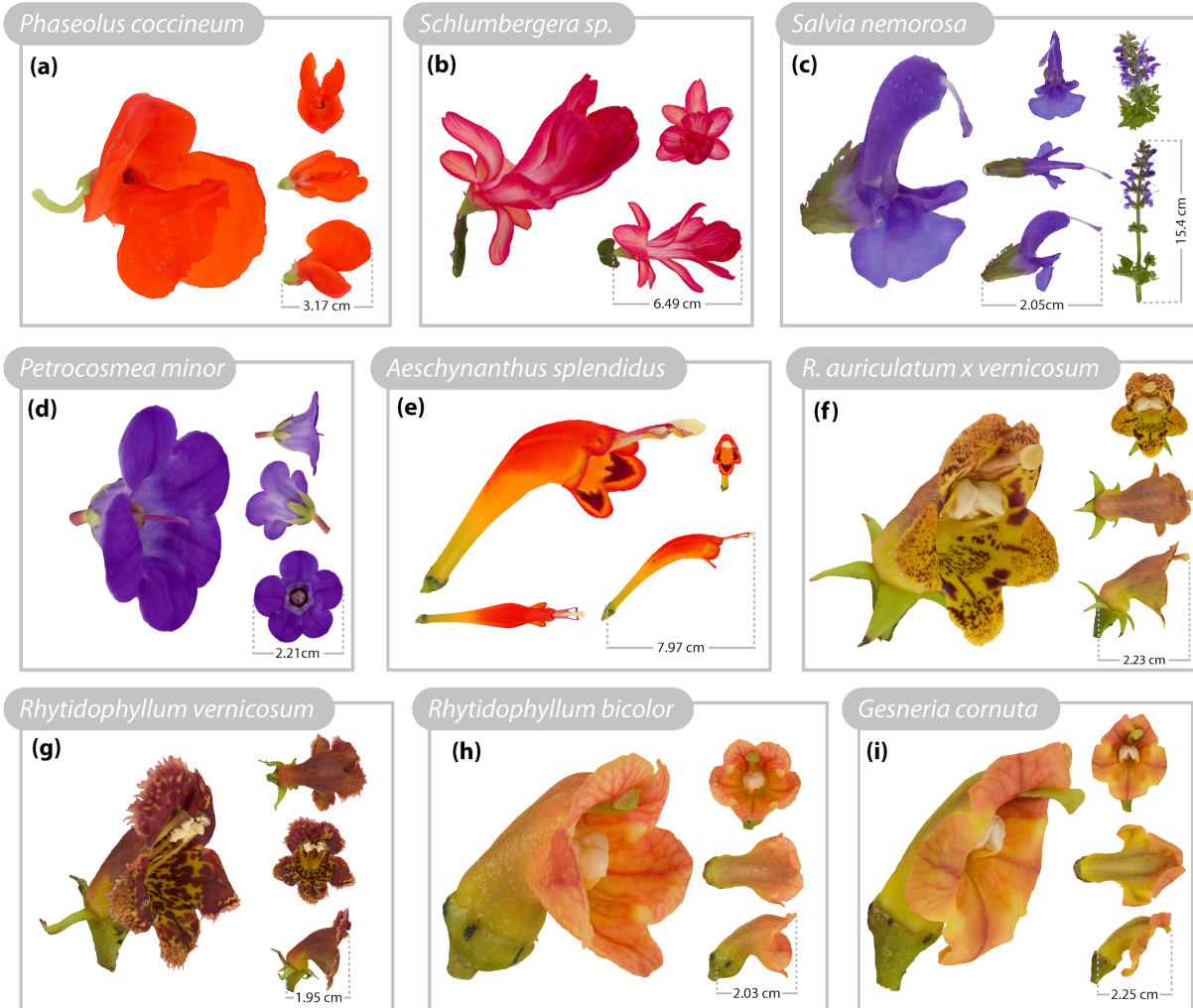
Figure 11. 3D textured models derived from non-Gesnericeae (a-c) and Gesneriaceae flowers (d-i) using photogrammetry. *Phaseolus coccineum*, Fabaceae (a), *Schlumbergera sp.*, Cactaceae (b), *Salvia nemorosa*, Lamiaceae (c). *Petrocosmea minor* (d), *Aeschynanthus splendidus* (e), the hybrid *Rhytidophyllum* x *vernicosum* (f), *Rhytidophyllum vernicosum* (g), *Rhytidophyllum bicolor* (h), and *Gesneria cornuta* (i), Gesneriaceae. The model of the inflorescence of *S. nemorosa* is illustrated under two different viewing angles (c).

3.2. Photogrammetry vs. microCT comparison

To compare the models obtained by photogrammetry with models obtained by microCT scanning, the flowers of five species (*Gesneria acaulis* 1328-2021, *Kohleria sp.* 1828-2013, *Paliavana prasinata* 1432-2010, *Rhytidophyllum exsertum* 112-1991 and *Rhytidophyllum tomentosum* 1327-2021) were sent to the Integrated Quantitative Biology Initiative (IQBI) platform at McGill University for microCT scanning and model reconstruction. Flowers were collected at the Montreal Botanical Garden and fixed in 4% Paraformaldehyde (PFA) in 1X Phosphate-buffered saline (PBS). The samples were gradually transferred to 70% ethanol from water and placed in 2%

ethanolic phosphotungstic acid (EPTA) in 70% ethanol stain for 15 days. Flowers were scanned in 1% agarose in 15 ml tubes at resolution 22μm at voltage 60V. The microCT models were reconstructed in Dragonfly (version 2020.2). The reconstruction of the models obtained from microCT took between 0.5 to 5h.

To allow a visual comparison of the models obtained by photogrammetry and microCT, we presented the flower models of three species side-by-side in different figures (Fig. **12** and Supporting Information Figs. **S1** and **S2**). All microCT models were also analysed alongside the photogrammetry models in a geometric morphometric analysis (see application example below). The microCT models were deposited in Morphosource in the same project as the photogrammetry models.

The surface meshes of models reconstructed with the microCT scans included holes as well as bumps due to the detection of hairs during the scanning step, but overall represented the morphology of flowers similarly to photogrammetry (see details in the floral shape analysis application example). Due to the softening of tissues during the staining process, flower parts were occasionally distorted and flowers with naturally recurved petals and/or sepals during the anthesis were slightly unfolded on the CT-based model compared to the photogrammetry model and the real flower (see for instance *Paliavana prasinata* in Fig. **12a,b,c,d**). Similar distortions of the corolla and sepals in microCT models are evident on the models of *G. rupincola* and *R. exsertum* (Supporting Information Fig. **S1**, and **S2**). Internal and non-visible organs were properly modelled using microCT scan, which could not be accurately reproduced using photogrammetry (Fig. **12e,f**). However, anther and stigma position can only be captured when visible from the flower opening (see Figs. **11** and **12**).
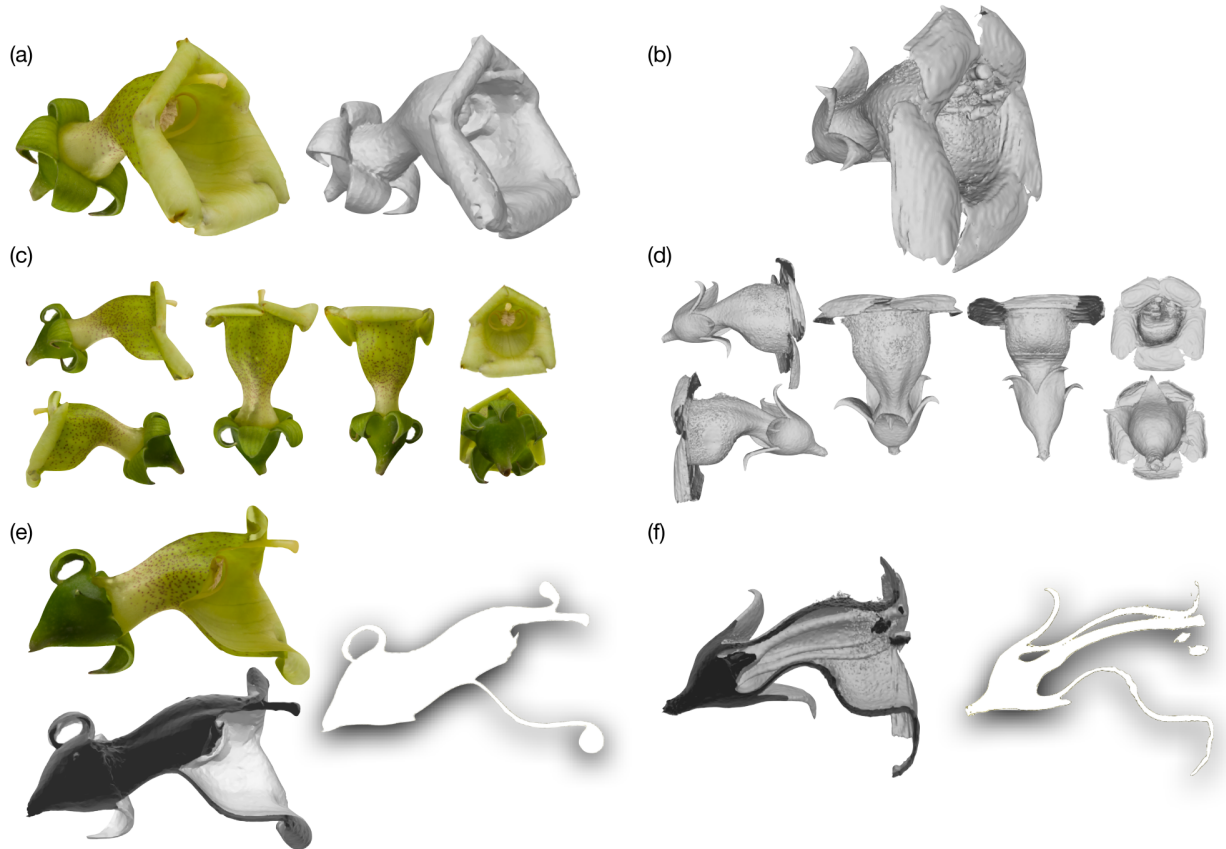
Figure 12. Comparison of 3D models of *Paliavana prasinata* derived from photogrammetry (left) and microCT (Micro Computed Tomography) scanning (right). The final solid models are represented for both photogrammetry (a - grey scale and colour) and microCT scan (b) under all viewing angles (c,d) (left and right lateral views, ventral, dorsal, anterior, and posterior views). Sections of these models are represented by half models (grey scale and colour) and median plane sections of both models along the x axis (e,f).

4. Application example

4.1. Material and methods

To demonstrate the potential use of flower models obtained from photogrammetry, we studied the shape and colour of 26 flowers from 18 species and one hybrid (*Rhytidophyllum auriculatum × vernicosum*) from the Gesneriaceae family that belong to three pollination syndromes: bird pollination, bat pollination, and mixed-pollination (see details in Supporting Information Notes **S1** and Table **S3**). We provide a brief description of the methods used here, but detailed materials and methods are available as supplementary information.

4.2. Floral shape analysis

The perianth of each flower was reconstructed in 3D using the described photogrammetry protocol above. We then used geometric morphometrics to compare the 3D flower shapes. Landmarks as well as semi-landmarks for curves and surfaces were placed on the flowers (see Supporting Information Methods **S1**, Fig. **S3**, and Table **S4**). After shape alignment using a generalized Procrustes analysis (GPA), the coordinates of the landmarks and semi-landmarks were projected onto the tangent space using principal component analysis (PCA) (Supporting Information Methods **S1**). The resulting morphospace places individuals from the same species very close to each other and allows the distinction of the pollination syndromes (Fig. **13** and Supporting Information Fig. **S4**). The estimated mean 3D shape of each syndrome also shows the main differences in shape between them (Supporting Information Fig. **S5**). The inclusion of the microCT flower models to the same morphospace shows that they fall very close to the photogrammetry models (Supporting Information Fig. **S6**).
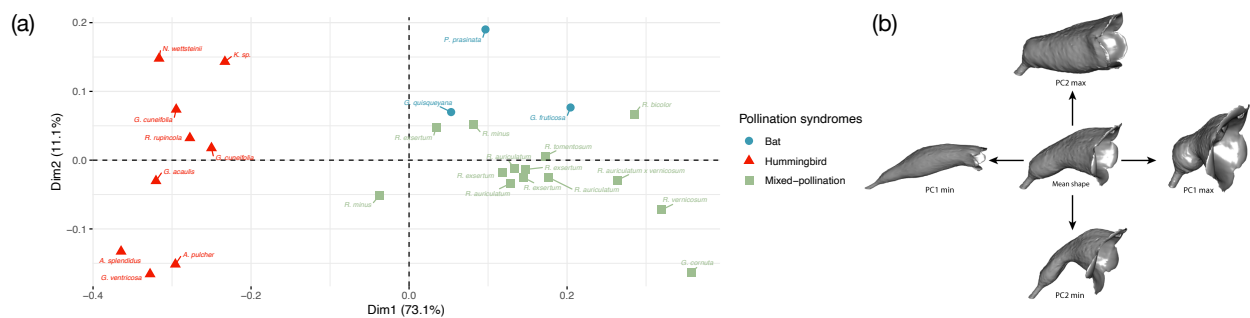
Figure 13. 3D floral morphospace and corresponding shape variation along the axes for individuals belonging to the *Gesneria*, *Rhytidophyllum*, *Nematanthus*, *Aeschynanthus*, *Kohleria*, and *Paliavana* genera. Specialists for bat (blue circles) and hummingbird pollination (red triangles) as well as mixed-pollination strategies (green squares) are represented along the first and second dimensions of the principal component analysis (PCA) (a). The mean 3D flower shape, as well as the maximum and minimum configurations of the 3D flower shape are shown for the first and second dimensions of the PCA (b).

4.3. Colour analysis

To illustrate the potential of the photogrammetric approach to study flower colour, the colour profiles of flowers were compared alongside the phylogeny of the 18 species of Gesneriaceae (see Supporting Information Methods **S2** for phylogeny reconstruction). The colour of each flower surface texture was quantified in eight categories (bins) in terms of red, blue, and green, which then allowed to compute a colour distance between flowers (see Supporting Information Methods **S3** and Fig. **S7**). The resulting distance matrix was used to build a phenogram and compared to the phylogenetic relationships (Fig. **14**). This example highlights that species tend to group

by pollination syndromes when considering flower colour and that similar colour patterns show evolutionary convergence in the Gesneriaceae.
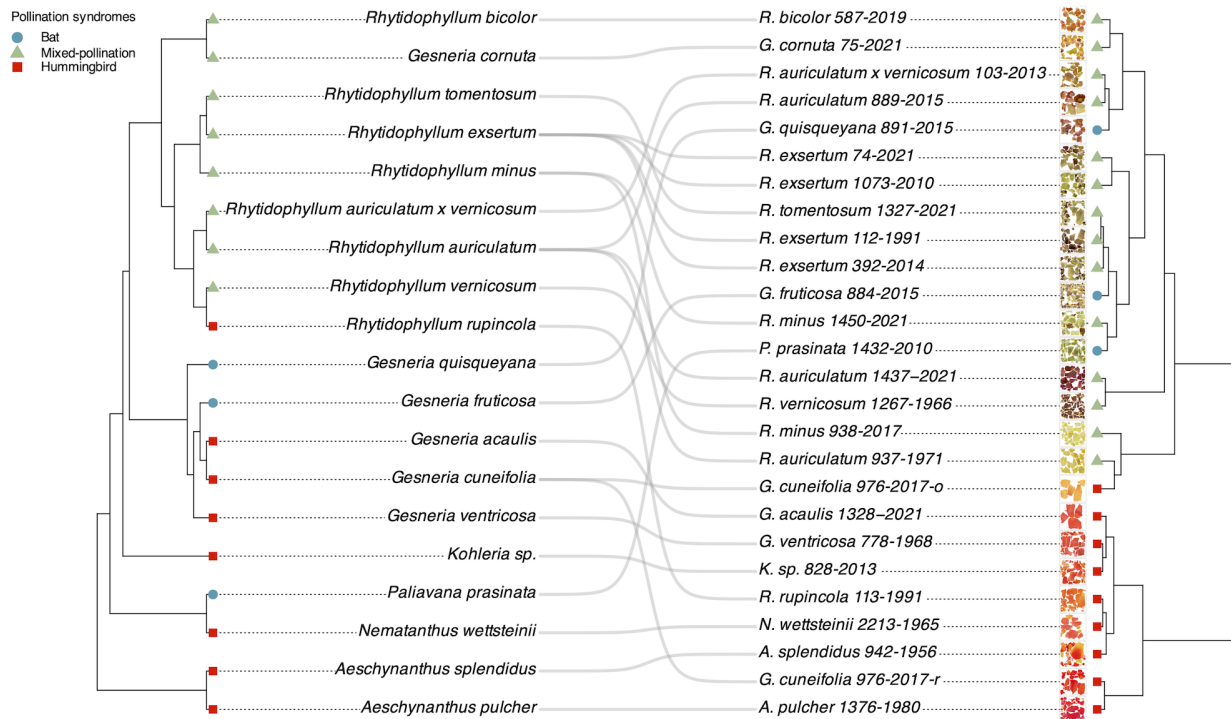
Figure 14. Tanglegram linking the phylogenetic relations of Gesneriaceae species (left) with the colour distance dendrogram from flower specimen colour using Ward's clustering method (right) according to their respective pollination syndromes.

5. Discussion

5.1. Relevance of ultra-close-range photogrammetry for the study of flowers

Flower shape has attracted much interest in several sub-fields of plant sciences, but relatively few studies have used 3D flower models, despite the importance of precisely quantifying the size, shape and colour of flowers in 3D given that the vast majority of flowers have to interact in a three dimensional environment to be fertilised. The main aspects of the methods currently used that may limit the number of 3D geometric morphometric studies on floral shape are the cost and lack of portability of microCT technologies. Although flowers can be fixed in the field in highly concentrated ethanol for later microCT scanning, doing so can damage or shrink flowers depending on their structure and thickness (Staedler et al., 2013; Dellinger et al., 2019). Moreover, contrasting reagents used to infiltrate the flower tissues prior to scanning may also produce additional leaching artefacts (Staedler et al., 2013). We observed slight anatomical

distortions in the flower models obtained with CT scans following fixation such as the unfolding of petals and sepals, distorting the shape and the relative positioning of the floral structures. Our microCT protocols could be improved to provide better and more accurate results; however, the use of standard protocols combined with an external service offers a fair comparison with our photogrammetry approach.

An array of flower sizes and colours for species belonging to the Gesneriaceae, Fabaceae, Lamiaceae, and Cactaceae were successfully reconstructed using photogrammetry. Various sizes of flowers as well as inflorescences can be rendered accurately and in detail and we were able to model all visible parts of the flowers, including the stigma and anthers in many species. The entire physical set-up (turntable, lightbox, tripod and colour chart) required to implement this method costs less than 600 US$, making this approach affordable for most laboratories that already own a suitable digital camera. Computer requirements are relatively reasonable for photogrammetry applications (16-32 GB of Random Access Memory (RAM), and 4-8 central processing units (CPUs)). The academic professional edition of the Agisoft Metashape software we used to reconstruct the 3D models currently costs 549 US$, although cheaper or open-source alternatives are available (see Medina et al. (2020)).

Ultra-close-range photogrammetry has several clear advantages over microCT–the gold standard in the field–for reconstructing 3D models of flowers. It is portable, affordable, time efficient both for image acquisition and model building, and can reconstruct the colour of the flower (see Table **4**). Yet, photogrammetry is also subject to some limitations (Table **4**). Most obviously, flower models can be reconstructed for only externally visible parts of the flower. Hidden structures, such as reproductive organs in some species, may remain hidden in particularly closed corollas. Floral dissection might in some cases provide the means to characterise concealed structures in 3D using photogrammetry, e.g., removal of the corolla, or simply cutting the sepals to reveal the base of the corolla, as we did in the application example using Gesneriaceae. In addition, concealed organs can be photographed and thus be visible on the model texture, allowing them to be analysed. But if concealed organs are of main interest for a given study, microCT is clearly the best option.

Some flower characteristics also likely complicate the 3D model reconstruction with photogrammetry. One of these is the often very thin surfaces of flowers. Missing surfaces or edges in the final 3D model often result from a miscalculation of the position of sufficiently close outer and inner surfaces of an object to be modelled. Depth data from sets of images may intersect, thus creating holes in the 3D mesh. A contrasting background and accurate masking of flowers allow recovery of thin structures at the extremities of the models such as fringed petals or stamen filament (e.g. see interactive flowers of *Rhytidophyllum vernicosum* and *Salvia nemorosa*). Shiny or translucent surfaces also represented a challenge because the reflection of light or the features that are detected behind the translucent petals are not fixed features on the surface, but are still captured in images. This issue can be solved by using a softer light during the photography

step. The presence of dense hairs on the flower also complicates model reconstruction because of the difficulty of adequately removing the background on photographs and because the resulting model is often rugged, although it can generally be corrected by smoothing the 3D surface. Finally, radially symmetrical or spherical objects with no clear visual landmarks are typically difficult to reconstruct using photogrammetry (Ijiri et al., 2018), such as some actinomorphic flowers. A straightforward solution is placing a few visually distinct markers on such flowers (i.e. coloured dots) to add artificial distinct features to help the software to align the photographs.

Overall, ultra-close-range photogrammetry is an useful alternative to microCT scanning and could be valuable for studies interested in the non-occluded parts of a flower and its colour. One interesting avenue is to combine CT-based and image-based approaches to get the advantages of both approaches, as demonstrated by Ijiri et al. (2018).

Characteristics	Approaches	
	Photogrammetry	**microCT scan**
3D reconstruction of occluded areas and internal structures	No	Yes
Model colour and texture	Yes	No
Portability	Yes	No, but flowers can be fixed on site
Adaptable to any type of flower	Yes, but very soft and hairy flowers and those with few clear visual landmarks are more difficult to reconstruct	yes
Deformation of structures	no	slight
Cost	from $2000	$200,000 to $1,000,000
Time requirements per flower	Setup and photography: 30min Colour calibration: 10min Reconstruction: 30min to 3h	Staining: typically > 14 days Scanning: 1h Segmentation: 30min to 5h

Table 4. Summary of the capabilities of both the microCT scan and photogrammetry approaches. Details on costs associated with photogrammetry are available in the Supporting Information Table **S1**.

5.2. Perspectives for floral morphology studies

5.2.1. Studying high-dimensional floral shape evolution

One obvious application of 3D flower models obtained by photogrammetry is to study floral shape. Different methods exist for characterising biological shapes in 3D. The most popular type of methods are geometric morphometrics that are based on the positioning of landmarks

(homologous points) and semi-landmarks (points that are positioned relative to others, along curves or surfaces). Landmark-free methods have also been developed and could be useful for smooth or featureless 3D surfaces for which landmark placement is not appropriate (Pomidor et al., 2016). Our worked example on Gesneriaceae showed how photogrammetry can be used to study the three-dimensional morphology of flowers. The accurate three-dimensional reconstruction of flowers combined with landmark-based geometric morphometrics allowed better discrimination and understanding of the 3D structure of the distinct pollination syndromes (Fig.**13**) compared to what can be obtained using 2D shape information from flowers in profile view (Joly et al., 2018).

5.2.2. Studying flower colour in 3D

One obvious advantage of photogrammetry over other approaches is to provide a very accurate reconstruction of flower colour in 3D. This opens many study opportunities as flower pigmentation is a major display signal for animal-pollinated plants. The complexity of floral colouration, including nectar guides, help pollinators limit the time they spend locating rewards, thus improving their foraging efficiency (Leonard and Papaj, 2011). Moreover, both biotic factors, such as pollinator abundance and the colour of co-occurring plants in the community, and abiotic factors such as solar radiation and low precipitation, can influence the colour perception and patterns of flowers (Dalrymple et al., 2020).

We showed that photogrammetry is a valuable tool to recover calibrated colour information from the entire 3D surface of flowers. 3D textures generated directly from calibrated high-quality photos in colour analyses can account for the totality of variation in flower pigmentation, avoiding biases caused by overlooked concealed surfaces or the distorted importance given certain regions of the flower (surfaces perpendicular to the camera compared to those that are more parallel) when using only a few 2D images in such analyses. Moreover, the presence of colour on 3D models could facilitate the distinction of structures that vary in colour but not so much in shape. For example, some species of Merianieae have stamen appendages that are distinguished from anthers primarily by their colour. Retaining colour on 3D models could thus help the positioning of these structures to test alternative hypotheses of floral modularity (Dellinger et al., 2019). The use of 3D models of flowers that retain colour information would greatly assist in distinguishing organs that differ in function and colour, but are difficult to distinguish based on shape.

Photography is a convenient way to collect morphological and reflectance data (colour) from specimens, and to facilitate research in ecology and evolution. However, the lack of tools to make objective colour measurements and the fact that cameras generally used in scientific studies produce uncalibrated photographs unreliable for quantitative colour measurements (Troscianko and Stevens, 2015). For this reason, a particular attention needs to be given to photo calibration and linearisation.

In addition, photography is not restricted to the visible spectrum (wavelength from 400 to 700 nm). Light can be detected by camera sensors in the UV range (320 to 400 nm) and IR (also called "heat radiation") or near-infrared (NIR) range (over 700 nm to about 1 mm), making it possible to incorporate these components of the light spectrum in 3D models. This could be important to understand patterns of reflectance evolution as most insect pollinators possess UV receptors (Chittka et al., 2001; Schiestl and Johnson, 2013), and self-heating flowers or inflorescences (Thien et al., 2000) as a reward or a means of enhancing the production and dissemination of floral scents (Seymour et al., 2003). Furthermore, images could be converted to correspond to different animal visual system sensitivities (cone-catch values) (Troscianko and Stevens, 2015).

5.2.3. Experimental studies

Advancements in 3D printing technology enable printing relatively small and intricate 3D models as well as remarkably detailed colour patterns, directly (using coloured filaments) or indirectly (by applying colour on models). In addition to colour, soft and flexible resins can be used thinly to resemble the soft tissues of flowers (see Supporting Information Fig. **S8** for an example of a colourless soft 3D printed artificial flower of a 3D model derived from photogrammetry). These methods should help expand the scope of experimental studies designed to test hypotheses about pollinator behaviour and flower shape, size and colour. As an example, printed artificial flowers and chimeric flowers made of artificial and natural flower parts were used to decouple and test the relative contributions of olfactory and visual signals to attract pollinators in a mimetic orchid *Dracula lafleurii* by Policha et al. (2016).

5.3. Natural history collections 3.0

Digitisation and archiving of information of material from natural history collections have revolutionised their current use. 3D modelling of natural history collections would further advance their value, accessibility and use. Such efforts are ongoing in entomological and ornithological collections using photogrammetry (Ströbel et al., 2018; Medina et al., 2020). Unlike zoological specimens, which generally retain their 3D shapes in collections, plant specimens are usually kept pressed in herbaria, thus losing most of their natural shape. Although morphological data can be extracted from herbarium specimens (e.g., Bilbao et al., 2021), morphological correlations between flower parts are generally lost. One strength of photogrammetry is that 2D data sets can be collected in the field to reconstruct 3D morphological features lost in herbarium specimens and can be subsequently linked to them in similar ways as other sources of information, such as genetic data or plants parts preserved separately from the specimens. Sharing such 3D models would significantly improve the quality of phenomic data obtainable from herbaria (Ströbel et al., 2018; Medina et al., 2020) or complement and extend the information on plant traits (morphological,

anatomical, functional, biochemical, phenological, and physiological) that is being centralised in global databases such as TRY (Kattge et al., 2011, 2020) and PROTEUS (Sauquet, 2019). Photogrammetry could also be extended to living collections, such as botanical gardens, thus improving access to such collections by providing access to virtual plants all year round and from anywhere in the world, creating new opportunities for scientific studies and outreach (Maschner et al., 2013). Open access databases dedicated to natural history, cultural heritage, and scientific collections are already available for such applications (Boyer et al., 2016).

6. Conclusions

Due to its simplicity and efficacy, photogrammetry has the potential to inspire new ways to quantify flower shape and colour and explore questions and collaborations in investigations of flowering plant evolution. Combined with genomic data, phenomic information obtained from 3D models using photogrammetry will open new areas of study of floral evolution. By combining practicality, reasonable costs, portability, and user friendly applications, photogrammetry has the potential to revolutionise studies of floral evolution and ecology.

7. Conflict of interests

The authors have no conflicts of interest to declare.

8. Acknowledgments

9. Data availability

The 3D model data are openly available in Morphosource at https://www.morphosource.org/, reference ID: 000369440.

Bibliography

Agisoft LLC (2021). Agisoft metashape user manual: Professional edition, version 1.7.

Artuso, S., Gamisch, A., Staedler, Y. M., Schönenberger, J., and Comes, H. P. (2021). Evidence for selectively constrained 3d flower shape evolution in a late miocene clade of malagasy bulbophyllum orchids. *New Phytologist*, 232(2):853–867.

Artuso, S., Gamisch, A., Staedler, Y. M., Schönenberger, J., and Comes, H. P. (2022). Evidence for an evo-devo-derived hypothesis on 3d flower shape modularity in a tropical orchid clade. *Evolution; International Journal of Organic Evolution*.

Bilbao, G., Bruneau, A., and Joly, S. (2021). Judge it by its shape: a pollinator-blind approach reveals convergence in petal shape and infers pollination modes in the genus erythrina. *American journal of botany*, 108(9):1716–1730.

Boyer, D. M., Gunnell, G. F., Kaufman, S., and McGeary, T. M. (2016). Morphosource: archiving and sharing 3-d digital specimen data. *The Paleontological Society Papers*, 22:157–181.

Chittka, L., Spaethe, J., Schmidt, A., and Hickelsberger, A. (2001). *Adaptation, constraint, and chance in the evolution of flower color and pollinator color vision*, page 106–126. Cambridge University Press.

Christiansen, F., Sironi, M., Moore, M. J., Di Martino, M., Ricciardi, M., Warick, H. A., Irschick, D. J., Gutierrez, R., and Uhart, M. M. (2019). Estimating body mass of free-living whales using aerial photogrammetry and 3d volumetrics. *Methods in Ecology and Evolution*, 10(12):2034–2044.

Cunliffe, A. M., Brazier, R. E., and Anderson, K. (2016). Ultra-fine grain landscape-scale quantification of dryland vegetation structure with drone-acquired structure-from-motion photogrammetry. *Remote Sensing of Environment*, 183:129–143.

Dalrymple, R. L., Kemp, D. J., Flores-Moreno, H., Laffan, S. W., White, T. E., Hemmings, F. A., and Moles, A. T. (2020). Macroecological patterns in flower colour are shaped by both biotic and abiotic factors. *New Phytologist*, 228(6):1972–1985.

Davies, T. G., Rahman, I. A., Lautenschlager, S., Cunningham, J. A., Asher, R. J., Barrett, P. M., Bates, K. T., Bengtson, S., Benson, R. B., Boyer, D. M., et al. (2017). Open data and digital morphology. *Proceedings of the Royal Society B: Biological Sciences*, 284(1852):20170194.

Dellinger, A. S., Artuso, S., Pamperl, S., Michelangeli, F. A., Penneys, D. S., Fernández-Fernández, D. M., Alvear, M., Almeda, F., Scott Armbruster, W., Staedler, Y., and Schönenberger, J. (2019). Modularity increases rate of floral evolution and adaptive success for functionally specialized pollination systems. *Communications Biology*, 2(1):1–11.

Evin, A., Souter, T., Hulme-Beaman, A., Ameen, C., Allen, R., Viacava, P., Larson, G., Cucchi, T., and Dobney, K. (2016). The use of close-range photogrammetry in zooarchaeology: Creating accurate 3d models of wolf crania to study dog domestication. *Journal of Archaeological Science: Reports*, 9:87–93.

Faegri, K. and van der Pijl, L. (1979). The principles of pollination ecology.

Fenster, C. B., Armbruster, W. S., Wilson, P., Dudash, M. R., and Thomson, J. D. (2004). Pollination syndromes and floral specialization. *Annual Reviews of Ecology Evolution and Systematic*, 35:375–403.

Florey, C. L. and Moore, P. A. (2019). Analysis and description of burrow structure in four species of freshwater crayfishes (decapoda: Astacoidea: Cambaridae) using photogrammetry to recreate casts as 3d models. *The Journal of Crustacean Biology*, 39(6):711–719.

Gamisch, A., Staedler, Y. M., Schönenberger, J., Fischer, G. A., and Comes, H. P. (2013). Histological and micro-ct evidence of stigmatic rostellum receptivity promoting auto-pollination in the madagascan orchid bulbophyllum bicoloratum. *PLoS One*, 8(8):e72688.

Giacomini, G., Scaravelli, D., Herrel, A., Veneziano, A., Russo, D., Brown, R. P., and Meloro, C. (2019). 3d photogrammetry of bat skulls: perspectives for macro-evolutionary analyses. *Evolutionary Biology*, 46(3):249–259.

Hsu, H.-C., Chou, W.-C., and Kuo, Y.-F. (2020). 3d revelation of phenotypic variation, evolutionary allometry, and ancestral states of corolla shape: a case study of clade corytholoma (subtribe ligeriinae, family gesneriaceae). *GigaScience*, 9(1):1–16.

Iglhaut, J., Cabo, C., Puliti, S., Piermattei, L., O'Connor, J., and Rosette, J. (2019). Structure from motion photogrammetry in forestry: A review. *Current Forestry Reports*, 5(3):155–168.

Ijiri, T., Todo, H., Hirabayashi, A., Kohiyama, K., and Dobashi, Y. (2018). Digitization of natural objects with micro ct and photographs. *PloS one*, 13(4):e0195852.

Joly, S., Lambert, F., Alexandre, H., Clavel, J., Léveillé-Bourret, E., and Clark, J. L. (2018). Greater pollination generalization is not associated with reduced constraints on corolla shape in Antillean plants. *Evolution*.

Kattge, J., Bönisch, G., Díaz, S., Lavorel, S., Prentice, I. C., Leadley, P., Tautenhahn, S., Werner, G. D., Aakala, T., Abedi, M., et al. (2020). Try plant trait database–enhanced coverage and open access. *Global change biology*, 26(1):119–188.

Kattge, J., Diaz, S., Lavorel, S., Prentice, I. C., Leadley, P., Bönisch, G., Garnier, E., Westoby, M., Reich, P. B., Wright, I. J., et al. (2011). Try–a global database of plant traits. *Global change biology*, 17(9):2905–2935.

Katz, D. and Friess, M. (2014). 3d from standard digital photography of human crania—a preliminary assessment. *American Journal of Physical Anthropology*, 154(1):152–158.

Leonard, A. S. and Papaj, D. R. (2011). 'x'marks the spot: The possible benefits of nectar guides to bees and plants. *Functional Ecology*, 25(6):1293–1301.

Linder, W. (2009). *Digital photogrammetry*, volume 1. Springer.

Luhmann, T., Robson, S., Kyle, S., and Boehm, J. (2013). *Close-range photogrammetry and 3D imaging*. Walter de Gruyter.

Maschner, H. D., Schou, C. D., and Holmes, J. (2013). Virtualization and the democratization of science: 3d technologies revolutionize museum research and access. In *2013 Digital Heritage*

International Congress (DigitalHeritage), volume 2, pages 265–271. IEEE.

Mathys, A., Brecko, J., and Semal, P. (2013). Comparing 3d digitizing technologies: what are the differences? In *2013 Digital Heritage International Congress (DigitalHeritage)*, volume 1, pages 201–204. IEEE.

Medina, J. J., Maley, J. M., Sannapareddy, S., Medina, N. N., Gilman, C. M., and McCormack, J. E. (2020). A rapid and cost-effective pipeline for digitization of museum specimens with 3d photogrammetry. *Plos one*, 15(8):e0236417.

Policha, T., Davis, A., Barnadas, M., Dentinger, B. T. M., Raguso, R. A., and Roy, B. A. (2016). Disentangling visual and olfactory signals in mushroom-mimicking Dracula orchids using realistic three-dimensional printed flowers. *New Phytologist*, pages n/a–n/a.

Pomidor, B. J., Makedonska, J., and Slice, D. E. (2016). A landmark-free method for three-dimensional shape analysis. *PloS one*, 11(3):e0150368.

Reich, D., Berger, A., von Balthazar, M., Chartier, M., Sherafati, M., Schönenberger, J., Manafzadeh, S., and Staedler, Y. M. (2020). Modularity and evolution of flower shape: the role of function, development, and spandrels in erica. *New Phytologist*, 226(1):267–280.

Rohlf, F. J. and Marcus, L. F. (1993). A revolution morphometrics. *Trends in ecology & evolution*, 8(4):129–132.

Sauquet, H. (2019). Proteus: A database for recording morphological data and fossil calibrations.

Schiestl, F. P. and Johnson, S. D. (2013). Pollinator-mediated evolution of floral signals. *Trends in ecology & evolution*, 28(5):307–315.

Seymour, R. S., White, C. R., and Gibernau, M. (2003). Heat reward for insect pollinators. *Nature*, 426(6964):243–244.

Staedler, Y. M., Masson, D., and Schönenberger, J. (2013). Plant tissues in 3d via x-ray tomography: simple contrasting methods allow high resolution imaging. *PloS one*, 8(9):e75295.

Ströbel, B., Schmelzle, S., Blüthgen, N., and Heethoff, M. (2018). An automated device for the digitization and 3d modelling of insects, combining extended-depth-of-field and all-side multi-view imaging. *ZooKeys*, (759):1–27.

Stuppy, W. H., Maisano, J. A., Colbert, M. W., Rudall, P. J., and Rowe, T. B. (2003). Three-dimensional analysis of plant structure using high-resolution x-ray computed tomography. *Trends in plant science*, 8(1):2–6.

Thien, L. B., Azuma, H., and Kawano, S. (2000). New perspectives on the pollination biology of basal angiosperms. *International Journal of Plant Sciences*, 161(S6):S225–S235.

Timerman, D. and Barrett, S. C. (2019). Comparative analysis of pollen release biomechanics in thalictrum: implications for evolutionary transitions between animal and wind pollination. *New Phytologist*, 224(3):1121–1132.

Troscianko, J. and Stevens, M. (2015). Image calibration and analysis toolbox–a free software suite for objectively measuring reflectance, colour and pattern. *Methods in Ecology and Evolution*, 6(11):1320–1331.

van der Niet, T., Zollikofer, C. P., de León, M. S. P., Johnson, S. D., and Linder, H. P. (2010). Three-dimensional geometric morphometrics for studying floral shape variation. *Trends in plant science*, 15(8):423–426.

Wang, C.-N., Hsu, H.-C., Wang, C.-C., Lee, T.-K., and Kuo, Y.-F. (2015). Quantifying floral shape variation in 3d using microcomputed tomography: a case study of a hybrid line between actinomorphic and zygomorphic flowers. *Frontiers in plant science*, 6:724.

Willmer, P. (2011). *Pollination and floral ecology*. Princeton University Press.

Troisième chapitre.

Impact of pollination syndromes on diversification rates in a neotropical insular system

par

Marion Leménager[1], John L. Clark[2], Silvana Martén-Rodríguez[3] et Simon Joly[4]

([1])   Université de Montréal, Institut de recherche en biologie végétale
([2])   Marie Selby Botanical Gardens, 1534 Mound Street Sarasota, FL 34236
([3])   Laboratorio Nacional de Análisis y Síntesis Ecológica, Escuela Nacional de Estudios Superiores–Morelia, Universidad Nacional Autónoma de México, Morelia, Michoacán C.P. 58190, México
([4])   Université de Montréal, Institut de recherche en biologie végétale
        Jardin Botanique de Montréal, 4101 Rue Sherbrooke E, Montréal, QC H1X 2B2, Canada

Cet article est en préparation.

RÉSUMÉ.

Des adaptations clés, ouvrant des niches écologiques inexplorées, peuvent potentiellement conduire à des changements écologiques significatifs, en particulier lorsque les ressources alternatives sont sous-utilisées, comme dans le cas de la colonisation de nouveaux environnements. Les changements peuvent contribuer à augmenter les taux de diversification en limitant l'extinction et en favorisant la spéciation. Les changements écologiques et les processus de diversification sont toutefois des processus distincts qui peuvent ne pas être corrélés. Dans les systèmes insulaires, les radiations adaptatives peuvent être motivées par la sous-utilisation de ressources alternatives et une dispersion limitée, ce qui favorise la spéciation géographique. Les stratégies de pollinisation représentent un aspect majeur de la reproduction des plantes et peuvent donc avoir un impact direct sur les taux de diversification. Les espèces généralistes bénéficient potentiellement de l'exploitation de niches de pollinisation plus larges et réussissent mieux à coloniser les îles et à y persister en raison de la réduction des risques d'extinction. Les archipels tels que les Antilles constituent un cadre idéal pour étudier les mécanismes évolutifs en raison de leur isolement et de l'évolution répétée des groupes d'espèces entre les îles. Dans les Antilles, les généralistes de la pollinisation, les colibris et les spécialistes des chauves-souris au sein des Gesneriaceae antillaises (Gesneriinae) représentent une étude de cas de la convergence évolutive des morphologies florales. Nous explorons ce groupe pour vérifier si les généralistes connaissent des taux de diversification plus élevés que les spécialistes dans ce contexte insulaire. Nous avons reconstruit la phylogénie des Gesneriinae et étudié la corrélation entre les syndromes de pollinisation et les taux de spéciation/extinction à l'aide de modèles de spéciation et d'extinction. Malgré l'hypothèse initiale d'un succès supérieur des généralistes, nous démontrons que la spécialisation n'est pas une impasse évolutive dans les archipels et qu'elle se diversifie au même rythme que les généralistes.

Mots clés : Diversification, syndromes de pollinisation, spécialiste, généraliste, Antilles, Gesneriaceae

ABSTRACT.

Key adaptations, opening unexplored ecological niches, can potentially drive significant ecological shifts, especially when alternative resources are underutilised, such as in the colonisation of novel environments. Shifts can contribute to increased diversification rates by limiting extinction and promoting speciation. However, ecological change and diversification are distinct processes that may not be correlated. In insular systems, adaptive radiation may be driven by the under-utilisation of alternative resources and limited dispersal, promoting geographic speciation. Pollination strategies represent a major aspect of plant reproduction, and thus can directly impact diversification rates. Generalist species potentially benefit from exploiting broader pollination niches and obtain higher success in colonising and persisting on islands due to reduced extinction risks. Archipelagos such as the Antilles provide an ideal setting to study evolutionary mechanisms by its isolation and replicated evolution of species groups among the islands. Within the Antilles, pollination generalists, hummingbirds and bat specialists within Antillean Gesneriaceae (Gesneriinae) represent a case study of the evolutionary convergence of floral morphologies. We explore this group to test whether generalists experience higher diversification rates than specialists in this insular context. We reconstructed the phylogeny of Gesneriinae and investigated the correlation between pollination syndromes and speciation/extinction rates using state speciation and extinction models. Despite the initial hypothesis of higher success of generalists, we demonstrate that specialisation is not an evolutionary dead end in archipelagos and diversifies at the same rate as generalists.

Keywords: Diversification, Pollination syndromes, Specialist, Generalist, Antilles, Gesneriaceae

1. Introduction

The emergence of key adaptations has the potential to drive significant ecological shifts, opening up previously unexplored ecological niches (Miller et al., 2023). These acquired traits may then directly facilitate speciation or mitigate extinction, ultimately contributing to a net increase in species richness or the rate of species diversification. However, the adaptive radiation phenomenon, characterised by the emergence of diverse ecological roles and role-specific adaptations within a lineage, may not necessarily result in increased diversification (Alfaro et al., 2009; Rabosky, 2014; Givnish, 2015). Notably, once established, many plant groups, particularly those on oceanic islands, diversify rapidly in morphology and ecology as a result of adaptive radiation (see Barrett, 1996).

In addition to exploiting a new adaptive zone, adaptive radiation may be promoted in contexts where alternative resources are underutilised by other species, such as the case of colonisation of remote insular systems (Givnish, 2015). Geographic speciation through limited dispersal or gene flow is also a process that can promote diversification without adaptive divergence (Givnish, 2015). As species diversification and shifts in ecology are distinct processes, it is interesting to test whether shifts in ecology are associated with increased diversification rates.

Transitions among pollination strategies can directly impact diversification rates as they impact the reproduction of flowering plants and their mating patterns (Wessinger et al., 2019). Specialisation has been in some instances considered an evolutionary dead end, with reduced net diversification rates relative to generalists, and a limited ability to evolve towards a more generalist strategy (Zenil-Ferguson et al., 2023). Alternatively, in an insular context, as pollinator resources in a newly colonised area may differ from those in the source area of immigrant plants, plants with a generalist pollination syndrome may be favoured, as the pollinator requirements of specialist plants may be a hindrance to their establishment on islands (Barrett, 1996). Pollinators of specialist plants may not be present in the same abundance, may have greater temporal variability, or may not have the same specific correspondence as in the environment of origin of the immigrant plants. For these reasons, species pollinated by a broader spectrum of pollinators might thus have greater success in colonising oceanic islands. This is primarily because generalist species could experience a reduced risk of extinction due to their ability to receive pollination from various sources. Indeed, it is well documented that generalists are generally associated with reduced risk of extinction (McKinney, 1997; Colles et al., 2009).

Archipelagos have played an essential role in the development of seminal theories in biogeography, but also in evolution and ecology, enabling a better understanding of the processes of species immigration, diversification and extinction (MacArthur and Wilson, 1963; Ricklefs and Bermingham, 2008; Warren et al., 2015). When islands are in extreme isolation, interactions between them and the mainland can be limited to one-way exchanges of organisms (immigration from the mainland to the archipelago), subject to stochasticity and the long-distance dispersal

abilities of organisms (Ricklefs and Bermingham, 2008). On the other hand, islands too close to the mainland may receive a large influx of immigrants, preventing the emergence of endemic species through genetic isolation (Ricklefs and Bermingham, 2008). Nestled between these two extremes, the geographical situation of the Antillean islands allows for a complex dynamic of interactions between mainland and archipelago organisms. The islands of the Antilles are sufficiently isolated geographically for the emergence and persistence of endemic species and close enough to the mainland to maintain dynamic exchanges of organisms (MacArthur and Wilson, 1963; Ricklefs and Bermingham, 2008). These and other characteristics (island diversity and geographical location) have led to characterising the Antilles as a biogeographic laboratory (Ricklefs and Bermingham, 2008). They offer ideal conditions for replicating ecological and evolutionary opportunities in various situations of isolation from the mainland, enabling us to highlight the processes leading to current patterns of diversity (Ricklefs and Bermingham, 2008; Regalado et al., 2018).

Within the Antilles, the repeated evolution of generalist syndromes from putative hummingbird specialist pollination type in Antillean Gesneriaceae (Martén-Rodríguez et al., 2010; Joly et al., 2018) constitutes an interesting setting to test assumptions on the impact of pollination syndromes on diversification in an insular context. The Gesneriinae is a monophyletic group of ca. 80 species mostly endemic to the Antilles. Five pollination syndromes have been characterised in Gesneriaceae (Martén-Rodríguez and Fenster, 2008; Martén-Rodríguez et al., 2009; Martén-Rodríguez et al., 2010; Martén-Rodríguez et al., 2015; Joly et al., 2018). Most species from this group are hummingbird specialists or mixed-pollinated by hummingbirds, bats, and insects, although a few species are also bat or moth specialists (Martén-Rodríguez et al., 2009; Martén-Rodríguez et al., 2010; Martén-Rodríguez et al., 2015). The generalist syndrome is unique to the Antilles in the New World Gesneriaceae (Martén-Rodríguez et al., 2009, 2015), suggesting that this strategy is more advantageous for insular plants, potentially representing an adaptive innovation in this environment. In this context, it seems plausible that species of Gesneriinae with the mixed-pollination syndrome have experienced a higher rate of diversification than pollination specialists, possibly due to a reduced extinction rate.

The generalist pollination syndrome emerging in Antillean Gesneriaceae has a distinct floral morphology that allows them to access a new niche space since they exploit more pollinators than specialists. However, whether this represents a key innovation that leads to diversification in this group remains unclear. To test whether generalists have higher diversification rates than specialists in a neotropical island system, we reconstructed the most extensive phylogeny of West Indian Gesneriinae from living collections or herbarium specimens as well as speciation- and extinction-dependent diversification models (SSE) to test correlations between the evolution of pollination syndromes and speciation and extinction rates.

2. Materials and Methods

2.1. Pollination syndromes

Pollination syndrome data was obtained from field-based information (Martén-Rodríguez and Fenster, 2008; Martén-Rodríguez et al., 2009; Martén-Rodríguez et al., 2010; Martén-Rodríguez et al., 2015; Faure and Joly, 2020), or inferred from floral morphological traits (shape and colour) as flower traits are accurate predictors for the pollination strategies in this clade (Martén-Rodríguez et al., 2009).

2.2. Phylogeny

2.2.1. General approach

Tackling macroevolutionary questions such as studying diversification rates requires a robust phylogenetic framework. This is often difficult to achieve when looking at a low number of loci, especially for lineages that have recently diverged such as the Gesneriinae or when incomplete lineage sorting or inter-specific gene flow may be taking place (Martín-Hernanz et al., 2019). Among next-generation sequencing (NGS) methods, genotyping-by-sequencing (GBS) makes it possible to reduce genome complexity to DNA fragments. These fragments, of which ends are then sequenced, make it possible to obtain thousands of new loci distributed throughout the genome (Miller et al., 2007; Andrews et al., 2016). We used a GBS approach to sequence a large number of loci from multiple individuals from all the species we could sample and we combined this information with previously Sanger-sequenced single-copy nuclear genes to reconstruct a species phylogeny.

2.2.2. Plant material for GBS molecular data

Leaf samples from 152 specimens representing 82 species were gathered from field collections, herbarium specimens(29 samples from the William and Steer Herbarium, NYBG, and 25 from the National Herbarium, Natural Museum of Natural History, Smithsonian Institution) and living collections for DNA extractions to generate GBS molecular data for Gesneriinae species.When possible, we tried to include specimens from distant locations and from different islands where applicable.

2.2.3. Genotyping-by-sequencing

DNA was extracted using a modified Small-scale CTAB (Cetyltrimethylammoniumbromide) DNA Extraction Protocol (Doyle and Doyle, 1987; Joly et al., 2006). We used a two-enzyme genotyping-by-sequencing approach to obtain genome fragments from extracted DNA (Poland

et al., 2012). Extracted DNA samples were sent to the Institut de Biologie Intégrative et de Systèmes (IBIS) Genomic analysis platform (Laval University, Québec) for genotyping by sequencing (GBS) using the `SbfI` (high fidelity) and `MspI` enzymes.Quality control checks on raw sequence data were done using the software FastQC (Andrews et al., 2010).

2.2.4. Assembly

We used the pipeline `iPyrad` version 0.9.77 to process the GBS sequence data using a *de novo* assembly approach without a reference sequence (Eaton and Overcast, 2020). The raw sequence data were filtered (maximum number of low quality base of 5, Phred QScore offset = 33) and demultiplexed according to internal barcodes associated with each sample. The *de novo* pipeline was executed using the settings as listed in Table S12. The loci that were exported for further analyses were those that had a coverage filter of a minimum of 20 samples per locus, two alleles maximum per individual to assume diploidy, a maximum of 20% SNPs per locus, a maximum of five indels per locus, and a maximum of 25% heterozygous sites per locus.

2.2.5. Bayesian inference of phylogenetic relationships

We selected a concatenation approach to build a multi-species tree of the phylogenetic relationships among Antillean Gesneriaceae. The five DNA markers (CHI, CYCLOIDEA, F3H, GAPDH, UF3GT) were retrieved from GenBank for n=47, n=62, n=52, n=32, n=40 species respectively including the outgroups. Samples with only DNA markers of the five targeted genes (no GBS loci) were not included in the present analysis. GBS loci and Sanger sequences were concatenated using `Concatenator` (Release v0.2.1) (Vences et al., 2022).

`RAxML` ('Randomized Axelerated Maximum Likelihood') version 8 (Stamatakis, 2014) was initially used to identify unstable individuals from the dataset. Samples that caused low bootstrap support when included in the phylogeny and had low loci coverage were excluded from the final phylogenetic analyses. Once the final alignment was obtained, a Bayesian MCMC phylogenetic analysis was performed in BEAST 2.7.5 (Bouckaert et al., 2019). The GTR + Γ (8 categories) + I substitution model was used for all genes, estimating substitution rates. An uncorrelated relaxed clock model was selected for all loci (Drummond et al., 2006), and a pure birth model (Yule model) was used as the tree prior. We ran one MCMC chain for 10 million iterations, sampling the parameters every 1000 steps (Drummond et al., 2002).

The chain-specific burn-in fraction was determined and removed by examining the trace plot in `TRACER` 1.7.2 (Rambaut et al., 2018). We ensured that sufficiently large effective sample sizes (> 100) were obtained for the posterior and likelihood. A Maximum Clade Credibility (MCC) tree was calculated in `TREEANNOTATOR` 2.7.5.

To obtain a species tree from the individual-based tree, we selected, for the species that were represented by more than one specimen, the sample that contained the most sequencing information in terms of nucleotides. The phylogenetic tree was then pruned to keep only species

with pollination syndrome confirmed or inferred to be hummingbird specialists, bat specialists, or mixed-pollinated species. The species tree was rescaled to a total length of 1 to facilitate diversification rates interpretation using `rescale.phylo` from the package `geiger` version 2.0.11 (Pennell et al., 2014).

2.3. Analyses of diversification

2.3.1. General approach

To assess the effect of pollination syndromes on diversification rates we used state speciation and extinction (SSE) models (Maddison et al., 2007; FitzJohn, 2012; Beaulieu and O'Meara, 2016; Nakov et al., 2018). These models use phylogenetic topology and branch length information to estimate speciation (λ) and extinction (μ) associated with specific character values and the transition rates between these character values. Several categories of models have been proposed over the years to account for multiple character states (Multiple or MuSSE models) (FitzJohn, 2012), to control the possibility that unobserved or hidden characters could affect the diversification rates (hidden states or HiSSE models), and to provide better null models to test for differences in diversification rates (see character-independent HiSSE or CID models in Beaulieu and O'Meara, 2016). We tested our hypotheses by comparing the fit of these different models.

2.3.2. Diversification analyses

In the diversification analyses, we considered that specialists and generalists had different diversification rates (binary coding) or that each syndrome had different diversification rates using multistate coding (specialist for bats, specialist for hummingbirds, and generalists). We compared models of diversification rates that affected the character of interest (two and three states MuSSE depending on whether the character was coded as binary or multistate), models that have hidden states that affect the diversification rates (two and three states MuHiSSE with two hidden states), and null models (null model and CID models that match the parameter complexity of the models with state-dependent diversification) for which the character states do not affect the diversification rates (Figure 15). For all models, the extinction fraction ($\epsilon_i = \mu_i/\lambda_i$) was set to be equal for all character states, but the turnover parameter differed among states depending on the models. For binary characters, we set a distinct parameter for turnover for specialists and generalists ($\tau_{specialist} \neq \tau_{generalist}$, which corresponds to $\tau_{hummingbird} = \tau_{bat} \neq \tau_{generalist}$) for the BiSSE model, and distinct turnover parameters for each syndrome in the MuSSE model ($\tau_{hummingbird} \neq \tau_{bat} \neq \tau_{generalist}$). Hidden states models were set with distinct turnover parameters for specialists and generalists (two states MuHiSSE) or for each syndrome (three states MuHiSSE), and different parameters for the different hidden states A and B (Figure 15 D and E). For all models, transition rates were set to be different among the three syndromes, and equal among hidden states for hidden states models. For the null model, we set the turnover

rates ($\tau_i = \lambda_i + \mu_i$) to be equal among all pollination syndromes, with no hidden character states. Additional character-independent (null) diversification models with two to six hidden states (CID-2, CID-4 and CID-6) were also fitted as nontrivial null models. To better account for missing data, for all models, the sampling fraction of each pollination syndrome was calculated using the ratio of sampled species in this study on the total number of known species belonging to each syndrome.

All models were fitted using the `hisse` R package version 2.1.11 (Beaulieu and O'Meara, 2016). Model selection was based on AICc weights using the function `GetAICWeights`. For models within 2 units of the AICc of the best model belonging to the same model category, we sampled parameter values within a 2 lnL region of the maximum likelihood estimation (MLE) using the function `SupportRegionMuHiSSE` from the package `hisse`, which adaptively samples the likelihood surface for each parameter to estimate confidence intervals that reflect the uncertainty in the MLE. The rates matrix including rates for turnover, extinction fraction, net diversification, speciation and extinction were retrieved using the function `MarginReconMuHiSSE` from the package `hisse` that estimates ancestral state estimation based on marginal reconstruction by estimating the likeliest states for both internal nodes and tips of the phylogeny using a marginal reconstruction algorithm. Speciation and extinction rates were retrieved by back transforming the estimated parameters following the equations for diversification rates ($r = \lambda - \mu$), extinction fraction ($\epsilon = \mu/\lambda$), extinction ($\mu = (\tau\epsilon)/(1 + \epsilon)$), speciation ($\lambda = \tau/(1 + \epsilon)$), and turnover ($\tau = \lambda + \mu$) (Beaulieu and O'Meara, 2016).

The ancestral state reconstruction of pollination syndromes was performed using the best model using node information from the function `MarginReconMuHiSSE` to represent the marginal probabilities of each syndrome calculated for each node as pie charts.
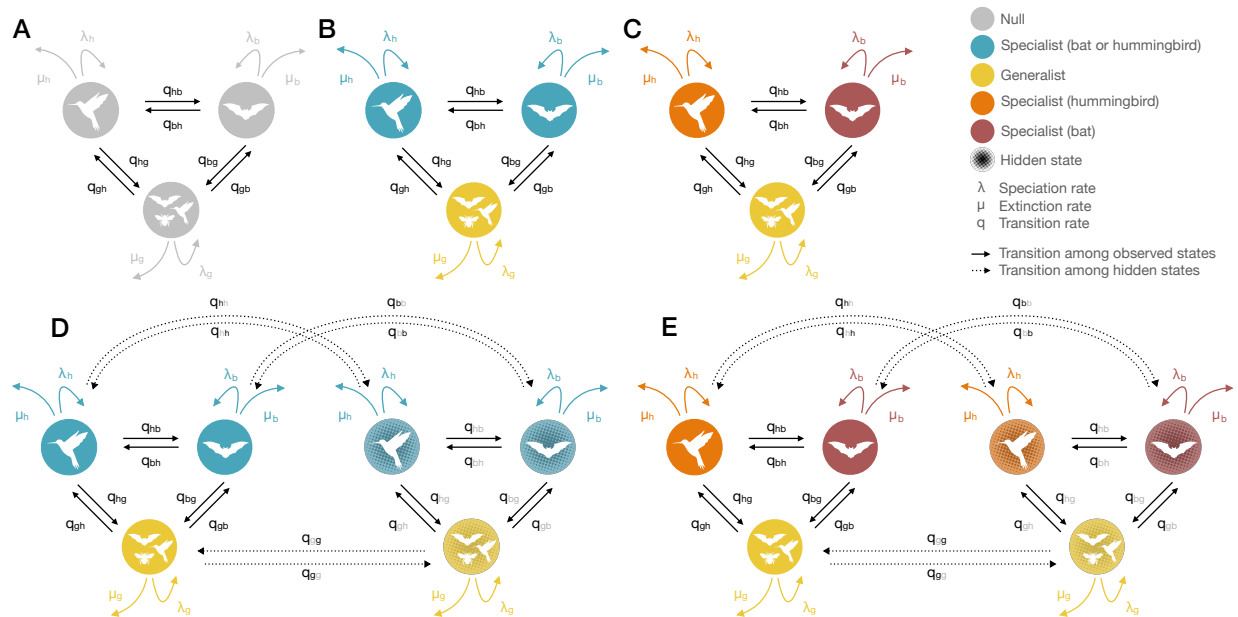
Figure 15. Schematic representation of the SSE models explored. The null model (A) does not account for differences in diversification rates among the three pollination syndromes. The MuSSE model uses either a binary categorisation of the pollination syndromes (B) into specialists or generalists to attribute different diversification rates of speciation (λ) and extinction (λ). The MuSSE model also can account for the three distinct pollination syndromes (C). Rates of transition among each syndrome are considered distinct in each of these models (arrows in black). The unobserved traits' effect is considered in the diversification patterns using hidden states (blank vs. patterned syndromes) in the MuHiSSE models, considering specialists vs. generalists (D) and considering the three pollination syndromes independently (E). Transition rates between hidden states are estimated to be the same among hidden states (dashed arrows).

3. Results

3.1. Genotyping-by-sequencing and locus selection

After filtering, 139 loci were retrieved using the GBS approach. A total of 22 samples were removed because they had a lack of loci after filtering (11 samples), or had low sample coverage (10 samples with fewer than 10 loci shared with other samples) (see Table S13 for details).

3.2. Phylogenetic relationships among Antillean Gesneriaceae

Using the GBS loci and the nuclear gene information, we reconstructed the phylogenetic relationships among 123 individuals from 73 species of Gesneriaceae, which represents 79% of all described Gesneriinae species (Acevedo-Rodríguez and Strong, 2012; Clark et al., 2020). More precisely, the tree contained 47 species of *Gesneria* L., 22 species of *Rhytidophyllum* Mart., one

species of *Bellonia*, *Pheidonocarpa corymbosa*, and two outgroup species (*Henckelia malayana* (Hook.fil.) A.Weber and *Kohleria sp.*) The species representation was similar for *Gesneria* (78.6%) and for *Rhytidophyllum* (80%), the two largest genera of Gesneriinae.

Internal nodes received high support throughout the tree, even for the backbone of the phylogeny with a posterior probability between 0.68 and 0.99 for the four most internal nodes of Gesneriinae (Figure 16). Most of the nodes are supported with a posterior probability (pp) > 0.90 and 44 nodes had a support of $pp = 1$ in total. A clade consisting of genera *Rhytidophyllum* and *Gesneria* received moderate support ($pp = 0.63$), and the two genera did not form reciprocally monophyletic groups due to the placement of *G. onacaensis* and *G. decapleura* with *Rhytidophyllum* and due to the grouping of *R. grande* within *Gesneria*. Low support was found for some nodes within *Gesneria* ($pp < 0.5$), especially for closely related species (e.g the *G. calycosa*, *G. jamaicensis*, *G. scabra* clade with a $pp < 0.5$), or for the clade that includes the hybrid species *G. cornuta* and its parents *G. bicolor* and *G. flava* (Joly et al., 2023).

Clade support was also good in the *Rhytidophyllum* group, except for the closely related species *R. exsertum*, *R. tomentosum*, *R. villosum*, and *R. crenulatum*, where species were not recovered as monophyletic. Samples of *R. auriculatum* individuals also did not necessarily group together, with high support ($pp > 0.8$). The only other case of a non-monophyletic species is *G. viridiflora*.
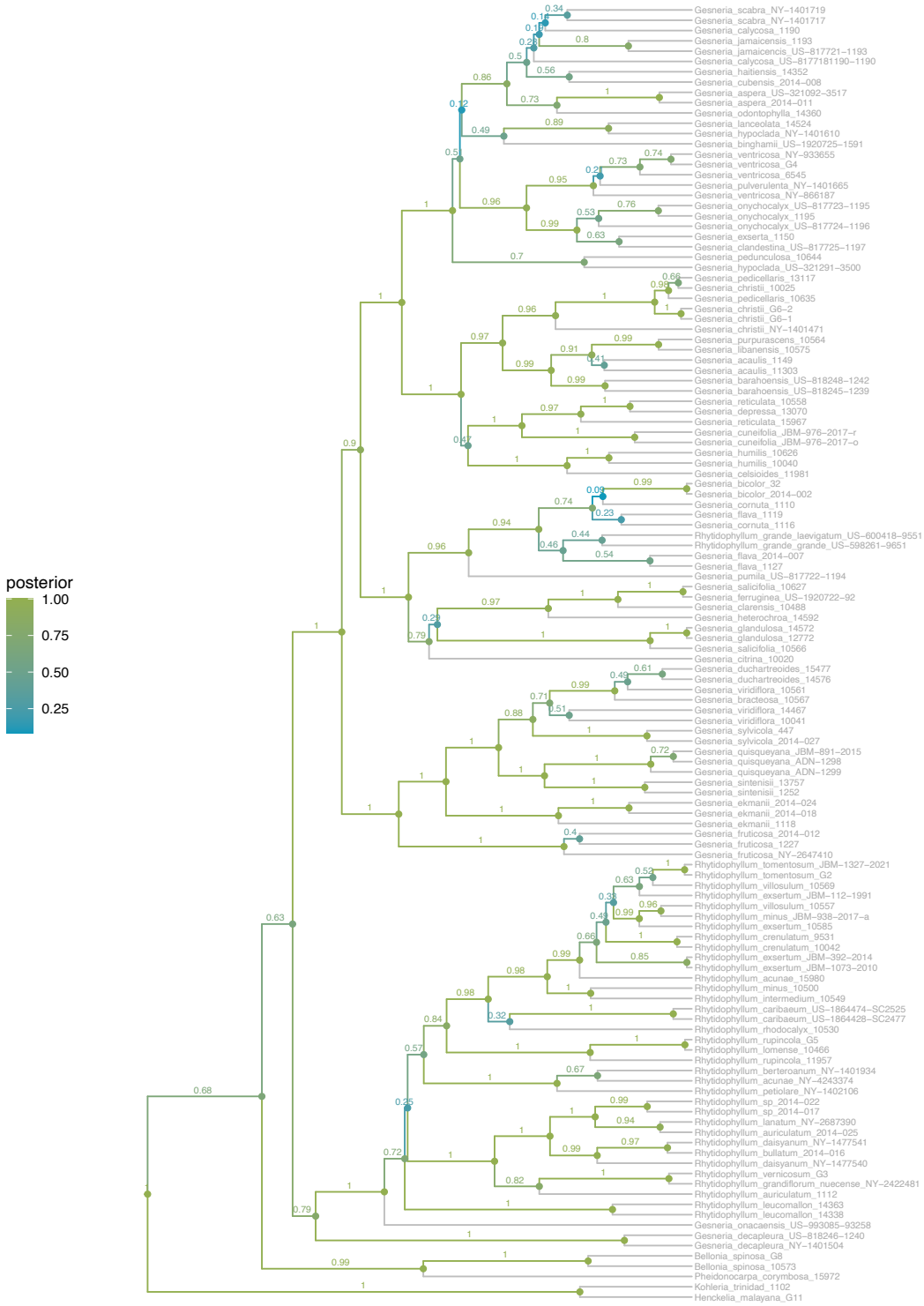
Figure 16. Complete maximum clade credibility (MCC) tree with node posterior probabilities of Antillean Gesneriaceae (Gesneriineae).

3.3. Diversification analysis

3.3.1. Model selection

To better incorporate sampling fraction bias, the sampling fraction f of each pollination syndrome was informed for all models. Half of the bat specialists were present in this study ($f_b = 0.55$), and most of the specialists for hummingbirds and generalists were taken into account ($f_h = 0.71$, $f_g = 0.82$).

Diversification rates did not seem to vary among pollination syndromes, as the trivial null model received the highest AICc weight ($w = 0.38$) (Table 5). The MuSSE that accounted for the three distinct pollination syndromes received the second highest score ($w = 0.21$) and is within 2 units of AICc from the best model. The non-trivial null model CID-2 was the third best model ($w = 0.17$), followed by the MuSSE model that accounted for a binary coding of the syndromes (specialists vs. generalists; $w = 0.14$). All other models received low weights ($w < 0.07$).

Table 5. Comparison of character-dependant (SSE) and character-independent (null and CID) models of diversification. The trivial null model assumes no variation in diversification rates. The MuSSE (specialist vs. generalists) model assumes a distinct diversification rate among specialists and generalists, and the MuSSE model (3 pollination strategies) attributes different diversification rates to bat specialists, hummingbird specialists, and generalists. Hidden characters linked to diversification rates (MuHiSSE) were also included. **nhs** the number of hidden states, **ndp** the number of diversification parameters (turnover + extinction fraction), **ntp** the number of transition parameters, δ the differences in AICc, and w the Akaike weights of alternative models.

Model	lnL	nhs	ndp	ntp	AIC	AICc	δ	w
trivial null	-56.53	1	2	6	129.05	131.58	0	0.38
MuSSE (3 pollination strategies)	-54.37	1	4	6	128.74	132.74	1.16	0.21
CID-2	-54.58	2	3	7	129.15	133.15	1.57	0.17
MuSSE (specialists vs. generalists)	-56.19	1	3	6	130.38	133.60	2.02	0.14
CID-3	-54.14	3	4	7	130.29	135.18	3.60	0.06
CID-4	-53.76	4	5	7	131.51	137.40	5.82	0.02
MuHiSSE (specialists vs. generalists)	-54.22	2	5	7	132.44	138.33	6.75	0.01
MuHiSSE (3 pollination strategies)	-52.93	2	7	7	133.86	142.10	10.52	0
CID-6	-53.74	6	7	7	135.49	143.72	12.14	0

3.3.2. Rates of diversification

Parameter estimates from the trivial null model suggest very low extinction rates ($\mu = 5.944e^{-09}$, scaled in units of total tree length), such that net diversification rates, speciation rates and turnover rates were the same ($\tau = r = \lambda = 2.884$)(Figure 17). The extinction fraction was also very low ($\epsilon = 2.061e^{-09}$).

The second best (MuSSE) model that accounted for distinct rates of diversification among the three pollination syndromes retrieved similar patterns of rate estimation for hummingbird specialist and generalist, but not for the bat specialist syndrome (Figure 17). Although very similar, net diversification rates were estimated to be slightly higher for hummingbirds ($r = 3.369$) than for generalists ($r = 3.258$). Net diversification was estimated to be extremely low for bat specialists ($r = 2.061e^{-09}$).
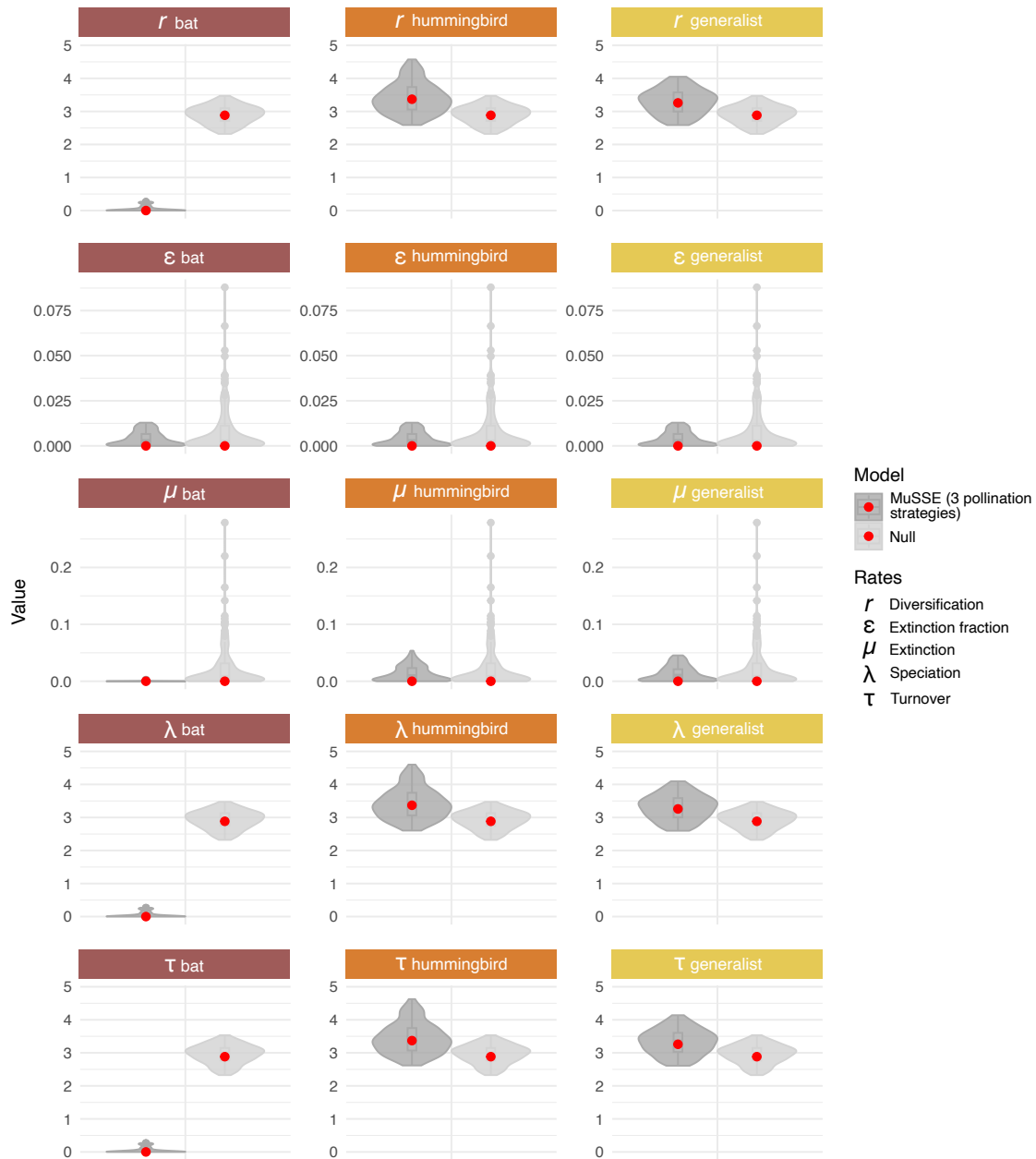
Figure 17. Diversification rates estimates obtained with the MuSSE (3 distinct pollination strategies) and null models. The red dots show the maximum likelihood estimates and the violin plots the confidence interval estimated by sampling point values within a 2 lnL region of the likelihood surface for diversification rates ($r = \lambda - \mu$), extinction fraction ($\epsilon = \mu/\lambda$), extinction ($\mu = (\tau\epsilon)/(1+\epsilon)$), speciation ($\lambda = \tau/(1+\epsilon)$), and turnover ($\tau = \lambda + \mu$).

3.3.3. Pollination syndrome shifts

The transition between syndromes was left free among each pollination syndrome (bat specialist, hummingbird specialist, and generalist). It differed among the null and MuSSE models

with distinct diversification rates among the three pollination syndromes (Figure 18). The highest transition rates obtained with both the null and MuSSE models were the ones between the bat and hummingbird strategies ($q > 1$). Shifts from generalist to bat specialist and hummingbird specialists were also relatively high for both the null and MuSSE models (Figure 18). The main differences between models were found for transition rates towards generalisation. The transition rate from bat specialist to generalist was close to 0 for the null model and the transition rate from hummingbird to generalist was almost 0 for the MuSSE model. For both models, however, transition rates were always greater from generalists to specialists than the opposite.
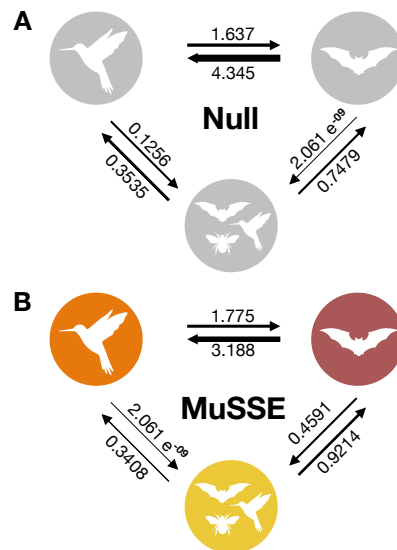
Figure 18. Transition rate matrices among pollination syndrome (bat specialist, hummingbird specialist, and generalist) for the null model (A) and for the MuSSE model that accounts for different rates of diversification for the three pollination distinct syndromes (B).

3.3.4. Ancestral state reconstruction of pollination syndromes

The ancestral state reconstruction (ASR) based on marginal reconstruction (MR) for the best-supported (null) model gives the probabilities of observing the character states at the internal nodes, considering the states at the tip of the tree. The ASR strongly supports that the generalist syndrome is ancestral to the group (Figure 19). All bat specialists appear as independent events of convergence. In the *Rhytidophyllum* clade, most species are generalists and the hummingbird pollination syndrome only appears as a recent convergence for *R. bullatum*, *R. berteroanum*, *R. acunae* and for the most recent ancestor (MRA) of the very close sister species *R. rupincola* and *R. lomense*.

In contrast, approximately half the *Gesneria* species have a specialist syndrome for humming-bird pollination, with a few ancestral switches from generalist to hummingbird specialist (for

G. citrina, and the two sister species *G. salicifolia* and *G. glandulosa*). A single reversion from hummingbird specialists towards a generalised pollination strategy was observed for *G. celsioides*.

Uncertainty on the internal nodes within the *Gesneria* clade switching from generalist to specialist for hummingbird (or bat specialist) highlights a possibility for additional convergences from a generalist syndrome towards hummingbird specialists instead of a single event. The bat syndrome takes on much more weight in deep nodes of the hummingbird pollinated *Gesneria*, which is not the case with the MuSSE models that account for distinct rates of diversification among the three pollination strategies (see Figure S18). In both cases, the generalist syndromes dominate the probabilities at the root of the tree, despite the presence of two hummingbird-pollinated species (*Pheidonocarpa corymbosa* and *G. decaleura*) that branch at the base of the tree.
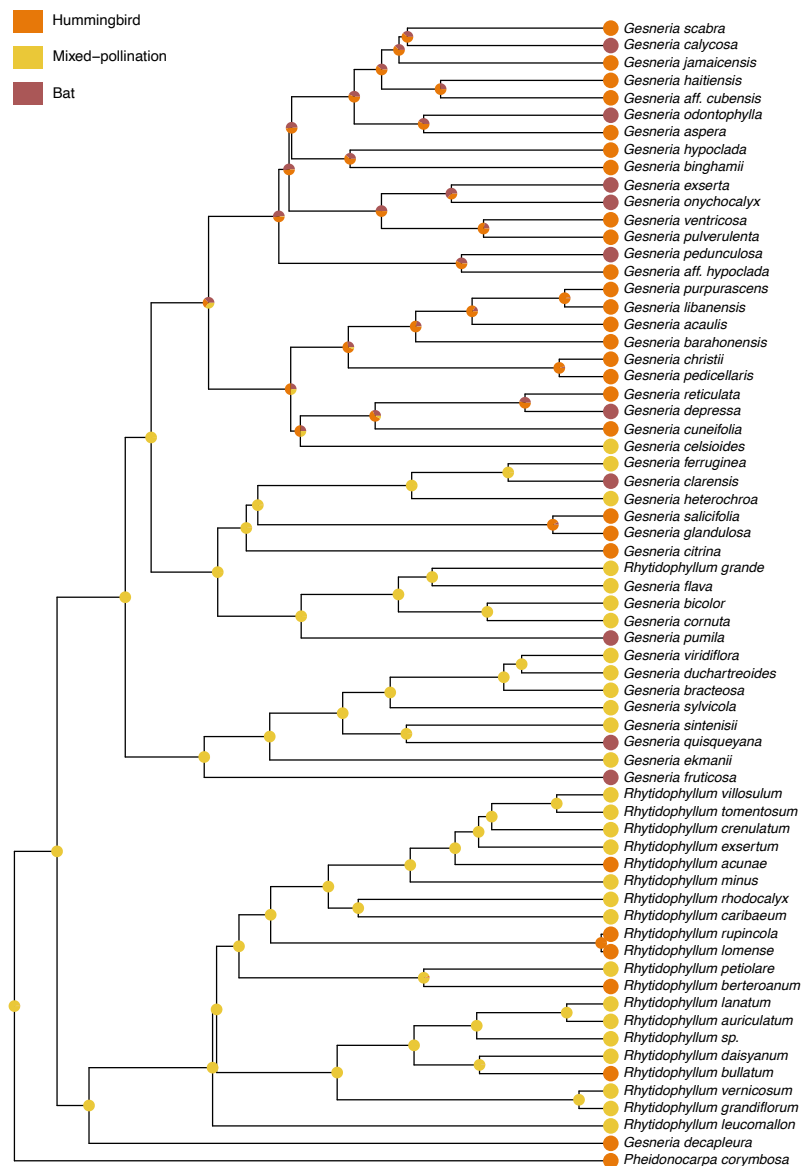
Figure 19. Ancestral state reconstruction according to the null MuSSE model of diversification of specialists for hummingbirds, bats and mixed-pollinated strategies of pollination across Antillean Gesneriaceae.

4. Discussion

4.1. Phylogeny of Antillean Gesneriaceae

Efforts have been made to describe and revise the taxonomy of Gesneriaceae, often characterised as a "taxonomist's nightmare" due to the constant revisions in the classification (Clark, 2020). At higher taxonomic levels, the backbone of the Gesneriaceae is well-resolved (Perret et al.,

2013), but not within Gesneriinae (Joly et al., 2018). The phylogeny we obtained represents the most comprehensive phylogeny of Antillean Gesneriaceae (Gesneriinae) through a combination of previously published and newly generated sequence data. It is consistent with previous studies in the placement of *Pheidonocarpa* L.E.Skog and *Bellonia* L. as sister genera to the Gesneriinae (see Smith et al., 2004a; Martén-Rodríguez et al., 2010; Watson, 2015) even though these relationships are not strongly supported. Several inconsistencies have been described in the literature concerning the monophyly of the genera *Rhytidophyllum* and *Gesneria*. The genus *Rhytidophyllum* has either been considered as monophyletic within a paraphyletic *Gesneria* (Zimmer et al., 2002; Joly et al., 2018) or both *Rhytidophyllum* and *Gesneria* have been supported as monophyletic (Smith et al., 2004a; Martén-Rodríguez et al., 2010; Watson, 2015). In our analyses, two species of *Gesneria* are placed in the *Rhytidophyllym* clade, suggesting the need for careful taxonomic assessment of the generic affinities of these two species, rather than bringing into doubt the monophyly of *Gesneria*.

Clark et al. (2020) had already noted the difficulty of assignning *Gesneria onacaensis* as either a *Gesneria* or *Rhytidophyllum*. Other species could also benefit from taxonomic revisions as they did not fall within the genus in which they have been placed. For example, our analyses place one species of *Rhytidophyllum*, *R. grande*, in the *Gesneria* clade.

However, by improving the scale and robustness of relationships, the present phylogeny also suggests the position of two new undescribed species of *Rhytidophyllum* as closely related to *R. lanatum* and to the *R. vernicosum* and *R. grandifolium* clade.

4.2. Diversification of specialists and generalists

Insular systems play a key role in advancing foundational theories in biogeography and elucidating the mechanisms driving diversification processes. They provide a unique opportunity to examine how specialist and generalist pollination syndromes directly impact speciation and extinction dynamics. Notably, the unique floral shapes associated with mixed pollination in the Gesneriinae (Martén-Rodríguez et al., 2009), observed solely in the Antilles amongst the New World Gesneriaceae (Martén-Rodríguez et al., 2015), suggest a possible advantageous strategy relative to specialists. Because extreme climatic perturbations can affect pollinator communities, relying on a single functional type of pollinator could increase species extinction risks with a specialised pollination syndrome. In this context, plants relying on a single pollinator species or functional type of pollinators, could be at high risk of extinction, whereas pollination generalists should be more resilient to the loss of a subset of the pollinator community (see review by Johnson and Steiner, 2000). In this context, specialists could represent an evolutionary dead-end.

The reconstruction of ancestral pollination syndromes in Gesneriinae resolves a generalist as the ancestral ancestor to all Gesneriinae. The generalist syndrome appears now as a plesiomorphic adaptation instead of resulting from distinct origins of this strategy (Martén-Rodríguez et al.,

2010; Joly et al., 2018). Evolution to a specialised syndrome for hummingbird pollination is mostly represented in a single clade of Gesneria with few cases of convergence across the phylogeny.

Contrary to our hypotheses, generalists do not have higher diversification rates, but rather similar rates to specialists, suggesting that pollination syndromes may not be the main driver of extensive diversification in our study group. Hummingbird specialists actually had slightly higher diversification rates than generalists, considering the second-best model selected. The generalist syndrome provided a means of shifting to more specialised strategies, either bat or hummingbird specialists. Interestingly, bat specialists had significantly lower diversification rates than hummingbird specialists. So generalists did have a higher diversification rate than some specialists – bats specialists – but not hummingbird species, highlighting the risk of categorising all specialists under a single umbrella.

Considering only pollination syndromes probably fails to capture the main adaptation driving diversification. Other factors may be at play in driving diversification patterns. The predominance of a single large group of species solely pollinated by hummingbirds may influence the model fitting and support the notion that other factors may have influenced the diversification rates of this particular clade. This could be due to an adaptive trait (e.g. the habit of the plant, like lithophytic rosettes or erect bushes) or to non-adaptive processes such as speciation through geographic isolation (see Givnish, 2015, for examples). Antillean Gesneriaceae also underwent a recent geographic isolation while colonising the different islands of the archipelago. Geographic isolation and limited dispersal among islands, alongside frequent cases of endemism within mountain habitats on islands, could also potentially influence the patterns of species diversification. The role of geographic modes of speciation within Antillean Gesneriaceae (Gesneriinae) might thus have strongly influenced diversification rates in this group. Additionally, the long life span of Gesneriinae could also provide a compensatory mechanism that delays the extinction of specialised species (see Johnson and Steiner, 2000), and thus mitigate model selection towards a multivariate model of evolution.

This context of geographical and temporal isolation in Antillean Gesneriaceae dovetails with broader theories on the evolution of specialists and generalists. Temporally stable environments should lead to the evolution of specialists whereas varying environments should advantage generalists (Kassen, 2002; Svanbäck et al., 2009). Similarly, specialists should be selected in spatially homogeneous environments and generalists in heterogeneous environments, although local adaptation of specialists is also possible in spatially heterogeneous habitats, with great costs of adaptation to other habitat patches (Kassen, 2002).Grinnellian specialists, which are geographically rare and therefore extinction-prone species, are also more likely to persist if they adopt a generalist strategy locally (Williams et al., 2006). Thus, species prone to extinction are more likely to persist if they adopt a more generalised strategy of resource exploitation.

Nevertheless, non-significant results could also arise from small sample sizes in the diversification analysis. Firstly, only about half (55%) of the knwown bat specialists were present in

our study, even though only a few species with this syndrome exist according to field observations. Though incomplete, the proportion of specialists and generalists was relatively high (71% and 82% respectively). Secondly, trait-dependant analyses of diversification depend on tree size (number of species) and tree robustness to get reliable estimates to detect the influence of traits on diversification rates. Including GBS data helped improve the phylogeny, but the number of tips is still relatively small even though it is an almost complete phylogeny of the Gesneriinae subtribe with a sampling ratio well above the recommended 25% (FitzJohn et al., 2009). Several species also had to be excluded due to a lack of pollination information and morphological data for inference of syndrome. In addition to unknown syndromes, a moth and bee specialist species respectively were not included. Despite the lack of convergence for these two syndromes within Gesneriinae, they represent an alternative avenue of adaptation.

5. Conclusions

Using the most extensive phylogeny for the model group of Antillean plants of Gesneriaceae to date, we explored how pollination strategies have played a role in the diversification patterns in this recently diverged group. Contrary to the initial hypothesis of higher success of generalists, we demonstrate that specialisation is not an evolutionary dead end in archipelagos and diversifies at the same rate as generalists. We also observed contrasting rates of evolution among bat and hummingbird specialists. More complex patterns of interplay between trait evolution, biotic interactions and geography may be at play in Antillean Gesneriaceae. The Antilles are a biodiversity hot-spot with high levels of endemism (Clark et al., 2020; Smith et al., 2004b) but most of the land areas of the archipelago remain largely unprotected (Smith et al., 2004b). New species are continuously being described in this group (Clark et al., 2020; Joly et al., 2023), and few pollination observations are available for most of the Gesneriinae species. More efforts to assess the diversity and pollination strategies in this group will improve our understanding of the evolutionary dynamics of specialists and generalists in the particular context of neotropical archipelagos and at larger scales between the mainland and island groupings.

6. Conflict of interest statement

The authors have no conflict of interest to declare.

7. Ackowledgments

William and Lynda Steere Herbarium at the New York Botanical Garden and the National Herbarium at the Natural Museum of Natural History, Smithsonian Institution for preparing and gifting specimens samples. Herbarium staff for maintaining and managing the collections. The

Bibliography

Acevedo-Rodríguez, P. and Strong, M. T. (2012). Catalogue of seed plants of the west indies. *Smithsonian Contributions to Botany*, 98.

Alfaro, M. E., Santini, F., Brock, C., Alamillo, H., Dornburg, A., Rabosky, D. L., Carnevale, G., and Harmon, L. J. (2009). Nine exceptional radiations plus high turnover explain species diversity in jawed vertebrates. *Proceedings of the National Academy of Sciences*, 106(32):13410–13414.

Andrews, K. R., Good, J. M., Miller, M. R., Luikart, G., and Hohenlohe, P. A. (2016). Harnessing the power of radseq for ecological and evolutionary genomics. *Nature Reviews Genetics*, 17(2):81.

Andrews, S. et al. (2010). Fastqc: a quality control tool for high throughput sequence data.

Barrett, S. C. H. (1996). The reproductive biology and genetics of island plants. *Philosophical Transactions of the Royal Society of London. Series B: Biological Sciences*, 351(1341):725–733.

Beaulieu, J. M. and O'Meara, B. C. (2016). Detecting hidden diversification shifts in models of trait-dependent speciation and extinction. *Systematic biology*, 65(4):583–601.

Bouckaert, R., Vaughan, T. G., Barido-Sottani, J., Duchêne, S., Fourment, M., Gavryushkina, A., Heled, J., Jones, G., Kühnert, D., De Maio, N., et al. (2019). Beast 2.5: An advanced software platform for bayesian evolutionary analysis. *PLoS computational biology*, 15(4):e1006650.

Clark, J. (2020). The caribbean gesneriaceae: an update on the classification of gesneria and rhytidophyllum. *Gesneriads*, 70:10–20.

Clark, J., Skog, L., Boggan, J., and Ginzbarg, S. (2020). Index to names of new world members of the gesneriaceae (subfamilies sanangoideae and gesnerioideae). *Rheedea*, 30(1):190.

Colles, A., Liow, L. H., and Prinzing, A. (2009). Are specialists at risk under environmental change? neoecological, paleoecological and phylogenetic approaches. *Ecology letters*, 12(8):849–863.

Doyle, J. J. and Doyle, J. L. (1987). A rapid dna isolation procedure for small quantities of fresh leaf tissue. *Phytochemical bulletin*.

Drummond, A. J., Ho, S. Y., Phillips, M. J., and Rambaut, A. (2006). Relaxed phylogenetics and dating with confidence. *PLoS biology*, 4(5):e88.

Drummond, A. J., Nicholls, G. K., Rodrigo, A. G., and Solomon, W. (2002). Estimating mutation parameters, population history and genealogy simultaneously from temporally spaced sequence data. *Genetics*, 161(3):1307–1320.

Eaton, D. A. and Overcast, I. (2020). ipyrad: Interactive assembly and analysis of radseq datasets. *Bioinformatics*, 36(8):2592–2594.

Faure, J. and Joly, S. (2020). Pollinator performance of the pollination generalist rhytidophyllum bicolor (gesneriaceae) in haiti 15 months after the matthew hurricane. *Selbyana*, 33(3).

FitzJohn, R. G. (2012). Diversitree: comparative phylogenetic analyses of diversification in r. *Methods in Ecology and Evolution*, 3(6):1084–1092.

FitzJohn, R. G., Maddison, W. P., and Otto, S. P. (2009). Estimating trait-dependent speciation and extinction rates from incompletely resolved phylogenies. *Systematic biology*, 58(6):595–611.

Givnish, T. J. (2015). Adaptive radiation versus 'radiation'and 'explosive diversification': why conceptual distinctions are fundamental to understanding evolution. *New Phytologist*, 207(2):297–303.

Johnson, S. D. and Steiner, K. E. (2000). Generalization versus specialization in plant pollination systems. *Trends in ecology & evolution*, 15(4):140–143.

Joly, S., Lambert, F., Alexandre, H., Clavel, J., Léveillé-Bourret, E., and Clark, J. L. (2018). Greater pollination generalization is not associated with reduced constraints on corolla shape in Antillean plants. *Evolution*.

Joly, S., Lambert, F., Cinea, W., and Clark, J. L. (2023). Three new gesneria species (gesneriaceae) support parc national pic macaya (haiti) as an important biodiversity hotspot. *Systematic Botany*, 48(1):34–43.

Joly, S., Starr, J. R., Lewis, W. H., and Bruneau, A. (2006). Polyploid and hybrid evolution in roses east of the rocky mountains. *American Journal of Botany*, 93(3):412–425.

Kassen, R. (2002). The experimental evolution of specialists, generalists, and the maintenance of diversity. *Journal of evolutionary biology*, 15(2):173–190.

MacArthur, R. H. and Wilson, E. O. (1963). An equilibrium theory of insular zoogeography. *Evolution*, 17(4):373–387.

Maddison, W. P., Midford, P. E., and Otto, S. P. (2007). Estimating a binary character's effect on speciation and extinction. *Systematic biology*, 56(5):701–710.

Martén-Rodríguez, S., Fenster, C. B., Agnarsson, I., Skog, L. E., and Zimmer, E. A. (2010). Evolutionary breakdown of pollination specialization in a caribbean plant radiation. *New Phytologist*, 188(2):403–417.

Martín-Hernanz, S., Aparicio, A., Fernández-Mazuecos, M., Rubio, E., Reyes-Betancort, J. A., Santos-Guerra, A., Olangua-Corral, M., and Albaladejo, R. G. (2019). Maximize resolution or minimize error? using genotyping-by-sequencing to investigate the recent diversification of helianthemum (cistaceae). *Frontiers in plant science*, 10:1416.

Martén-Rodríguez, S., Almarales-Castro, A., and Fenster, C. B. (2009). Evaluation of pollination syndromes in Antillean Gesneriaceae: evidence for bat, hummingbird and generalized flowers. *Journal of Ecology*, 97(2):348–359.

Martén-Rodríguez, S. and Fenster, C. B. (2008). Pollination Ecology and Breeding Systems of Five Gesneria Species from Puerto Rico. *Annals of Botany*, 102(1):23–30.

Martén-Rodríguez, S., Quesada, M., Castro, A.-A., Lopezaraiza-Mikel, M., and Fenster, C. B. (2015). A comparison of reproductive strategies between island and mainland Caribbean Gesneriaceae. *Journal of Ecology*, 103(5):1190–1204.

McKinney, M. L. (1997). Extinction vulnerability and selectivity: combining ecological and paleontological views. *Annual review of ecology and systematics*, 28(1):495–516.

Miller, A. H., Stroud, J. T., and Losos, J. B. (2023). The ecology and evolution of key innovations. *Trends in Ecology & Evolution*, 38(2):122–131.

Miller, M. R., Dunham, J. P., Amores, A., Cresko, W. A., and Johnson, E. A. (2007). Rapid and cost-effective polymorphism identification and genotyping using restriction site associated dna (rad) markers. *Genome research*, 17(2):240–248.

Nakov, T., Beaulieu, J. M., and Alverson, A. J. (2018). Accelerated diversification is related to life history and locomotion in a hyperdiverse lineage of microbial eukaryotes (diatoms, bacillariophyta). *New Phytologist*, 219(1):462–473.

Pennell, M. W., Eastman, J. M., Slater, G. J., Brown, J. W., Uyeda, J. C., FitzJohn, R. G., Alfaro, M. E., and Harmon, L. J. (2014). geiger v2. 0: an expanded suite of methods for fitting macroevolutionary models to phylogenetic trees. *Bioinformatics*, 30(15):2216–2218.

Perret, M., Chautems, A., De Araujo, A. O., and Salamin, N. (2013). Temporal and spatial origin of gesneriaceae in the new world inferred from plastid dna sequences. *Botanical Journal of the Linnean Society*, 171(1):61–79.

Poland, J. A., Brown, P. J., Sorrells, M. E., and Jannink, J.-L. (2012). Development of high-density genetic maps for barley and wheat using a novel two-enzyme genotyping-by-sequencing approach. *PloS one*, 7(2):e32253.

Rabosky, D. L. (2014). Automatic detection of key innovations, rate shifts, and diversity-dependence on phylogenetic trees. *PloS one*, 9(2).

Rambaut, A., Drummond, A. J., Xie, D., Baele, G., and Suchard, M. A. (2018). Posterior summarization in bayesian phylogenetics using tracer 1.7. *Systematic biology*, 67(5):901–904.

Regalado, L., Lóriga, J., Bechteler, J., Beck, A., Schneider, H., and Heinrichs, J. (2018). Phylogenetic biogeography reveals the timing and source areas of the adiantum species (pteridaceae) in the west indies, with a special focus on cuba. *Journal of Biogeography*, 45(3):541–551.

Ricklefs, R. and Bermingham, E. (2008). The west indies as a laboratory of biogeography and evolution. *Philosophical Transactions of the Royal Society B: Biological Sciences*, 363(1502):2393–2413.

Smith, J. F., Draper, S. B., Hileman, L. C., and Baum, D. A. (2004a). A phylogenetic analysis within tribes gloxinieae and gesnerieae (gesnerioideae: Gesneriaceae). *Systematic Botany*, 29(4):947–958.

Smith, M., Hedges, S., Buck, W., Hemphill, A., Inchaustegui, S., Ivie, M., Martina, D., Maunder, M., and Francisco-Ortega, J. (2004b). Caribbean islands. In CEMEX, M., editor, *Hotspots revisited: earth's biologically richest and most threatened terrestrial ecoregions*, Cemex books

on nature, pages 112–118. Agrupacion Sierra Madre.

Stamatakis, A. (2014). Raxml version 8: a tool for phylogenetic analysis and post-analysis of large phylogenies. *Bioinformatics*, 30(9):1312–1313.

Svanbäck, R., Pineda-Krch, M., and Doebeli, M. (2009). Fluctuating population dynamics promotes the evolution of phenotypic plasticity. *The American Naturalist*, 174(2):176–189.

Vences, M., Patmanidis, S., Kharchev, V., and Renner, S. S. (2022). Concatenator, a user-friendly program to concatenate dna sequences, implementing graphical user interfaces for mafft and fasttree. *Bioinformatics Advances*, 2(1):vbac050.

Warren, B. H., Simberloff, D., Ricklefs, R. E., Aguilée, R., Condamine, F. L., Gravel, D., Morlon, H., Mouquet, N., Rosindell, J., Casquet, J., et al. (2015). Islands as model systems in ecology and evolution: Prospects fifty years after macarthur-wilson. *Ecology Letters*, 18(2):200–217.

Watson, D. R. (2015). *Resolving generic boundaries in Rhytidophyllum and Gesneria: A molecular phylogeny of the Caribbean subtribe gesneriinae (gesneriaceae)*. M.s., Department of Biological Sciences in the Graduate School of The University of Alabama, Ann Arbor, United States.

Wessinger, C. A., Rausher, M. D., and Hileman, L. C. (2019). Adaptation to hummingbird pollination is associated with reduced diversification in penstemon. *Evolution letters*, 3(5):521–533.

Williams, Y. M., Williams, S. E., Alford, R. A., Waycott, M., and Johnson, C. N. (2006). Niche breadth and geographical range: ecological compensation for geographical rarity in rainforest frogs. *Biology letters*, 2(4):532–535.

Zenil-Ferguson, R., McEntee, J. P., Burleigh, J. G., and Duckworth, R. A. (2023). Linking ecological specialization to its macroevolutionary consequences: An example with passerine nest type. *Systematic Biology*, 72(2):294–306.

Zimmer, E. A., Roalson, E. H., Skog, L. E., Boggan, J. K., and Idnurm, A. (2002). Phylogenetic relationships in the gesnerioideae (gesneriaceae) based on nrdna its and cpdna trnl-f and trne-t spacer region sequences. *American journal of Botany*, 89(2):296–311.

Discussion

L'objectif de cette thèse était de mieux comprendre l'interaction entre les pressions de sélection liées à des stratégies de pollinisation distinctes et les compromis adaptatifs aux échelles micro et macroévolutives. En utilisant le groupe des Gesneriaceae des Antilles (Gesneriinae), leurs stratégies de pollinisation spécialisées et généralistes et leurs morphologies florales ont été étudiées aux échelles intraspécifique à interspécifique, micro- à macro-évolutive, et 2D à 3D.

L'évolution de la forme des fleurs, et leur variation intra-spécifique

Résumé des résultats

Le premier chapitre explore le rôle des principales stratégies de pollinisation observées chez les Gesneriinae, c'est à dire la spécialisation pour la pollinisation par les colibris et la stratégie généralistes, sur les modèles évolutifs suivis par la variation intraspécifique de la forme de leurs corolle, soit l'ensemble des pétales de la fleur. Selon l'hypothèse de variation de niche, étant donné que la pollinisation est effectuée par divers groupes fonctionnels de pollinisateurs et qu'elles exploitent donc une niche écologique plus large, les espèces généralistes devraient avoir une morphologie florale plus variable que les spécialistes. La caractérisation de la forme des profils des fleurs des Gesneriinae et l'analyse de leurs formes selon trois analyses phylogénétiques comparatives ont pu mettre en évidence le rôle crucial joué par les stratégies de pollinisation dans la variation de leur morphologie florale, tant au niveau micro- qu'au niveau macro-évolutif. Les trois approches utilisées (PGLS, mcMORPH, JIVE) prennent différemment en compte la dimensionnalité de la morphologie des fleurs (la morphologie complète ou une décomposition de la forme selon les axes principaux de variation), les syndromes ancestraux (l'utilisation de simulation de syndromes ancestraux), et l'erreur associée à l'estimation de la variance (l'utilisation de la variance calculée par espèce ou l'utilisation de chaque valeurs individuelles par espèces). En tenant compte de ces trois approches, cette étude suggère que les stratégies généralistes montrent une plus grande variation intraspécifique de la forme de la corolle que les stratégies spécialisées, bien que les résultats obtenus avec l'approche JIVE soient plus ambigus. Selon ces résultats, les généralistes semblent tendre à évoluer vers des profils de fleurs qui sont d'autant plus variables au niveau de leur tubularité que leur courbure en comparaison avec les spécialistes des colibris. Ces résultats

soutiennent l'hypothèse de la variation de niche, mais démontrent également que tous les aspects de la corolle ne suivent vraisemblablement pas le même patron de variation.

L'évolution de la variance intraspécifique est rarement considérée à l'échelle macroévolutive malgré l'influence des forces sélectives qui s'appliquent à cette échelle (Gaboriau et al., 2020). La prise en compte du rôle de l'évolution de la variation intraspécifique de la morphologie florale de concert avec les stratégies de pollinisation est novatrice en ce sens. Ce premier chapitre appuie l'idée qu'il est important de prendre en compte la variation intraspécifique comme composante sous sélection dans la modélisation des traits phénotypiques en lien avec les régimes de sélection, et non pas considérer la variation intraspécifique comme biais de mesures des traits.

Perspectives

Les stratégies de pollinisation des Gesneriinae ne se résument cependant pas aux deux stratégies étudiées dans le premier chapitre. Dans le but de mieux comprendre comment évolue la forme des fleurs selon les stratégies de pollinisation des Gesneriinae, le fait d'inclure le troisième syndrome le plus représenté chez les Gesneriinae, c'est à dire les spécialistes pour les chauves-souris, permettrait aussi de comparer la variation entre systèmes spécialisés, et entre plusieurs systèmes spécialisés et les généralistes. Le fait d'inclure la stratégie de pollinisation par les chauves-souris dans le cadre de cette étude serait d'autant plus intéressant que la forme des fleurs de cette stratégie sont relativement similaires à celles des généralistes. Par exemple, les spécialistes pour la pollinisation par les chauves-souris *Gesneria fruticosa* (L.) Kuntze et *Gesneria quisqueyana* Alain ont des morphologies semblables à *Gesneria bicolor* (Rub.) Simon Joly & J.L.Clark et *Rhytidophyllum exsertum* Griseb., qui sont des généralistes (voir chapitre 2). La forme moyenne des fleurs appartenant à ces deux syndromes sont aussi très semblables (voir chapitre 2 également). Ajouter le syndrome spécialisé pour la pollinisation par les chauve-souris pourrait aussi nous en apprendre plus sur les contraintes mécaniques d'attraction et d'exclusion de certains pollinisateurs pour ces 3 syndromes. Les fleurs généralistes et spécialistes des chauve-souris sont suffisamment similaires dans leur ouverture pour permettre la pollinisation par les chauve souris qui ont besoin de s'introduire dans la fleur, mais la constriction de la corolle des généralistes force les colibris à toucher les organes reproducteurs en se plaçant proche de la paroi supérieur de la corolle où se trouvent les organes reproducteurs pour accéder au nectar au delà de la constriction. Le premier axe de l'ACP du premier chapitre représente la variation des fleurs de Gesneriinae selon leur tubularité, et donc l'exclusion des pollinisateurs autres que des colibris, et le second et troisième axe de l'ACP représentent la variation du degré de constriction de la corolle et l'incurvation de la corolle. Inclure les espèces spécialistes pour les chauve-souris permettrait ainsi de distinguer plus précisément les forces de sélection sur la variation de la constriction et l'ouverture de la corolle. Inclure les espèces spécialistes pour les chauves-souris permettrait également de rejoindre le troisième chapitre de cette thèse où les trois syndromes principaux des Gesneriinae ont pu être pris en compte. Ce sont en tout 4 espèces de spécialistes pour les chauves-souris qui pourraient

d'ores et déjà être prises en compte avec le jeu de données collecté pour cette étude, autant d'un point de vue génétique que morphologique.

Selon la mécanique actuelle des méthodes utilisées dans le premier chapitre, la caractérisation de la forme des fleurs pourrait dores et déjà se faire plus précisément qu'avec l'utilisation de profils de fleurs uniquement. Pour une partie des fleurs utilisées dans ce premier chapitre, des images de face sont disponibles grâce à la collaboration avec John L. Clark et ses efforts d'échantillonnage. Il serait possible de transformer le jeu de données actuel, et d'associer les profils de fleurs à leurs faces individuelles de façon orthogonales afin de les analyser simultanément en pseudo-3D (Schat et al., 2020; Faure et al., 2023). Au delà de la pseudo-3D, il serait aussi intéressant de caractériser plus précisément la variation intraspécifique des fleurs en 3D par espèce. Bien que l'obtention de ces nouvelles données, notamment plusieurs individus par espèce, représente d'un défi majeur, l'utilisation de la photogrammétrie devrait pouvoir faciliter cette tâche.

En plus d'une meilleure estimation de la variation inter et intraspécifique, l'estimation complète de la distribution des traits à l'intérieur des espèces pourrait aussi nous permettre de tester le rôle de la variation comme facteur structurant en écologie des communautés à l'échelle locale et régionale, du fait que la variation intraspécifique permet d'augmenter la coexistence et l'utilisation des ressources des espèces (Violle et al., 2012).

L'évolution de la morphologie florale en trois dimensions

Résumé des résultats

Des caractéristiques traditionnellement utilisées pour décrire des syndromes (couleur, récompense, parfum, forme) peuvent être difficiles à quantifier, et mener à des catégorisations subjectives, et très peu d'études se basent sur de la morphométrie pour quantifier la forme des fleurs (Dellinger, 2020). Afin de prendre en compte toute la complexité tridimensionnelle des fleurs, dans le second chapitre j'ai démontré que l'approche de la photogrammétrie était une méthode pertinente pour caractériser les patrons de variation morphologiques floraux (forme et couleur) en trois dimensions de façon quantitative. En plus de capturer la complexité des fleurs, l'utilisation de la 3D permet aussi d'éviter l'approximation et les erreurs de mesures de la forme du vivant (Cardini et al., 2014). La photogrammétrie devrait représenter un grand pas en avant pour facilement quantifier objectivement les traits morphologiques impliqués dans les syndromes de pollinisation pour une diversité de morphologies florales au delà des formes de fleurs typiques des Gesneriaceae, telles que les fleurs de Fabaceae, Cactaceae, et Lamiaceae (présentées comme exemples), et autant zygomorphes qu'actinomorphes, à corolle tubulaire ou pétales libres, et de tailles tout autant variées. Il a été montré que la photogrammétrie est une alternative à la tomodensitométrie (microCT) qui nécessite peu d'investissement et d'équipement. Les besoins matériels minimaux nécessaires à la numérisation des fleurs pour la photogrammétrie permettent

également une grande flexibilité de transport, et ainsi la facilitation de cette approche sur le terrain. L'approche de la photogrammétrie a ainsi le potentiel de stimuler la recherche sur l'évolution et l'écologie des fleurs en fournissant un moyen simple d'accéder à des données morphologiques tridimensionnelles provenant d'une variété de types de fleurs.

Pour accompagner la démonstration de la pertinence de la photogrammétrie pour modéliser la morphologie florale en trois dimensions, un exemple d'application a pu être présenter en utilisant les Gesneriinae. Dans cet exemple, la forme des fleurs ainsi que leur coloration ont pu être explorées. L'analyse de la forme des fleurs tridimensionnelle montre une claire distinction entre les stratégies spécialistes pour les colibris, spécialistes pour les chauves-souris, et les généralistes. Les spécialistes pour les chauves-souris occupent un espace morphologique proche de celui des généralistes, mais sans pour autant se recouper. Il a aussi pu être proposé que selon leur coloration, les espèces spécialistes pour colibri se regroupent ensemble d'une part, ainsi que les généralistes et spécialistes des chauves-souris d'autre part, bien qu'avec quelques sous groupes qui semblent se distinguer. Les espèces spécialistes des chauves-souris ne se regroupent pas ensemble, mais plutôt avec des sous-groupes de généralistes du fait de leur coloration très variables (verte à points mauves pour *P. prasinata*, vertes et mauves foncées pour *G. fruticosa*, et mauves et orange pour *G. quisqueyana*). En plus de la variation de la forme des fleurs des généralistes, les espèces pollinisées par plusieurs types fonctionnels de pollinisateurs semblent aussi beaucoup varier selon leur coloration.

Perspectives biologiques

En plus de caractériser la corolle des fleurs en trois dimensions, la photogrammétrie permet de reconstruire toutes les structures visibles lors de la numérisation des fleurs. L'analyse morphologique qui a été effectuée dans le second chapitre en guise d'exemple se base sur la forme et couleur de la corolle, mais une direction future pour un projet d'étude de l'évolution de la forme des fleurs à plus large échelle serait d'incorporer les structures reproductrices et les sépales dans la modélisation des fleurs et l'analyse morphologique. La combinaison de la numérisation et de la dissection de différentes parties de la fleurs permettraient d'obtenir des données morphologique sur la position de tous les organes impliqués dans l'attraction des pollinisateurs.

Il pourra être ainsi exploré le rôle de la spécialisation et généralisation sur la modularité des fleurs, c'est à dire si des sous ensembles de traits floraux sont intégrés, et donc si des ensembles de traits co-varient indépendamment d'autres sous-ensembles de traits (Klingenberg, 2014). En particulier les hypothèses d'attraction-reproduction (séparation des structures pour l'attraction des pollinisateurs avec celles pour la reproduction), d'efficacité (séparation des structures pour l'attraction des pollinisateurs avec celles pour la reproduction et l'efficacité de la pollinisation), et de développement (modularité dominée par l'origine développementale des structures) pourraient être explorées en lien avec les syndromes de pollinisation en utilisant le groupe modèle des Gesneriaceae (Dellinger et al., 2019; Reich et al., 2020; Artuso et al., 2021).

En parallèle de la morphologie, la couleur pourra être explorée de façon plus objective. La présence de sous-groupes de généralistes chez les Gesneriaceae laissent penser que la couleur de la surface totale de la fleur pourrait suivre des patrons évolutifs distincts de la forme des fleurs. Il existe déjà des outils de détection et quantification de motifs de variation de coloration (Van Belleghem et al., 2018), mais ce n'est pas encore le cas pour des structures en 3D. L'intégration de tels outils pourraient permettre d'identifier des patrons distincts de coloration pour l'attraction de pollinisateurs. Les Gesneriaceae Antillaises pourraient à nouveau servir de modèle d'étude dans ce cas là, du fait de la grande variation de couleurs (blanches, vertes, jaunes, rouges, pourpres, vertes) et de variations d'ornementation à l'intérieur de la corolle.

Intégrer la diversité de la morphologie florale dans un espace morphologique plus grand en prenant en compte à la fois la forme et la couleur de la corolle, du calice, et la position des structures impliquées dans le dépôt et la réception du pollen, devraient permettre de mieux distinguer les traits qui caractérisent morphologiquement les syndromes de pollinisation. Élargir l'étude à grande échelle taxonomique permettra ainsi de détecter de nouveaux groupes de syndromes du point de vue de leur morphologie. Ce sont principalement le syndrome de pollinisation pour les insectes, le syndrome de pollinisation spécialisé pour la pollinisation par les abeilles et la spécialisation pour la pollinisation par les colibris qui sont retrouvés à large échelle taxonomique chez les Gesneriaceae (Serrano-Serrano et al., 2017).

Perspectives expérimentales

La modélisation 3D permet aussi l'impression de fleurs 3D pour le développement de schémas expérimentaux qui permettent de découpler et quantifier le potentiel des différents signaux d'attraction des pollinisateurs, tels que les signaux visuels (forme et couleur) et les signaux olfactifs (Policha et al., 2016). Il pourra être intéressant de tester si les variations de colorations des fleurs généralistes influencent les proportions des pollinisateurs qui les visitent du fait que plusieurs groupes semblent se distinguer les uns des autres au niveau de leur coloration (chapitre 2).

En lien avec une étude de la modularité des différentes structures qui composent les fleurs, la possibilité de modifier artificiellement la forme des fleurs trait par trait permettrait aussi de déterminer la direction de la sélection des traits floraux impliqués dans la transition d'un syndrome à un autre. Par exemple, Castellanos et al. (2004) ont investigué chez *Penstemon barbatus* (pollinisée presque exclusivement par des colibris) et *Penstemon strictus* (pollinisée par des Hymenotpères) les traits floraux adaptés pour exclure des pollinisateurs moins efficaces (e.g. abeilles), avec ou sans améioration du transfert du pollen par des pollinisateurs plus efficaces (e.g. les oiseaux). La modification artificielle fine des différentes structures et le développement des outils d'impression 3D pourraient permettre de telles expériences à grande échelle. En particulier, il serait intéressant de voir chez les Gesneriinae comment la modification de l'exsertion des anthères, la courbure des fleurs, la présence d'une poche prononcée à la base de la corolle (fleur hypocyrtoïde), la présence

d'une constriction au milieu de la fleur et l'ouverture de la corolle affectent le transfert de pollen par leurs différents pollinisateurs.

Perspectives de collaborations

Suite à la publication de l'article de méthode présentant l'approche de la photogrammétrie comme outil de reconstruction des fleurs en trois dimensions (deuxième chapitre), le protocole qui a été développé et proposer pour application a pu être utilisé dans d'autres laboratoires. Par exemple, JianJun Jin du laboratoire Eaton à l'Université Columbia (États-Unis) a notamment pu reprendre le protocole de photogrammétrie et développer une étape d'empilement de focus (de l'anglais *focus-stacking*) afin d'améliorer la netteté des images à la source du processus de photogrammétrie, et ainsi la facilitation de la détection de la surface de la fleurs numérisée pour en reconstruire la surface en trois dimensions. La proposition d'amélioration de l'automatisation de cette étape a pu donner suite à l'intégration de cette étape dans le protocole original de photo-grammétrie par Loudmila Jelinscaia Lagou de l'université de Munich (Allemagne) et l'Université de Montréal. Cet exemple de collaboration open source est à mon sens une belle démonstration de la rapidité à laquelle la photogrammétrie peut être apprivoisée et développée. Cela laisse penser que rapidement, la morphologie florale de familles de plantes variées pourront être obtenues facile-ment, et ainsi élargir l'échelle taxonomique de notre exemple d'application de la photogrammétrie dans l'étude de la forme et la couleur des Gesneriinae en lien avec leurs stratégies de pollinisation. La mise en avant de la photogrammétrie et de la plate-forme MorphoSource devraient permettre la facilitation de collaboration à large échelle humaine également.

Perspectives éducatives

Un parallèle intéressant à ce second chapitre est qu'historiquement, les premiers modèles 3D de fleurs ont initialement été conçus dans le but d'enseigner la botanique. Le Dr. Goodale, fondateur du musée botanique de l'Université d'Harvard, souhaitait disposer de modèles réalistes du règne végétal pour enseigner la botanique lorsque seuls des modèles approximatifs en papier mâché ou en cire étaient disponibles. Les artisans Leopold et Rudolf Blaschka ont été commissionnés dans ce but et ont produit entre 1887 et 1936 près de 4300 modèles en verres représentant 780 espèces de plantes et leurs différents structures d'une infime précision et fidélité botanique "*as if we had the natural plant before us*" (Deane, 1894; Rossi-Wilcox, 2015). Ces modèle sont d'une incroyable précision, et présentent les différentes structures des plantes, y compris leurs fleurs, et des sections dont la taille a été augmentée jusqu'à 250 fois leur taille actuelle (e.g. sections longitudinales et/ou transversales d'ovaires, de fleurs, ou de fruits critiques pour l'identification taxonomique des plantes) (Rossi-Wilcox, 2015). La collection Ware de modèles de plantes en verre Blaschka représente ainsi une des premières collections de modèles 3D de plantes. En plus des modèles de plantes, ce sont aussi des modèles de près de 16 genres d'insectes qui ont également été réalisés afin d'illustrer les mécanismes de pollinisation, différents étapes de la floraison, les

adaptations pour la pollinisation croisée, les structures qui produisent du nectar pour récompenser les pollinisateurs et attirent les voleurs de nectar, et les relations plantes-insectes mutualistes mais aussi des plantes carnivores et leurs proies (Rossi-Wilcox, 2015). C'est une révolution botanique pour l'époque qui a soulevé l'intérêt du public pour la botanique et les systèmes de reproduction des plantes, et qui peut se reproduire à nouveau aujourd'hui par l'utilisation de ce nouveau type de ressource 3D numérique pour la mise en valeur des collections de plantes auprès du publique, et pour l'enseignement.

En ce sens, l'amélioration de l'accessibilité des collections botaniques depuis n'importe où et n'importe quand, autant par la numérisation des herbiers, les collections des plantes en trois dimensions, et l'accès aux plantes à la fois dans les collections physiques et numériques, a le potentiel de créer de nouvelles opportunités pour l'étude des plantes et la vulgarisation des sciences (Maschner et al., 2013).

Les stratégies de pollinisation et la diversification des plantes

Résumé des résultats

Du fait que les stratégies de pollinisation représentent un aspect majeur de la reproduction des angiospermes, les modes de pollinisation peuvent directement influencer le taux de diversification des plantes, c'est à dire leurs taux de spéciation et d'extinction (Wessinger et al., 2019; Zenil-Ferguson et al., 2023). Les adaptations florales qui permettent d'utiliser une niche écologique encore inexplorée ou sous-exploitée peuvent contribuer à limiter leur extinction ou favoriser la spéciation dans le processus de colonisation des les îles (Barrett, 1996; Miller et al., 2023). Dans un troisième chapitre, j'ai exploré l'idée que les espèces avec une stratégie de pollinisation généralistes devraient donc bénéficier de l'exploitation de niches de pollinisation plus larges et ainsi devraient pouvoir mieux réussir à coloniser et persister dans les Antilles en raison de la réduction de leurs risques d'extinction. Ce qui a pu être observé est que les espèces généralistes qui exploitent une plus large niche de pollinisation réussissent à persister dans les Antilles, sans pour autant que ce soit au détriment des espèces spécialisées pour les colibris. Lors de la prise en compte des trois stratégies de pollinisation principalement retrouvées chez les Gesneriinae de façon distincte dans les modèles de diversification, les spécialistes pour les colibris et les généralistes ont des taux de diversification qui sont relativement similaires, tandis que la stratégie de pollinisation pour les chauves-souris a des taux de diversification comparativement très faibles. La spécialisation de la pollinisation pour les colibris n'est ainsi pas une impasse évolutive dans les Antilles. Les espèces spécialistes des colibris se diversifient ainsi autant que les généralistes. Grâce à la reconstruction extensive des liens de parentés entre les Gesneriaceae Antillaises et de leurs syndromes ancestraux, il a également pu être montré que la stratégie généraliste est ancestrale au groupe, et qu'une réversion vers une stratégie spécialiste pour les colibris est survenue bien plus tard, et plusieurs fois au cours du temps.

Perspectives méthodologiques

L'échantillonnage disponible pour cette étude reste toutefois limitant. Bien que l'approche par génotypage-par-séquençage (GBS) qui a été utilisée pour reconstruire relations de parentés entre espèces des Gesneriinae nous ai permis d'obtenir l'arbre phylogénétique le plus complet pour ce groupe, obtenir les espèces manquantes à l'appel nous permettrait d'avoir un meilleur contrôle du biais de la fraction d'échantillonnage des syndromes de population. Près de la moitié des espèces spécialistes des chauves-souris n'ont pas pu être collectées pour la phylogénie, et autour de 20% sont manquantes pour les syndromes spécialistes des colibris et des généralistes. L'omission de biais d'échantillonnage pour les analyses de diversification faisait plutôt pencher le choix vers un modèle d'estimation du taux de diversification dépendant de l'état des traits (SSE) multivarié (voir S14).

En plus des données phylogénétiques, ce sont aussi des données d'observation des pollinisateurs de plusieurs espèces qui seraient importantes à obtenir afin de confirmer les syndromes de pollinisation qui ont été inférés. De telles informations seraient précieuses afin de valider les syndromes actuellement utilisés chez les Gesneriinae, mais aussi afin de pouvoir mieux caractériser les syndromes généralistes au sein du groupe. Comme semble le suggérer le deuxième chapitre, il existe peut être des sous groupes de généralistes, qui pourraient dépendre de la proportion relative des visites de colibris et des chauves-souris chez ces espèces. Déterminer avec précision les guildes de pollinisateurs qui visitent les espèces identifiées comme ayant un syndrome généraliste permettrait sûrement d'identifier des régimes de sélection distincts au sein des généralistes, qui pourrait ainsi avoir un rôle sur les taux de diversification du groupe.

Du fait que les conclusions biologiques tirées d'analyses phylogénétiques comparatives sont sensibles à l'incertitude liée à l'échantillonnage, il serait intéressant de quantifier la robustesse face à cette incertitude, et ne pas surestimer la fiabilité des conclusions tirées. Cependant, la taille de la phylogénie actuelle pourrait déjà être limitante pour explorer ce genre d'analyse de sensibilité. Dans la même idée, il pourrait aussi être utile de faire un analyse de puissance en simulant des données à partir du modèle ajusté et en testant des fourchettes de valeurs de diversification, dans le but de comparer les simulations avec les données empiriques et ainsi voir si il est possible de correctement détecter une réelle différence de diversification entre les différents syndromes de pollinisation.

Enfin, pour consolider les conclusions du troisième chapitre et vérifier si les spécialistes ont peu d'opportunité de réversion vers une stratégie généraliste, une autre piste pourrait consister à estimer conjointement la phylogénie et les taux de diversification en utilisant l'approche RevBayes pour aborder les mêmes types de questions que celles abordées dans le troisième chapitre, et savoir si les spécialistes tendent effectivement à se diriger vers une impasse évolutive (Zenil-Ferguson et al., 2023). En plus de cette approche Bayesienne, il serait aussi utile d'explorer la dynamique

évolutive des Gesneriinae, c'est à dire d'identifier où se situent les changements de taux de diversification à travers l'arbre phylogénétique (Rabosky, 2014; Rabosky et al., 2014).

Perspectives biologiques

Notre point de vue sur la stratégie généraliste a ainsi beaucoup changé grâce au troisième chapitre, notamment sur son origine ancestrale à la base des Gesneriinae, malgré une stratégie spécialiste des colibris présente chez les groupes externes à notre groupe d'étude. La stratégie généraliste semble plus ancienne qu'initialement estimée (Martén-Rodríguez et al., 2010; Joly et al., 2018), et maintenue à travers le temps. Il n'y a pas une seule stratégie qui domine les Gesneriinae dans les Antilles du fait que les généralistes et spécialistes des colibris sont majoritairement représentés en proportions égales, mais les stratégies plus minoritaires sont aussi des stratégies retrouvées sur le continent. C'est notamment le cas du syndrome de pollinisation par les abeilles. La spécialisation pour les colibris et la spécialisation pour les insectes/abeilles sont les deux stratégies les plus observées en dehors des Antilles chez les Gesneriaceae. Il semble ainsi important d'élargir l'étude de la forme des fleurs à plus grande échelle en incorporant le syndrome spécialisé pour la pollinisation par les insectes du fait de son rôle prépondérant à travers les Gesneriaceae.

Les Gesneriaceae et leurs syndromes

Le concept de syndrome de pollinisation

À travers les trois chapitres, le thème dominant des stratégies de pollinisation revient. Cependant, l'utilisation du concept de syndrome de pollinisation peut être affinées dans le groupe des Gesneriinae (Dellinger, 2020). Au sein d'un même syndrome de pollinisation, des espèces de Gesneriaceae peuvent être pollinisées par des espèces de pollinisateurs distincts (e.g. des espèces de colibris différentes), d'autant plus si les espèces d'intérêt ne sont pas en sympatrie. Les guildes de pollinisateurs peuvent également varier à différentes l'échelle spatiales et temporelles. Les facteurs tels que l'influence des ouragans sur les populations de plantes mais aussi de pollinisateurs et la segmentation des habitats en îles distinctes mais aussi au sein des îles jouent également un rôle important qui n'est pas pris en compte explicitement dans les trois chapitres de cette thèse. Déterminer les stratégies de pollinisation à travers le temps, à différentes échelles temporelles, permettrait de mieux comprendre comment l'isolation et ainsi les pressions de sélection ont effectivement lieu sur l'isolation de la reproduction.

La forme des fleurs à plus grande échelle taxonomique

Les Gesneriaceae sont caractérisées par une diversité florale flagrante. Chez les Gesneriinae, la forme des fleurs appartenant au syndrome de pollinisation par les colibris sont assez similaires, c'est à dire tubulaires, rouges à jaunes, avec une ouverture restreinte. Mais il semble exister plus

de variation au sein de ce syndrome à plus grande échelle taxonomique qui serait pertinente à prendre en compte pour pouvoir mieux déterminer les différents syndromes de pollinisation au sein des Gesneriaceae, mais aussi pour mieux comprendre les patrons de diversification morphologiques au sein de ce groupe. En particulier, chez les espèces pollinisées par les colibris on retrouve notamment des fleurs bilabiées ou avec la présence d'une poche très prononcée à la base de la fleur (fleur hypocyrtoïde) ainsi qu'une ouverture du tube de la corolle très restreinte, où encore la présence d'éperon chez les Gesneriaceae mais que l'on ne retrouve pas nécessairement chez les Gesneriinae. La forme des fleurs pollinisées par les colibris à plus large échelle tout en restant au sein des Gesneriaceae pourraient nous montrer des patrons de variation complètement différents. Par exemple *Columnea pendens* F.Tobar, J.L.Clark & J.F.Sm. et *Columnea ceticeps* J.L.Clark & J.F.Sm., qu'on retrouve en Colombie et au Nord de l'Équateur ont des fleurs bilabiées allongées rouges. Dans le Nord Ouest de l'Amérique du Sud, *Columnea ericae* Mansf. a aussi une fleur bilabiée allongée mais jaune, ce qui est le cas également de *Columnea guttata* Poepp. & Endl., restreinte dans le Nord des Andes, bien que les pétales libres soient moins prononcés. Il y a aussi certaines espèces qui ont la présence d'un éperon très prononcé comme chez *Gasteranthus atratus* Wiehler (observée uniquement en Équateur, dans le nord des Andes). Un autre exemple de morphologie très différente pour la pollinisation par les colibris est celle de *Pearcea hypocyrtiflora* (Hook.fil.) Regel en Équateur qui a une petite fleur en forme de bulle, avec une ouverture très restreinte. C'est le cas aussi de *Pachycaulos huancabambae* J. L. Clark & Moonlight qui a une forme particulière comme *N. wettsteinii* (présente dans l'analyse de morphologie florale du deuxième chapitre) avec une toute petite ouverture mais une énorme poche. *Trichodrymonia hypocyrta* (Wiehler) M.M. Mora & J.L. Clark ressemble énormément, mais a une fleur complètement blanche, avec des sépales très grandes et rouges (présente dans les Andes d'Équateur). En plus de la constriction de la corolle, l'exsertion des anthères sert aussi à améliorer la compatibilité morphologique des fleurs avec les colibris qui les pollinisent (Serrano-Serrano et al., 2017; Castellanos et al., 2004). L'emplacement des parties impliquées dans la reproduction semble ainsi important à prendre en compte.

La flexibilité de la morphométrie géométrique permettrait de prendre en compte ces différentes structures pour étendre l'analyse de la forme des fleurs de Gesneriaceae et leurs stratégies de pollinisation à plus grande échelle. Il est par exemple possible de déterminer des régions comme étant présentes à travers l'ensemble des données, où en régions individuelles, ce qui permet de les indiquer comme manquantes lorsque la structure n'est pas présente sur une fleur en particulier. Ce qui pourrait rendre l'étude de la morphologie florale à large échelle taxonomique, et ainsi la prise en compte d'un large éventail de diversité de morphologies florales difficile est le fait que certaines fleurs pourraient nécessiter d'utiliser des gabarits différents pour chaque configuration des patrons de landmarks à placer (voir Bardua et al., 2019). Par exemple, suite à la publication du second chapitre, de nouvelles espèces de Gesneriaceae en dehors du groupe des Gesneriinae nous ont montré que garder les mêmes ensembles de landmarks et semi-landmarks de courbes

nécessite d'utiliser un nouveau gabarit pour placer correctement les landmarks de surface pour des fleurs pollinisées par les abeilles, qui sont presque complètement à pétales libres et actinomorphes (résultats non publiés).

Difficiles à prendre en compte en 2D, mais possible à incorporer dans l'analyse des fleurs en 3D, les franges sur la marge des pétales pourraient aussi être importante dans la définition des syndromes de pollinisation. Par exemple, la plupart des espèces de *Drymonia* ont des corolles en cloches avec la présence de franges qui sont impliquées dans la pollinisation pour les abeilles Euglossine , et des fleurs qui ont la présence d'une poche et d'une constriction de la corolle qui sont pollinisées par des colibris (fleurs hypocyrtoïdes) (Clark et al., 2015). Ce sont des structures qui pourraient avoir une influence sur les pollinisateurs qui les visitent, et ainsi avoir des patrons de variation florale et de diversification différents de ce qu'on a observé dans le groupe des Gesneriinae.

Malgré d'évidents défis techniques associés à l'incorporation d'une telle variation de morphologies florales au sein d'un même projet de morphologie comparative, les premiers essais d'étendre l'analyse des formes florales à plus grande échelle sont cependant encourageants.

Conclusion

Les stratégies d'extrême spécialisation sont souvent au centre des recherches, au dépens des espèces ayant des stratégies plus généralistes, mettant en évidence une sous-estimation de leur importance fonctionnelle et écologique et une surestimation de l'ubiquité des stratégies spécialisées (Waser et al., 1996; Waser, 2006). Cette thèse replace la stratégie de pollinisation au centre du tableau, et démontre son importance de par l'évolution complexe et conservée de cette stratégie au cours du temps, et de l'incidence des processus micro-évolutifs de variation morphologiques florales à l'échelle macroévolutive.

Les variations temporelles des conditions climatiques passées et actuelles et les perturbations des habitats ont également tendance à favoriser les espèces généralistes, au détriment des espèces spécialistes (Kassen, 2002; Clavel et al., 2011). Compte tenu de l'instabilité de l'environnement des Caraïbes due aux impacts anthropogéniques et climatiques, la compréhension du rôle des stratégies de pollinisation sur la diversité et l'évolution florales dans cette région est un sujet pertinent et sensible.

Bibliographie

Artuso, S., Gamisch, A., Staedler, Y. M., Schönenberger, J., and Comes, H. P. (2021). Evidence for selectively constrained 3d flower shape evolution in a late miocene clade of malagasy bulbophyllum orchids. *New Phytologist*, 232(2) :853–867.

Bardua, C., Felice, R. N., Watanabe, A., Fabre, A.-C., and Goswami, A. (2019). A practical guide to sliding and surface semilandmarks in morphometric analyses. *Integrative Organismal Biology*, 1(1) :obz016.

Barrett, S. C. H. (1996). The reproductive biology and genetics of island plants. *Philosophical Transactions of the Royal Society of London. Series B : Biological Sciences*, 351(1341) :725–733.

Cardini, A. et al. (2014). Missing the third dimension in geometric morphometrics : how to assess if 2d images really are a good proxy for 3d structures ? *Hystrix*, 25 :73–81.

Castellanos, M., Wilson, P., and Thomson, J. (2004). 'anti-bee'and 'pro-bird'changes during the evolution of hummingbird pollination in penstemon flowers. *Journal of evolutionary biology*, 17(4) :876–885.

Clark, J. L., Clavijo, L., and Muchhala, N. (2015). Convergence of anti-bee pollination mechanisms in the neotropical plant genus drymonia (gesneriaceae). *Evolutionary Ecology*, 29 :355–377.

Clavel, J., Julliard, R., and Devictor, V. (2011). Worldwide decline of specialist species : toward a global functional homogenization ? *Frontiers in Ecology and the Environment*, 9(4) :222–228.

Deane, W. (1894). The ware collection of blaschka glass models of flowers at harvard. *Botanical Gazette*, 19(4) :144–148.

Dellinger, A. S. (2020). Pollination syndromes in the 21st century : where do we stand and where may we go ? *New Phytologist*, 228(4) :1193–1213.

Dellinger, A. S., Artuso, S., Pamperl, S., Michelangeli, F. A., Penneys, D. S., Fernández-Fernández, D. M., Alvear, M., Almeda, F., Scott Armbruster, W., Staedler, Y., and Schönenberger, J. (2019). Modularity increases rate of floral evolution and adaptive success for functionally specialized pollination systems. *Communications Biology*, 2(1) :1–11.

Faure, J., Volz, V., and Joly, S. (2023). Variation in flower size and shape of impatiens capensis is correlated with urbanization in montreal, canada. *Ecology and Evolution*, 13(12) :e10826.

Gaboriau, T., Mendes, F. K., Joly, S., Silvestro, D., and Salamin, N. (2020). A multi-platform package for the analysis of intra-and interspecific trait evolution. *Methods in Ecology and Evolution*, 11(11) :1439–1447.

Joly, S., Lambert, F., Alexandre, H., Clavel, J., Léveillé-Bourret, E., and Clark, J. L. (2018). Greater pollination generalization is not associated with reduced constraints on corolla shape in Antillean plants. *Evolution*.

Kassen, R. (2002). The experimental evolution of specialists, generalists, and the maintenance of diversity. *Journal of evolutionary biology*, 15(2) :173–190.

Klingenberg, C. P. (2014). Studying morphological integration and modularity at multiple levels : concepts and analysis. *Philosophical Transactions of the Royal Society B : Biological Sciences*, 369(1649) :20130249.

Martén-Rodríguez, S., Fenster, C. B., Agnarsson, I., Skog, L. E., and Zimmer, E. A. (2010). Evolutionary breakdown of pollination specialization in a caribbean plant radiation. *New Phytologist*,

188(2) :403–417.

Maschner, H. D., Schou, C. D., and Holmes, J. (2013). Virtualization and the democratization of science : 3d technologies revolutionize museum research and access. In *2013 Digital Heritage International Congress (DigitalHeritage)*, volume 2, pages 265–271. IEEE.

Miller, A. H., Stroud, J. T., and Losos, J. B. (2023). The ecology and evolution of key innovations. *Trends in Ecology & Evolution*, 38(2) :122–131.

Policha, T., Davis, A., Barnadas, M., Dentinger, B. T. M., Raguso, R. A., and Roy, B. A. (2016). Disentangling visual and olfactory signals in mushroom-mimicking Dracula orchids using realistic three-dimensional printed flowers. *New Phytologist*, pages n/a–n/a.

Rabosky, D. L. (2014). Automatic detection of key innovations, rate shifts, and diversity-dependence on phylogenetic trees. *PloS one*, 9(2).

Rabosky, D. L., Grundler, M., Anderson, C., Title, P., Shi, J. J., Brown, J. W., Huang, H., and Larson, J. G. (2014). Bammtools : an r package for the analysis of evolutionary dynamics on phylogenetic trees. *Methods in Ecology and Evolution*, 5(7) :701–707.

Reich, D., Berger, A., von Balthazar, M., Chartier, M., Sherafati, M., Schönenberger, J., Manafzadeh, S., and Staedler, Y. M. (2020). Modularity and evolution of flower shape : the role of function, development, and spandrels in erica. *New Phytologist*, 226(1) :267–280.

Rossi-Wilcox, S. M. (2015). A brief history of harvard's glass flowers collection and its development. *Journal of Glass Studies*, pages 197–211.

Schat, L., Vink, S., Hemerik, A., Schranz, M., Bakker, F., et al. (2020). Capturing variation in floral shape ; a virtual3d based morphospace for pelargonium. *PeerJ PrePrints*.

Serrano-Serrano, M. L., Rolland, J., Clark, J. L., Salamin, N., and Perret, M. (2017). Hummingbird pollination and the diversification of angiosperms : an old and successful association in gesneriaceae. *Proceedings of the Royal Society B : Biological Sciences*, 284(1852) :20162816.

Van Belleghem, S. M., Papa, R., Ortiz-Zuazaga, H., Hendrickx, F., Jiggins, C. D., Owen McMillan, W., and Counterman, B. A. (2018). patternize : an r package for quantifying colour pattern variation. *Methods in ecology and evolution*, 9(2) :390–398.

Violle, C., Enquist, B. J., McGill, B. J., Jiang, L., Albert, C. H., Hulshof, C., Jung, V., and Messier, J. (2012). The return of the variance : intraspecific variability in community ecology. *Trends in ecology & evolution*, 27(4) :244–252.

Waser, N. M. (2006). Specialization and generalization in plant-pollinator interactions : a historical perspective. *Plant-pollinator interactions : From specialization to generalization*, pages 3–17.

Waser, N. M., Chittka, L., Price, M. V., Williams, N. M., and Ollerton, J. (1996). Generalization in pollination systems, and why it matters. *Ecology*, 77(4) :1043–1060.

Wessinger, C. A., Rausher, M. D., and Hileman, L. C. (2019). Adaptation to hummingbird pollination is associated with reduced diversification in penstemon. *Evolution letters*, 3(5) :521–533.

Zenil-Ferguson, R., McEntee, J. P., Burleigh, J. G., and Duckworth, R. A. (2023). Linking ecological specialization to its macroevolutionary consequences : An example with passerine nest type. *Systematic Biology*, 72(2) :294–306.

Bibliographie

Acevedo-Rodríguez, P. and Strong, M. T. (2012). Catalogue of seed plants of the west indies. *Smithsonian Contributions to Botany*, (98) :1–1192.

Acevedo-Rodríguez, P. and Strong, M. T. (2012). Catalogue of seed plants of the west indies. *Smithsonian Contributions to Botany*, 98.

Adams, D., Collyer, M., Kaliontzopoulou, A., and Baken, E. (2021). Geomorph : Software for geometric morphometric analyses. r package version 4.0.

Adams, D. C. and Otárola-Castillo, E. (2013). geomorph : an r package for the collection and analysis of geometric morphometric shape data. *Methods in Ecology and Evolution*, 4(4) :393–399.

Agisoft LLC (2021). Agisoft metashape user manual : Professional edition, version 1.7.

Aigner, P. A. (2001). Optimality modeling and fitness trade-offs : when should plants become pollinator specialists ? *Oikos*, 95(1) :177–184.

Akaike, H. (1987). Factor analysis and aic. In *Selected Papers of Hirotugu Akaike*, pages 371–386. Springer.

Alfaro, M. E., Santini, F., Brock, C., Alamillo, H., Dornburg, A., Rabosky, D. L., Carnevale, G., and Harmon, L. J. (2009). Nine exceptional radiations plus high turnover explain species diversity in jawed vertebrates. *Proceedings of the National Academy of Sciences*, 106(32) :13410–13414.

Altshuler, D. L. and Wylie, D. R. (2020). Hummingbird vision. *Current Biology*, 30(3) :R103–R105.

Andrews, K. R., Good, J. M., Miller, M. R., Luikart, G., and Hohenlohe, P. A. (2016). Harnessing the power of radseq for ecological and evolutionary genomics. *Nature Reviews Genetics*, 17(2) :81.

Andrews, S. et al. (2010). Fastqc : a quality control tool for high throughput sequence data.

Armbruster, W. S. (2014). Floral specialization and angiosperm diversity : phenotypic divergence, fitness trade-offs and realized pollination accuracy. *AoB Plants*, 6.

Armbruster, W. S. (2017). The specialization continuum in pollination systems : diversity of concepts and implications for ecology, evolution and conservation. *Functional Ecology*, 31(1) :88–100.

Armbruster, W. S. and Baldwin, B. G. (1998). Switch from specialized to generalized pollination. *Nature*, 394(6694) :632–632.

Artuso, S., Gamisch, A., Staedler, Y. M., Schönenberger, J., and Comes, H. P. (2021). Evidence for selectively constrained 3d flower shape evolution in a late miocene clade of malagasy bulbophyllum orchids. *New Phytologist*, 232(2) :853–867.

Artuso, S., Gamisch, A., Staedler, Y. M., Schönenberger, J., and Comes, H. P. (2022). Evidence for an evo-devo-derived hypothesis on 3d flower shape modularity in a tropical orchid clade. *Evolution ; International Journal of Organic Evolution*.

Baken, E., Collyer, M., Kaliontzopoulou, A., and Adams, D. (2021). gmshiny and geomorph v4.0 : new graphical interface and enhanced analytics for a comprehensive morphometric experience.

Baldwin, B. G. and Sanderson, M. J. (1998). Age and rate of diversification of the hawaiian silversword alliance (compositae). *Proceedings of the National Academy of Sciences*, 95(16) :9402–9406.

Bardua, C., Felice, R. N., Watanabe, A., Fabre, A.-C., and Goswami, A. (2019). A practical guide to sliding and surface semilandmarks in morphometric analyses. *Integrative Organismal Biology*, 1(1) :obz016.

Barrett, S. C. H. (1996). The reproductive biology and genetics of island plants. *Philosophical Transactions of the Royal Society of London. Series B : Biological Sciences*, 351(1341) :725–733.

Beaulieu, J. M. and O'Meara, B. C. (2016). Detecting hidden diversification shifts in models of trait-dependent speciation and extinction. *Systematic biology*, 65(4) :583–601.

Bilbao, G., Bruneau, A., and Joly, S. (2021). Judge it by its shape : a pollinator-blind approach reveals convergence in petal shape and infers pollination modes in the genus erythrina. *American journal of botany*, 108(9) :1716–1730.

Bolnick, D. I., Amarasekare, P., Araújo, M. S., Bürger, R., Levine, J. M., Novak, M., Rudolf, V. H., Schreiber, S. J., Urban, M. C., and Vasseur, D. A. (2011). Why intraspecific trait variation matters in community ecology. *Trends in ecology & evolution*, 26(4) :183–192.

Bolnick, D. I., Svanbäck, R., Araújo, M. S., and Persson, L. (2007). Comparative support for the niche variation hypothesis that more generalized populations also are more heterogeneous. *Proceedings of the National Academy of Sciences*, 104(24) :10075–10079.

Bookstein, F. L. (1997). Shape and the information in medical images : A decade of the morphometric synthesis. *Computer Vision and Image Understanding*, 66(2) :97–118.

Bouckaert, R., Vaughan, T. G., Barido-Sottani, J., Duchêne, S., Fourment, M., Gavryushkina, A., Heled, J., Jones, G., Kühnert, D., De Maio, N., et al. (2019). Beast 2.5 : An advanced software platform for bayesian evolutionary analysis. *PLoS computational biology*, 15(4) :e1006650.

Boyer, D. M., Gunnell, G. F., Kaufman, S., and McGeary, T. M. (2016). Morphosource : archiving and sharing 3-d digital specimen data. *The Paleontological Society Papers*, 22 :157–181.

Brokaw, A. F. and Smotherman, M. (2020). Role of ecology in shaping external nasal morphology in bats and implications for olfactory tracking. *PLoS One*, 15(1) :e0226689.

Cardini, A. et al. (2014). Missing the third dimension in geometric morphometrics : how to assess if 2d images really are a good proxy for 3d structures ? *Hystrix*, 25 :73–81.

Castellanos, M., Wilson, P., and Thomson, J. (2004). 'anti-bee'and 'pro-bird'changes during the evolution of hummingbird pollination in penstemon flowers. *Journal of evolutionary biology*, 17(4) :876–885.

Chittka, L., Spaethe, J., Schmidt, A., and Hickelsberger, A. (2001). *Adaptation, constraint, and chance in the evolution of flower color and pollinator color vision*, page 106–126. Cambridge University Press.

Christiansen, F., Sironi, M., Moore, M. J., Di Martino, M., Ricciardi, M., Warick, H. A., Irschick, D. J., Gutierrez, R., and Uhart, M. M. (2019). Estimating body mass of free-living whales using aerial photogrammetry and 3d volumetrics. *Methods in Ecology and Evolution*, 10(12) :2034–2044.

Clark, J. (2020). The caribbean gesneriaceae : an update on the classification of gesneria and rhytidophyllum. *Gesneriads*, 70 :10–20.

Clark, J., Skog, L., Boggan, J., and Ginzbarg, S. (2020). Index to names of new world members of the gesneriaceae (subfamilies sanangoideae and gesnerioideae). *Rheedea*, 30(1) :190.

Clark, J. L., Clavijo, L., and Muchhala, N. (2015). Convergence of anti-bee pollination mechanisms in the neotropical plant genus drymonia (gesneriaceae). *Evolutionary Ecology*, 29 :355–377.

Clark, J. L., Funke, M. M., Duffy, A. M., and Smith, J. F. (2012). Phylogeny of a neotropical clade in the gesneriaceae : more tales of convergent evolution. *International Journal of Plant Sciences*, 173(8) :894–916.

Clavel, J., Aristide, L., and Morlon, H. (2018). A penalized likelihood framework for high-dimensional phylogenetic comparative methods and an application to new-world monkeys brain evolution. *Systematic biology*, 68(1) :93–116.

Clavel, J., Escarguel, G., and Merceron, G. (2015). mvmorph : an r package for fitting multivariate evolutionary models to morphometric data. *Methods in Ecology and Evolution*, 6(11) :1311–1319.

Clavel, J., Julliard, R., and Devictor, V. (2011). Worldwide decline of specialist species : toward a global functional homogenization ? *Frontiers in Ecology and the Environment*, 9(4) :222–228.

Colles, A., Liow, L. H., and Prinzing, A. (2009). Are specialists at risk under environmental change ? neoecological, paleoecological and phylogenetic approaches. *Ecology letters*, 12(8) :849–863.

Cronk, Q. and Ojeda, I. (2008). Bird-pollinated flowers in an evolutionary and molecular context. *Journal of experimental botany*, 59(4) :715–727.

Cunliffe, A. M., Brazier, R. E., and Anderson, K. (2016). Ultra-fine grain landscape-scale quantification of dryland vegetation structure with drone-acquired structure-from-motion photogrammetry. *Remote Sensing of Environment*, 183 :129–143.

Dalrymple, R. L., Kemp, D. J., Flores-Moreno, H., Laffan, S. W., White, T. E., Hemmings, F. A., and Moles, A. T. (2020). Macroecological patterns in flower colour are shaped by both biotic and abiotic factors. *New Phytologist*, 228(6) :1972–1985.

Davies, T. G., Rahman, I. A., Lautenschlager, S., Cunningham, J. A., Asher, R. J., Barrett, P. M., Bates, K. T., Bengtson, S., Benson, R. B., Boyer, D. M., et al. (2017). Open data and digital morphology. *Proceedings of the Royal Society B : Biological Sciences*, 284(1852) :20170194.

Deane, W. (1894). The ware collection of blaschka glass models of flowers at harvard. *Botanical Gazette*, 19(4) :144–148.

Dellinger, A. S. (2020). Pollination syndromes in the 21st century : where do we stand and where may we go ? *New Phytologist*, 228(4) :1193–1213.

Dellinger, A. S., Artuso, S., Pamperl, S., Michelangeli, F. A., Penneys, D. S., Fernández-Fernández, D. M., Alvear, M., Almeda, F., Scott Armbruster, W., Staedler, Y., and Schönenberger, J. (2019). Modularity increases rate of floral evolution and adaptive success for functionally specialized pollination systems. *Communications Biology*, 2(1) :1–11.

Delpino, F. (1874). Ulteriori osservazioni e considerazioni sulla dicogamia nel regno vegetale. 2 (iv). delle piante zoidifile. *Atti della Societa Italiana Scientia Naturale*, 16 :151–349.

Devictor, V., Clavel, J., Julliard, R., Lavergne, S., Mouillot, D., Thuiller, W., Venail, P., Villeger, S., and Mouquet, N. (2010). Defining and measuring ecological specialization. *Journal of Applied Ecology*, 47(1) :15–25.

Doyle, J. J. and Doyle, J. L. (1987). A rapid dna isolation procedure for small quantities of fresh leaf tissue. *Phytochemical bulletin*.

Drummond, A. J., Ho, S. Y., Phillips, M. J., and Rambaut, A. (2006). Relaxed phylogenetics and dating with confidence. *PLoS biology*, 4(5) :e88.

Drummond, A. J., Nicholls, G. K., Rodrigo, A. G., and Solomon, W. (2002). Estimating mutation parameters, population history and genealogy simultaneously from temporally spaced sequence data. *Genetics*, 161(3) :1307–1320.

Eaton, D. A. and Overcast, I. (2020). ipyrad : Interactive assembly and analysis of radseq datasets. *Bioinformatics*, 36(8) :2592–2594.

Evin, A., Souter, T., Hulme-Beaman, A., Ameen, C., Allen, R., Viacava, P., Larson, G., Cucchi, T., and Dobney, K. (2016). The use of close-range photogrammetry in zooarchaeology : Creating accurate 3d models of wolf crania to study dog domestication. *Journal of Archaeological Science : Reports*, 9 :87–93.

Faegri, K. and van der Pijl, L. (1979). The principles of pollination ecology.

Faegri, K. and Van Der Pijl, L. (2013). *Principles of pollination ecology*. Elsevier.

Faure, J. and Joly, S. (2020). Pollinator performance of the pollination generalist rhytidophyllum bicolor (gesneriaceae) in haiti 15 months after the matthew hurricane. *Selbyana*, 33(3).

Faure, J., Volz, V., and Joly, S. (2023). Variation in flower size and shape of impatiens capensis is correlated with urbanization in montreal, canada. *Ecology and Evolution*, 13(12) :e10826.

Fenster, C. B. (1991). Selection on floral morphology by hummingbirds. *Biotropica*, 23(1) :98–101.

Fenster, C. B., Armbruster, W. S., Wilson, P., Dudash, M. R., and Thomson, J. D. (2004). Pollination syndromes and floral specialization. *Annual Reviews of Ecology Evolution and Systematic*, 35 :375–403.

Fernández-i Marín, X. (2016). ggmcmc : Analysis of MCMC samples and Bayesian inference. *Journal of Statistical Software*, 70(9) :1–20.

FitzJohn, R. G. (2012). Diversitree : comparative phylogenetic analyses of diversification in r. *Methods in Ecology and Evolution*, 3(6) :1084–1092.

FitzJohn, R. G., Maddison, W. P., and Otto, S. P. (2009). Estimating trait-dependent speciation and extinction rates from incompletely resolved phylogenies. *Systematic biology*, 58(6) :595–611.

Florey, C. L. and Moore, P. A. (2019). Analysis and description of burrow structure in four species of freshwater crayfishes (decapoda : Astacoidea : Cambaridae) using photogrammetry to recreate casts as 3d models. *The Journal of Crustacean Biology*, 39(6) :711–719.

Friedman, W. E. (2009). The meaning of darwin's "abominable mystery". *American Journal of Botany*, 96(1) :5–21.

Fritsch, P. W. and McDowell, T. D. (2003). Biogeography and phylogeny of caribbean plants—introduction. *Systematic Botany*, 28(2) :376–378.

Funk, W. C., Lovich, R. E., Hohenlohe, P. A., Hofman, C. A., Morrison, S. A., Sillett, T. S., Ghalambor, C. K., Maldonado, J. E., Rick, T. C., Day, M. D., et al. (2016). Adaptive divergence despite strong genetic drift : genomic analysis of the evolutionary mechanisms causing genetic differentiation in the island fox (urocyon littoralis). *Molecular ecology*, 25(10) :2176–2194.

Futuyma, D. J. and Peterson, S. C. (1985). Genetic variation in the use of resources by insects. *Annual review of entomology*, 30(1) :217–238.

Gaboriau, T., Mendes, F. K., Joly, S., Silvestro, D., and Salamin, N. (2020). A multi-platform package for the analysis of intra-and interspecific trait evolution. *Methods in Ecology and Evolution*, 11(11) :1439–1447.

Gamisch, A., Staedler, Y. M., Schönenberger, J., Fischer, G. A., and Comes, H. P. (2013). Histological and micro-ct evidence of stigmatic rostellum receptivity promoting auto-pollination in the madagascan orchid bulbophyllum bicoloratum. *PLoS One*, 8(8) :e72688.

Giacomini, G., Scaravelli, D., Herrel, A., Veneziano, A., Russo, D., Brown, R. P., and Meloro, C. (2019). 3d photogrammetry of bat skulls : perspectives for macro-evolutionary analyses. *Evolutionary Biology*, 46(3) :249–259.

Givnish, T. J. (2015). Adaptive radiation versus 'radiation'and 'explosive diversification' : why conceptual distinctions are fundamental to understanding evolution. *New Phytologist*, 207(2) :297–303.

Gómez, J. M., Perfectti, F., and Klingenberg, C. P. (2014). The role of pollinator diversity in the evolution of corolla-shape integration in a pollination-generalist plant clade. *Philosophical Transactions of the Royal Society B : Biological Sciences*, 369(1649) :20130257.

Gonzalez-Gutierrez, K., Castaño, J. H., Perez-Torres, J., and Mosquera-Mosquera, H. R. (2022). Structure and roles in pollination networks between phyllostomid bats and flowers : a systematic review for the americas. *Mammalian Biology*, 102(1) :21–49.

Gower, J. C. (1975). Generalized procrustes analysis. *Psychometrika*, 40(1) :33–51.

Grafen, A. (1989). The phylogenetic regression. *Philosophical Transactions of the Royal Society of London. B, Biological Sciences*, 326(1233) :119–157.

Grant, P. and Price, T. (1981). Population variation in continuously varying traits as an ecological genetics problem. *American Zoologist*, 21(4) :795–811.

Grant, P. R. (1981). Speciation and the adaptive radiation of darwin's finches : The complex diversity of darwin's finches may provide a key to the mystery of how intraspecific variation is transformed into interspecific variation. *American Scientist*, 69(6) :653–663.

Gunz, P. and Mitteroecker, P. (2013). Semilandmarks : a method for quantifying curves and surfaces. *Hystrix, the Italian Journal of Mammalogy*, 24(1) :103–109.

Gómez, J. M., Perfectti, F., Abdelaziz, M., Lorite, J., and Muñoz-Pajares, A. J. (2014). Evolution of pollination niches in a generalist plant clade. *New Phytologist*, 205(1) :440–453.

Harmon, L. J., Andreazzi, C. S., Débarre, F., Drury, J., Goldberg, E. E., Martins, A. B., Melián, C. J., Narwani, A., Nuismer, S. L., Pennell, M. W., et al. (2019). Detecting the macroevolutionary signal of species interactions. *Journal of evolutionary biology*, 32(8) :769–782.

Heled, J. and Drummond, A. J. (2010). Bayesian Inference of Species Trees from Multilocus Data. *Molecular Biology and Evolution*, 27(3) :570–580.

Herrmann, N. C., Stroud, J. T., and Losos, J. B. (2021). The evolution of 'ecological release'into the 21st century. *Trends in Ecology & Evolution*, 36(3) :206–215.

Hsu, H.-C., Chou, W.-C., and Kuo, Y.-F. (2020). 3d revelation of phenotypic variation, evolutionary allometry, and ancestral states of corolla shape : a case study of clade corytholoma (subtribe ligeriinae, family gesneriaceae). *GigaScience*, 9(1) :1–16.

Huelsenbeck, J. P., Nielsen, R., and Bollback, J. P. (2003). Stochastic mapping of morphological characters. *Systematic Biology*, 52(2) :131–158.

Iglhaut, J., Cabo, C., Puliti, S., Piermattei, L., O'Connor, J., and Rosette, J. (2019). Structure from motion photogrammetry in forestry : A review. *Current Forestry Reports*, 5(3) :155–168.

Ijiri, T., Todo, H., Hirabayashi, A., Kohiyama, K., and Dobashi, Y. (2018). Digitization of natural objects with micro ct and photographs. *PloS one*, 13(4) :e0195852.

Iturralde-Vinent, M. A. (2006). Meso-cenozoic caribbean paleogeography : implications for the historical biogeography of the region. *International Geology Review*, 48(9) :791–827.

Jeffreys, H. (1935). Some tests of significance, treated by the theory of probability. In *Mathematical proceedings of the Cambridge philosophical society*, volume 31, pages 203–222. Cambridge University Press.

Johnson, S. D. (2010). The pollination niche and its role in the diversification and maintenance of the southern african flora. *Philosophical Transactions of the Royal Society B : Biological Sciences*, 365(1539) :499–516.

Johnson, S. D. and Steiner, K. E. (2000). Generalization versus specialization in plant pollination systems. *Trends in ecology & evolution*, 15(4) :140–143.

Joly, S., Lambert, F., Alexandre, H., Clavel, J., Léveillé-Bourret, E., and Clark, J. L. (2018). Greater pollination generalization is not associated with reduced constraints on corolla shape in Antillean plants. *Evolution*.

Joly, S., Lambert, F., Cinea, W., and Clark, J. L. (2023). Three new gesneria species (gesneriaceae) support parc national pic macaya (haiti) as an important biodiversity hotspot. *Systematic Botany*, 48(1) :34–43.

Joly, S., Starr, J. R., Lewis, W. H., and Bruneau, A. (2006). Polyploid and hybrid evolution in roses east of the rocky mountains. *American Journal of Botany*, 93(3) :412–425.

Kass, R. E. and Raftery, A. E. (1995). Bayes factors. *Journal of the American Statistical Association*, 90(430) :773–795.

Kassambara, A. and Mundt, F. (2020). *factoextra : Extract and Visualize the Results of Multivariate Data Analyses*. R package version 1.0.7.

Kassen, R. (2002). The experimental evolution of specialists, generalists, and the maintenance of diversity. *Journal of evolutionary biology*, 15(2) :173–190.

Katoh, K. and Standley, D. M. (2013). Mafft multiple sequence alignment software version 7 : improvements in performance and usability. *Molecular biology and evolution*, 30(4) :772–780.

Kattge, J., Bönisch, G., Díaz, S., Lavorel, S., Prentice, I. C., Leadley, P., Tautenhahn, S., Werner, G. D., Aakala, T., Abedi, M., et al. (2020). Try plant trait database–enhanced coverage and open access. *Global change biology*, 26(1) :119–188.

Kattge, J., Diaz, S., Lavorel, S., Prentice, I. C., Leadley, P., Bönisch, G., Garnier, E., Westoby, M., Reich, P. B., Wright, I. J., et al. (2011). Try–a global database of plant traits. *Global change biology*, 17(9) :2905–2935.

Katz, D. and Friess, M. (2014). 3d from standard digital photography of human crania—a preliminary assessment. *American Journal of Physical Anthropology*, 154(1) :152–158.

Kendall, D. G. (1984). Shape manifolds, procrustean metrics, and complex projective spaces. *Bulletin of the London Mathematical Society*, 16(2) :81–121.

Klingenberg, C. P. (2014). Studying morphological integration and modularity at multiple levels : concepts and analysis. *Philosophical Transactions of the Royal Society B : Biological Sciences*,

369(1649) :20130249.

Kostikova, A., Silvestro, D., Pearman, P. B., and Salamin, N. (2016). Bridging inter-and intraspecific trait evolution with a hierarchical bayesian approach. *Systematic biology*, 65(3) :417–431.

Kuppler, J., Albert, C. H., Ames, G. M., Armbruster, W. S., Boenisch, G., Boucher, F. C., Campbell, D. R., Carneiro, L. T., Chacón-Madrigal, E., Enquist, B. J., et al. (2020). Global gradients in intraspecific variation in vegetative and floral traits are partially associated with climate and species richness. *Global Ecology and Biogeography*, 29(6) :992–1007.

Lagomarsino, L. P., Condamine, F. L., Antonelli, A., Mulch, A., and Davis, C. C. (2016). The abiotic and biotic drivers of rapid diversification in a ndean bellflowers (campanulaceae). *New Phytologist*, 210(4) :1430–1442.

Lagomarsino, L. P., Forrestel, E. J., Muchhala, N., and Davis, C. C. (2017). Repeated evolution of vertebrate pollination syndromes in a recently diverged andean plant clade. *Evolution*, 71(8) :1970–1985.

Lartillot, N. (2023). Identifying the best approximating model in bayesian phylogenetics : Bayes factors, cross-validation or waic ? *Systematic Biology*, 72(3) :616–638.

Lemmon, A. R. and Moriarty, E. C. (2004). The importance of proper model assumption in bayesian phylogenetics. *Systematic Biology*, 53(2) :265–277.

Leonard, A. S. and Papaj, D. R. (2011). 'x'marks the spot : The possible benefits of nectar guides to bees and plants. *Functional Ecology*, 25(6) :1293–1301.

Lewis, P. O. (2001). A likelihood approach to estimating phylogeny from discrete morphological character data. *Systematic biology*, 50(6) :913–925.

Linder, W. (2009). *Digital photogrammetry*, volume 1. Springer.

Losos, J. B. (2017). *Improbable destinies : Fate, chance, and the future of evolution*. Penguin.

Losos, J. B. and Ricklefs, R. E. (2009). Adaptation and diversification on islands. *Nature*, 457(7231) :830–836.

Luhmann, T., Robson, S., Kyle, S., and Boehm, J. (2013). *Close-range photogrammetry and 3D imaging*. Walter de Gruyter.

MacArthur, R. H. and Wilson, E. O. (1963). An equilibrium theory of insular zoogeography. *Evolution*, 17(4) :373–387.

MacArthur, R. H. and Wilson, E. O. (1967). *Island biogeography*. Princeton.

Maddison, W. P., Midford, P. E., and Otto, S. P. (2007). Estimating a binary character's effect on speciation and extinction. *Systematic biology*, 56(5) :701–710.

Mahler, D. L., Revell, L. J., Glor, R. E., and Losos, J. B. (2010). Ecological opportunity and the rate of morphological evolution in the diversification of greater antillean anoles. *Evolution : International Journal of Organic Evolution*, 64(9) :2731–2745.

Martén-Rodríguez, S. and Fenster, C. B. (2010). Pollen limitation and reproductive assurance in antillean gesnerieae : a specialists vs. generalist comparison. *Ecology*, 91(1) :155–165.

Martén-Rodríguez, S., Fenster, C. B., Agnarsson, I., Skog, L. E., and Zimmer, E. A. (2010). Evolutionary breakdown of pollination specialization in a caribbean plant radiation. *New Phytologist*, 188(2) :403–417.

Martín-Hernanz, S., Aparicio, A., Fernández-Mazuecos, M., Rubio, E., Reyes-Betancort, J. A., Santos-Guerra, A., Olangua-Corral, M., and Albaladejo, R. G. (2019). Maximize resolution or minimize error? using genotyping-by-sequencing to investigate the recent diversification of helianthemum (cistaceae). *Frontiers in plant science*, 10 :1416.

Martén-Rodríguez, S., Almarales-Castro, A., and Fenster, C. B. (2009). Evaluation of pollination syndromes in Antillean Gesneriaceae : evidence for bat, hummingbird and generalized flowers. *Journal of Ecology*, 97(2) :348–359.

Martén-Rodríguez, S. and Fenster, C. B. (2008). Pollination Ecology and Breeding Systems of Five Gesneria Species from Puerto Rico. *Annals of Botany*, 102(1) :23–30.

Martén-Rodríguez, S., Quesada, M., Castro, A.-A., Lopezaraiza-Mikel, M., and Fenster, C. B. (2015). A comparison of reproductive strategies between island and mainland Caribbean Gesneriaceae. *Journal of Ecology*, 103(5) :1190–1204.

Maschner, H. D., Schou, C. D., and Holmes, J. (2013). Virtualization and the democratization of science : 3d technologies revolutionize museum research and access. In *2013 Digital Heritage International Congress (DigitalHeritage)*, volume 2, pages 265–271. IEEE.

Mathys, A., Brecko, J., and Semal, P. (2013). Comparing 3d digitizing technologies : what are the differences? In *2013 Digital Heritage International Congress (DigitalHeritage)*, volume 1, pages 201–204. IEEE.

McKinney, M. L. (1997). Extinction vulnerability and selectivity : combining ecological and paleontological views. *Annual review of ecology and systematics*, 28(1) :495–516.

Medina, J. J., Maley, J. M., Sannapareddy, S., Medina, N. N., Gilman, C. M., and McCormack, J. E. (2020). A rapid and cost-effective pipeline for digitization of museum specimens with 3d photogrammetry. *Plos one*, 15(8) :e0236417.

Miller, A. H., Stroud, J. T., and Losos, J. B. (2023). The ecology and evolution of key innovations. *Trends in Ecology & Evolution*, 38(2) :122–131.

Miller, M. R., Dunham, J. P., Amores, A., Cresko, W. A., and Johnson, E. A. (2007). Rapid and cost-effective polymorphism identification and genotyping using restriction site associated dna (rad) markers. *Genome research*, 17(2) :240–248.

Myers, N., Mittermeier, R. A., Mittermeier, C. G., Da Fonseca, G. A., and Kent, J. (2000). Biodiversity hotspots for conservation priorities. *Nature*, 403(6772) :853.

Nakov, T., Beaulieu, J. M., and Alverson, A. J. (2018). Accelerated diversification is related to life history and locomotion in a hyperdiverse lineage of microbial eukaryotes (diatoms, bacillariophyta). *New Phytologist*, 219(1) :462–473.

Olesen, J. M. and Jordano, P. (2002). Geographic patterns in plant–pollinator mutualistic networks. *Ecology*, 83(9) :2416–2424.

Ollerton, J. (2017). Pollinator diversity : distribution, ecological function, and conservation. *Annual Review of Ecology, Evolution, and Systematics*, 48 :353–376.

Ollerton, J., Alarcón, R., Waser, N. M., Price, M. V., Watts, S., Cranmer, L., Hingston, A., Peter, C. I., and Rotenberry, J. (2009). A global test of the pollination syndrome hypothesis. *Annals of botany*, 103(9) :1471–1480.

Ollerton, J., Winfree, R., and Tarrant, S. (2011). How many flowering plants are pollinated by animals ? *Oikos*, 120(3) :321–326.

Paradis, E. and Schliep, K. (2019). ape 5.0 : an environment for modern phylogenetics and evolutionary analyses in R. *Bioinformatics*, 35 :526–528.

Patterson, B. D. (1983). Grasshopper mandibles and the niche variation hypothesis. *Evolution*, 37(2) :375–388.

Pennell, M. W., Eastman, J. M., Slater, G. J., Brown, J. W., Uyeda, J. C., FitzJohn, R. G., Alfaro, M. E., and Harmon, L. J. (2014). geiger v2. 0 : an expanded suite of methods for fitting macroevolutionary models to phylogenetic trees. *Bioinformatics*, 30(15) :2216–2218.

Perez, S. I., Bernal, V., and Gonzalez, P. N. (2006). Differences between sliding semi-landmark methods in geometric morphometrics, with an application to human craniofacial and dental variation. *Journal of anatomy*, 208(6) :769–784.

Perret, M., Chautems, A., De Araujo, A. O., and Salamin, N. (2013). Temporal and spatial origin of gesneriaceae in the new world inferred from plastid dna sequences. *Botanical Journal of the Linnean Society*, 171(1) :61–79.

Petanidou, T. and Potts, S. G. (2006). Mutual use of resources in mediterranean plant–pollinator communities : how specialized are pollination webs. *Plant–pollinator interactions : from specialization to generalization*, pages 220–244.

Pinheiro, J., Bates, D., DebRoy, S., Sarkar, D., and R Core Team (2021). *nlme : Linear and Nonlinear Mixed Effects Models*. R package version 3.1-153.

Plummer, M., Best, N., Cowles, K., and Vines, K. (2006). Coda : Convergence diagnosis and output analysis for mcmc. *R News*, 6(1) :7–11.

Poland, J. A., Brown, P. J., Sorrells, M. E., and Jannink, J.-L. (2012). Development of high-density genetic maps for barley and wheat using a novel two-enzyme genotyping-by-sequencing approach. *PloS one*, 7(2) :e32253.

Policha, T., Davis, A., Barnadas, M., Dentinger, B. T. M., Raguso, R. A., and Roy, B. A. (2016). Disentangling visual and olfactory signals in mushroom-mimicking Dracula orchids using realistic three-dimensional printed flowers. *New Phytologist*, pages n/a–n/a.

Pomidor, B. J., Makedonska, J., and Slice, D. E. (2016). A landmark-free method for three-dimensional shape analysis. *PloS one*, 11(3) :e0150368.

R Core Team (2021). *R : A Language and Environment for Statistical Computing*. R Foundation for Statistical Computing, Vienna, Austria.

Rabosky, D. L. (2014). Automatic detection of key innovations, rate shifts, and diversity-dependence on phylogenetic trees. *PloS one*, 9(2).

Rabosky, D. L., Grundler, M., Anderson, C., Title, P., Shi, J. J., Brown, J. W., Huang, H., and Larson, J. G. (2014). Bammtools : an r package for the analysis of evolutionary dynamics on phylogenetic trees. *Methods in Ecology and Evolution*, 5(7) :701–707.

Rambaut, A., Drummond, A. J., Xie, D., Baele, G., and M.A.Suchard (2018a). Tracer v1.7. `http://beast.community/tracer`.

Rambaut, A., Drummond, A. J., Xie, D., Baele, G., and Suchard, M. A. (2018b). Posterior summarization in bayesian phylogenetics using tracer 1.7. *Systematic biology*, 67(5) :901–904.

Regalado, L., Lóriga, J., Bechteler, J., Beck, A., Schneider, H., and Heinrichs, J. (2018). Phylogenetic biogeography reveals the timing and source areas of the adiantum species (pteridaceae) in the west indies, with a special focus on cuba. *Journal of Biogeography*, 45(3) :541–551.

Reich, D., Berger, A., von Balthazar, M., Chartier, M., Sherafati, M., Schönenberger, J., Manafzadeh, S., and Staedler, Y. M. (2020). Modularity and evolution of flower shape : the role of function, development, and spandrels in erica. *New Phytologist*, 226(1) :267–280.

Revell, L. J. (2009). Size-correction and principal components for interspecific comparative studies. *Evolution*, 63(12) :3258–3268.

Revell, L. J. (2010). Phylogenetic signal and linear regression on species data. *Methods in Ecology and Evolution*, 1(4) :319–329.

Revell, L. J. (2012). phytools : an r package for phylogenetic comparative biology (and other things). *Methods in Ecology and Evolution*, 3(2) :217–223.

Ricklefs, R. and Bermingham, E. (2008a). The west indies as a laboratory of biogeography and evolution. *Philosophical Transactions of the Royal Society B : Biological Sciences*, 363(1502) :2393–2413.

Ricklefs, R. and Bermingham, E. (2008b). The west indies as a laboratory of biogeography and evolution. *Philosophical Transactions of the Royal Society B : Biological Sciences*, 363(1502) :2393–2413.

Rohlf, F. J. (2010). tpsrelw, relative warps analysis. *Department of Ecology and Evolution, State University of New York at Stony Brook, Stony Brook, NY*.

Rohlf, F. J. and Marcus, L. F. (1993). A revolution morphometrics. *Trends in ecology & evolution*, 8(4) :129–132.

Rohlf, F. J. and Slice, D. (1990). Extensions of the procrustes method for the optimal superimposition of landmarks. *Systematic Biology*, 39(1) :40–59.

Roncal, J., Nieto-Blázquez, M. E., Cardona, A., and Bacon, C. D. (2020). Historical biogeography of caribbean plants revises regional paleogeography. *Neotropical diversification : Patterns and processes*, pages 521–546.

Rosas-Guerrero, V., Aguilar, R., Martén-Rodríguez, S., Ashworth, L., Lopezaraiza-Mikel, M., Bastida, J. M., and Quesada, M. (2014). A quantitative review of pollination syndromes : do floral

traits predict effective pollinators ? *Ecology letters*, 17(3) :388–400.

Rosas-Guerrero, V., Quesada, M., Armbruster, W. S., Pérez-Barrales, R., and Smith, S. D. (2011). Influence of pollination specialization and breeding system on floral integration and phenotypic variation in ipomoea. *Evolution*, 65(2) :350–364.

Rossi-Wilcox, S. M. (2015). A brief history of harvard's glass flowers collection and its development. *Journal of Glass Studies*, pages 197–211.

Sahli, H. F. and Conner, J. K. (2011). Testing for conflicting and nonadditive selection : floral adaptation to multiple pollinators through male and female fitness. *Evolution : International Journal of Organic Evolution*, 65(5) :1457–1473.

Salzburger, W. (2018). Understanding explosive diversification through cichlid fish genomics. *Nature Reviews Genetics*, 19(11) :705–717.

Sauquet, H. (2019). Proteus : A database for recording morphological data and fossil calibrations.

Schat, L., Vink, S., Hemerik, A., Schranz, M., Bakker, F., et al. (2020). Capturing variation in floral shape ; a virtual3d based morphospace for pelargonium. *PeerJ PrePrints*.

Schiestl, F. P. and Johnson, S. D. (2013). Pollinator-mediated evolution of floral signals. *Trends in ecology & evolution*, 28(5) :307–315.

Schlager, S. (2017). Morpho and rvcg–shape analysis in r : R-packages for geometric morphometrics, shape analysis and surface manipulations.

Schneider, C. A., Rasband, W. S., and Eliceiri, K. W. (2012). Nih image to imagej : 25 years of image analysis. *Nature methods*, 9(7) :671–675.

Serrano-Serrano, M. L., Rolland, J., Clark, J. L., Salamin, N., and Perret, M. (2017). Hummingbird pollination and the diversification of angiosperms : an old and successful association in gesneriaceae. *Proceedings of the Royal Society B : Biological Sciences*, 284(1852) :20162816.

Seymour, R. S., White, C. R., and Gibernau, M. (2003). Heat reward for insect pollinators. *Nature*, 426(6964) :243–244.

Siefert, A., Violle, C., Chalmandrier, L., Albert, C. H., Taudiere, A., Fajardo, A., Aarssen, L. W., Baraloto, C., Carlucci, M. B., Cianciaruso, M. V., et al. (2015). A global meta-analysis of the relative extent of intraspecific trait variation in plant communities. *Ecology letters*, 18(12) :1406–1419.

Skog, L. E. (1976). *A study of the tribe Gesnerieae, with a revision of Gesneria (Gesneriaceae, Gesnerioideae)*, volume no.29 (1976). Washington Smithsonian Institution Press 1969-. https ://www.biodiversitylibrary.org/bibliography/100822.

Smith, J. F., Draper, S. B., Hileman, L. C., and Baum, D. A. (2004a). A phylogenetic analysis within tribes gloxinieae and gesnerieae (gesnerioideae : Gesneriaceae). *Systematic Botany*, 29(4) :947–958.

Smith, M., Hedges, S., Buck, W., Hemphill, A., Inchaustegui, S., Ivie, M., Martina, D., Maunder, M., and Francisco-Ortega, J. (2004b). Caribbean islands. In CEMEX, M., editor, *Hotspots revisited : earth's biologically richest and most threatened terrestrial ecoregions*, Cemex books

on nature, pages 112–118. Agrupacion Sierra Madre.

Smith, S. A. and Walker, J. F. (2019). PyPHLAWD : A python tool for phylogenetic dataset construction. *Methods in Ecology and Evolution*, 10 :104–108.

Staedler, Y. M., Masson, D., and Schönenberger, J. (2013). Plant tissues in 3d via x-ray tomography : simple contrasting methods allow high resolution imaging. *PloS one*, 8(9) :e75295.

Stamatakis, A. (2014). Raxml version 8 : a tool for phylogenetic analysis and post-analysis of large phylogenies. *Bioinformatics*, 30(9) :1312–1313.

Stebbins, G. L. (1970). Adaptive radiation of reproductive characteristics in angiosperms, i : pollination mechanisms. *Annual review of ecology and systematics*, 1(1) :307–326.

Ströbel, B., Schmelzle, S., Blüthgen, N., and Heethoff, M. (2018). An automated device for the digitization and 3d modelling of insects, combining extended-depth-of-field and all-side multi-view imaging. *ZooKeys*, (759) :1–27.

Stuppy, W. H., Maisano, J. A., Colbert, M. W., Rudall, P. J., and Rowe, T. B. (2003). Three-dimensional analysis of plant structure using high-resolution x-ray computed tomography. *Trends in plant science*, 8(1) :2–6.

Svanbäck, R., Pineda-Krch, M., and Doebeli, M. (2009). Fluctuating population dynamics promotes the evolution of phenotypic plasticity. *The American Naturalist*, 174(2) :176–189.

Taylor, A., Weigelt, P., König, C., Zotz, G., and Kreft, H. (2019). Island disharmony revisited using orchids as a model group. *New Phytologist*, 223(2) :597–606.

Thien, L. B., Azuma, H., and Kawano, S. (2000). New perspectives on the pollination biology of basal angiosperms. *International Journal of Plant Sciences*, 161(S6) :S225–S235.

Thomson, J. D. and Wilson, P. (2008). Explaining evolutionary shifts between bee and hummingbird pollination : convergence, divergence, and directionality. *International Journal of Plant Sciences*, 169(1) :23–38.

Timerman, D. and Barrett, S. C. (2019). Comparative analysis of pollen release biomechanics in thalictrum : implications for evolutionary transitions between animal and wind pollination. *New Phytologist*, 224(3) :1121–1132.

Troscianko, J. and Stevens, M. (2015). Image calibration and analysis toolbox–a free software suite for objectively measuring reflectance, colour and pattern. *Methods in Ecology and Evolution*, 6(11) :1320–1331.

Uyeda, J. C., Caetano, D. S., and Pennell, M. W. (2015). Comparative analysis of principal components can be misleading. *Systematic Biology*, 64(4) :677–689.

Van Belleghem, S. M., Papa, R., Ortiz-Zuazaga, H., Hendrickx, F., Jiggins, C. D., Owen McMillan, W., and Counterman, B. A. (2018). patternize : an r package for quantifying colour pattern variation. *Methods in ecology and evolution*, 9(2) :390–398.

van der Niet, T., Zollikofer, C. P., de León, M. S. P., Johnson, S. D., and Linder, H. P. (2010). Three-dimensional geometric morphometrics for studying floral shape variation. *Trends in plant science*, 15(8) :423–426.

Van Valen, L. (1965). Morphological variation and width of ecological niche. *The American Naturalist*, 99(908) :377–390.

Vences, M., Patmanidis, S., Kharchev, V., and Renner, S. S. (2022). Concatenator, a user-friendly program to concatenate dna sequences, implementing graphical user interfaces for mafft and fasttree. *Bioinformatics Advances*, 2(1) :vbac050.

Violle, C., Enquist, B. J., McGill, B. J., Jiang, L., Albert, C. H., Hulshof, C., Jung, V., and Messier, J. (2012). The return of the variance : intraspecific variability in community ecology. *Trends in ecology & evolution*, 27(4) :244–252.

Vogel, S. (1954). *Blütenbiologische typen als elemente der Sippengliederung*. Number 1. G. Fischer.

Vogel, S. (1969). Chiropterophilie in der neotropischen flora neue mitteilungen iii. *Flora oder Allgemeine botanische Zeitung. Abt. B, Morphologie und Geobotanik*, 158(4-5) :289–323.

Wang, C.-N., Hsu, H.-C., Wang, C.-C., Lee, T.-K., and Kuo, Y.-F. (2015). Quantifying floral shape variation in 3d using microcomputed tomography : a case study of a hybrid line between actinomorphic and zygomorphic flowers. *Frontiers in plant science*, 6 :724.

Warren, B. H., Simberloff, D., Ricklefs, R. E., Aguilée, R., Condamine, F. L., Gravel, D., Morlon, H., Mouquet, N., Rosindell, J., Casquet, J., et al. (2015). Islands as model systems in ecology and evolution : Prospects fifty years after macarthur-wilson. *Ecology Letters*, 18(2) :200–217.

Waser, N. M. (2006). Specialization and generalization in plant-pollinator interactions : a historical perspective. *Plant-pollinator interactions : From specialization to generalization*, pages 3–17.

Waser, N. M., Chittka, L., Price, M. V., Williams, N. M., and Ollerton, J. (1996). Generalization in pollination systems, and why it matters. *Ecology*, 77(4) :1043–1060.

Watson, D. R. (2015). *Resolving generic boundaries in Rhytidophyllum and Gesneria : A molecular phylogeny of the Caribbean subtribe gesneriinae (gesneriaceae)*. M.s., Department of Biological Sciences in the Graduate School of The University of Alabama, Ann Arbor, United States.

Weber, A., Clark, J. L., and Möller, M. (2013). A new formal classification of Gesnericeae. *Selbyana Special Issue : Proceedings of the World Gesneriad Research Conference 2010 (2013)*, Vol. 31(No. 2) :28.

Weller, H. I. and Westneat, M. W. (2019). Quantitative color profiling of digital images with earth mover's distance using the r package colordistance. *PeerJ*, 7 :e6398.

Wessinger, C. A., Rausher, M. D., and Hileman, L. C. (2019). Adaptation to hummingbird pollination is associated with reduced diversification in penstemon. *Evolution letters*, 3(5) :521–533.

Westerband, A., Funk, J., and Barton, K. (2021). Intraspecific trait variation in plants : a renewed focus on its role in ecological processes. *Annals of botany*, 127(4) :397–410.

Williams, Y. M., Williams, S. E., Alford, R. A., Waycott, M., and Johnson, C. N. (2006). Niche breadth and geographical range : ecological compensation for geographical rarity in rainforest frogs. *Biology letters*, 2(4) :532–535.

Willmer, P. (2011). *Pollination and floral ecology*. Princeton University Press.

Xie, W., Lewis, P. O., Fan, Y., Kuo, L., and Chen, M.-H. (2011). Improving marginal likelihood estimation for bayesian phylogenetic model selection. *Systematic biology*, 60(2) :150–160.

Yang, Z. (1994a). Estimating the pattern of nucleotide substitution. *Journal of molecular evolution*, 39(1) :105–111.

Yang, Z. (1994b). Maximum likelihood phylogenetic estimation from dna sequences with variable rates over sites : approximate methods. *Journal of Molecular evolution*, 39(3) :306–314.

Zenil-Ferguson, R., McEntee, J. P., Burleigh, J. G., and Duckworth, R. A. (2023). Linking ecological specialization to its macroevolutionary consequences : An example with passerine nest type. *Systematic Biology*, 72(2) :294–306.

Zhaoran, X. and Skog, L. (1990). A study of bellonia l. (gesneriacea).

Zimmer, E. A., Roalson, E. H., Skog, L. E., Boggan, J. K., and Idnurm, A. (2002). Phylogenetic relationships in the gesnerioideae (gesneriaceae) based on nrdna its and cpdna trnl-f and trne-t spacer region sequences. *American journal of Botany*, 89(2) :296–311.

Annexes

Annexe - Premier chapitre

The following Supporting Information is available for this article :

Figure S1. Landmarks (6 large dots) and sliding semi-landmarks (26 small dots) placement to characterise floral shape profiles. Landmarks are placed at the tip of the dorsal and ventral petals, at the intersection between the free and fused parts of the corolla, and at the base of the corolla. Sliding semi-landmarks are placed along the curves of the fused portion of the corolla tube (base of corolla lobes), dorsally and ventrally respectively.
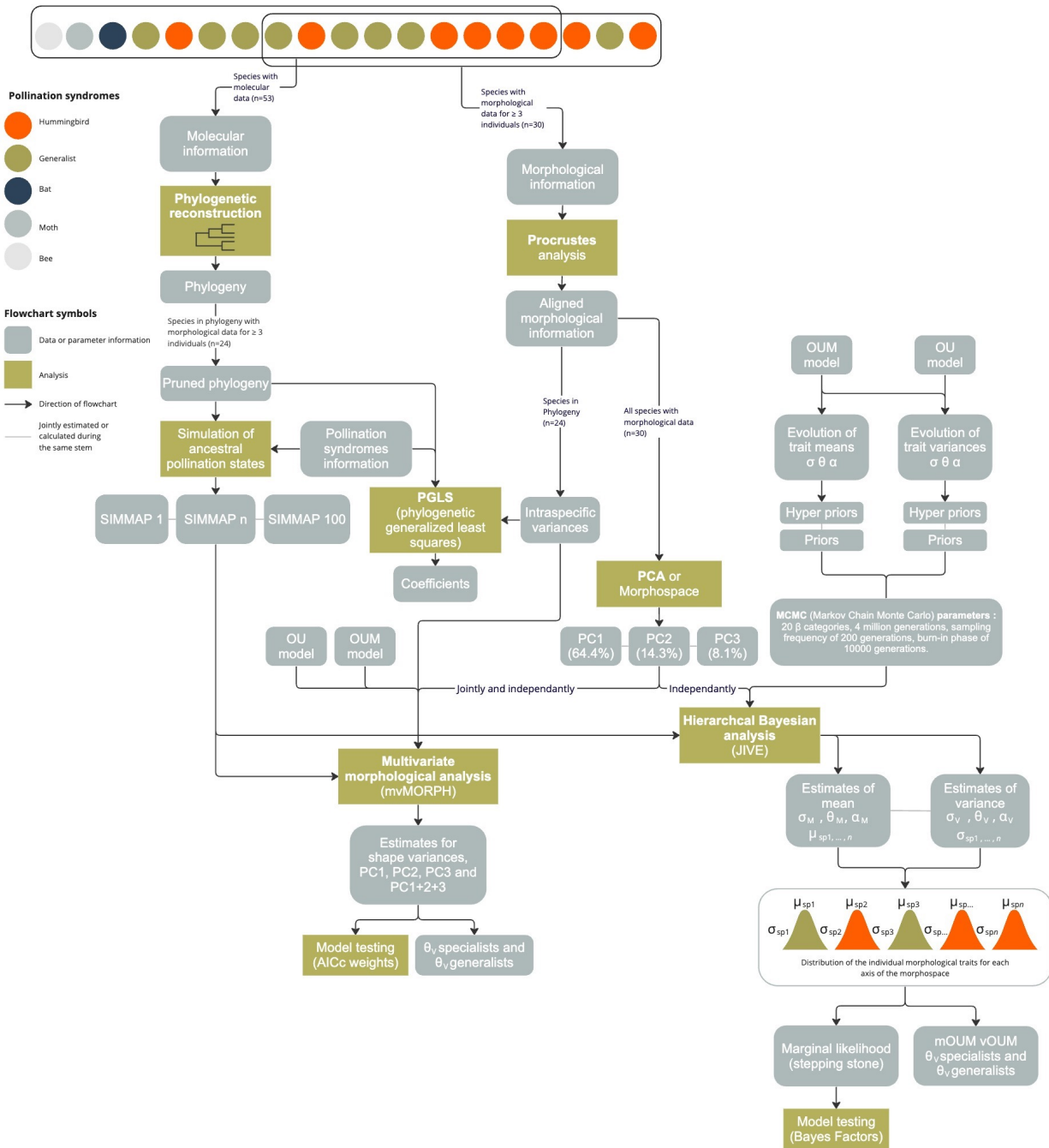
Figure S2. Methods flowchart. Individual flowers and their pollination syndromes are represented at the top of the chart. Downstream analyses are then represented by green squares, and information (molecular, morphological, results, models of evolution, and their parameter values) are represented by grey squares.

Tableau S1. Number of profiles per species to characterise intraspecific floral shape. Confirmed pollination syndromes are indicated in darker colours and inferred pollination syndromes are indicated in lighter colours : in orange for specialists for hummingbirds and green for mixed-pollination syndrome. Confirmed specialist for hummingbirds syndrome ⬤, inferred specialist for hummingbirds syndrome ⬤, confirmed mixed-pollination syndrome ⬤, inferred mixed-pollination syndrome ⬤.

Species	Sample size	Present in phylogeny
⬤ *Gesneria acaulis* L.	5	Yes
⬤ *Gesneria bicolor* (Rub.) Simon Joly & J.L.Clark	25	Yes
⬤ *Gesneria bracteosa* Urb.	4	Yes
⬤ *Gesneria citrina* Urb.	9	Yes
⬤ *Gesneria cuneifolia* (DC.) Fritsch	13	Yes
⬤ *Gesneria duchartreoides* (C. Wright) Urb.	5	No
⬤ *Gesneria ekmanii* Urb.	4	Yes
⬤ *Gesneria flava* Lambert, Simon Joly & J.L.Clark	3	Yes
⬤ *Gesneria glandulosa* (Griseb.) Urb.	9	No
⬤ *Gesneria harrisii* Urb.	3	No
⬤ *Gesneria libanensis* Linden ex C. Morren	4	No
⬤ *Gesneria nipensis* Britton & P. Wilson	3	Yes
⬤ *Gesneria pedicellaris* Alain	10	Yes
⬤ *Gesneria purpurascens* Urb.	4	Yes
⬤ *Gesneria reticulata* (Griseb.) Urb	10	Yes
⬤ *Gesneria salicifolia* (Griseb.) Urb.	30	Yes
⬤ *Gesneria sintenisii* Urb.	21	Yes
⬤ *Gesneria ventricosa* Sw.	8	Yes
⬤ *Gesneria viridiflora* (Decne.) Kuntze	8	Yes
⬤ *Gesneria viridiflora* (Decne.) Kuntze subsp. *acrochordonanthe* L.E.Skog	3	No
⬤ *Rhytidophyllum auriculatum* Hook.	14	Yes
⬤ *Rhytidophyllum berteroanum* Mart.	3	Yes
⬤ *Rhytidophyllum crenulatum* DC.	4	Yes
⬤ *Rhytidophyllum exsertum* Griseb.	27	Yes
⬤ *Rhytidophyllum grandiflorum* Xu & L.E.Skog ex Zanoni, & Jiménez Rodr.	3	Yes
⬤ *Rhytidophyllum leucomallon* Hanst.	7	Yes
⬤ *Rhytidophyllum lomense* (Urb.) C.V. Morton	4	No
⬤ *Rhytidophyllum minus* Urb.	10	Yes
⬤ *Rhytidophyllum rupincola* (Urb.) C.V. Morton	5	Yes
⬤ *Rhytidophyllum tomentosum* (L.) Mart.	3	Yes

Tableau S2. Pollination syndrome information for *Gesneria* and *Rhytidophyllum* species

Genus	Species	Pollinator	Confirmed	Reference
Gesneria	*acaulis*	hummingbird	yes	(Martén-Rodríguez et al., 2009; Martén-Rodríguez et al., 2010; Martén-Rodríguez et al., 2015)
Gesneria	*bicolor*	mixed-pollination	yes	(Faure and Joly, 2020)
Gesneria	*bracteosa*	mixed-pollination	no	(Joly et al., 2018)
Gesneria	*citrina*	hummingbird	yes	(Martén-Rodríguez and Fenster, 2008; Martén-Rodríguez et al., 2009; Martén-Rodríguez et al., 2010; Martén-Rod
Gesneria	*cuneifolia*	hummingbird	yes	(Martén-Rodríguez and Fenster, 2008; Martén-Rodríguez et al., 2009; Martén-Rodríguez et al., 2010; Martén-Rod
Gesneria	*duchartreoides*	mixed-pollination	no	(Joly et al., 2018)
Gesneria	*ekmanii*	mixed-pollination	no	(Joly et al., 2018)
Gesneria	*flava*	mixed-pollination	no	
Gesneria	*glandulosa*	hummingbird	no	(Joly et al., 2018)
Gesneria	*harrisii*	hummingbird	no	(Joly et al., 2018)
Gesneria	*libanensis*	hummingbird	no	(Joly et al., 2018)
Gesneria	*nipensis*	hummingbird	no	(Joly et al., 2018)
Gesneria	*pedicellaris*	hummingbird	yes	(Martén-Rodríguez et al., 2009; Martén-Rodríguez et al., 2010; Martén-Rodríguez et al., 2015)
Gesneria	*purpurascens*	hummingbird	yes	(Martén-Rodríguez et al., 2015)
Gesneria	*reticulata*	hummingbird	yes	(Martén-Rodríguez and Fenster, 2008; Martén-Rodríguez et al., 2010; Martén-Rodríguez et al., 2015)
Gesneria	*salicifolia*	hummingbird	no	(Joly et al., 2018)
Gesneria	*sintenisii*	mixed-pollination	yes	(Martén-Rodríguez and Fenster, 2008; Martén-Rodríguez et al., 2009, 2015)
Gesneria	*ventricosa*	hummingbird	yes	(Martén-Rodríguez et al., 2009; Martén-Rodríguez et al., 2010; Martén-Rodríguez et al., 2015)
Gesneria	*viridiflora* subsp. *viridiflora*	mixed-pollination	yes	(Martén-Rodríguez et al., 2010; Martén-Rodríguez et al., 2015)
Gesneria	*viridiflora* subsp. *acrochordonanthe*	mixed-pollination	no	
Rhytidophyllum	*auriculatum*	mixed-pollination	yes	(Martén-Rodríguez et al., 2009; Martén-Rodríguez et al., 2010)
Rhytidophyllum	*berteroanum*	hummingbird	yes	(Joly et al., 2018)
Rhytidophyllum	*crenulatum*	mixed-pollination	yes	(Martén-Rodríguez et al., 2010)
Rhytidophyllum	*exsertum*	mixed-pollination	yes	(Martén-Rodríguez et al., 2015)
Rhytidophyllum	*grandiflorum*	mixed-pollination	yes	(Martén-Rodríguez et al., 2009; Martén-Rodríguez et al., 2010; Martén-Rodríguez et al., 2015)
Rhytidophyllum	*leucomallon*	mixed-pollination	yes	(Martén-Rodríguez et al., 2009; Martén-Rodríguez et al., 2010; Martén-Rodríguez et al., 2015)
Rhytidophyllum	*lomense*	hummingbird	no	(Joly et al., 2018)
Rhytidophyllum	*minus*	mixed-pollination	yes	(Martén-Rodríguez et al., 2009, 2015; Joly et al., 2018)
Rhytidophyllum	*rupincola*	hummingbird	yes	(Martén-Rodríguez et al., 2010)
Rhytidophyllum	*tomentosum*	mixed-pollination	yes	(Martén-Rodríguez et al., 2010)

Tableau S3. Images of flower profiles information and their attributions. The new images added to the data set of Joly et al. (2018) are marked in the last column with a no.

Species	File name	Attribution	In Joly et al. (2018)
Gesneria acaulis	GES_acaulis_APR72R1_13.jpg		yes
Gesneria acaulis	GES_acaulis_G877_G940_G1238_1.jpg		yes
Gesneria acaulis	GES_acaulis_JLC_11303_02.jpg	John L. Clark	yes
Gesneria acaulis	GES_acaulis_MartenRodriguez_Cuba_sn_indiv.bas.jpg	Silvana Marten-Rodriguez	yes
Gesneria acaulis	GES_acaulis_side_JLC_14532_07.jpg	John L. Clark	no
Gesneria bicolor	RHY_bicolor_2014-001.jpg	Francois Lambert	yes
Gesneria bicolor	RHY_bicolor_JLC_14321_109.jpg	John L. Clark	yes
Gesneria bicolor	RHY_bicolor_JLC_14364_05.jpg	John L. Clark	yes
Gesneria bicolor	RHY_bicolor_JLC_14493_07.jpg	John L. Clark	yes
Gesneria bicolor	RHY_bicolor_side_JLC_14370_10.jpg	John L. Clark	no
Gesneria bicolor	RHY_bicolor_side_JLC_14494_19.jpg	John L. Clark	no
Gesneria bicolor	RHY_bicolor-1_side_img5627.jpg	Simon Joly	no
Gesneria bicolor	RHY_bicolor-10_side_img5662.jpg	Simon Joly	no
Gesneria bicolor	RHY_bicolor-11_side_img5667.jpg	Simon Joly	no
Gesneria bicolor	RHY_bicolor-12_side_img5670.jpg	Simon Joly	no
Gesneria bicolor	RHY_bicolor-13_side_img5678.jpg	Simon Joly	no
Gesneria bicolor	RHY_bicolor-14_side_img5687.jpg	Simon Joly	no
Gesneria bicolor	RHY_bicolor-15-1_side_img5691.jpg	Simon Joly	no
Gesneria bicolor	RHY_bicolor-15-2_side_img5695.jpg	Simon Joly	no
Gesneria bicolor	RHY_bicolor-2_side_img5630.jpg	Simon Joly	no
Gesneria bicolor	RHY_bicolor-3_side_img5634.jpg	Simon Joly	no
Gesneria bicolor	RHY_bicolor-4_side_img5637.jpg	Simon Joly	no
Gesneria bicolor	RHY_bicolor-6_side_img5640.jpg	Simon Joly	no
Gesneria bicolor	RHY_bicolor-7_side_img5648.jpg	Simon Joly	no
Gesneria bicolor	RHY_bicolor-8_side_img5654.jpg	Simon Joly	no
Gesneria bicolor	RHY_bicolor-9_side_img5658.jpg	Simon Joly	no
Gesneria bicolor	RHY_bicolor-grande_Joly_27janv2018-1_side_img5914.jpg	Simon Joly	no
Gesneria bicolor	RHY_bicolor-grande_Joly_27janv2018-2_side_img5916.jpg	Simon Joly	no
Gesneria bicolor	RHY_bicolor-grande_Joly_sn_25janv2018_side_img5842.jpg	Simon Joly	no
Gesneria bicolor	RHY_bicolor-grande_Joly1116-1_img5586.jpg	Simon Joly	no
Gesneria bracteosa	GES_bracteosa_JLC_10567_53.jpg	John L. Clark	yes
Gesneria bracteosa	GES_bracteosa_side_JLC_15442_007.jpg	John L. Clark	no
Gesneria bracteosa	GES_bracteosa_side_JLC_15468_12.jpg	John L. Clark	no

Gesneria bracteosa	GES_bracteosa_side_JLC_15500_27.jpg	John L. Clark	no
Gesneria citrina	GES_citrina_G888_Dec_1965_1.jpg		yes
Gesneria citrina	GES_citrina_IMG_5510_side_PuertoRico_Lambert.jpg	François Lambert	no
Gesneria citrina	GES_citrina_IMG_5532_side_PuertoRico_Lambert.jpg	François Lambert	no
Gesneria citrina	GES_citrina_JLC_10021_07.jpg	John L. Clark	yes
Gesneria citrina	GES_citrina_MartenRodriguez_PuertoRico_sn.jpg	Silvana Marten-Rodriguez	no
Gesneria citrina	GES_citrina_MarteRodriguez_Puerto-Rico_DSC0530.jpg	Silvana Marten-Rodriguez	no
Gesneria citrina	GES_citrina_MarteRodriguez_Puerto-Rico_sn3.jpg	Silvana Marten-Rodriguez	no
Gesneria citrina	GES_citrina_Puerto_Rico_1965_Talpey_SN_01.jpg	Thomas E. Talpey	NA
Gesneria citrina	GES_citrina_urban_2.jpg		no
Gesneria cuneifolia	GES_cuneifolia_APR_72R9_1.jpg		yes
Gesneria cuneifolia	GES_cuneifolia_Cornell_857_Florida_Talpey_SN_01.jpg	Thomas E. Talpey	NA
Gesneria cuneifolia	GES_cuneifolia_Dunn_1.jpg		yes
Gesneria cuneifolia	GES_cuneifolia_G784_G857_1.jpg		yes
Gesneria cuneifolia	GES_cuneifolia_G857_Puerto_Rico_Tapley_1965_2.jpg	Thomas E. Talpey	yes
Gesneria cuneifolia	GES_cuneifolia_G869_G857_G763_1.jpg		yes
Gesneria cuneifolia	GES_cuneifolia_G869_Puerto_Rico_1963_Tapley_10_5_BH_4.jpg	Thomas E. Talpey	yes
Gesneria cuneifolia	GES_cuneifolia_iNaturalist_150193941.jpeg	iNaturalist ©jingyilu	no
Gesneria cuneifolia	GES_cuneifolia_JBM.jpg	Etienne Leveille-Bourret	yes
Gesneria cuneifolia	GES_cuneifolia_july_1980_1.jpg		yes
Gesneria cuneifolia	GES_cuneifolia_Quebradillas_Tapley_1.jpg	Thomas E. Talpey	no
Gesneria cuneifolia	GES_cuneifolia_USBRG_1997_200_2.jpg	US Botanical Research Gardens	no
Gesneria cuneifolia	GES_cuneifolia_USBRG_85_116_4.jpg	US Botanical Research Gardens	no
Gesneria duchartreoides	GES_duchartreoides_JLC_12791_067.jpg	John L. Clark	yes
Gesneria duchartreoides	GES_duchartreoides_side_JLC_15964_07.jpg	John L. Clark	no
Gesneria duchartreoides	GES_duchartreoides_side_JLC_15973_092.jpg	John L. Clark	no
Gesneria duchartreoides	GES_duchartroides_JLC_14576_68.jpg	John L. Clark	no
Gesneria duchartreoides	GES_duchartroides_JLC_15034_64.jpg	John L. Clark	no
Gesneria ekmanii	GES_ekmanii_JLC_14525_21.jpg	John L. Clark	no
Gesneria ekmanii	GES_ekmanii_Lambert2014-024-3.jpg	Francois Lambert	no
Gesneria ekmanii	RHY_ekmanii_2014-020.jpg	Francois Lambert	yes
Gesneria ekmanii	RHY_ekmanii_2014-024.jpg	Francois Lambert	yes
Gesneria flava	RHY_espèce_nov_Macaya_side_JLC_14460_027.jpg	John L. Clark	no
Gesneria flava	RHY_espèce_nov_Macaya_side_JLC_14492_06.jpg	John L. Clark	no
Gesneria flava	RHY_nov.sp._2014-010.jpg	Francois Lambert	yes
Gesneria glandulosa	GES_glandulosa_JJLC_15063_21.jpg	John L. Clark	no
Gesneria glandulosa	GES_glandulosa_JLC_12772_023.jpg	John L. Clark	yes
Gesneria glandulosa	GES_glandulosa_JLC_14572_064.jpg	John L. Clark	no

Species	Filename	Photographer	
Gesneria glandulosa	GES_glandulosa_side_01_1919_Cuba_Almarales-Castro.jpg	Abel Almarales-Castro	no
Gesneria glandulosa	GES_glandulosa_side_02_1924_Cuba_Almarales-Castro.jpg	Abel Almarales-Castro	no
Gesneria glandulosa	GES_glandulosa_side_03_1927_Cuba_Almarales-Castro.jpg	Abel Almarales-Castro	no
Gesneria glandulosa	GES_glandulosa_side_04_1929_Cuba_Almarales-Castro.jpg	Abel Almarales-Castro	no
Gesneria glandulosa	GES_glandulosa_side_05_1918_Cuba_Almarales-Castro.jpg	Abel Almarales-Castro	no
Gesneria glandulosa	GES_glandulosa_side_JLC_15961_069.jpg	John L. Clark	no
Gesneria harrisii	GES_harrisii_Jamaica_Guaco_Rock_3.jpg	Thomas E. Talpey	yes
Gesneria harrisii	GES_harrisii_Jamaica_Nov_05_1964_Talpey_19_Guaco_Rock_07.jpg	Thomas E. Talpey	no
Gesneria harrisii	GES_harrisii_Tapley_1964.jpg	Thomas E. Talpey	yes
Gesneria libanensis	GES_libanensis_JLC_10575_01.jpg	John L. Clark	no
Gesneria libanensis	GES_libanensis_JLC_15057_34.jpg	John L. Clark	no
Gesneria libanensis	GES_libanensis_side_JLC_15957_035.jpg	John L. Clark	no
Gesneria libanensis	GES_libanensis_side_JLC_15978_059.jpg	John L. Clark	no
Gesneria lomensis	RHY_lomense_side_JLC_10466_11.jpg	John L. Clark	no
Gesneria lomensis	RHY_lomensis_JLC_10469_23.jpg	John L. Clark	yes
Gesneria lomensis	RHY_lomensis_JLC_10470_24.jpg	John L. Clark	yes
Gesneria lomensis	RHY_lomensis_JLC_10471_01.jpg	John L. Clark	yes
Gesneria nipensis	GES_nipensis_JLC_10577_30.jpg	John L. Clark	yes
Gesneria nipensis	GES_nipensis_JLC_10578_05.jpg	John L. Clark	yes
Gesneria nipensis	GES_nipensis_side_JLC_15952_089.jpg	John L. Clark	no
Gesneria pedicellaris	GES_pedicellaris_1964_Dominican_Republic_Talpey_SN_01.jpg	Thomas E. Talpey	NA
Gesneria pedicellaris	GES_pedicellaris_405_1.jpg		no
Gesneria pedicellaris	GES_pedicellaris_dunn_1.jpg		no
Gesneria pedicellaris	GES_pedicellaris_G1364_2.jpg		no
Gesneria pedicellaris	GES_pedicellaris_G898_G883_G1231_1.jpg		yes
Gesneria pedicellaris	GES_pedicellaris_JBM.jpg	Etienne Leveille-Bourret	yes
Gesneria pedicellaris	GES_pedicellaris_JLC_10635_04_2.jpg	John L. Clark	no
Gesneria pedicellaris	GES_pedicellaris_JLC_11328_13.jpg	John L. Clark	yes
Gesneria pedicellaris	GES_pedicellaris_JLC_14536_14.jpg	John L. Clark	no
Gesneria pedicellaris	GES_pedicellaris_pauciflora_sacatilis_1.jpg		yes
Gesneria purpurascens	GES_purpurascens_JLC_10564_025.jpg	John L. Clark	no
Gesneria purpurascens	GES_purpurascens_JLC_12769_057.jpg	John L. Clark	no
Gesneria purpurascens	GES_purpurascens_JLC_15061_11.jpg	John L. Clark	no
Gesneria purpurascens	GES_purpurascens_side_JLC_15963_08.jpg	John L. Clark	no
Gesneria reticulata	GES_reticulata_dominicanrepublic_talpey_1972_1.jpg	Thomas E. Talpey	yes
Gesneria reticulata	GES_reticulata_G784_3.jpg		yes
Gesneria reticulata	GES_reticulata_IMG_5465_side_PuertoRico_Lambert.jpg	François Lambert	no
Gesneria reticulata	GES_reticulata_IMG_5470_side_PuertoRico_Lambert.jpg	François Lambert	no

Gesneria reticulata	GES_reticulata_IMG_5472_side_PuertoRico_Lambert.jpg	François Lambert	no
Gesneria reticulata	GES_reticulata_IMG_5480_side_PuertoRico_Lambert.jpg	François Lambert	no
Gesneria reticulata	GES_reticulata_JLC_13762_19.jpg	John L. Clark	no
Gesneria reticulata	GES_reticulata_JLC_14490_55.jpg	John L. Clark	no
Gesneria reticulata	GES_reticulata_side_JLC_15967_029.jpg	John L. Clark	no
Gesneria reticulata	GES_reticulata_USBRG_1997_205_2.jpg	US Botanical Research Gardens	yes
Gesneria salicifolia	GES_salicifolia_JLC_10566_38.jpg	John L. Clark	no
Gesneria salicifolia	GES_salicifolia_JLC_14565_071.jpg	John L. Clark	no
Gesneria salicifolia	GES_salicifolia_JLC_14566_11.jpg	John L. Clark	no
Gesneria salicifolia	GES_salicifolia_JLC_15058_21.jpg	John L. Clark	no
Gesneria salicifolia	GES_salicifolia_side_01_1829(Largo)_Cuba_Almarales-Castro.jpg	Abel Almarales-Castro	no
Gesneria salicifolia	GES_salicifolia_side_01_1831(Largo)_Cuba_Almarales-Castro.jpg	Abel Almarales-Castro	no
Gesneria salicifolia	GES_salicifolia_side_01_2069_Cuba_Almarales-Castro.jpg	Abel Almarales-Castro	no
Gesneria salicifolia	GES_salicifolia_side_02_1827(Largo)_Cuba_Almarales-Castro.jpg	Abel Almarales-Castro	no
Gesneria salicifolia	GES_salicifolia_side_02_1833(Largo)_Cuba_Almarales-Castro.jpg	Abel Almarales-Castro	no
Gesneria salicifolii	GES_salicifolia_side_02_1837(Largo)_Cuba_Almarales-Castro.jpg	Abel Almarales-Castro	no
Gesneria salicifolia	GES_salicifolia_side_02_2071_Cuba_Almarales-Castro.jpg	Abel Almarales-Castro	no
Gesneria salicifolia	GES_salicifolia_side_02_2072_Cuba_Almarales-Castro.jpg	Abel Almarales-Castro	no
Gesneria salicifolia	GES_salicifolia_side_03_1838(Largo)_Cuba_Almarales-Castro.jpg	Abel Almarales-Castro	no
Gesneria salicifolia	GES_salicifolia_side_03_1839(Largo)_Cuba_Almarales-Castro.jpg	Abel Almarales-Castro	no
Gesneria salicifolia	GES_salicifolia_side_03_1841(Largo)_Cuba_Almarales-Castro.jpg	Abel Almarales-Castro	no
Gesneria salicifolia	GES_salicifolia_side_03_2073_Cuba_Almarales-Castro.jpg	Abel Almarales-Castro	no
Gesneria salicifolia	GES_salicifolia_side_03_2075_Cuba_Almarales-Castro.jpg	Abel Almarales-Castro	no
Gesneria salicifolia	GES_salicifolia_side_04_2078_Cuba_Almarales-Castro.jpg	Abel Almarales-Castro	no
Gesneria salicifolia	GES_salicifolia_side_04_2080_Cuba_Almarales-Castro.jpg	Abel Almarales-Castro	no
Gesneria salicifolia	GES_salicifolia_side_05_2082_Cuba_Almarales-Castro.jpg	Abel Almarales-Castro	no
Gesneria salicifolia	GES_salicifolia_side_05_2084.jpg	Abel Almarales-Castro	no
Gesneria salicifolia	GES_salicifolia_side_06_2086_Cuba_Almarales-Castro.jpg	Abel Almarales-Castro	no
Gesneria salicifolia	GES_salicifolia_side_06_2087_Cuba_Almarales-Castro.jpg	Abel Almarales-Castro	no
Gesneria salicifolia	GES_salicifolia_side_06_2089_Cuba_Almarales-Castro.jpg	Abel Almarales-Castro	no
Gesneria salicifolia	GES_salicifolia_side_07_2093_Cuba_Almarales-Castro.jpg	Abel Almarales-Castro	no
Gesneria salicifolia	GES_salicifolia_side_07_2095_Cuba_Almarales-Castro.jpg	Abel Almarales-Castro	no
Gesneria salicifolia	GES_salicifolia_side_08_2097_Cuba_Almarales-Castro.jpg	Abel Almarales-Castro	no
Gesneria salicifolia	GES_salicifolia_side_08_2099_Cuba_Almarales-Castro.jpg	Abel Almarales-Castro	no
Gesneria salicifolia	GES_salicifolia_side_JLC_15960_148.jpg	John L. Clark	no
Gesneria salicifolia	GES_salicifolia_side_JLC_15976_048.jpg	John L. Clark	no
Gesneria sintenisii	GES_sintenisii_20181206_110637_side_PuertoRico_Lambert.jpg	Francois Lambert	no
Gesneria sintenisii	GES_sintenisii_20181206_111121_side_PuertoRico_Lambert.jpg	Francois Lambert	no

Species	Filename	Photographer	
Gesneria sintenisii	GES_sintenisii_20181206_111126_side_PuertoRico_Lambert.jpg	Francois Lambert	no
Gesneria sintenisii	GES_sintenisii_IMG_5283_side_PuertoRico_Lambert.jpg	Francois Lambert	no
Gesneria sintenisii	GES_sintenisii_IMG_5295_side_PuertoRico_Lambert.jpg	Francois Lambert	no
Gesneria sintenisii	GES_sintenisii_IMG_5298_side_PuertoRico_Lambert.jpg	Francois Lambert	no
Gesneria sintenisii	GES_sintenisii_IMG_5301_side_PuertoRico_Lambert.jpg	Francois Lambert	no
Gesneria sintenisii	GES_sintenisii_IMG_5307_side_PuertoRico_Lambert.jpg	Francois Lambert	no
Gesneria sintenisii	GES_sintenisii_IMG_5319_side_PuertoRico_Lambert.jpg	Francois Lambert	no
Gesneria sintenisii	GES_sintenisii_IMG_5325_side_PuertoRico_Lambert.jpg	Francois Lambert	no
Gesneria sintenisii	GES_sintenisii_IMG_5329_side_PuertoRico_Lambert.jpg	Francois Lambert	no
Gesneria sintenisii	GES_sintenisii_IMG_5351_side_PuertoRico_Lambert.jpg	Francois Lambert	no
Gesneria sintenisii	GES_sintenisii_IMG_5354_side_PuertoRico_Lambert.jpg	Francois Lambert	no
Gesneria sintenisii	GES_sintenisii_IMG_5356_side_PuertoRico_Lambert.jpg	Francois Lambert	no
Gesneria sintenisii	GES_sintenisii_IMG_5357_side_PuertoRico_Lambert.jpg	Francois Lambert	no
Gesneria sintenisii	GES_sintenisii_IMG_5358_side_PuertoRico_Lambert.jpg	Francois Lambert	no
Gesneria sintenisii	GES_sintenisii_IMG_5392_side_PuertoRico_Lambert.jpg	Francois Lambert	no
Gesneria sintenisii	GES_sintenisii_IMG_5400_side_PuertoRico_Lambert.jpg	Francois Lambert	no
Gesneria sintenisii	GES_sintenisii_IMG_5407_side_PuertoRico_Lambert.jpg	Francois Lambert	no
Gesneria sintenisii	GES_sintenisii_MartenRodriguez1252.jpg	Silvana Marten-Rodriguez	no
Gesneria ventricosa	GES_ventricosa_dunn_4.jpg		yes
Gesneria ventricosa	GES_ventricosa_G940_3.jpg		yes
Gesneria ventricosa	GES_ventricosa_iNaturalist_22293191.jpeg	iNaturalist ©Elizabeth Haber	no
Gesneria ventricosa	GES_ventricosa_iNaturalist_43872598.jpeg	iNaturalist ©reefguard	no
Gesneria ventricosa	GES_ventricosa_JBM.jpg	Etienne Leveille-Bourret	yes
Gesneria ventricosa	GES_ventricosa_JLC_13076_04.jpg	John L. Clark	no
Gesneria ventricosa	GES_ventricosa_JLC_14534_13.jpg	John L. Clark	no
Gesneria ventricosa	GES_ventricosa_JLC_6545_2.jpg	John L. Clark	yes
Gesneria viridiflora subsp. *acrochordonanthe*	GES_viridiflora_acrochordonanthe_2014-028.jpg	Francois Lambert	yes
Gesneria viridiflora subsp. *acrochordonanthe*	GES_viridiflora_acrochordonanthe_JLC_14467_090.jpg	John L. Clark	no
Gesneria viridiflora subsp. *acrochordonanthe*	GES_viridiflora_acrochordonanthe_JLC_14522_045.jpg	John L. Clark	no
Gesneria viridiflora subsp. *viridiflora*	GES_viridiflora_JLC_10509_35.jpg	John L. Clark	yes
Gesneria viridiflora subsp. *viridiflora*	GES_viridiflora_JLC_10509_91.jpg	John L. Clark	no
Gesneria viridiflora subsp. *viridiflora*	GES_viridiflora_JLC_10540_01.jpg	John L. Clark	yes
Gesneria viridiflora subsp. *viridiflora*	GES_viridiflora_JLC_10552_21.jpg	John L. Clark	yes
Gesneria viridiflora subsp. *viridiflora*	GES_viridiflora_JLC_10554_20.jpg	John L. Clark	yes
Gesneria viridiflora subsp. *viridiflora*	GES_viridiflora_JLC_10555_29.jpg	John L. Clark	yes
Gesneria viridiflora subsp. *viridiflora*	GES_viridiflora_JLC_12797_14.jpg	John L. Clark	yes
Gesneria viridiflora subsp. *viridiflora*	GES_viridiflora_side_JLC_15984_248.jpg	John L. Clark	no
Rhytidophyllum auriculatum	RHY_auriculatum_2014-014.jpg	Francois Lambert	yes

Rhytidophyllum auriculatum	RHY_auriculatum_2014-025.jpg	Francois Lambert	yes
Rhytidophyllum auriculatum	RHY_auriculatum_iNaturalist_33974904.jpeg	iNaturalist ©Martin Reith	no
Rhytidophyllum auriculatum	RHY_auriculatum_JBM.jpg	Etienne Leveille-Bourret	yes
Rhytidophyllum auriculatum	RHY_auriculatum_JLC_14319_34.jpg	John L. Clark	yes
Rhytidophyllum auriculatum	RHY_auriculatum_JLC_14387_37.jpg	John L. Clark	yes
Rhytidophyllum auriculatum	RHY_auriculatum_JLC_14434_01.jpg	John L. Clark	yes
Rhytidophyllum auriculatum	RHY_auriculatum_JLC_14499_10.jpg	John L. Clark	yes
Rhytidophyllum auriculatum	RHY_auriculatum_JLC_14523_028.jpg	John L. Clark	yes
Rhytidophyllum auriculatum	RHY_auriculatum_USBRG_97_113_1.jpg	US Botanical Research Gardens	yes
Rhytidophyllum auriculatum	RHY_auriculatum-Macaya_Joly1112-1_img5547.jpg	Simon Joly	no
Rhytidophyllum auriculatum	RHY_auriculatum-Macaya_Joly1112-2_img5557.jpg	Simon Joly	no
Rhytidophyllum auriculatum	RHY_auriculatum-Macaya_Joly1112-4_img5561.jpg	Simon Joly	no
Rhytidophyllum auriculatum	RHY_auriculatum-Macaya_Joly1112-5_img5567.jpg	Simon Joly	no
Rhytidophyllum berteroanum	RHY_berteroanum_77_227_4.jpg		yes
Rhytidophyllum berteroanum	RHY_berteroanum_G1398_G1257_G841_1.jpg		yes
Rhytidophyllum berteroanum	RHY_berteroanum_JUL81W5_16.jpg		yes
Rhytidophyllum crenulatum	RHY_crenulatum_JLC_10042_38.jpg	John L. Clark	yes
Rhytidophyllum crenulatum	RHY_crenulatum_JLC_10580_10.jpg	John L. Clark	yes
Rhytidophyllum crenulatum	RHY_crenulatum_JLC_10582_02.jpg	John L. Clark	yes
Rhytidophyllum crenulatum	RHY_crenulatum_JLC_12803_09.jpg	John L. Clark	yes
Rhytidophyllum exsertum	RHY_exsertum_JBM.jpg	Etienne Leveille-Bourret	yes
Rhytidophyllum exsertum	RHY_exsertum_JLC_10508_12.jpg	John L. Clark	yes
Rhytidophyllum exsertum	RHY_exsertum_JLC_10538_07.jpg	John L. Clark	yes
Rhytidophyllum exsertum	RHY_exsertum_JLC_10546_07.jpg	John L. Clark	yes
Rhytidophyllum exsertum	RHY_exsertum_JLC_10551_03.jpg	John L. Clark	yes
Rhytidophyllum exsertum	RHY_exsertum_JLC_10565_08.jpg	John L. Clark	yes
Rhytidophyllum exsertum	RHY_exsertum_JLC_10569_05.jpg	John L. Clark	yes
Rhytidophyllum exsertum	RHY_exsertum_JLC_10571_07.jpg	John L. Clark	no
Rhytidophyllum exsertum	RHY_exsertum_JLC_10579_01.jpg	John L. Clark	yes
Rhytidophyllum exsertum	RHY_exsertum_JLC_10585_18.jpg	John L. Clark	yes
Rhytidophyllum exsertum	RHY_exsertum_JLC_12770_23.jpg	John L. Clark	yes
Rhytidophyllum exsertum	RHY_exsertum_JLC_12787_14.jpg	John L. Clark	yes
Rhytidophyllum exsertum	RHY_exsertum_side_JLC_10557_30.jpg	John L. Clark	no
Rhytidophyllum exsertum	RHY_exsertum_side_JLC_14559_15.jpg	John L. Clark	no
Rhytidophyllum exsertum	RHY_exsertum_side_JLC_14569_23.jpg	John L. Clark	no
Rhytidophyllum exsertum	RHY_exsertum_side_JLC_14577_33.jpg	John L. Clark	no
Rhytidophyllum exsertum	RHY_exsertum_side_JLC_14594_36.jpg	John L. Clark	no
Rhytidophyllum exsertum	RHY_exsertum_side_JLC_15036_18.jpg	John L. Clark	no

Rhytidophyllum exsertum	RHY_exsertum_side_JLC_15056_13.jpg	John L. Clark	no
Rhytidophyllum exsertum	RHY_exsertum_side_JLC_15059_08.jpg	John L. Clark	no
Rhytidophyllum exsertum	RHY_exsertum_side_JLC_15060_26.jpg	John L. Clark	no
Rhytidophyllum exsertum	RHY_exsertum_side_JLC_15496_21.jpg	John L. Clark	no
Rhytidophyllum exsertum	RHY_exsertum_side_JLC_15547_17.jpg	John L. Clark	no
Rhytidophyllum exsertum	RHY_exsertum_side_JLC_15954_064.jpg	John L. Clark	no
Rhytidophyllum exsertum	RHY_exsertum_side_JLC_15974_15.jpg	John L. Clark	no
Rhytidophyllum exsertum	RHY_exsertum_side_JLC_15977_021.jpg	John L. Clark	no
Rhytidophyllum exsertum	RHY_exsertum_side_JLC_15985_011.jpg	John L. Clark	no
Rhytidophyllum grandiflorum	RHY_grandiflorum_1965_Dominican_Republic_Talpey_SN_02.jpg	Thomas E. Talpey	NA
Rhytidophyllum grandiflorum	RHY_grandiflorum_APR72r9_8.jpg		yes
Rhytidophyllum grandiflorum	RHY_grandiflorum_side_SEP70r9_25.jpg		no
Rhytidophyllum minus	RHY_intermedium_2018_3.jpg		NA
Rhytidophyllum minus	RHY_intermedium_JBM-936-2017.jpg	Jardin Botanique de Montréal	no
Rhytidophyllum minus	RHY_intermedium_JLC_10547_10.jpg	John L. Clark	yes
Rhytidophyllum minus	RHY_intermedium_JLC_10549_12.jpg	John L. Clark	no
Rhytidophyllum minus	RHY_minus_JLC_10500_34.jpg	John L. Clark	yes
Rhytidophyllum minus	RHY_minus_MartenRodriguez_Cuba_sn.jpg	Silvana Marten-Rodriguez	no
Rhytidophyllum minus	RHY_minus_side_JLC_10547_17.jpg	John L. Clark	no
Rhytidophyllum minus	RHY_minus_side_JLC_10549_14.jpg	John L. Clark	no
Rhytidophyllum minus	RHY_minus_side_JLC_14595_11.jpg	John L. Clark	no
Rhytidophyllum minus	RHY_minus_side_JLC_15982_053.jpg	John L. Clark	no
Rhytidophyllum leucomallon	RHY_leucomallon_G1232_1.jpg		yes
Rhytidophyllum leucomallon	RHY_leucomallon_iNaturalist_29524256.jpeg	iNaturalist © Martin Reith	no
Rhytidophyllum leucomallon	RHY_leucomallon_iNaturalist_44060147.jpeg	iNaturalist ©Martin Reith	no
Rhytidophyllum leucomallon	RHY_leucomallon_JLC_14338_031.jpg	John L. Clark	yes
Rhytidophyllum leucomallon	RHY_leucomallon_JLC_14497_09.jpg	John L. Clark	yes
Rhytidophyllum leucomallon	RHY_leucomallon_JLC_14498_10.jpg	John L. Clark	yes
Rhytidophyllum leucomallon	RHY_leucomallon_side_JLC_14363_02.jpg	John L. Clark	no
Rhytidophyllum rupincola	RHY_rupincola_JBM.jpg	Etienne Leveille-Bourret	yes
Rhytidophyllum rupincola	RHY_rupincola_JLC_11308_18.jpg	John L. Clark	yes
Rhytidophyllum rupincola	RHY_rupincola_JLC_11957_36.jpg	John L. Clark	yes
Rhytidophyllum rupincola	RHY_rupincola_side_JLC_11950_013.jpg	John L. Clark	no
Rhytidophyllum rupincola	RHY_rupincola_usbrg_97_117.jpg	US Botanical Research Gardens	no
Rhytidophyllum tomentosum	RHY_tomentosum_iNaturalist_14124900.jpeg	iNaturalist ©Rich Hoyer	no
Rhytidophyllum tomentosum	RHY_tomentosum_JBM.jpg	Etienne Leveille-Bourret	yes
Rhytidophyllum tomentosum	RHY_tomentosum_jlc_10477_06.jpg	John L. Clark	yes

Figure S3. Scree plot of the principal component analysis (PCA), or morphospace. The first three principal components representing 86.6% of the total floral shape variation were selected for downstream analyses.
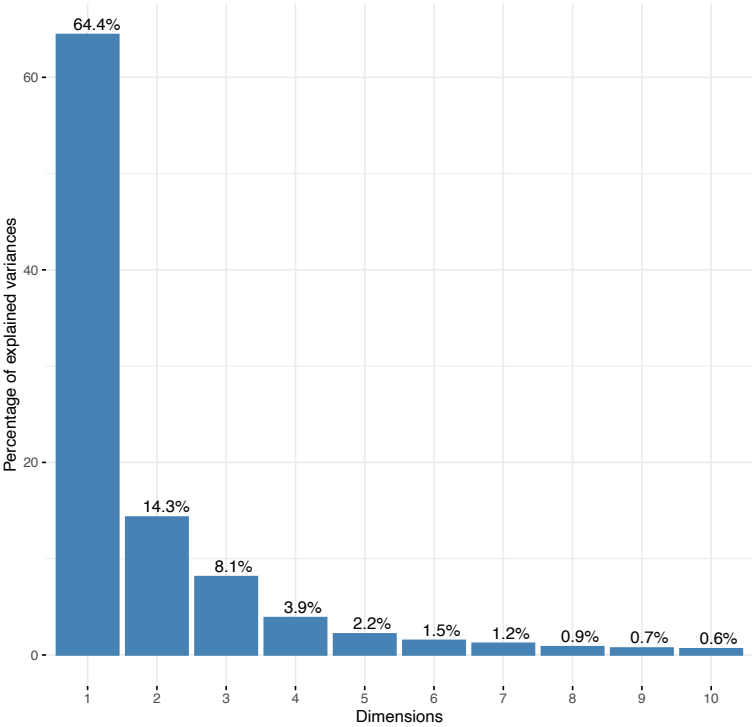
Tableau S4. Sequences information used in the phylogenetic reconstruction of the Antillean Gesneriaceae phylogeny using five nuclear genes.

Genus	Species	Collector	Collector number	GCYC	F3H	UF3GT	CHI	GADPH
Bellonia	spinosa	Léveillé-Bourret, Étienne ; Alexandre, Hermine ; Lambert, François	G8		MF318654	MF318561	MF318807	
Bellonia	spinosa	Clark, J.	10573	MF318728			MF318806	MF318613
Codonoboea	malayana	Léveillé-Bourret, Étienne ; Alexandre, Hermine ; Lambert, François	G11	MF318772	MF318723		MF318867	
Gesneria	acaulis	Clark, J.	11303	MF318730	MF318715		MF318829	MF318646
Gesneria	acaulis	Marten-Rodriguez, Silvana	1188	GU323229				
Gesneria	aspera	Lambert, F	2014-011	MF318731	MF318682		MF318849	
Gesneria	barahonensis	Marten-Rodriguez, Silvana	1242	sequenced	sequenced	sequenced	sequenced	sequenced
Gesneria	barahonensis	Marten-Rodriguez, Silvana	1239	GU323230				
Gesneria	bicolor	Lambert, F	2014-002	MF318779	MF318698	MF318594	MF318859	MF318623
Gesneria	bicolor	Lambert, F	2014-001	MF318778	MF318697	MF318593	MF318858	MF318621
Gesneria	bracteosa	Clark, J.	10567	MF318732	MF318705	MF318605	MF318869	MF318642
Gesneria	calycosa	Marten-Rodriguez, Silvana	1190	GU323231	sequenced	sequenced	sequenced	sequenced
Gesneria	celsioides	Clark, J.	11981	MF318733	MF318683	MF318600	MF318833	
Gesneria	christii	Léveillé-Bourret, Étienne ; Alexandre, Hermine ; Lambert, François	G6	MF318735	MF318673	MF318579	MF318839	MF318649
Gesneria	christii	Clark, J.	10025	MF318734	MF318672		MF318838	
Gesneria	christii	Smithsonian Institution living collection	94-507	AY363923				
Gesneria	citrina	Clark, J.	10021	MF318736	MF318679			
Gesneria	citrina	Marten-Rodriguez, Silvana	1248	GU323232				
Gesneria	clandestina	Marten-Rodriguez, Silvana	1197	GU323233	sequenced		sequenced	
Gesneria	clarensis	Clark, J.	10488	MF318737	MF318674	MF318588	MF318860	MF318650
Gesneria	cubensis	Lambert, F	2014-008	MF318738	MF318714		MF318850	
Gesneria	cubensis	Marten-Rodriguez, Silvana	1232	GU323234				
Gesneria	cuneifolia	Marten-Rodriguez, Silvana	1247	GU323235				
Gesneria	ekmanii	Lambert, F	2014-018	MF318797	MF318718	MF318597	MF318863	
Gesneria	ekmanii	Lambert, F	2014-024	MF318742	MF318720		MF318864	
Gesneria	ekmanii	Lambert, F	2014-020	MF318741	MF318719	MF318580	MF318865	MF318643

Gesneria	*ekmanii*	Acevedo	13892	GU323237				
Gesneria	*flava*	no voucher	2014-007	MF318793	MF318694	MF318590	MF318855	MF318619
Gesneria	*flava*	Lambert, F	2014-010	MF318795	MF318696	MF318592	MF318857	MF318622
Gesneria	*flava*	Lambert, F	2014-009	MF318794	MF318695	MF318591	MF318856	MF318620
Gesneria	*fruticosa*	Marten-Rodriguez, Silvana	1227	GU323238	sequenced	sequenced	sequenced	sequenced
Gesneria	*fruticosa*	Lambert, F	2014-012	MF318743	MF318711	MF318581	MF318851	MF318644
Gesneria	*humilis*	Clark, J.	10626	MF318747	MF318684	MF318603	MF318836	MF318615
Gesneria	*humilis*	Clark, J.	10040	MF318744	MF318699	MF318601	MF318834	MF318614
Gesneria	*humilis*	Clark, J.	10472	MF318745	MF318700	MF318602	MF318835	MF318616
Gesneria	*humilis*	Clark, J.	10574	MF318746			MF318837	
Gesneria	*humilis*	Chautems, A.	1179	AY423156				
Gesneria	*jamaicensis*	Marten-Rodriguez, Silvana	1193	GU323239	sequenced	sequenced	sequenced	sequenced
Gesneria	*lanceolata*	Marten-Rodriguez, Silvana	1238	sequenced	sequenced	sequenced	sequenced	sequenced
Gesneria	*nipensis*	Clark, J.	10577	MF318748	MF318710			
Gesneria	*onychocalyx*	Marten-Rodriguez, Silvana	1195	GU323240	sequenced		sequenced	
Gesneria	*pedicellaris*	Clark, J.	10635	MF318749	MF318675	MF318612	MF318840	
Gesneria	*pedicellaris*	Marten-Rodriguez, Silvana	1229	GU323241				
Gesneria	*pedunculosa*	Clark, J.	10644	MF318750	MF318701	MF318582	MF318852	
Gesneria	*pedunculosa*	Marten-Rodriguez, Silvana	1251	GU323242				
Gesneria	*pumila*	Marten-Rodriguez, Silvana	1194	GU323244	sequenced	sequenced		sequenced
Gesneria	*purpurascens*	Clark, J.	10564	MF318751	MF318716	MF318587	MF318831	MF318647
Gesneria	*quisqueyana*	no voucher	ADN-1298	MF318753	MF352014			
Gesneria	*quisqueyana*	no voucher	ADN-1299	MF318754	MF318707	MF318606		
Gesneria	*quisqueyana*	no voucher	ADN1297	MF318752				
Gesneria	*quisqueyana*		LAH400-10		MF318703			
Gesneria	*quisqueyana*		LAH454-12		MF318704			
Gesneria	*quisqueyana*	Marten-Rodriguez, Silvana	1230	GU323245				
Gesneria	*reticulata*	Clark, J.	10558	MF318755	MF318680	MF318598	MF318832	
Gesneria	*reticulata*	Marten-Rodriguez, Silvana	1221	GU323246				
Gesneria	*salicifolia* var. *salicifolia*	Clark, J.	10566	MF318757	MF318676		MF318862	MF318645
Gesneria	*salicifolia* var. *ferruginea*	Clark, J.	10627	MF318756		MF318589	MF318861	MF318651
Gesneria	*sintenisii*	Clark, J.	13757	MF318759	MF318708	MF318611	MF318841	
Gesneria	*sintenisii*	Martén-Rodríguez, Silvana	1252	GU323250		MF352012		
Gesneria	*sintenisii*	Monsegur-Rivera, Omar A. ; Sanchez, B	863	MF318760		MF318607		
Gesneria	*sylvicola*	Lambert, F	2014-027	MF318764	MF352013	MF352011	MF318842	

Gesneria	*sylvicola*	Hahn, L. ; Clase, Theodoro S. ; De Los Santos, Carlos	447	MF352015		MF318608		
Gesneria	*sylvicola*	Lambert, F	2014-028	MF318765	MF318722	MF318585	MF318843	
Gesneria	*tuberosa*	Peguero, B.	4717	GU323248				
Gesneria	*ventricosa* subsp. *ventricosa*	Léveillé-Bourret, Étienne ; Alexandre, Hermine	G4	MF318762	MF318712	MF318583	MF318853	MF318640
Gesneria	*ventricosa*	Clark, J.	6545	MF318761	MF318677			MF318617
Gesneria	*ventricosa*	Marten-Rodriguez, Silvana	1112A	GU323249				
Gesneria	*viridiflora* subsp. *viridiflora*	Clark, J.	10561	MF318770	MF318725	MF318586	MF318866	
Gesneria	*viridiflora* subsp. *viridiflora*	Clark, J.	10041	MF318766		MF318610	MF318845	
Gesneria	*viridiflora* subsp. *acrochordonanthe*	Clark, John L. ; Cinea, William ; Henrys, I. ; Despagne, M. ; Sturla, M.	14467	MF318763	MF318702		MF318846	
Gesneria	*viridiflora* subsp. *viridiflora*	Clark, J.	10524	MF318768	MF318706	MF318584		
Gesneria	*viridiflora* subsp. *viridiflora*	Clark, J.	10509	MF318767	MF318726	sequenced	MF318854	
Gesneria	*viridiflora* subsp. *viridiflora*	Clark, J.	10540	MF318769	MF318709	MF318609		
Gesneria	*yamuriensis*	Clark, J.	10575	MF318771	MF318717	MF318599	MF318830	MF318648
Kohleria	sp. 'trinidad'	Joly, S.	1102	MF318773			MF318868	
Rhytidophyllum	*auriculatum*	Lambert, F	2014-025	MF318776	MF318668	MF318573		
Rhytidophyllum	*auriculatum*	Joly, S.	1100	MF318777	MF318658	MF318564		MF318641
Rhytidophyllum	*auriculatum*	Lambert, F	2014-014	MF318775	MF318687	MF318565	MF318824	MF318635
Rhytidophyllum	*auriculatum*	Marten-Rodriguez, Silvana	1222	GU323253				
Rhytidophyllum	*berteroanum*	Marten-Rodriguez, Silvana	1226	GU323254				
Rhytidophyllum	*bullatum*	Lambert, F	2014-016	MF318780	MF318670	MF318574	MF318847	
Rhytidophyllum	*crenulatum*	Clark, J.	9531	MF318781	MF318659	MF318576	MF318848	MF318630
Rhytidophyllum	*crenulatum*	Clark, John L.	10580	GU323255				
Rhytidophyllum	*earlei*	Clark, J.	10486	MF318740	MF318689	MF318595	MF318820	MF318625
Rhytidophyllum	*earlei*	Clark, J.	10458	MF318739	MF318686	MF318563	MF318818	MF318624
Rhytidophyllum	*exsertum*	Clark, J.	10585	sequenced	MF318713		MF318809	
Rhytidophyllum	*exsertum*	Clark, J.	10038	MF318782	MF318660	MF318566	MF318810	MF318633
Rhytidophyllum	*exsertum*	Léveillé-Bourret, Étienne ; Alexandre, Hermine	G1	MF318783	MF318661	MF318568	MF318812	MF318637
Rhytidophyllum	*exsertum*	Skog, L.	1197-14	GU323256				
Rhytidophyllum	*grandiflorum*	Marten-Rodriguez, Silvana	1224	GU323257				
Rhytidophyllum	*intermedium*	Clark, J.	10549	MF318784	MF318721	MF318569	MF318816	MF318629
Rhytidophyllum	*leucomallon*	Acevedo, P.	13966	GU323258				
Rhytidophyllum	*lomense*	Clark, J.	10466	MF318785	MF318691		MF318821	MF318626
Rhytidophyllum	*lomense*	Clark, J.	10469	MF318786	MF318692	MF318572	MF318823	MF318628

Genus	species	Collector	Number					
Rhytidophyllum	*minus*	Clark, J.	10500	MF318787	MF318666	MF318577	MF318815	
Rhytidophyllum	*onacaensis*	E. Carbono	9085	MF318788	MF318678	MF318575	MF318826	MF318618
Rhytidophyllum	*rhodocalyx*	Clark, J.	10530	MF318789	MF318662	MF318578	MF318827	
Rhytidophyllum	*rupincola*	Léveillé-Bourret, Étienne ; Alexandre, Hermine	G5	MF318792	MF318693	MF318596		MF318636
Rhytidophyllum	*rupincola*	Clark, J.	11957	MF318791	MF318685		MF318819	MF318634
Rhytidophyllum	*rupincola*	Clark, J.	11261	MF318790	MF318690		MF318822	MF318627
Rhytidophyllum	*rupincola*	Marten-Rodriguez, Silvana	1253	GU323247				
Rhytidophyllum	*sp.*	Lambert, F	2014-017	MF318796	MF318669		MF318828	
Rhytidophyllum	*sp.*	Lambert, F	2014-022	MF318798	MF318671		MF318825	
Rhytidophyllum	*tomentosum*	Léveillé-Bourret, Étienne ; Alexandre, Hermine	G2	MF318799	MF318663	MF318570	MF318817	MF318638
Rhytidophyllum	*tomentosum*	Marten-Rodriguez, Silvana	1191	GU323260				
Rhytidophyllum	*tomentosum*	Smithsonian Institution living collection	SI77-235	AY363926				
Rhytidophyllum	*vernicosum*	Léveillé-Bourret, Étienne ; Alexandre, Hermine	G3 (JBM-1267-1966)	MF318800	MF318724	MF318604	MF318844	MF318652
Rhytidophyllum	*vernicosum*	Marten-Rodriguez, Silvana	1246	GU323261				
Rhytidophyllum	*villosulum*	Clark, J.	10557	MF318803	MF318657	MF318562	MF318808	MF318632
Rhytidophyllum	*villosulum*	Clark, J.	10465	MF318801	MF318664	MF318567	MF318811	MF318631
Rhytidophyllum	*villosulum*	Clark, J.	10569	MF318804	MF318665		MF318814	
Rhytidophyllum	*villosulum*	Clark, J.	10538	MF318802	MF318667	MF318571	MF318813	MF318639
Sinningia	*incarnata*	Clark, J.	8849	MF318805	MF318727			

Figure S4. Phylogeny of *Rhytidophylum*, *Gesneria* and *Bellonia* species (Gesnerieae). Numbers in circles on the branches represent clade posterior probabilities.
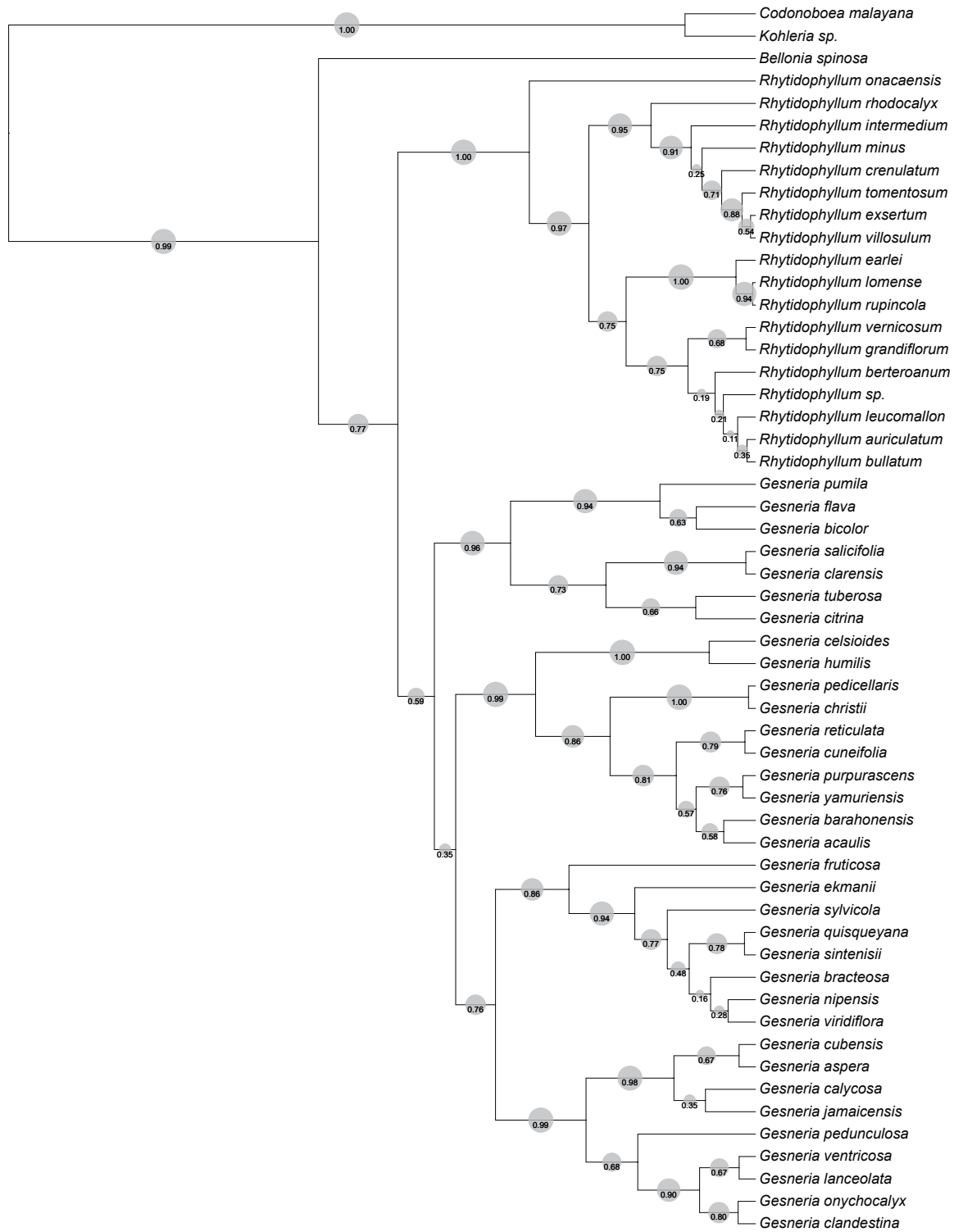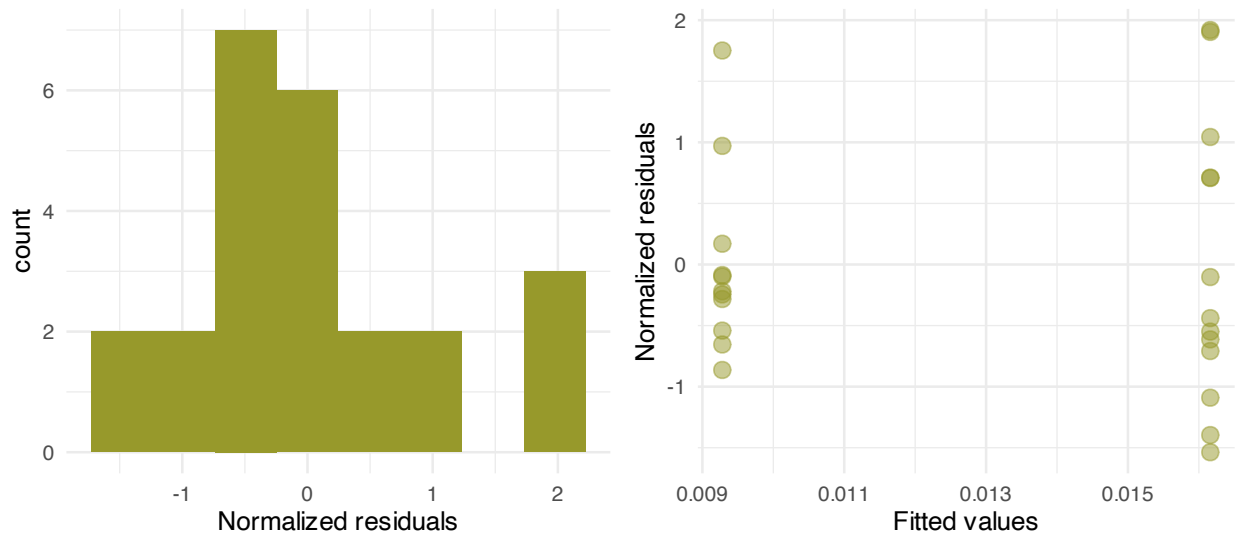
Figure S5. Residuals vs fitted plot for the phylogenetic generalised least square (PGLS) regression.

Tableau S5. Bayes Factors (BF) comparing the fit of the univariate (OU) and multivariate model (OUM) of evolution of the complete dataset of 100 simulations of ancestral pollination strategies (SIMMAP 1 to 100), for the first three principal components of the floral morphospace (PC1 to PC3).

SIMMAP	PC1	PC2	PC3	SIMMAP	PC1	PC2	PC3
1	5.32	0.97	-1.79	51	1.54	-0.97	0.29
2	0.49	-2.22	3.23	52	11.46	3.29	-6.67
3	11.02	-21.81	-3.49	53	4.27	-0.36	0.51
4	-1.92	0.66	2.77	54	4.45	-8.09	-1.69
5	-2.49	-5.50	-0.20	55	0.90	-3.38	-6.70
6	5.79	1.93	2.50	56	-4.21	-1.66	0.96
7	0.88	4.57	7.65	57	4.87	-1.74	4.21
8	4.09	9.23	-3.39	58	-2.51	2.44	0.52
9	4.97	-5.27	-1.45	59	-1.22	-2.17	4.31
10	-2.83	-13.39	3.58	60	-0.84	-5.15	9.99
11	1.48	-1.40	-1.18	61	2.05	-10.17	-3.11
12	-1.50	-4.38	-1.79	62	-3.71	-6.09	2.30
13	-5.81	-5.82	0.81	63	2.70	-5.83	-5.39
14	-2.13	7.32	0.66	64	-2.80	-9.75	-3.59
15	2.83	-2.28	2.87	65	-2.64	-11.58	-3.55
16	10.98	-20.69	2.08	66	6.17	-7.89	1.32
17	-5.90	-2.31	-3.66	67	5.64	-12.43	-4.86
18	-3.78	-6.40	-5.56	68	13.47	-12.10	9.41
19	1.87	-1.89	-3.81	69	-7.19	-1.78	9.33
20	4.06	-4.38	-7.72	70	4.69	-1.08	-2.06
21	-0.15	-14.94	-10.54	71	2.44	-4.61	0.05
22	4.25	-9.97	-1.32	72	-0.55	-7.92	-1.42
23	-2.64	5.73	3.04	73	12.20	-3.42	1.53
24	-0.16	1.28	-6.23	74	-2.38	-3.88	4.27
25	8.33	-5.45	-2.23	75	2.88	-12.67	4.68
26	-1.78	-19.35	-1.06	76	1.63	-7.48	15.25
27	-0.14	1.73	-3.72	77	4.19	-0.79	-4.05
28	6.55	-6.79	-12.99	78	8.20	3.20	2.95
29	0.01	-9.99	-0.92	79	1.50	4.73	-9.93
30	-3.69	4.48	-3.81	80	2.99	-1.53	0.43
31	3.27	-2.65	-4.93	81	0.37	-16.28	-1.62
32	-17.36	-2.23	-6.53	82	8.28	-2.42	-1.52
33	3.02	-6.74	0.96	83	-3.82	7.21	0.27
34	-4.13	3.56	-5.01	84	14.76	0.23	0.79
35	-0.84	-1.15	1.34	85	1.27	-5.68	7.48
36	0.92	3.13	8.11	86	4.89	-2.10	-1.81
37	-3.78	-4.77	2.39	87	-2.05	-9.65	-13.06
38	0.46	-9.87	-3.66	88	5.15	-4.66	7.94
39	-2.09	-8.14	-2.49	89	2.34	-8.03	3.32
40	-2.75	-16.75	-3.96	90	-0.23	-4.79	-1.07
41	0.62	1.56	-2.99	91	7.63	-7.81	1.47
42	6.88	-7.88	0.54	92	-2.06	-14.02	-3.53
43	1.25	12.04	2.71	93	-5.54	-11.35	-2.84
44	1.21	-2.42	-2.14	94	-1.14	-0.33	-5.41
45	0.31	-3.30	-4.88	95	-1.01	-3.36	7.83
46	-3.99	-13.26	-8.68	96	6.57	-3.96	18.30
47	-2.02	2.20	-6.68	97	-0.71	-11.81	-1.04
48	-0.57	-2.96	5.17	98	2.93	-10.21	-1.13
49	-1.29	2.98	5.89	99	1.29	-1.71	-1.46
50	-3.10	3.17	3.72	100	3.59	-10.20	-6.92

Tableau S6. Summary statistics of the estimated parameter values per principal component (PC) for the two models, averaged over all stochastic simulations (SIMMAPs).

	PC1						PC2						PC3					
	Summary			Quantiles			Summary			Quantiles			Summary			Quantiles		
Model : mean OUM variance OU	Mean	SD	Naive SE	2.5%	25%	50%	Mean	SD	Naive SE	2.5%	25%	50%	Mean	SD	Naive SE	2.5%	25%	50%
posterior	326.70	11.57	0.12	308.63	318.25	325.26	360.57	13.45	0.13	339.13	350.82	358.90	361.52	13.43	0.13	336.06	352.55	360.22
log likelihood	320.62	6.00	0.06	308.43	316.34	320.80	336.63	4.26	0.04	328.81	334.28	336.65	334.19	4.40	0.04	326.12	331.25	334.31
prior mean	37.91	9.78	0.10	19.47	30.60	38.44	31.05	2.60	0.03	25.64	29.48	31.33	32.36	2.51	0.03	27.43	30.82	32.51
prior log variance	-15.86	10.50	0.11	-30.03	-22.58	-17.64	3.51	14.61	0.15	-21.34	-7.97	-0.45	5.86	13.59	0.14	-13.78	-4.34	3.51
mean α	24.64	10.33	0.10	9.05	16.95	22.06	0.96	0.72	0.01	0.07	0.46	0.77	5.93	4.86	0.05	0.33	2.52	4.83
mean σ^2	0.18	0.15	0.00	0.02	0.06	0.12	0.02	0.01	0.00	0.01	0.02	0.02	0.06	0.05	0.00	0.01	0.03	0.04
mean θ hummingbird	0.24	0.02	0.00	0.18	0.22	0.23	-0.07	0.12	0.00	-0.30	-0.16	-0.06	-0.01	0.05	0.00	-0.12	-0.04	-0.01
mean θ mixed-pollination	-0.21	0.02	0.00	-0.25	-0.22	-0.21	0.04	0.12	0.00	-0.21	-0.03	0.04	0.04	0.06	0.00	-0.07	0.02	0.04
log variance α	6.74	3.99	0.04	1.49	3.81	5.85	8.08	4.52	0.05	1.34	4.92	7.14	8.48	6.07	0.06	1.26	4.54	7.05
log variance σ^2	4.25	3.44	0.03	0.23	1.65	3.09	1.42	1.50	0.02	0.06	0.30	0.96	1.17	1.52	0.02	0.04	0.23	0.57
log variance θ	-5.81	0.59	0.01	-7.27	-5.90	-5.68	-5.85	0.54	0.01	-7.71	-5.83	-5.74	-5.92	0.63	0.01	-8.16	-5.89	-5.76
Model : mean OUM variance OUM	Mean	SD	Naive SE	2.5%	25%	50%	Mean	SD	Naive SE	2.5%	25%	50%	Mean	SD	Naive SE	2.5%	25%	50%
posterior	327.50	11.97	0.12	308.20	318.20	325.59	356.01	14.33	0.14	331.30	346.16	354.68	362.09	13.66	0.14	338.47	351.61	361.82
log likelihood	321.34	6.00	0.06	307.06	318.75	321.47	336.38	4.44	0.04	326.60	333.52	336.81	334.30	3.90	0.04	326.03	331.50	334.32
prior mean	37.44	10.11	0.10	18.89	30.77	36.77	31.48	2.36	0.02	25.80	29.84	31.85	32.40	2.31	0.02	28.25	30.76	32.61
prior log variance	-13.33	11.61	0.12	-33.16	-21.37	-15.39	1.33	15.49	0.15	-24.90	-10.26	-1.26	8.39	13.93	0.14	-14.76	-2.03	7.34
mean α	23.31	11.07	0.11	6.22	14.90	22.04	0.88	0.87	0.01	0.04	0.32	0.61	6.49	4.83	0.05	1.10	2.94	4.85
mean σ^2	0.16	0.14	0.00	0.03	0.07	0.12	0.02	0.01	0.00	0.01	0.01	0.02	0.07	0.05	0.00	0.02	0.03	0.05
mean θ hummingbird	0.24	0.02	0.00	0.18	0.22	0.23	-0.06	0.12	0.00	-0.32	-0.12	-0.04	-0.02	0.03	0.00	-0.11	-0.03	-0.01
mean θ mixed-pollination	-0.20	0.02	0.00	-0.25	-0.22	-0.21	0.07	0.13	0.00	-0.24	-0.00	0.06	0.03	0.04	0.00	-0.03	0.01	0.03
log variance α	7.62	4.98	0.05	1.48	3.82	6.91	9.46	5.73	0.06	1.37	4.96	8.33	7.76	5.19	0.05	1.12	4.22	6.69
log variance σ^2	3.50	2.58	0.03	0.25	1.50	3.11	2.03	2.39	0.02	0.03	0.38	1.33	0.87	0.92	0.01	0.03	0.17	0.54
log variance θ hummingbird	-6.24	0.55	0.01	-7.84	-6.43	-6.10	-5.78	0.53	0.01	-7.69	-5.81	-5.68	-6.15	0.73	0.01	-8.87	-6.10	-6.00
log variance θ mixed-pollination	-5.53	0.56	0.01	-6.81	-5.60	-5.40	-5.92	0.51	0.01	-7.72	-5.94	-5.81	-5.75	0.63	0.01	-8.02	-5.73	-5.60

Tableau S7. Effective sample size (ESS) for the parameters of the model of the combined Markov-Chain Monte-Carlo (MCMC) chains from all ancestral pollination syndrome map along the phylogenetic tree (SIMMAP) (n=100)

	PC1 mOUM vOU	PC2 mOUM vOU	ESS PC3 mOUM vOU	PC1 mOUM vOUM	PC2 mOUM vOUM	PC3 mOUM vOUM
log.lik	61309.79	70491.73	67008.86	62659.55	70615.70	64466.00
logvar.alpha	61034.46	23905.63	23336.38	34835.13	22715.32	22811.39
logvar.sigma_sq	52979.99	26449.04	25310.77	46052.83	28557.39	21187.55
logvar.theta	306458.69	331071.92	394075.85	-	-	-
logvar.theta_hummingbird	-	-	-	190817.02	325108.00	287370.86
logvar.theta_mixed.pollination	-	-	-	377657.65	252859.28	370206.76
mean.alpha	5587.35	14806.36	181602.15	5417.43	14455.74	168800.14
mean.sigma_sq	3320.00	2805.54	2779.53	3363.13	2796.27	2746.18
mean.theta_hummingbird	62966.89	620455.42	686961.60	64111.59	621262.12	674100.33
mean.theta_mixed.pollination	70332.12	516778.86	1043092.64	72174.97	506294.47	1019109.07
posterior	18805.83	4538.83	4051.82	14056.49	5387.01	3361.80
prior.logvar	39419.29	52470.94	44733.67	38828.83	47402.60	40702.81
prior.mean	578.84	505.09	464.11	596.25	503.27	466.07

Bibliographie

Faure, J. and Joly, S. (2020). Pollinator performance of the pollination generalist rhytidophyllum bicolor (gesneriaceae) in haiti 15 months after the matthew hurricane. *Selbyana*, 33(3).

Joly, S., Lambert, F., Alexandre, H., Clavel, J., Léveillé-Bourret, E., and Clark, J. L. (2018). Greater pollination generalization is not associated with reduced constraints on corolla shape in Antillean plants. *Evolution*.

Martén-Rodríguez, S., Fenster, C. B., Agnarsson, I., Skog, L. E., and Zimmer, E. A. (2010). Evolutionary breakdown of pollination specialization in a caribbean plant radiation. *New Phytologist*, 188(2) :403–417.

Martén-Rodríguez, S., Almarales-Castro, A., and Fenster, C. B. (2009). Evaluation of pollination syndromes in Antillean Gesneriaceae : evidence for bat, hummingbird and generalized flowers. *Journal of Ecology*, 97(2) :348–359.

Martén-Rodríguez, S. and Fenster, C. B. (2008). Pollination Ecology and Breeding Systems of Five Gesneria Species from Puerto Rico. *Annals of Botany*, 102(1) :23–30.

Martén-Rodríguez, S., Quesada, M., Castro, A.-A., Lopezaraiza-Mikel, M., and Fenster, C. B. (2015). A comparison of reproductive strategies between island and mainland Caribbean Gesneriaceae. *Journal of Ecology*, 103(5) :1190–1204.

Annexe - Deuxième chapitre

The following Supporting Information is available for this article :

Tableau S8. Summary of the materials used to scan and reconstruct three-dimensional flower models and their approximate price in 2022. Alternative materials can be considered, and we give as an example the specific materials we used when relevant.

Material	Description	Price (USD)
Photography		
Camera	Digital Single-Lens Reflex (DSLR) (e.g. Canon t2i)	from $500
Macro lens	A preferably fixed lens (e.g. Canon 60mm f/2.8 Macro lens)	from $400
Tripod	Preferably flexible, such as a gorillapod	e.g. $80
Stepping motor and turntable kit	Genie mini II, Shoot smooth rotating video and interactive 360° images of objects. Full iOS and Android App control via Bluetooth. Battery life : 6hrs video and 15hrs time-lapse. Panning payload 8.8lbs/4kgs	$328.00
Lightbox	A portable photo studio, e.g. Neewer 20"/50cm foldable portable photography lighting kit (Neewer Technology Co. LTD, Shenzhen, China), adjustable brightness with 120 LED lights, CRI (colour Rendering Index) of 85+, 6000-6500K colour temperature, needs to be powered by a portable battery in the field, white, grey, and black backdrops. In the bracket of light intensities possible for this lightbox, we used an intermediate light intensity. [maximum ;usually used ; minimum] lux light intensities correspond to [3140 ;2680 ;1330] lux for a white backdrop and [330 ;305 ;238] Lux with a black backdrop.	$79.99
External battery	Powering source for in-field photo capture, essentially for the lightbox or to recharge batteries	optional
Flower mounting and identification		
Flower	Freshly cut flower with peduncle and floral receptacle	/
Labels and container	Identification and storage of fresh flowers to avoid damage and avoid wilting	/
Turntable labels	Identification to species, collector, collection number, date, locality, and coordinates, and the chunk number. To use as a separate photo before each run of photos.	/
Razor blade	To remove sepals	/
Small block of dense foam	To fix flowers in place with a pin at the center of the turntable.	/
Entomological pins	To pin through the peduncle or floral receptacle and fix the flower on the turntable.	/
Scale	A 1 cm scale as reference	/
Color calibration		
Color chart	A color reference to calibrate RAW photos (e.g. X-rite ColorChecker Passport)	e.g. $99.00
Color calibration software	ColorChecker Camera Calibration, Xrite software for automatic color profile creation	Free
Photo editing software	Adobe Photoshop Lightroom, editing software for image color calibration in batch	Payment plans vary
DNG conversion software	Adobe DNG converter, to convert Camera Raw files from supported cameras to the more widely used DNG raw files	Free
Model reconstruction		
3D reconstruction from photogrammetry software	Agisoft Metashape Pro Software	$549 Academic price

Tableau S9. Summary of camera and turn table settings used to scan flowers.

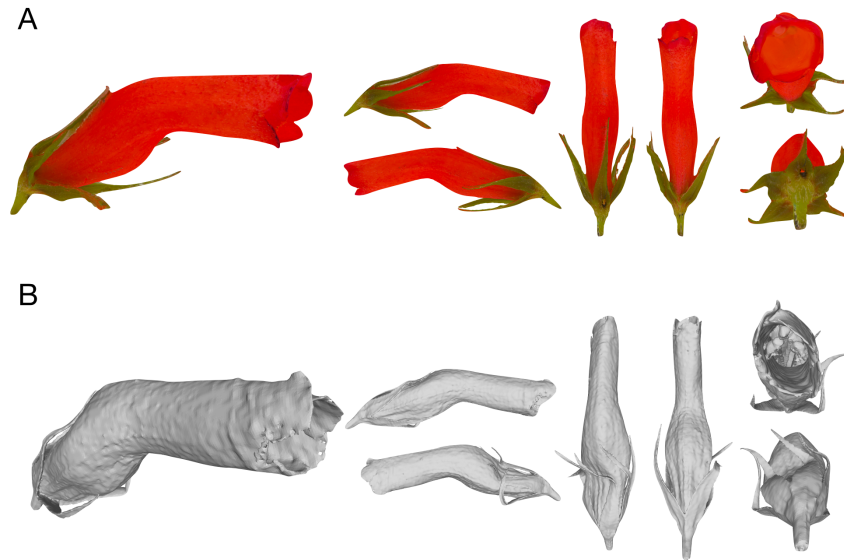| Parameter	Value
Camera settings	
Aperture	F/16
Sensibility	ISO 100 (lowest)
Exposure time	1/20s (depending on light settings)
Turn table settings	
Number of photos	20 per camera height (high, mid, low) and per flower side (ventral and dorsal)
Wait time	2s

Figure S6. Three-dimensional models of flowers of *Gesneria acaulis* (75-2021) obtained from photogrammetry (A) and CT scanning (B)

Figure S7. Three-dimensional models of flowers of *Rhytidophyllum exsertum* (112-1991) obtained from photogrammetry (A) and CT scanning (B)

Notes S1 - Taxonomic groups and flower material

A sample of Gesneriaceae species was used to further illustrate the utility of photogrammetry to study of the evolution of floral shape and colour. Flowers of the Gesneriaceae vary extensively in colour and shape, often in association with different pollination systems (Serrano-Serrano et al., 2017). In Antillean species, pollination systems range from specialists (bat, bird, bee, or moth pollinated) to mixed-pollination (birds, bats, and insects) (Martén-Rodríguez and Fenster, 2008; Martén-Rodríguez et al., 2009, 2015) and the same pollination systems and associated floral traits have evolved several times in this group (Martén-Rodríguez et al., 2015; Joly et al., 2018). The clade is thus ideal for studying the evolution of flower shape and colour during convergent evolution of specialist and mixed-pollination systems (Losos and Ricklefs, 2009).

3D flower models were reconstructed for a selected number of specimens from the living collections of the Montreal Botanical Garden (Quebec, Canada). The flowers of 25 individuals representing 17 species and one hybrid were used (see Table S3), mainly from the Gesneriinae (*Gesneria* and *Rhytidophyllum* species) and Ligeriinae tribes (*Paliavana prasinata*), and four additional bird pollinated species (*Aeschynanthus pulcher*, *Aeschynanthus splendidus*, *Kohleria sp.* and *Nematanthus wettsteinii*). Sepals were removed with a scalpel before photo acquisition to expose corolla bases and facilitate shape characterisation. A 3D flower model was reconstructed for each flower as described in our protocol. Available pollinator information was obtained from the literature for 15 species (Martén-Rodríguez and Fenster, 2008; Martén-Rodríguez et al., 2009; Martén-Rodríguez et al., 2010; Martén-Rodríguez et al., 2015; Faure and Joly, 2020). For species without field observations of pollinators, the pollination syndromes were inferred based on previous characterisations (Vogel, 1969; Martén-Rodríguez and Fenster, 2008; Martén-Rodríguez et al., 2009; Martén-Rodríguez et al., 2010; Martén-Rodríguez et al., 2015; Joly et al., 2018) (see Table **S3**). We refer generically to the bird pollination syndrome for brevity because of our small sample, even though the Antillean bird-pollinated species are mainly pollinated by hummingbirds (Martén-Rodríguez et al., 2010).

Tableau S10. Species and collection numbers associated with the Botanical Garden of Montreal database of the specimens used to reconstruct 3D models of flowers. Each species is associated with a pollination syndrome. The bibliographic reference identifying the pollination syndromes of each species is also listed. Pollination syndromes that are not confirmed were inferred.

Genus	species	Collection number	Syndrome	Confirmed	Litterature
Aeschynanthus	*pulcher*	1376-1980	Bird	no	
Aeschynanthus	*splendidus*	942-1956	Bird	no	
Gesneria	*acaulis*	1328-2021	Hummingbird	yes	Martén-Rodríguez et al. (2009); Martén-Rodríguez et al. (2010); Martén-Rodríguez et al. (2015)
Gesneria	*cornuta*	75-2021	Mixed-pollination	no	
Gesneria	*cuneifolia*	976-2017	Hummingbird	yes	Martén-Rodríguez and Fenster (2008) Martén-Rodríguez et al. (2009); Martén-Rodríguez et al. (2010); Martén-Rodríguez et al. (2015)
Gesneria	*cuneifolia*	976-2017	Hummingbird	yes	Martén-Rodríguez and Fenster (2008) Martén-Rodríguez et al. (2009); Martén-Rodríguez et al. (2010); Martén-Rodríguez et al. (2015)
Gesneria	*fruticosa*	884-2015	Bat	yes	Martén-Rodríguez et al. (2009); Martén-Rodríguez et al. (2010); Martén-Rodríguez et al. (2015)
Gesneria	*quisquesana*	891-2015	Bat	yes	Martén-Rodríguez et al. (2009); Martén-Rodríguez et al. (2010); Martén-Rodríguez et al. (2015)
Gesneria	*ventricosa*	778-1968	Hummingbird	yes	Martén-Rodríguez et al. (2009); Martén-Rodríguez et al. (2010); Martén-Rodríguez et al. (2015)
Kohleria	*sp.*	828-2013	Bird	no	
Nemathantus	*wettsteinii*	2213-1965	Bird	no	
Paliavana	*prasinata*	1432-2010	Bat	yes	Vogel (1969)
Rhytidophyllum	*auriculatum*	889-2015	Mixed-pollination	yes	Martén-Rodríguez et al. (2009); Martén-Rodríguez et al. (2010)
Rhytidophyllum	*auriculatum*	937-1971	Mixed-pollination	yes	Martén-Rodríguez et al. (2009); Martén-Rodríguez et al. (2010)
Rhytidophyllum	*auriculatum* - red flowers	1437-2021	Mixed-pollination	no	
Rhytidophyllum	*auriculatum* x *vernicosum*	103-2013	Mixed-pollination	no	
Rhytidophyllum	*bicolor*	587-2019	Mixed-pollination	yes	Martén-Rodríguez et al. (2015); Joly et al. (2018)
Rhytidophyllum	*exsertum*	1073-2010	Mixed-pollination	yes	Martén-Rodríguez et al. (2015)
Rhytidophyllum	*exsertum*	112-1991	Mixed-pollination	yes	Martén-Rodríguez et al. (2015)
Rhytidophyllum	*exsertum*	392-2014	Mixed-pollination	yes	Martén-Rodríguez et al. (2015)
Rhytidophyllum	*exsertum*	74-2021	Mixed-pollination	no	Joly et al. (2018)
Rhytidophyllum	*minus*	938-2017	Mixed-pollination	no	Joly et al. (2018)
Rhytidophyllum	*minus*	1450-2021	Mixed-pollination	no	Joly et al. (2018)
Rhytidophyllum	*rupincola*	113-1991	Hummingbird	yes	Martén-Rodríguez et al. (2010)
Rhytidophyllum	*tomentosum*	1327-2021	Mixed-pollination	yes	Martén-Rodríguez et al. (2010)
Rhytidophyllum	*vernicosum*	1267-1966	Mixed-pollination	yes	Martén-Rodríguez et al. (2009); Martén-Rodríguez et al. (2010); Martén-Rodríguez et al. (2015)

Methods S1 - 3D Geometric morphometrics

To compare the flower morphologies of species from 3D models, landmarks and semi-landmarks were placed on each flower model using the software Stratovan Checkpoint (Stratovan Corporation, Davis, California, U.S.). Landmarks were placed on homologous features of each flower (see Fig. **S1** and Table **S4** for details). A total of 10 landmarks and 233 curve semi-landmarks were manually placed on each flower, delimiting the corolla tube and petal lobes (Fig. **1q**). 20 semi-landmarks were placed along the dorsal and ventral side of the flowers and 21 along each petal lobe margins, 7 between each sepal landmarks at the basis of the corolla, and 17 at the base of each petal lobes, delimiting the beginning of the corolla tube between each petal lobes. Surface landmarks were then semi-automatically placed on each flower using a simple 3D truncated conical template (a very simplified flower; Fig. **1p**). The conical template includes the same number of landmarks and curves semi-landmarks as the flowers and a grid of additional surface semi-landmarks. The landmarks of the flowers and template were loaded in R version 4.0.5 (R Core Team, 2021) and the surface semi-landmarks of the template were automatically applied (patched) on each flower model using the Morpho R package version 2.8 (Schlager, 2017). See Bardua et al. (2019) for more information on the use of templates for mapping surface semi-landmarks. The landmarks of the different models were aligned by generalised Procrustes analysis (GPA) using the geomorph R package version 4.0.0 (Baken et al., 2021; Adams et al., 2021). The landmark coordinates were then projected onto the tangent space using principal component analysis (PCA) to represent the morphological variation at a lower dimensional space using the function prcomp from the stats R package version 4.0.5 (R Core Team, 2021). The mean 3D flower shape of all specimens, the extreme shapes at either end of each principal component axis, and the mean shape of each syndrome were estimated using the function mshape from the geomorph R package (Baken et al., 2021; Adams et al., 2021). The corresponding 3D meshes were calculated using the function warpRefMesh from the same package. This function warps the surface of the reference floral shape onto the target landmarks of the mean shape. The surface of *R. auriculatum* (accession number 889-2015) was used for this analysis as it represents an approximation of an intermediate floral shape, and the resulting mean surface was then used as a reference to be warped on the extremes of the PC axes and pollination syndromes shapes.
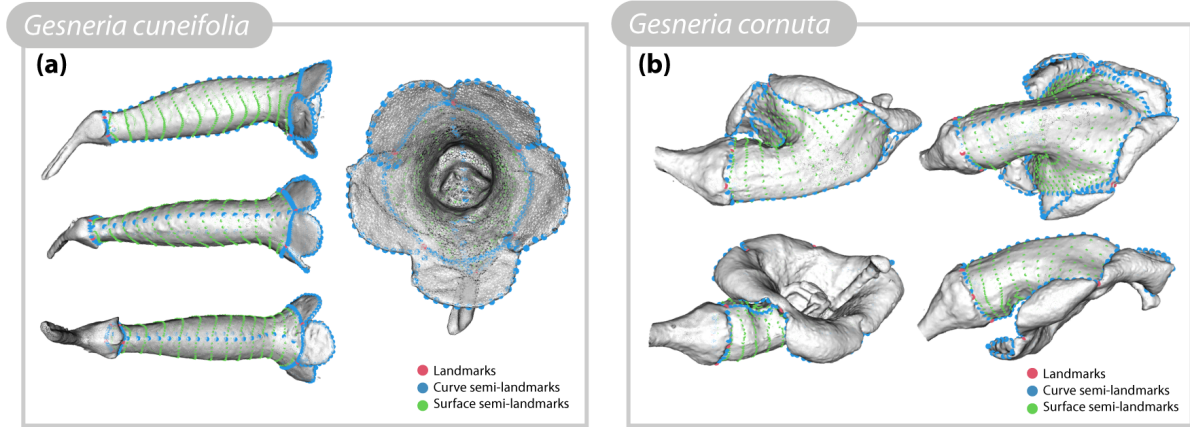
Figure S8. Example of landmarks and semi-landmarks placement on the corolla of *Gesneria cuneifolia* (a) and *Gesneria cornuta* (b).

Tableau S11. Identification of the landmark and semi-landmarks used for curves and surfaces. Landmarks and semi-landmarks for dorsal, ventral, petal margin, and petal basis curves were placed manually in Stratovan Checkpoint. Semi-landmarks for surfaces were placed automatically in R. 5 landmarks were placed at the intersection of petal lobes, 5 landmarks at the intersection of sepals, marked with ink on the flower receptacle after sepal removal. Sliding semi-landmarks were used to characterize curves and to help with the automatic placement of the surface semi-landmarks (see Bardua et al., 2019). 20 semi-landmarks were placed along the dorsal and ventral side of the flowers and 21 along each petal lobe margins, 7 between each sepal landmarks at the basis of the corolla, and 17 at the base of each petal lobes, delimiting the beginning of the corolla tube between each petal lobes.

Landmark	ID	points	sliders
Petal 1	1	1	
Petal 2	2	1	
Petal 3	3	1	
Petal 4	4	1	
Petal 5	5	1	
Sepal 1	6	1	
Sepal 2	7	1	
Sepal 3	8	1	
Sepal 4	9	1	
Sepal 5	10	1	
Curve dorsal	1,11 :29	20	19
Curve ventral	8, 30 :48	20	19
Curve margin Petal1-Petal2	1,49 :67,2	21	19
Curve margin Petal2-Petal3	2,68 :86,3	21	19
Curve margin Petal3-Petal4	3,87 :105,4	21	19
Curve margin Petal4-Petal5	4,106 :124,5	21	19
Curve margin Petal5-Petal1	5,125 :143, 1	21	19
Curve Sepal1-Sepal2	6,144 :148,7	7	5
Curve Sepal2-Sepal3	7,149 :153,8	7	5
Curve Sepal3-Sepal4	8,154 :158,9	7	5
Curve Sepal4-Sepal5	9,159 :163,10	7	5
Curve Sepal5-Sepal1	10,164 :168,6	7	5
Curve base Petal1-Petal2	1,169 :183,2	17	15
Curve base Petal2-Petal3	2,184 :198,3	17	15
Curve base Petal3-Petal4	3,199 :213,4	17	15
Curve base Petal4-Petal5	4,214 :228,5	17	15
Curve base Petal5-Petal1	5,229 :243,1	17	15
Surface tube	244 :789		
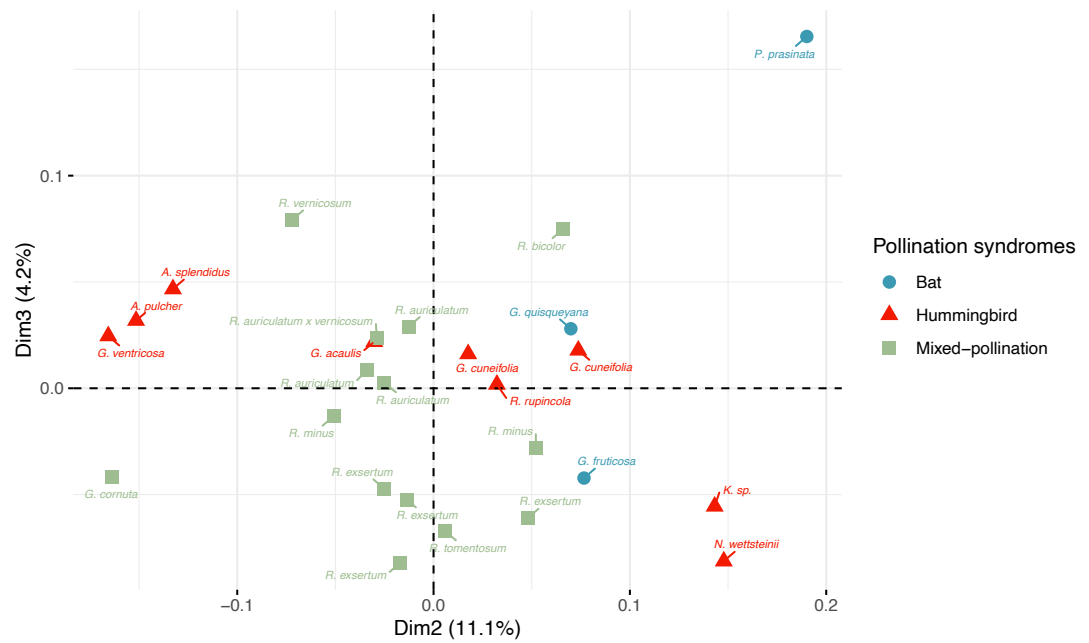
(a)
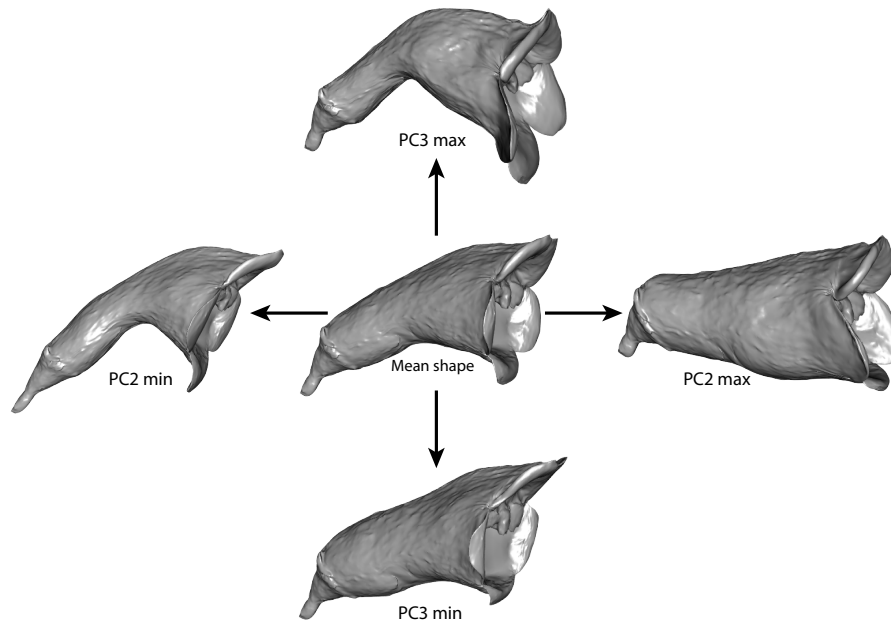
(b)

Figure S9. Morphospace of individual 3D floral shape variation along the second and third principal axes of the PCA (a). Each flower is represented according to its pollination syndrome. Multidimensional floral shape variation according to pollination syndromes in the Gesneriaceae (b).
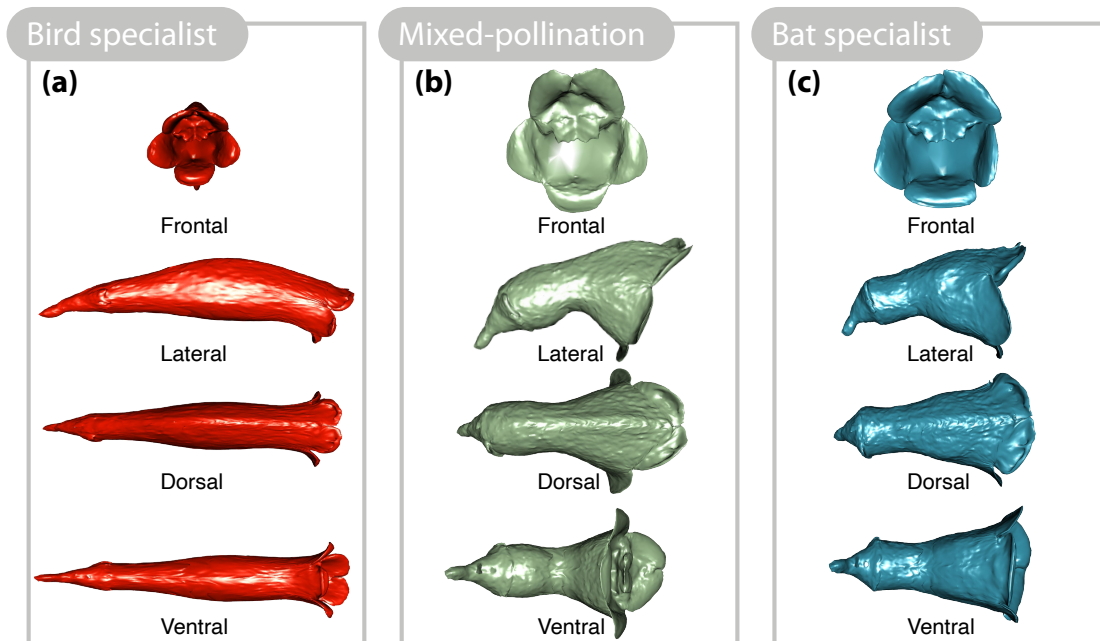
Figure S10. Mean floral shapes for three pollination syndromes : bird specialists (a), mixed-pollination (b), and bat specialists (c). These models were obtained by warping the mean flower shape on the mean morphospace coordinates of each syndrome.
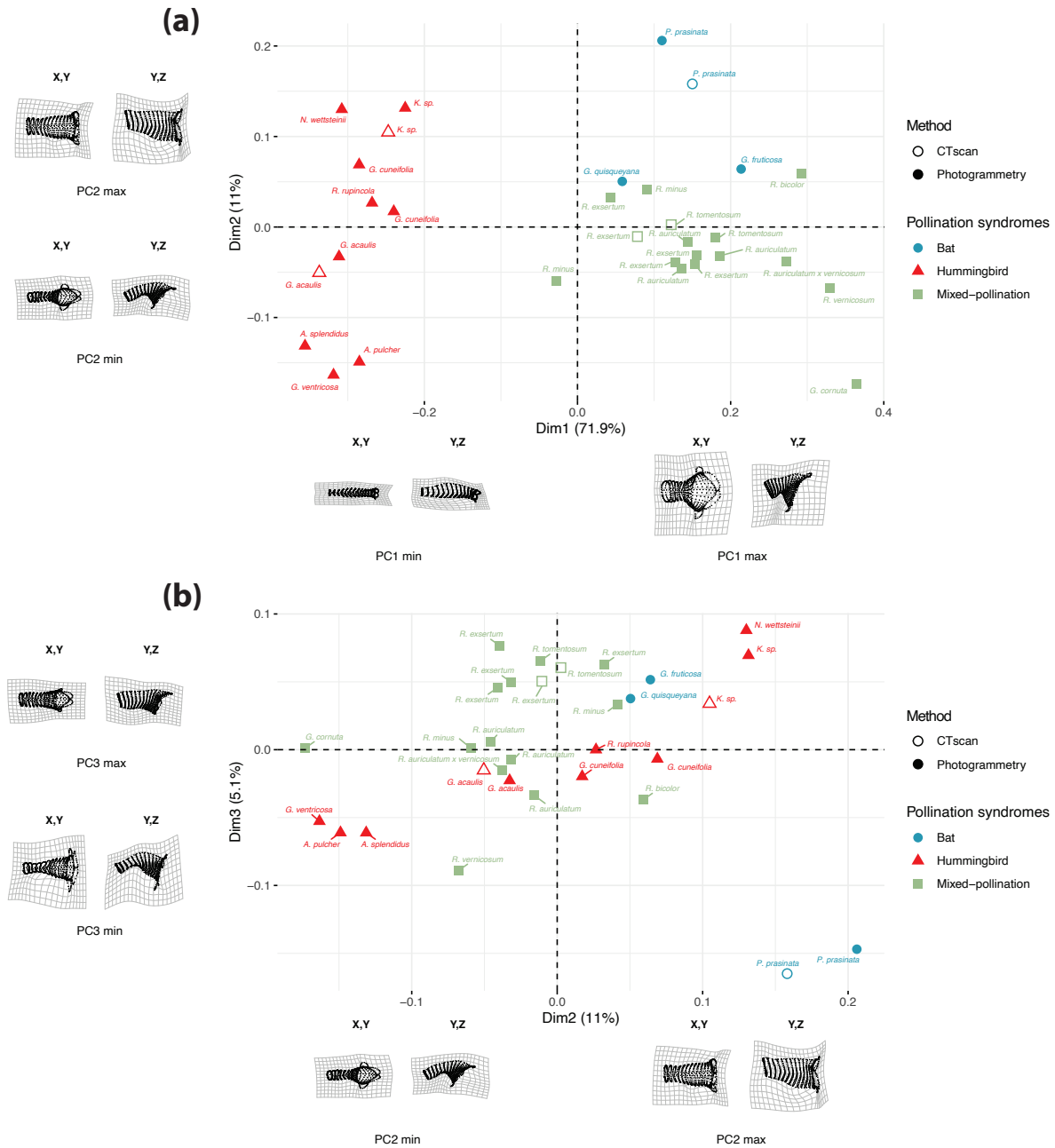
Figure S11. Principal component analysis of floral shapes of Gesneriaceae according to pollination syndromes and the method used to reconstruct the 3D floral shapes. The Thin Plate Splines (TPS) deformation grids represent the lateral and dorsal deformation of the mean floral shape along each principal component axes (PC), for PC1 and PC2 (a) and PC2 and PC3 (b).

Methods S2 - Phylogenetic analysis

We used PyPHLAWD (Smith and Walker, 2019) to generate a multiple sequence alignment of genes available in GenBank for the studied species. We used the plant sequence database pln.08122019 available from the PyPHLAWD website (built December 8th, 2019). Blastn settings in PyPHLAWD were 0.55 for the length limit, 10-10 for the e-value limit and 20 for percentage identity. The phylogeny was reconstructed using RAxML using a GTR GAMMA model partitioned by gene. *Aeschynanthus acuminatus* was used as a replacement for *A. pulcher* and *A. splendidus*, as no molecular data were available for the latter species. The sequences for this species also served to root the phylogeny. *Besleria notabilis* was included to help with the phylogenetic analysis but was pruned following the analysis. *Kohleria spicata* was used to place *Kohleria sp.*, an undescribed natural hybrid. *Paliavana prasinata*, the hybrid *Rhytidophyllum auriculatum* × *vernicosum* as well as *Gesneria cornuta*, a new hybrid (Joly and Clark, unpublished data), were added manually to the final phylogeny. This phylogeny was not used to draw firm conclusions on the evolution of flowers in the group but rather to illustrate the potential for examining the phylogenetic relationships among the species modeled in 3D with photogrammetry.

Methods S3 - Flower colour variation analysis

A quantitative colour comparison of flowers was performed using the calibrated surface textures (Fig. **1r**) and the colordistance R package version 1.1.2 (Weller and Westneat, 2019). Textures of each flower were imported in R and pixels were treated as three-dimensional coordinates in an RGB colour space (Fig. **1s**). Each image pixels were sorted into 8 colour bins using RGB channels by dividing the 3D colour space of each flower texture into the defined number of clusters. Each bin is characterized by its colour attributes (R, G ,B) representing the average RGB colour values of the pixels in that category, and its density represents the proportion of the pixels present in that category. The 8 colour clusters were calculated for the entire texture dataset using the getHistList function (Weller and Westneat, 2019). A colour distance matrix (CDM) between flowers was then calculated using earth mover's distance (EMD) between the histograms of each flower, taking both the colour information and frequency of each bin (Weller and Westneat, 2019). A tanglegram was built with the cophylo function of the phytools R package version 0.7.80 (Revell, 2012) and was used to visualize and compare the phylogenetic tree of Gesneriaceae and a dendrogram of the flower colour distance matrix representing the colour similarities between the flower models. Ward's minimum variance method was used as the clustering method. This method aims to find compact, spherical clusters.
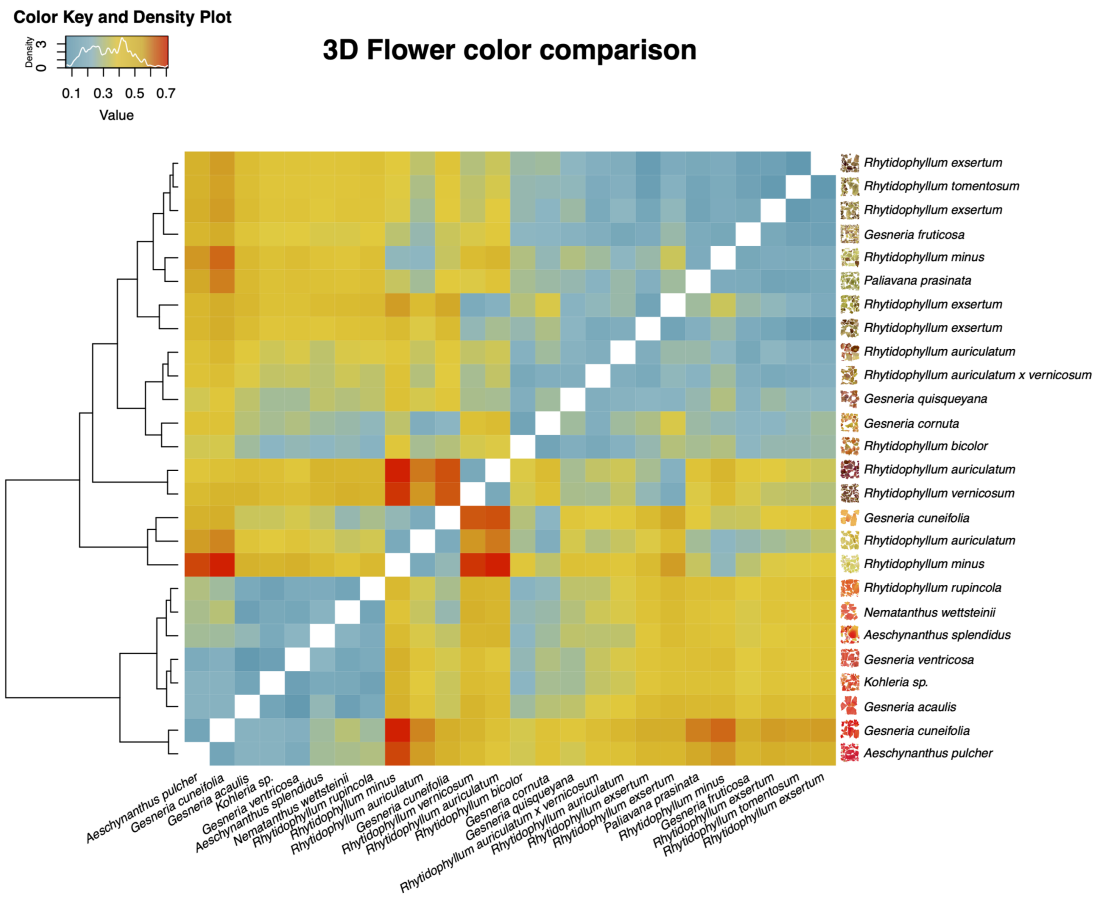
Figure S12. Colour distance matrix heatmap and dendrogram using Ward's distance.

Figure S13. Example of a 3D-printed flower of *Gesneria cornuta* in clear and soft resin. We used the Form 3 3D-printer from Formlabs (Somerville, Massachusetts, U.S.) to print Gesneriaceae flowers. After they were printed, the models were rinsed in fresh isopropyl alcohol (IPA), the supports used to stabilise the models while being printed were removed, and the final models were post-curated using heat and 405 nm light.

Bibliographie

Adams, D., Collyer, M., Kaliontzopoulou, A., and Baken, E. (2021). Geomorph : Software for geometric morphometric analyses. r package version 4.0.

Baken, E., Collyer, M., Kaliontzopoulou, A., and Adams, D. (2021). gmshiny and geomorph v4.0 : new graphical interface and enhanced analytics for a comprehensive morphometric experience.

Bardua, C., Felice, R. N., Watanabe, A., Fabre, A.-C., and Goswami, A. (2019). A practical guide to sliding and surface semilandmarks in morphometric analyses. *Integrative Organismal Biology*, 1(1) :obz016.

Faure, J. and Joly, S. (2020). Pollinator performance of the pollination generalist rhytidophyllum bicolor (gesneriaceae) in haiti 15 months after the matthew hurricane. *Selbyana*, 33(3).

Joly, S., Lambert, F., Alexandre, H., Clavel, J., Léveillé-Bourret, E., and Clark, J. L. (2018). Greater pollination generalization is not associated with reduced constraints on corolla shape in Antillean plants. *Evolution*.

Losos, J. B. and Ricklefs, R. E. (2009). Adaptation and diversification on islands. *Nature*, 457(7231) :830–836.

Martén-Rodríguez, S., Fenster, C. B., Agnarsson, I., Skog, L. E., and Zimmer, E. A. (2010). Evolutionary breakdown of pollination specialization in a caribbean plant radiation. *New Phytologist*, 188(2) :403–417.

Martén-Rodríguez, S., Almarales-Castro, A., and Fenster, C. B. (2009). Evaluation of pollination syndromes in Antillean Gesneriaceae : evidence for bat, hummingbird and generalized flowers. *Journal of Ecology*, 97(2) :348–359.

Martén-Rodríguez, S. and Fenster, C. B. (2008). Pollination Ecology and Breeding Systems of Five Gesneria Species from Puerto Rico. *Annals of Botany*, 102(1) :23–30.

Martén-Rodríguez, S., Quesada, M., Castro, A.-A., Lopezaraiza-Mikel, M., and Fenster, C. B. (2015). A comparison of reproductive strategies between island and mainland Caribbean Gesneriaceae. *Journal of Ecology*, 103(5) :1190–1204.

R Core Team (2021). *R : A Language and Environment for Statistical Computing*. R Foundation for Statistical Computing, Vienna, Austria.

Revell, L. J. (2012). phytools : an r package for phylogenetic comparative biology (and other things). *Methods in Ecology and Evolution*, 3(2) :217–223.

Schlager, S. (2017). Morpho and rvcg–shape analysis in r : R-packages for geometric morphometrics, shape analysis and surface manipulations.

Serrano-Serrano, M. L., Rolland, J., Clark, J. L., Salamin, N., and Perret, M. (2017). Hummingbird pollination and the diversification of angiosperms : an old and successful association in gesneriaceae. *Proceedings of the Royal Society B : Biological Sciences*, 284(1852) :20162816.

Smith, S. A. and Walker, J. F. (2019). PyPHLAWD : A python tool for phylogenetic dataset construction. *Methods in Ecology and Evolution*, 10 :104–108.

Vogel, S. (1969). Chiropterophilie in der neotropischen flora neue mitteilungen iii. *Flora oder Allgemeine botanische Zeitung. Abt. B, Morphologie und Geobotanik*, 158(4-5) :289–323.

Weller, H. I. and Westneat, M. W. (2019). Quantitative color profiling of digital images with earth mover's distance using the r package colordistance. *PeerJ*, 7 :e6398.

Annexe - Deuxième chapitre
Protocole de photogrammétrie

Dans le second chapitre de cette thèse, un protocole de photogrammétrie a été établi afin de reconstruire en trois dimensions la structure de fleurs. La version en ligne de ce protocole est hébergée sur la plateforme GitHub, et le protocole qui suit est également visualisable en ligne à l'adresse suivante : `http://www.plantevolution.org/photogrammetry-protocol/`.

Flower photogrammetry and 3D modeling protocol

Marion Leménager

Jérôme Burkiewicz

Loudmila Jelinscaia Lagou

Daniel Schoen

Diana Constanza Diaz Cardona

Simon Joly

2024-02-01

1 About

This protocol is an evolving protocol used in the Joly lab at the Université de Montréal (Canada)

This protocol describes how to obtain three-dimensional (3D) reconstructions of flowers using photogrammetry. It describes in details the set-up, settings and steps that has worked for us for building accurate flower models, but other approaches are certainly possible. Hence, we hope this protocol serves as a starting point rather than a final protocol. We welcome any comments.

1.1 Citation

Leménager, M., J. Burkiewicz, D. J. Schoen, S. Joly. Studying flowers in 3D using photogrammetry. New Phytologist. 237(5): 1922-1933.

1.2 Contributing

This protocol was produced with bookdown and is hosted on github. Please do not hesitate to fork the protocol, modify it and make pull requests to improve it!

1.3 Disclaimer

We provide this protocol as guidelines, without any guaranty. It has worked well for us for many types of flowers, but there is no guaranty that it will work on all flowers.

2 Materials

2.1 Lighting

It is important to have good lighting conditions to take the photographs. To optimize the lighting conditions, we use a Neewer portable lighting box to recreate lighting studio conditions and reduce shading on the object to a maximum. This lightbox needs to be powered from an outlet or from an external battery. The color of the background used should contrast with the color of the flowers to be photographed.

2.2 Turntable

We use an automated turntable and shutter release device (Syrp Genie mini II and turntable) to rotate each flower around itself (360°) and trigger a predetermined number of pictures from the camera to get pictures from all around the flower. The Genie Mini II has several hours of autonomy depending on its use, but it can be plugged in a source of energy during the process (external battery, plug, or usb). This device is easily controlled and set remotely via its application "Syrp" (Figure 2.1) on any kind of smartphone (although not all Android versions) with Bluetooth (Appstore or Playstore) after the device has been paired with your phone and after any updates suggested by the device has been done.

We also use a 1 cm scale placed adjacently to the flower, and include a label describing the species name, collection number, date of collection, location, and coordinates.

Figure 2.1: Syrp application

2.3 Camera

It is important to have very sharp pictures for optimal model reconstruction. Ideally, the whole flower should be in focus to maximize the amount of details captured. This could be achieved with focus bracketing (i.e., shooting a series of pictures of the flower at different focus distances) and subsequently, focus stacking (i.e., combining the series of pictures to produce a sharp image with a greater depth of field than any single image; Figure 2.2). Focus bracketing can be easily achieved with a camera that provides this option (we use Canon EOS 90D with a fixed macro lens EF 100mm f/2.8L MACRO IS USM), while focus stacking can be done using software like Helicon Focus (paid) or Enfuse (free in Linux).
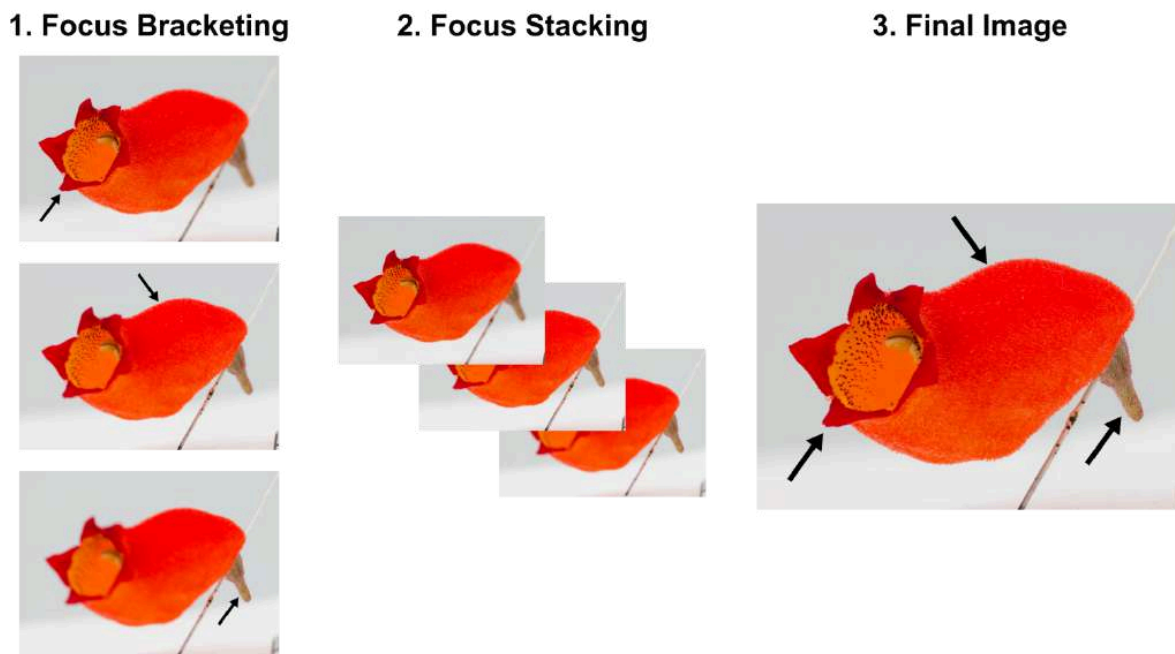
Figure 2.2: A simplified visual summary of the focus stacking process. (1) Focus bracketing: The camera shoots a series of pictures at different focus distances. (2) Focus Stacking: The series of pictures is combined using specialised software. (3) Final Image: The final image is sharp, with a greater depth of field than any single image taken during focus bracketing. The black arrows show the parts of the flower in focus.

However, using a professional camera and doing focus bracketing and stacking are not necessary. We also obtained good results with a Canon T2i/550D camera that shoots 18.0 MP RAW photos (5184 x 3456 pixels) and a fixed macro lens (60mm f/2.8 Macro lens).

In general, avoid using a lens that isn't fixed; zooming in and out can create artifacts during the model reconstruction. Ideally the flower should take a large portion of the photographs for best results. Depending on the weight of the camera, a flexible or a rigid tripod could be used. If a short flexible table-top tripod can safely support your camera and prevent its movement during the shooting, we

recommend it for easier and quicker modification of the camera angle at which we take each series of photos. Otherwise, opt for a rigid collapsible tripod, as it is crucial to avoid camera movement, especially during focus bracketing.

2.4 Color chart

To calibrate the photos for color, we use a Xrite ColorChecker Passport Photo 2. The main target that we use is the classic target with a 24-patch color reference target to create Digital Negative (DNG) (Adobe Systems Incorporated (2012)) camera profiles from a raw photo (called DNG conversion), and the 75% neutral gray patch to calibrate for light exposure.
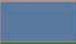
		sRGB		
		R	G	B
1	Dark Skin	115	82	68
2	Light Skin	194	150	130
3	Blue Sky	98	122	157
4	Foliage	87	108	67
5	Blue Flower	133	128	177
6	Bluish Green	103	189	170
7	Orange	214	126	144
8	Purplish Blue	80	91	166
9	Moderate Red	193	90	99
10	Purple	94	60	108
11	Yellow Green	157	188	64
12	Orange Yellow	224	163	46
13	blue	56	61	150
14	Green	70	148	73
15	Red	175	54	60
16	Yellow	231	199	31
17	Magenta	187	86	149
18	Cyan	8	133	161
19	White (5%)	243	243	242
20	Neutral 8 (26%)	200	200	200
21	Neutral 65 (44%)	160	160	160
22	Neutral 5 (62%)	122	122	122
23	Neutral 35 (75%)	85	85	85
24	Black (86%)	52	52	52

Figure 2.3: Xrite color chart details for standard Red Green and Blue (sRGB) values. The 75% neutral gray has values of 0.33 (85/255) for Red Green Blue channels in the LightRoom software

2.5 Softwares

To convert RAW photos (CR2 or CR3 for Canon Raw Version 2 or 3 image files, respectively) to DNG files, we either use directly Adobe Lightroom Classic to export in DNG format the CR2 photos or Adobe DNG converter. To calibrate the photos according to the color chart, we use the Xrite Color Checker software to create DCP camera profiles from DNG files, and Adobe Lightroom to use these profiles and apply them on an entire set of photos that need the same calibration. To do focus stacking, we first cluster the series of images to be combined based on time intervals using ExifTool and then we use Helicon Focus to stack them. Both can be easily done from the command line using the python scripts provided by the Eaton Lab. To reconstruct the 3D models from photos, we use Agisoft Metashape.

2.6 Flowers

Collect fresh flowers from the plant, label them and store them in a cool place or with the tip of the pedicel in some water to prevent accelerated wilting. Different flowers will wilt at different paces. Flowers are pinned through the floral receptacle or pedicel using entomological pins in dense foam at the center of the turntable. Alternatively, flowers can be secured in a truncated pipette tip, itself fixed on the turntable, or with alligator clips to rapidly fix the flowers.

> Store flowers in 50mL Eppendorf tubes or in foam box no more than an hour before taking photos of them.

> In some cases, it is necessary to remove sepals from the flower before building the model to accurately study the corolla shape. To do this, use a razor blade and mark the sepal intersections with a waterproof pen. The marks will help for the model construction and more importantly landmarks positioning.

2.7 Summary of materials and software

Materials	Description	Price (USD)
Photography		
Camera	Digital Single-Lens Reflex (DSLR) (e.g., Canon t2i or Canon EOS 90D for taking images without or with focus bracketing, respectively)	from $500
Macro lens	A preferably fixed focal-length lens (e.g., Canon 60mm f/2.8 Macro lens for the Canon t2i camera, or Canon EF 100mm f/2.8L MACRO IS USM for the Canon EOS 90D camera)	from $400
Tripod	Preferably flexible (e.g. Gorillapod), or collapsible	from $30
Stepping motor and turntable kit	Syrp Genie mini II and turntable, used to shoot smooth rotating video and interactive 360° images of objects. Full iOS and Android App control via Bluetooth. Battery life: 6hrs video and 15hrs time-lapse. Panning payload 8.8lbs/4kgs	$328

Materials	Description	Price (USD)
Lightbox	A portable photo studio, e.g. Neewer Lightbox 20"/50cm foldable portable photography lighting kit (Neewer Technology Co. LTD, Shenzhen, China), adjustable brightness with 120 LED lights, CRI (colour Rendering Index) of 85+, 6000-6500K colour temperature, needs to be powered by a portable battery in the field and comes with white, grey, black and orange backdrops. In the bracket of light intensities possible for this lightbox, we used an intermediate light intensity. [maximum;usually used; minimum] lux light intensities correspond to [3140;2680;1330] lux for a white backdrop and [330;305;238] lux with a black backdrop.	e.g. $89
External battery	Powering source for in-field photo capture, essentially for the lightbox or to recharge batteries	optional
Flower mounting and identification		
Flower	Freshly cut flower with pedicel and floral receptacle	/
Labels and container	Identification and storage of fresh flowers to avoid damage and avoid wilting	/

Materials	Description	Price (USD)
Turntable labels	To provide information on species, collector, collection number, date, locality, and coordinates, and the chunk number. To use as a separate photo before each run of photos.	/
Razor blade	To remove flower parts (e.g., sepals)	/
Small block of dense foam attached to the center of a paper disk	To fix flowers in place with a pin at the center of the turntable. The foam and the paper disk should have the same color as the backdrop used.	/
Entomological pins	To pin through the peduncle or floral receptacle and fix the flower on the turntable.	/
Scale	A 1 cm scale to use as reference	/
Colour calibration		
Color chart	A color reference to calibrate RAW photos (e.g. X-rite ColorChecker Passport)	e.g. $90
Color calibration software	ColorChecker Camera Calibration, Xrite software for automatic color profile creation	Free
Photo editing software	Adobe Photoshop Lightroom, editing software for image color calibration in batch	Payment plans vary

Materials	Description	Price (USD)
DNG conversion software	Adobe DNG converter, to convert Camera Raw files from supported cameras to the more widely used DNG raw files	Free
Focus stacking (optional)		
Image clustering software	ExifTool, to cluster the images taken with focus bracketing from each angle based on time intervals	Free
Focus stacking software	Helicon Focus Pro (Mac OS X, Windows) or Enfuse (Linux), to focus stack the clustered images and produce a sharp image with a high depth of field	Payment plans vary
Python scripts	Python scripts developed by the Eaton Lab to use ExifTool and Helicon Focus through the command line for faster processing	Free
Model reconstruction		
3D reconstruction from photogrammetry software	Agisoft Metashape Pro Software	$549 Academic price

References

Adobe Systems Incorporated. 2012. "Digital Negative (DNG) Specification, Version 1.4.0.0." Adobe Systems Incorporated: San Jose, CA, USA, 2012.

3 Settings and preparation

3.1 Camera and tripod settings and preparation

To obtain the best picture quality for model reconstruction, we need an optimal combination of the light sensibility of the sensor (ISO), the duration of exposure and the focal of the objective (F). As mentioned, it is preferable to use a fixed lens (one that doesn't allow zooming) to facilitate the model reconstruction in the processing step because the software can't take zooming into account in the reconstruction process. Maximizing the light source allows us to use the lowest ISO to get crisper images. Adjust the time exposure to allow the right amount of light to go to the sensor, avoiding low key and high key photos (i.e., under/over exposed photos). This may be adjusted according to the subject (light or dark colored subject or background) or if different lighting conditions are used.

A flexible tripod (Figure 3.1) can be used to easily and quickly adjust several camera heights (high, middle, and low) close to the subject. If this option cannot safely support your camera and prevent its movement during the shooting, opt for a rigid collapsible tripod, as it is crucial to avoid camera movement, especially during focus bracketing (Figure 3.2).

Figure 3.1: Flexible tripod.

Figure 3.2: Collapsible tripod.

3.1.1 Camera settings

The standard settings have to be adjusted depending on the flower (mostly colour and conditions).

3.1.1.1 Without focus stacking

If not doing focus stacking, we often use the following settings: M (Manual Exposure) mode dial, 1/20s exposure time (shutter speed), F/16 aperture, ISO 100, and standard exposure on the light meter. Using the "Manual Exposure" on the camera dial and setting the focal F to F16 will maximize the depth of field without lowering the image quality.

Use the manual focus setting on the side of the lens (Figure 3.3) to avoid camera trigger malfunction when the flower doesn't land on the detector. If the focus setting is set to automatic and the flower is off centered during rotation, the camera might not be able to focus (on the background) and thus, prevent the camera trigger. On manual, the camera will always be triggered by the turntable, even if the focus isn't optimal.

Because the subject is moving and may be off centered on the turntable, the focus may need to be adjusted while the turntable runs. For this you can pause the turntable, manually adjust the focus, and resume the spin.

In general, we save pictures as RAW files (ML setting on the camera display) to be able to post-process them for color calibration (Figure 3.4). A RAW photo of the color chart with an identical set of lighting conditions and camera settings as the flower to be photographed is needed for each flower photos series. If several flowers are processed one after the other without variation of light conditions, only one chart photo is needed.

> The nicer and the sharper the photographs, the easier it will be to build the models. So make sure that the flower is always in focus. Shade or high light reflectance can also impair model reconstruction, so pay attention to these while taking the pictures.

Figure 3.3: Camera (Canon T2i/550D) and lens (60mm f/2.8 Macro lens) used to take RAW photos. The red arrows (from top to bottom) depict the button to get manual focus, the ISO button and the Manual Exposure mode dial.

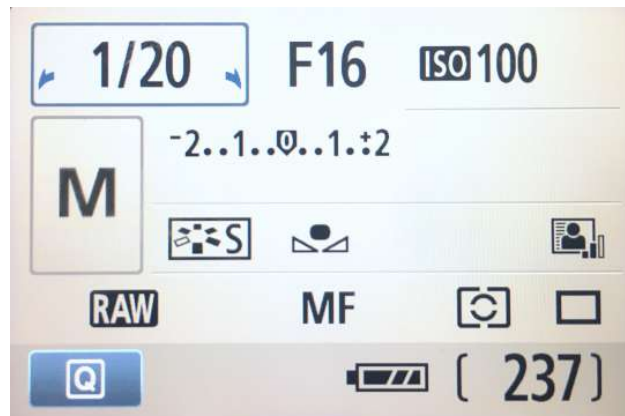Figure 3.4: Camera settings interface of the Canon t2i/550D (no focus stacking).

3.1.1.2 With focus stacking

If you decide to do focus stacking for your project, check the manual of your camera for optimal parameters during focus bracketing as they may slightly differ from what we use. For a Canon EOS 90D camera, we use the following settings: M (Manual Exposure) mode dial, 1/20 exposure time, F/11

aperture, ISO 100, Auto Focus (AF) lens focus mode, RAW image format (Figure 3.5, Figure 3.6).We usually use the *Zone AF* method and enable *Continuous AF* (On the camera screen, Shooting Menu, Tab 6).

Turn off the *Image Review* option (On the camera screen, Shooting Menu, Tab 1) to prevent delays after taking each set of pictures. To enable focus bracketing on EOS 90D, press the "START-STOP" button to enter the *Live View Shooting Mode*, then enable *Focus Bracketing* (On the camera screen, Shooting Menu, Tab 5). If using an EF 100mm f/2.8L MACRO IS USM lens, disable *Exposure Smoothing* (option within *Focus Bracketing*), otherwise it may cause changes in image brightness.

The optimal number of shots and focus increments depend on the size of the flower, as well as its position and distance from the camera (Figure 3.7). For example, from the highest camera position, 8 images with a focus increment of 4 works good for a ~2.5x1x1cm (LxWxH) tubular flower, but from an en-face camera angle (i.e. the flower opening facing the camera), 10-12 images with a focus increment of 3 may work better. Test what parameters would produce the smallest number of shots with each part of your flower in focus in each case. Generally, the higher the number of shots, the smaller the focus increments can be.

If the camera fails to capture all parts of the flower in focus, the turntable can be paused to make the appropriate adjustments. This may be the number of shots and focus increments, and/or the starting focal point, which should ideally be on the flower part nearest to the lens. Following the adjustment, the spin may be resumed to continue with image capturing. To save time, optimize the number of shots and focus increments from the start to avoid adjustments during image capturing, and help the camera focus by tapping on the part of the flower nearest to the lens after each rotation, before the camera is triggered. This part will be in focus in the first image taken at each rotation point, while the focus will gradually shift to points further from the lens with each subsequent image.

Figure 3.5: Camera (Canon EOS 90D) and lens (EF 100m f/2.8L MACRO IS USM) used to take RAW photos for focus stacking. Arrow on the lens: Focus mode button set to Auto Focus (AF). Arrows on the camera body (from top to bottom): ISO button, Manual Exposure mode dial and "START-STOP" button (for *Live View Shooting Mode*).
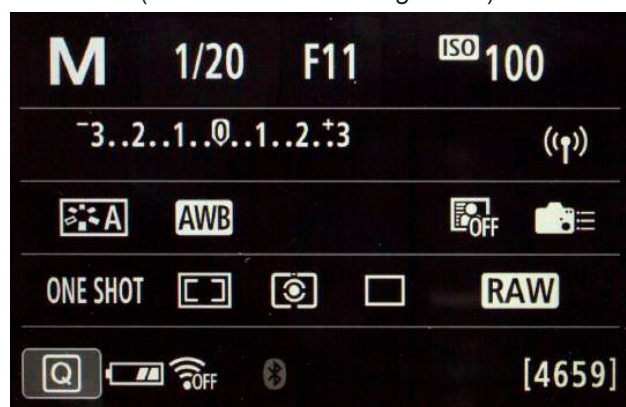
Figure 3.6: Camera settings interface of the Canon EOS 90D, used for projects with focus stacking.
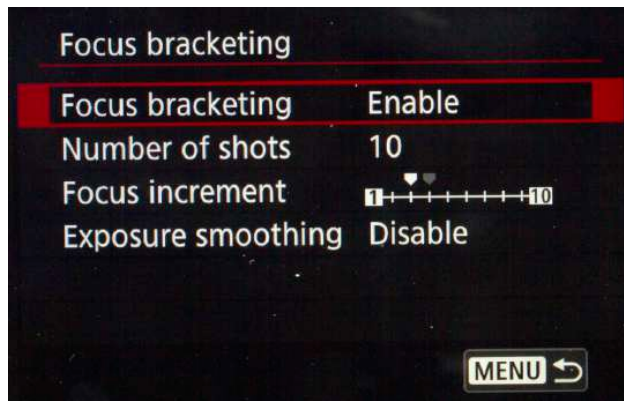
Figure 3.7: Focus bracketing settings of the Canon EOS 90D.

3.1.2 Optional: custom camera white balance

Optionally, you can begin by setting a personalized white balance (WB) in your camera with the light gray scale on the chart:

1. For a Canon camera, take a picture of the gray scale;

2. Choose *Custom WB* in your camera settings (Figure 3.8);

3. Select *Custom* and use the picture of the grey scale to define your custome white balance (Figure 3.9). Be careful, you will still require to linearize and calibrate each photo afterwards.

However, the color chart will always be the reference for post-processing the color calibration of each photo. This optional section only helps to have a better preview of the photos.
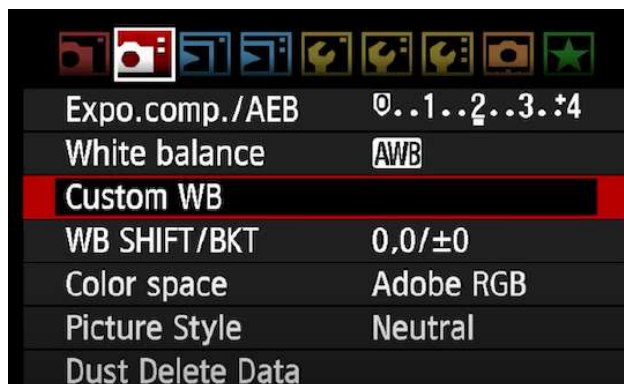
Figure 3.8: Custom whhite balance parameter.
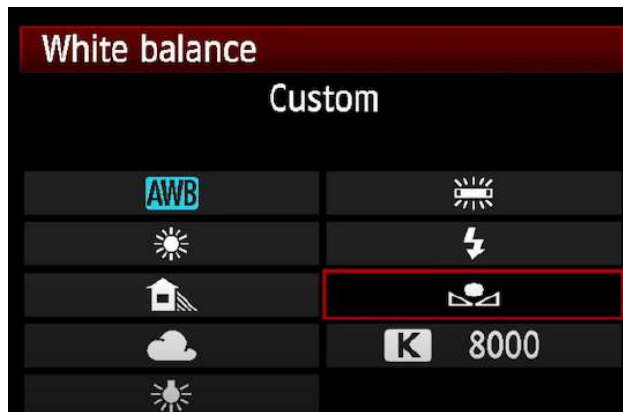
Figure 3.9: How to select a custom white balance.

3.2 Turntable settings and preparation

If not doing focus stacking, for each run (one 360° spin of the turntable), we use a wait time of 2s to allow the camera time to save the images on the SD card after it is triggered, and the flower to stabilize after each rotation. If doing focus stacking, we use a wait time of 6-8s depending on the number of shots and focus increments.

1. Connect the shutter release to your camera and the turntable Syrp Genie II (Figure 3.10).

2. Turn the turntable on (to turn it off, hold the *on* button for 3 seconds).

3. Connect the Syrp Genie II to your device, and do the updates if required (needs an internet connection).

4. Click on *Create Content > Turntable* (Figures 3.11, 3.12).

5. Make sure the turntable orientation is inverted in the detailed settings (Figure 3.13)

6. In parameters (Figure 3.14), select 20 photos for each run, and the appropriate amount of waiting time depending on if you are doing focus stacking (6-8s) or not (2s; move-wait-shoot-wait-move). If it is too quick, some pictures won't be able to be saved as the camera needs a delay to save them on the memory card. The spinning device will take the first picture then proceed to a move-shoot-move run until the last photo.

7. Place the white background paper disk with the foam block on the turntable to contrast with the flower. If your flower is pale, then use a different background (colored or darker). Ideally, the color of the disk and the foam block should be the exact same as the color of the backdrop in the lightbox as this will help when applying masks later.

Figure 3.10: Camera shutter release port.
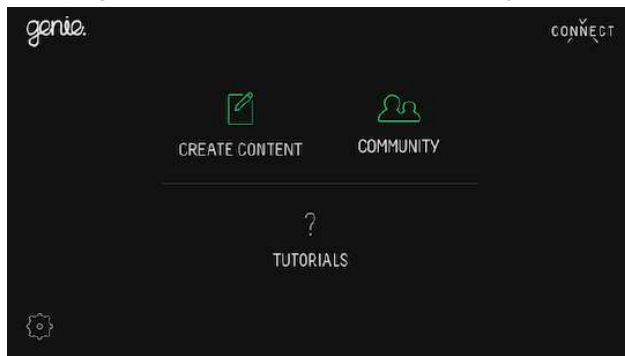
Figure 3.11: Camera shutter release port.
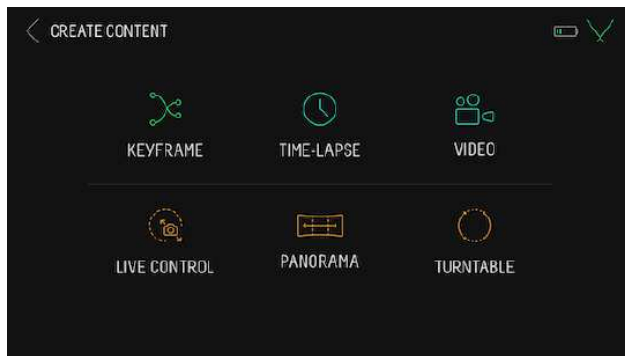
Figure 3.12: Camera shutter release port.
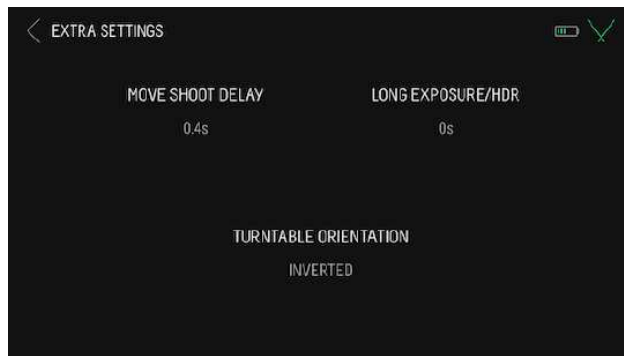
Figure 3.13: Genie detailed settings.
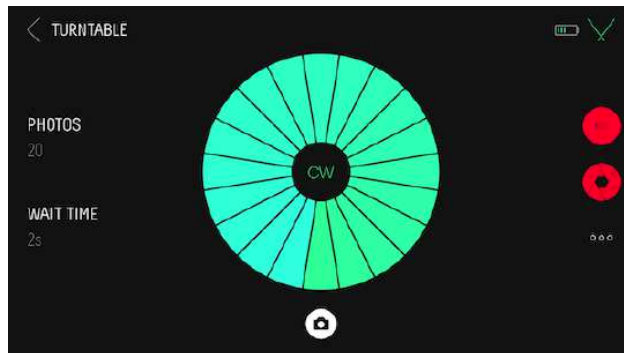
Figure 3.14: Start recording with the turntable.

3.3 Summary of settings

Parameter	Value
Camera settings	
Aperture	F/16 (no focus stacking) or F11 (focus stacking)
Sensibility	ISO 100 (lowest)
Exposure time	1/20s (depending on light settings)
Turntable settings	
Number of photos	20 per camera height (high, mid, low)
Wait time	2s (no focus stacking) or 6-8s (focus stacking)

4 Image capture step-by-step

4.1 Take a picture of the color chart

1. Camera settings:

   a. **Without focus stacking**: Set the camera settings to F/16, ISO 100, 1/20s, and RAW format.

   b. **With focus stacking**: Set the camera settings to F/11 (depends on the ideal settings of your camera and lens for focus bracketing), ISO 100, 1/20s, and RAW format.

2. Verify that you have enough space on your SD card for RAW photos:

   a. **Without focus stacking**: A minimum of 163 photos, accounting for photos of labels and chart.

   b. **With focus stacking**: The total number of photos depends on the number of shots at each rotation point and the number of flower positions used (usually around 1,500 photos +-200).

3. Verify that the placement of your turntable inside the lightbox will allow to capture correctly the flower you are about to photograph (distance from opening of the lightbox) and that the 1/20s shutter speed captures enough light from your flower by taking an initial photo of your flower.

4. If satisfactory go to the next step. The goal here is to have a definite set of settings that will match both your flower photos and a color chart to subsequently calibrate all your photos that have the same light conditions and camera settings.

5. Place the color chart where the flower will be placed, without shadows, and exposed under the same light as the flower will be (angled towards the LED source light in the lightbox). The camera settings and lighting cannot be changed after this. If the lighting or the camera settings are modified, the color chart needs to be taken again to correct the corresponding photos.

6. Place the camera so that the entire chart is visible.

7. Take a picture of the color chart in RAW format (if you are doing focus stacking for your project, disable the focus bracketing function for this step). Make sure to incorporate all color squares and the corners of the chart as shown below (Figure 4.1).

Figure 4.1: Colour chart photo taken at the beginning of the process to calibrate the photos in post process.

4.2   Flower placement & image capture

To reconstruct an accurate 3D model, it is very important to have pictures of all the parts and details of the flowers and from several angles. Also, the photographs need to overlap with each other for proper alignment in the first steps of the reconstruction. For this reason, several pictures will be taken of each flower, from different perspectives and all around the flower. We suggest that flowers are photographed from at least two positions (e.g., Figure 4.2). For more complex flowers, three positions may be required: horizontal, vertical, and upside down (Figure 4.3). Note that it is better to take more photos than less because if we can drop some pictures during the model reconstruction, it is impossible to come back and take more pictures if we realize that we should have.

Figure 4.2: Two flower positions that are normally suficient for Gesneriaceae flowers.

Figure 4.3: More complex flowers can require the pictures to be taken from three flower positions.

214

> For Gesneriaceae, we first suggest a standard and an upside-down position (Figure 4.2) of the flower as this generally gives satisfactory results. For more complex flowers, three positions may be required: horizontal, vertical, and upside down (Figure 4.3).

1. Clip the camera on the tripod and place it at one of the three position required per flower position: high, mid, and low position (see Figure 4.4. Make sure to not use different camera orientations (landscape vs. portrait).

2. If sepals need to be removed, use a razor blade to cut them at the base and mark the sepal intersections with a waterproof pen to keep track of the morphological structures.

3. Pin the flower through the pedicel or the floral receptacle and through a block of dense foam or malleable gum using an entomological pin. You can use several pins to avoid any sliding of the flower during the image capture process.

4. Make sure to place the flower so that it is wholly encompassed in the camera frame as much as possible. It is best to have the subject take as much space as possible in the camera frame to capture every details overall than having it entirely in the camera frame but with poor detail quality. What counts the most is getting several overlapping photos of each feature. Make sure that the flower is not in contact with anything as this would deform it and create problems during the model reconstruction.

5. For flowers with very uniform color or with radial symmetry, it may be helpful to place dots on the corolla using a waterproof pen to facilitate manual marker positioning and/or automated pixel position detection in the reconstruction step.

6. Place a scale (e.g., 1 cm) directly below the flower.

7. Take a picture of the flower with the label for each new positioning of the flower. This will help to identify each group of images during model reconstruction.

8. If you are doing focus stacking, enable *Focus Bracketing* function at this point and optimize the number of shots and focus increments so that you get each flower part in focus in at least one image. Tap on the part of the flower that is nearest to the lens before the first picture is taken at each rotation point, if it is not already in focus at that moment.

9. Press the *REC* button on your smartphone using the turntable interface to start the spin of the turntable and automated image capture.

10. Verify occasionally the focus on the flower while the flower rotates by pressing the square button (stop) and manually adjust the focus if needed, then press *REC* to resume your spin. You can also help the camera focus by tapping on the flower before the camera is triggered at each rotation point.

Figure 4.4: The three camera positions from which pictures should be taken for each flower position.

Adjust the number of flower positions and number of photos according to each flower. For intricate flowers, or flowers that can't be captured entirely with only two positions (ventral and dorsal), you can place the flower on an another position (Figure 4.3). On the contrary, if the flower can't be placed on several positions, you may need to increase the number of photos per camera height in order to have sufficient information for the software to reconstruct accurate 3D models.

5   Image post processing

5.1   File names and storage

We found that it is critical to have a very organized structure for saving files, especially when several people are working on the same project. We propose here what has been working so far for us.

In a species folder named with the name of the species (*Genus_species*), there should be a distinct folder for each individual photographed, usually with a different collection number. If the same individual has been photographed several times, the date of photos acquisition should be appended to the folder name to discriminate them. We also indicate in the folder name whether the individual has been photographed with or without sepals.

For each flower, we have one folder for uncalibrated photos, one for calibrated photos, and one for the model. The RAW picture of the color chart should be placed in the uncalibrated photos.

To distinguish which photo goes in which chunk, a photo of the label is taken at the beginning of each chunk (each set of photos per side of flower). We suggest to place the photos from different chunks in different folders once the photos are calibrated. The date of when the photos are taken is important because it helps matching the calibration to the right DNG file. If more than one set of photos with different lighting or camera settings are taken, make sure to distinguish the color charts that correspond to each set of photos.

```
Genus_species
  GEN_species_CollectionNumber
    sepal_DD.MM.YYYY or no_sepals_DD.MM.YYYY
      Model
        MetashapeProject
        MetashapeProjectFolder.files
        model.obj
        model.ply
        texture.jpg
      01_Photos_to_calibrate
        Place here all the RAW photos and color chart
      02_Photos_calibrated
        Place here all the calibrated photos, that you can organize per chunk
```

If you are doing focus stacking, you can also create the following two folders in addition to the above:

```
      03_Photos_clustered
        Place here the calibrated photos that have been clustered based on time intervals into
separate subfolders containing series of pictures taken using the Focus Bracketing function at each
rotation point
      04_Photos_focus_stacked
        Place here all the final images after focus stacking
```

5.2   Image color calibration

5.2.1   Creating color profiles

We present here three ways to create camera profiles. The first one allows to manually check the automatic detection of the color chart, the second and third ones are fully automatic (on MacOS and windows respectively).

This does not linearize the photos. For further details on color calibration, read Troscianko and Stevens (2015).

Method 1 : Manual creation of color profiles

1. This method uses the Xrite ColorChecker Camera Calibration software and Adobe DNG converter software (Figure 5.1).

2. Create a new empty folder called DNG.

3. Copy the RAW file representing your color chart in your DNG folder, and rename it accordingly (e.g. Color_chart_DD.MM.YYYY).

4. Open DNG converter and select the DNG folder you created in the first step. You can't select a specific file, you need to select a folder, and the software will convert all the files within this folder. Default parameters are fine for step 2-4. It will export the RAW file in the DNG folder to a DNG file with the same file name (Figure 5.2).

5. Open the Color Checker Camera Calibration software and drag and drop the newly created DNG file in the software. The software will automatically draw a grid around it. Make sure that the green grid fits the chart, avoiding edge effects on each square of color (Figure 5.3.

6. Click on *Create Profile* and save it under Color_Chart_DD.MM.YYYY (Figure 5.4.
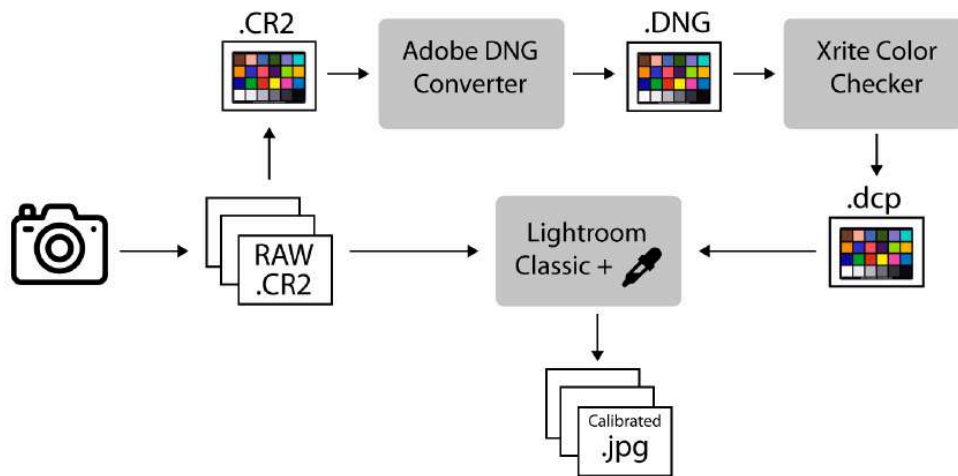
Figure 5.1: Image color calibration workflow.
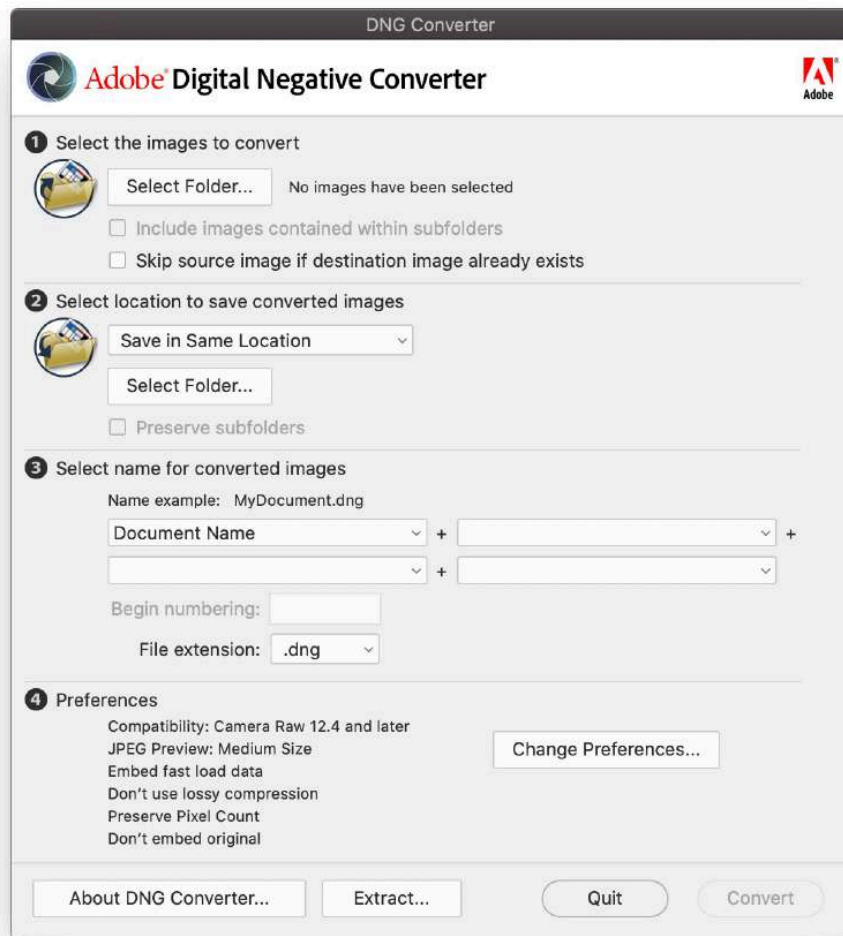
Figure 5.2: Convert RAW chart to DNG in Adobe DNG Converter.
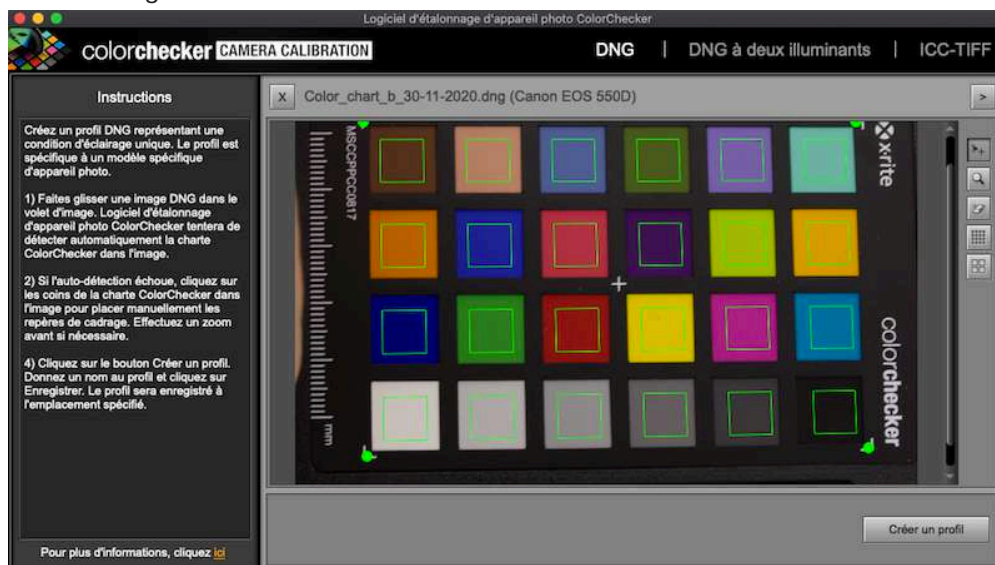
Figure 5.3: Align grid on chart in ColorChecker Camera Calibration.

Figure 5.4: Export the color profile.

Method 2: X-Rite Color Checker plug-in installation and automatic creation of color profiles on MacOS

1. Directly in Adobe Lightroom, you can add ColorChecker Camera Calibration as a module to a means of exporting files directly into a color profile.

    1. Click on *File > Export > Plug-in Manager* (or *gestionnaire des modules externes* in the left bottom corner).

    2. Click on *Add*.

    3. Navigate to *Library > Application Support > Adobe > Lightroom > Modules*.

    4. Select *XRiteColorCheckerPassport.lrplugin* and then click on *Add Plug-in* and *Done*.

2. Click on the color chart then *File > Export >* Choose *Xrite presets* from the drop down menu.

3. Name your profile then *> Export*.

4. It will go through ColorCheckerCamera calibration to automatically create the profile.

5. Restart Lightroom as indicated.

Method 3: X-Rite Color Checker plug-in installation and automatic creation of color profiles on Windows

1. Get the Xrite ColorChecker Camera Calibration software and download the *PC Version*. Save the *CameraCalibrationSetup.exe* in your downloads, for example, and run the program.

2. If Adobe Lightroom Classic is already installed on your computer, the installation program should proposed you to install the Adobe Photoshop Lightroom plug-in (Figure 5.5). Install it.

3. Once the plug-in is installed, run Adobe Lightroom Classic and import your color chart (*File > Import*).

4. Click on *File > Export* and in the drop-down menu, select *X-Rite Preselection* (Figure 5.6). Name your profile, and click on *Export*.

5. Restart Lightroom as indicated.

6. Run the setps 4 and 5 each time you want to create a new color profile witht the color chart.
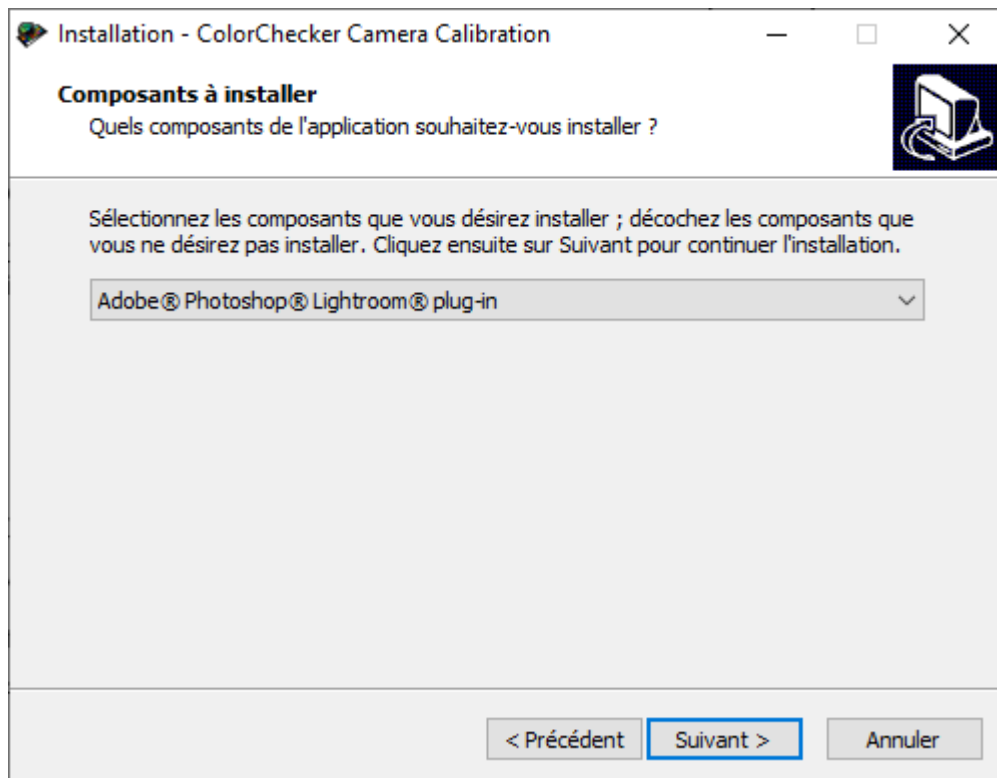
Figure 5.5: Color Checker plug-in for Lightroom installation.
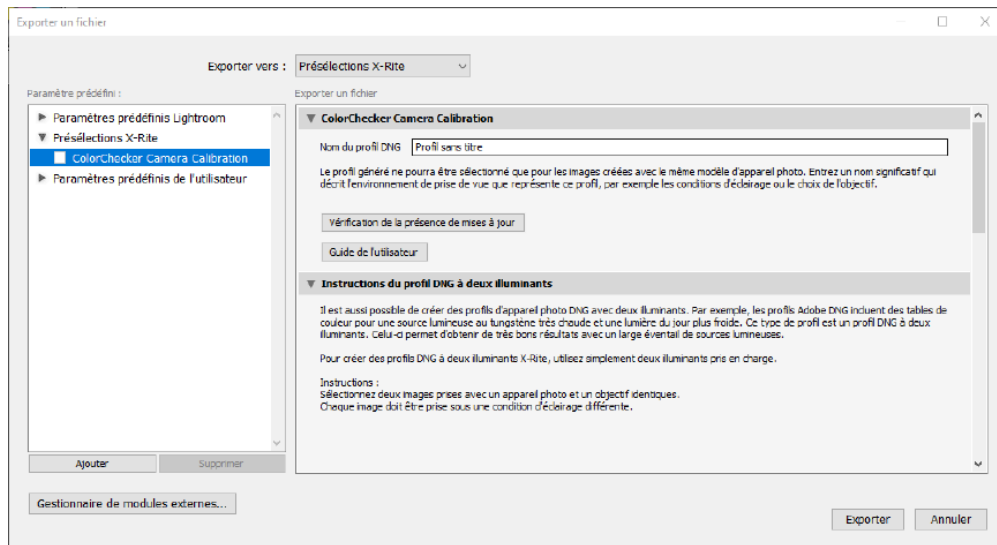
Figure 5.6: Color chart profile exportation.

5.2.2 Color and exposure calibration from profiles

1. Import your photos in Lightroom Classic. *File* > *Import* then select your folder of RAW photos.

2. Select the photo of the color chart.

3. Go to the *Development* module.

4. Select the color profile corresponding to the color chart you have selected (see Figure 5.7 and 5.8 to manually add a color profile) to calibrate the photo of the chart with its own calibration profile.
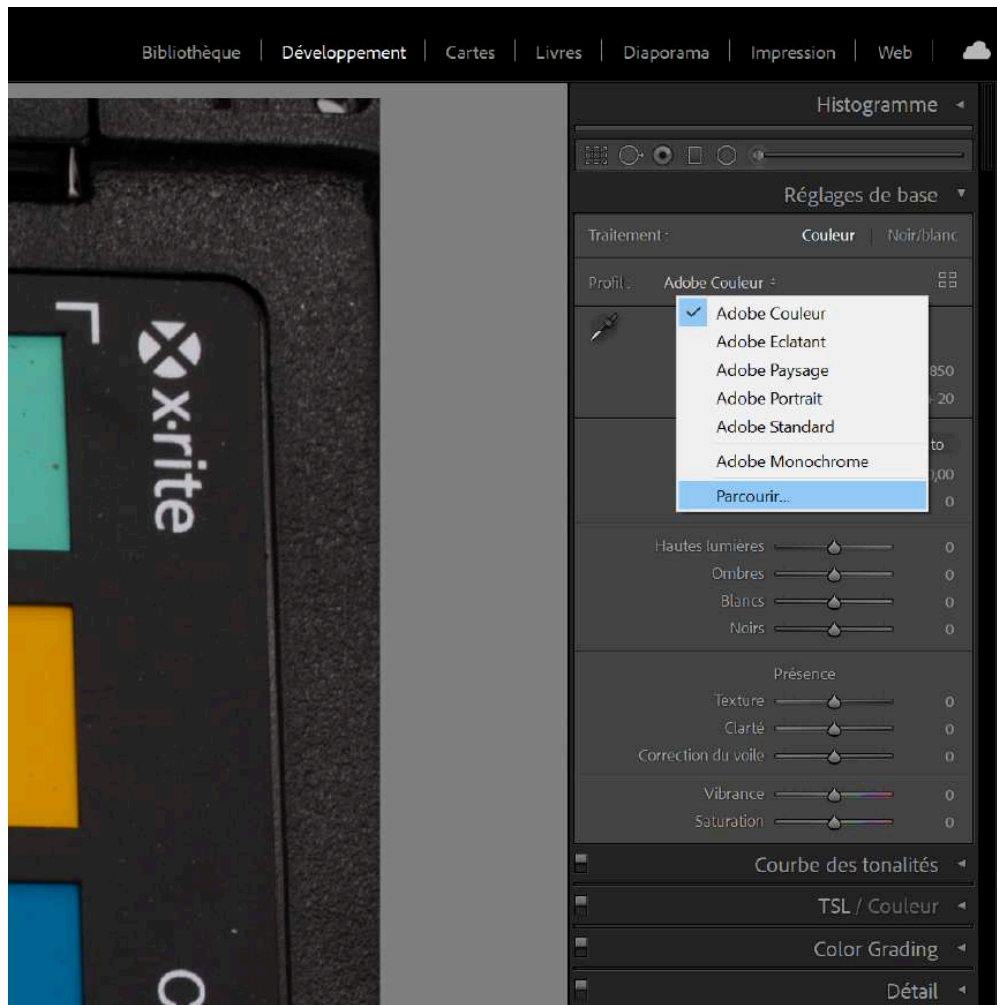
Figure 5.7: Add a new color profile.
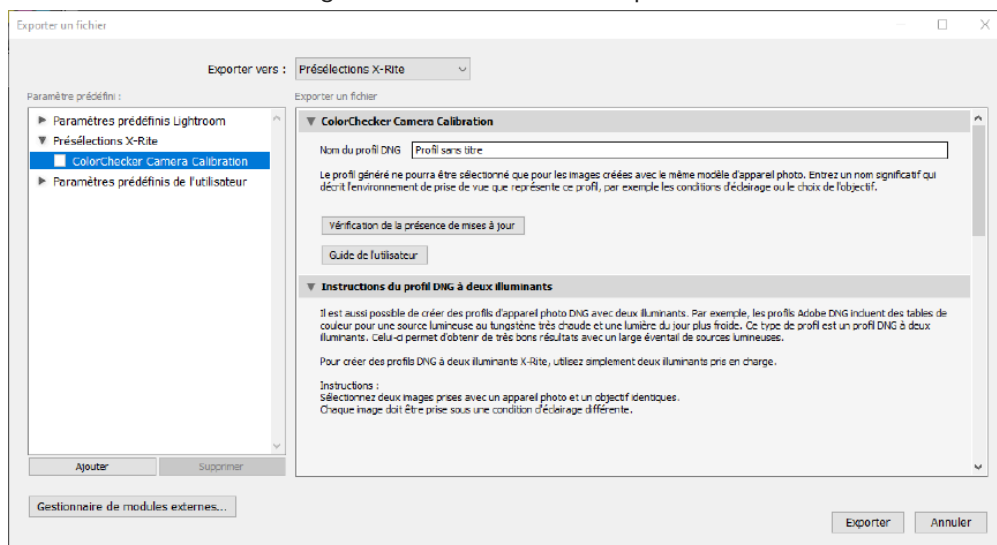
Figure 5.8: After adding a profile with the + sign, select it in the list below.

5. Use the eyedropper over the 75% gray scale (the dark gray patch right before the black patch on the color chart). Do not click on the photo with the eye dropper, only hover over it.

6. Adjust the RGB values the eyedropper indicates on the 75% gray scale by changing the exposure setting to make them as close as possible to 0.33 0.33 0.33 (corresponding to 85/255 for each of the red, blue, and green class). The exposure is now adjusted in addition to the color calibration, but only on the chart image.

7. To apply the modifications we just did to all the photos, go to the *Library* module, select all the photos (*Cmd+A* or *Ctrl+A*), and make sure that the one for which you made changes is highlighted (in white compared to the light gray of the newly selected images).

8. Go back to the *Development* module and click on the *Synchronize* option, check the profile and exposure boxes in the pop-up window and click on *Synchronize* (see Figure 5.9).
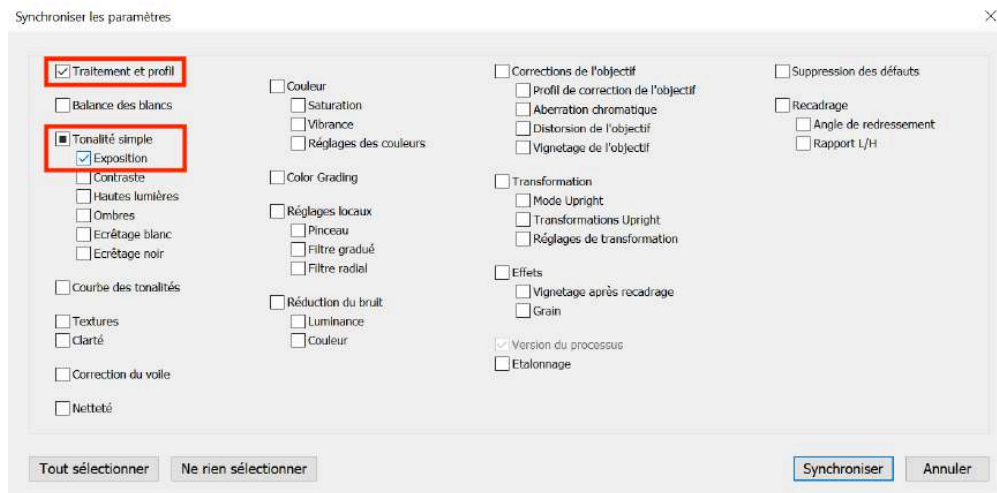
Figure 5.9: Synchronize your settings made to the photo of the chart to all the other photos and check the two categories you modified (color profile and exposure).

5.2.3 Export calibrated files

1. Select all the photos you need to export or all of them (*Cmd+A* or *Ctrl+A*).

2. Click on *File > Export*.

3. You can create presets that you will only need to create once to always export the same way in Adobe Lightroom (example Figure 5.10), and add personalized file names such as "_color_calibrated" at the end of each image file.

   a. Without focus stacking: Save the calibrated images as JPEG.
   b. With focus stacking: Save the calibrated images as TIFF (300 PPI). Make sure to include all metadata.

4. The calibrated folders can be saved into their own folder, and further divided into different subfolders representing different chunks (easily distinguishable by the separation created by a photo of the label).

225
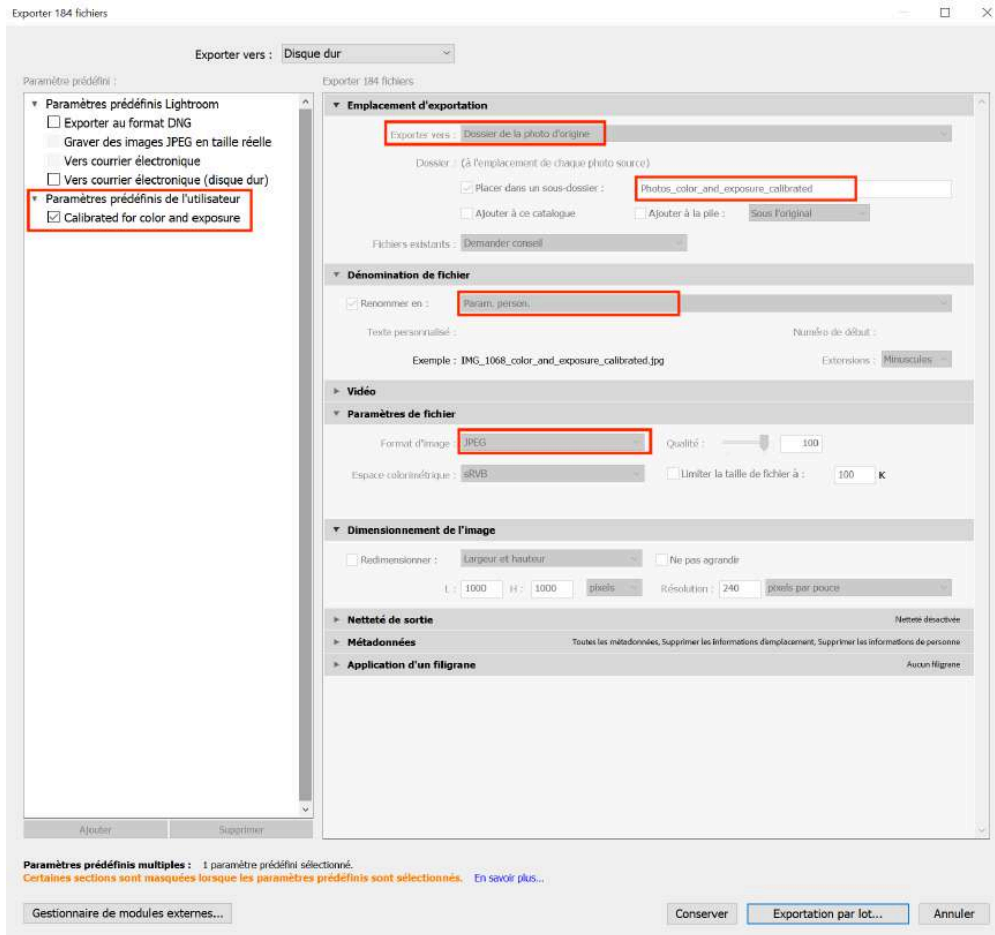
Figure 5.10: You can export using your own personalized parameters and then export in batch your selection in a specific folder within your folder of uncalibrated photos for easy access. This method can thus work for any folder of uncalibrated photos.

5.3 Image clustering (one folder at a time)

Note: This step is only necessary if you chose to do *focus stacking* in your project.

If you used the *Focus Bracketing* function during image capture and wish to proceed with focus stacking, you can make the process easier by first grouping (i.e., *clustering*) the series of photos taken at each angle and rotation point in separate subfolders. This way, each folder will contain images that can be stacked together as they depict the same flower angle and rotation point but with different focus distances.

This can be achieved using ExifTool. ExifTool extracts time-stamps from the metadata of images and can be used to separate the image clusters from each other based on time intervals. The time intervals between photos taken at each rotation point (i.e., at the same exact perspective, but with different focus

distances) is smaller than between photos taken between two rotation points (i.e., after the turntable changes the flower angle) when using the *Focus Bracketing* function.

To make image clustering faster, a python script developed by the Eaton Lab can be used (cluster_photos_by_time_intervals.py).

Command structure:

```
python3 cluster_photos_by_time_intervals.py -i <input folder with calibrated images> -o <o
```

Example:

```
python3 cluster_photos_by_time_intervals.py -i 02_Photos_calibrated -o 03_Photos_clustered
```

After running the command above, you will have a `03_Photos_clustered` folder containing subfolders with the different image clusters, distinguished by angle and rotation numbers based on their time-stamps.

5.4 Focus stacking (one folder at a time)

Note: This step is only necessary if you chose to do *focus stacking* in your project.

With the image groups taken at each rotation point and angle separated into different folders, they can now be easily focus stacked to produce one image per cluster with the whole flower in focus. Similarly to image clustering, this can be achieved by running another python script developed by the Eaton Lab (helicon_focus.py).

Command structure:

```
python3 helicon_focus.py -i <input folder with clustered images> -o <output folder with fo
```

Example:

```
python3 cluster_photos_by_time_intervals.py -i 03_Photos_clustered -o 04_Photos_focus_stac
```

Now you should have a `04_Photos_focus_stacked` folder containing one focus stacked image corresponding to each angle and rotation point cluster.

5.5 Alternatively: Cluster and focus stack photos from multiple folders at once

In case you would like to cluster and focus stack images of multiple specimens at once, to make the process even faster, you could also use the Automated Pipeline Scripts developed by the Eaton Lab.

You can use these scripts for all steps (i.e., from image calibration to focus stacking) or modify them according to your preferences and needs. We normally do the calibration step manually in Adobe Lightroom Classic as it does not take significantly more time and allows for calibrating both the colors and exposure of the images.

To make the scripts work, we save the calibrated images in a subfolder directly in the corresponding RAW image folder, for example in `3D_Modelization/Genus_species_A/01_Photos_calibrated/`, with the RAW images being in `3D_Modelization/Genus_species_A/`, while the directory containing the `3D_Modelization/` contains other folders that are similarly structured for other species.

```
3D_Modelization
  Genus_species_A
    RAW_photo_A1.CR3
    RAW_photo_A2.CR3
    RAW_photo_A3.CR3
    ...
    01_Photos_calibrated
      Calibrated_photo_A1.tif
      Calibrated_photo_A.tif2
      Calibrated_photo_A3.tif
      ...
  Genus_species_B
    RAW_photo_B1.CR3
    RAW_photo_B2.CR3
    RAW_photo_B3.CR3
    ...
    01_Photos_calibrated
      Calibrated_photo_B1.tif
      Calibrated_photo_B2.tif
      Calibrated_photo_B3,tif
      ...
  ...
```

For the sake of simplifying the following examples, `3d_Modelization/` would represent the path to your working directory that contains all your folders.

First, you need to create a text file containing a list of folder names in your working directory, i.e., the folders names in the directory `3D_Modelization/` following the example above. `cd` to this directory and run the following command:

```
ls -b1A >> folder_name.txt
```

This command will create a `folder_name.txt` file in your working directory with the names of all the folders in it. Then you need to create a text file containing the list of the RAW photo names within these folders.

Command structure:

```
for i in `cat folder_name.txt`; do cd 3D_Modelization/${i} && ls *.CR3 | sed -e 's!.CR3!!'
```

Now, aside from the RAW photos and the subfolder with the calibrated .tif photos, the `Genus_species_#/` folders within the `3D_Modelization/` directory should contain a `photo_names.txt` file with a list of the names of all the RAW photos in each folder.

We usually run the following modified automated script for processing multiple folders at once.

 • Automated script structure for clustering and focus stacking photos from multiple folders at once:

```
for i in `cat 3D_Modelization/folder_name.txt`
    do python3 cluster_photos_by_time_intervals.py -i 3D_Modelization/${i}/01_Photos_calib
    python3 helicon_focus.py -i 3D_Modelization/${i}/02_Photos_clustered -o 3D_Modelizatio
done
```

The `for` loop above should create two new subfolders in each of your `3D_Modelization/Genus_species_#/` directories:

1. `02_Photos_clustered`, containing the calibrated photos that have been clustered by angle and rotation points based on time intervals.

2. `03_Photos_focus_stacked`, containing the final focus stacked photos.

Although the original automated pipeline script by the Eaton Lab includes a step for resizing the photos after focus stacking, we do not typically include this step in the process as the photos' dimensions before and after focus stacking remains the same most of the time. Additionally, changing the images' dimensions to a different ratio can distort the shape of your 3D Model.

For those few images whose dimensions do change after focus stacking (for us it's normally no more that 3 per specimen), during the masking step in Agisoft Metashape it will notify you that the background image you are using does not have the same size as some of the images. You can find those unmasked photos and create a background images using their dimensions for masking them. However, as mentioned, this happens rarely.

If you wish to resize all your images after focus stacking following the original script, you will need to install `imagemagick`, which could be done using *homebrew*.

```
brew install imagemagick
```

- Automated script structure for clustering, focus stacking, and resizing photos from multiple folders at once:

```
for i in `cat 3D_Modelization/folder_name.txt`
    do python3 cluster_photos_by_time_intervals.py -i 3D_Modelization/${i}/01_Photos_calib
    python3 helicon_focus.py -i 3D_Modelization/${i}/02_Photos_clustered -o 3D_Modelizatio
    cd 3D_Modelization/${i}/03_Photos_focus_stacked && ls -b1A | sed -e 's!.tiff!!' >> sta
    for i in `cat stacking_names.txt`
        do convert ./${i}.tiff -resize 5300x3500! ./${i}.tiff
    done
done
```

Remember to add the path to your python script files if they are not located in your working directory, as well as modify the final image size if you wish it to be different.

References

Troscianko, Jolyon, and Martin Stevens. 2015. "Image Calibration and Analysis Toolbox–a Free Software Suite for Objectively Measuring Reflectance, Colour and Pattern." *Methods in Ecology and Evolution* 6 (11): 1320–31.

6   3D model reconstruction in Agisoft Metashape

6.1   Download Agisoft Metashape

Download the Agisoft Metashape professional edition software here. Make sure that your computer fills the minimum system requirements. The standard edition doesn't allow the use of the scale option, which we will need to add a scale to our models.

Figure 6.1: Agisoft Metashape Logo.

6.2   Initial tweaks

Agisoft Metashape can use graphic cards at certain steps of the model construction such as image matching and depth maps calculation. To enable the use of the graphic hardware (GPU):

- Select Preferences command from the *Tools* menu (v. <2.0) or *MetashapePro* menu (v. >2.0).

- In *Preferences* dialog select *GPU* tab.

- Select available GPU devices in *GPU* tab of the *Preferences* window.

This step has to be done only once.

This protocol has been elaborated using the version 1.7.1 of Agisoft Metashape. The latest version of Metashape is now version 2.0.3, but we still made the following changes. In order to obtain accurate thin structures, such as petal margin, and avoid holes in your mesh in Agisoft Metashape versions older than 2.0 (as far as we know) you will need to activate ONCE the *Visibility consistent mesh* function in *Tools > Preferences > Advanced >Tweaks*, then *Add* and fill in *Parameters* with *BuildModel/tvl1_mesh* and select

the value as *False* (figure 6.2). Additionally, to use the anterior version of the depth maps generation process, add ONCE the tweak: *BuildDepthMaps/pm_enable* and set the value to *False* (figure 6.3). For Agisoft Metashape 2.0.x (as far as we know) the *Preferences* are located in the *MetashapePro* menu.
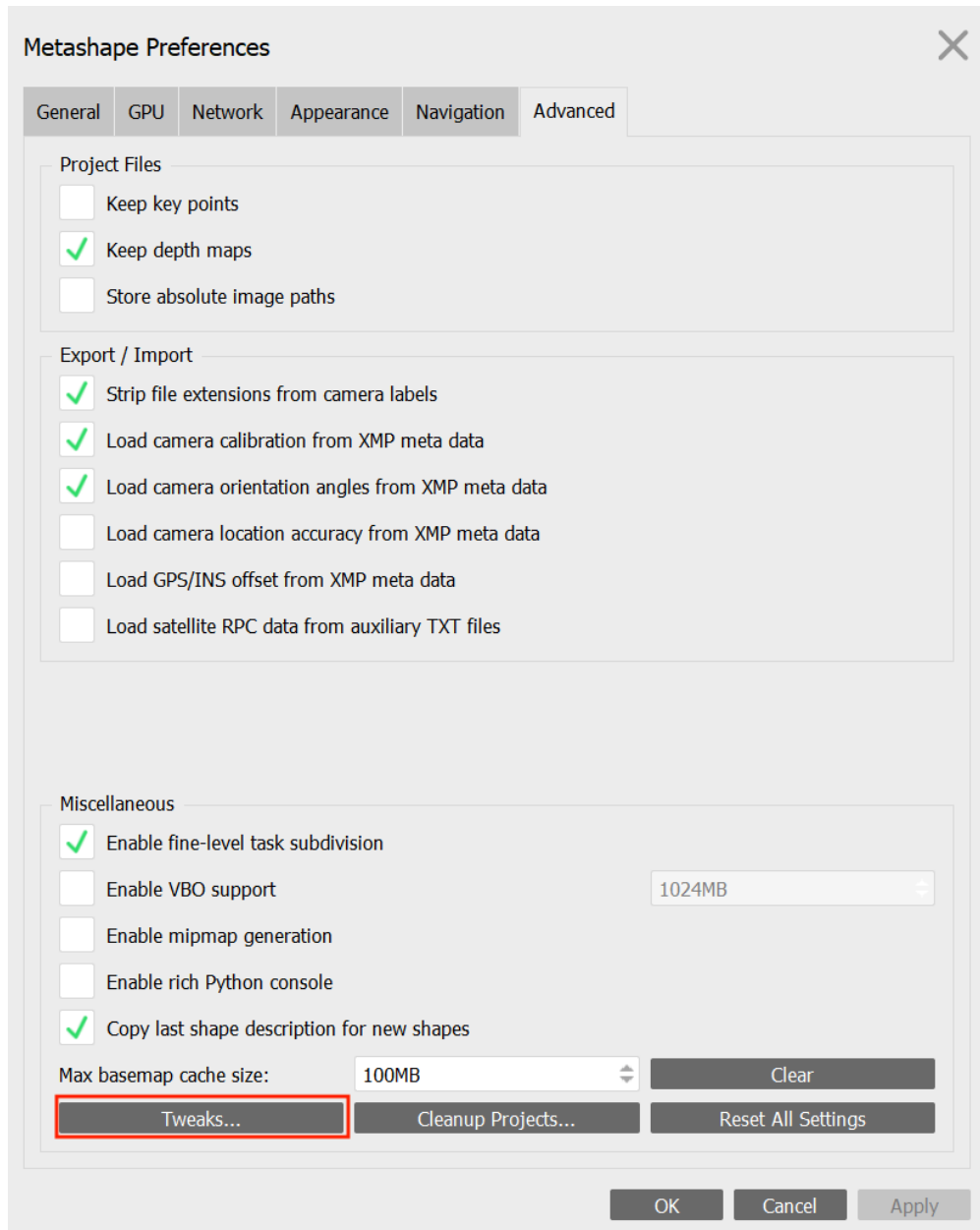
Figure 6.2: Tweaks settings (A).
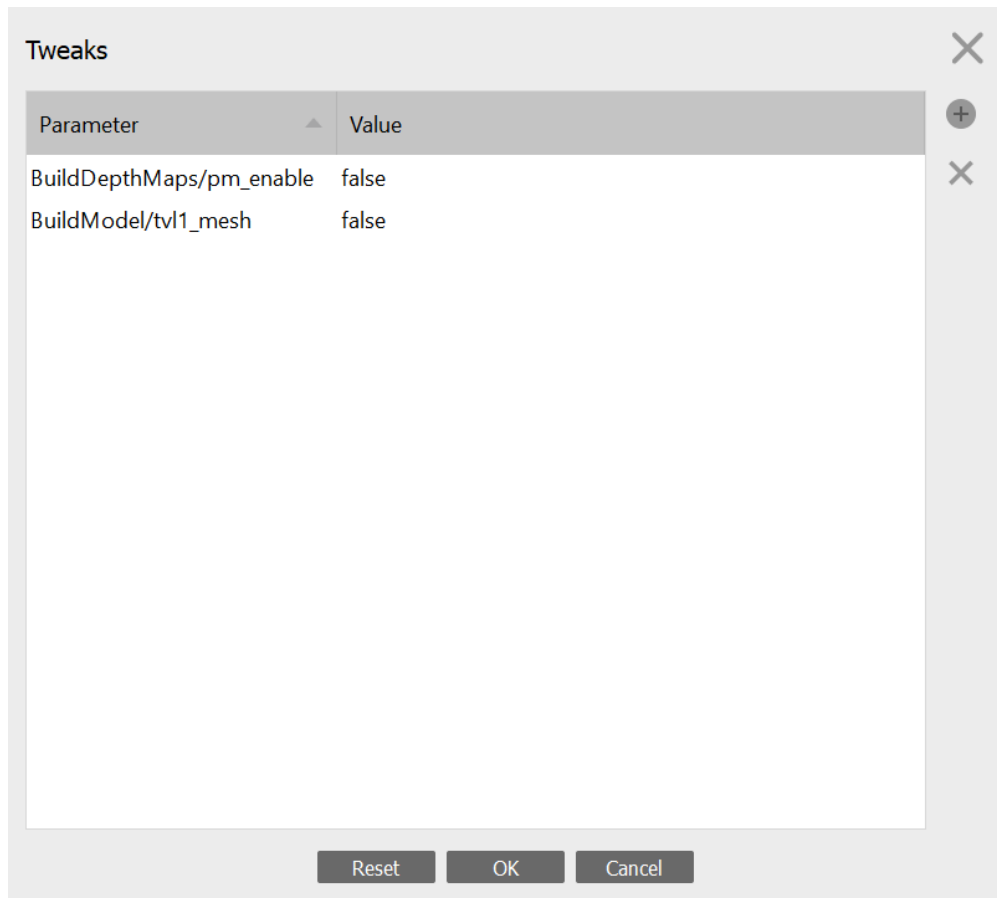
Figure 6.3: Tweaks settings (B).

6.3 Overview of the model building pipeline

To build a model, we need to do the following steps: (1) Import the calibrated photos, (2) Apply masks to remove the background of the photos, (3) Align the photos, (4) Calculate depth maps, (5) Build the 3D model (mesh), and (6) Reconstruct the final texture (model color). There could be different approaches for each of the steps and options will be given below.

One important thing to consider is whether to align all the photos simultaneously or proceed by groups of photos (i.e., "chunks") that correspond to each flower position. The first approach is quicker and normally results in more accurate models. However, it does not work all the time. We recommend to try the first approach and if it fails, to use the alternative approach, which is to divide the pictures in different "chunks" that will create partial 3D models that will be subsequently merged.

6.4 Photo importation

Go to *Workflow*, click on *Add Photos*, and click *Open*. Once the photos are imported, they are in a single "chunk".

To try to align all the photos simultaneously (ideal approach), you need to arrange them in "Image Groups" ot "Camera Groups" (e.g., select the photos, right click, *Move Images/Cameras > New Image/Camera Group*)*, where each camera group contains all pictures taken with the same flower orientation and camera angle. Once this is done, you can add the first photo of each set of photos representing the label, right click on this photo and select *Disable Cameras* or *Disable Images**. This allows you to not take it into account while reconstructing the model, but to keep all the information about the flower in your Metashape project.

*__Note__: Depending on the version of Agisoft Metashape, some functions use either the word "camera(s)" (v.<2.0) or "image(s)" (v.>2.0) as far as we know.

6.5 Mask application

Masks represent selected areas that are excluded from the feature detection procedure when applied to key points detection. When several keypoints are detected as the same point (matched as projections of the same 3D point on different photos), then it is considered as a tie point. If masks are applied to tie points, then if a key point is masked in at least one image, it will not be considered. You can thus use a single or just a few masks with the second method and apply masks to tie points. It is however possible to automatically apply masks on each photo to better constrain key point detection and then apply masks to keypoints. Using masks helps in removing points from being detected in the background during the image alignment procedure. You can see examples here on the Agisoft helpdesk portal.

Step-by-step mask application workflow

1. Duplicate one of your photos, and fill it in black (or the main color of your background) in any image manipulation software, and rename it to *background.jpg* or *background.tif* depending on the format of your photos. You can also take a picture of the lightbox without your flower just before starting to shoot and use this image as background. This sometimes work better.

2. Right click on a photo in one of your chunk in your Metashape project.

3. Click on *Masks*, *Import Masks* (Figure 6.4) and in the box that appears select the method *From Background* and operation *Replacement*.

4. Enter the same name as the name of the background image you created in step 1.

5. Depending on the flower and how contrasting its color is relatively to the background, the value for *Tolerance* can vary between approximately 40 and 60 (Figure 6.5). For some pale flowers you may need a lower tolerance value (e.g. 30 or lower).

6. Test different values of tolerance on a single photo first and when you have a value that is satisfactory (i.e., that creates a mask with the border of the flower well defined), you can select *Apply to > Entire workspace*.

7. Click *OK*.

8. This will automatically produce masks around the flowers for all the photos in all your chunks. This is why we need a contrasting background color behind the flower.

9. Check for masks that need touch ups (see next section).
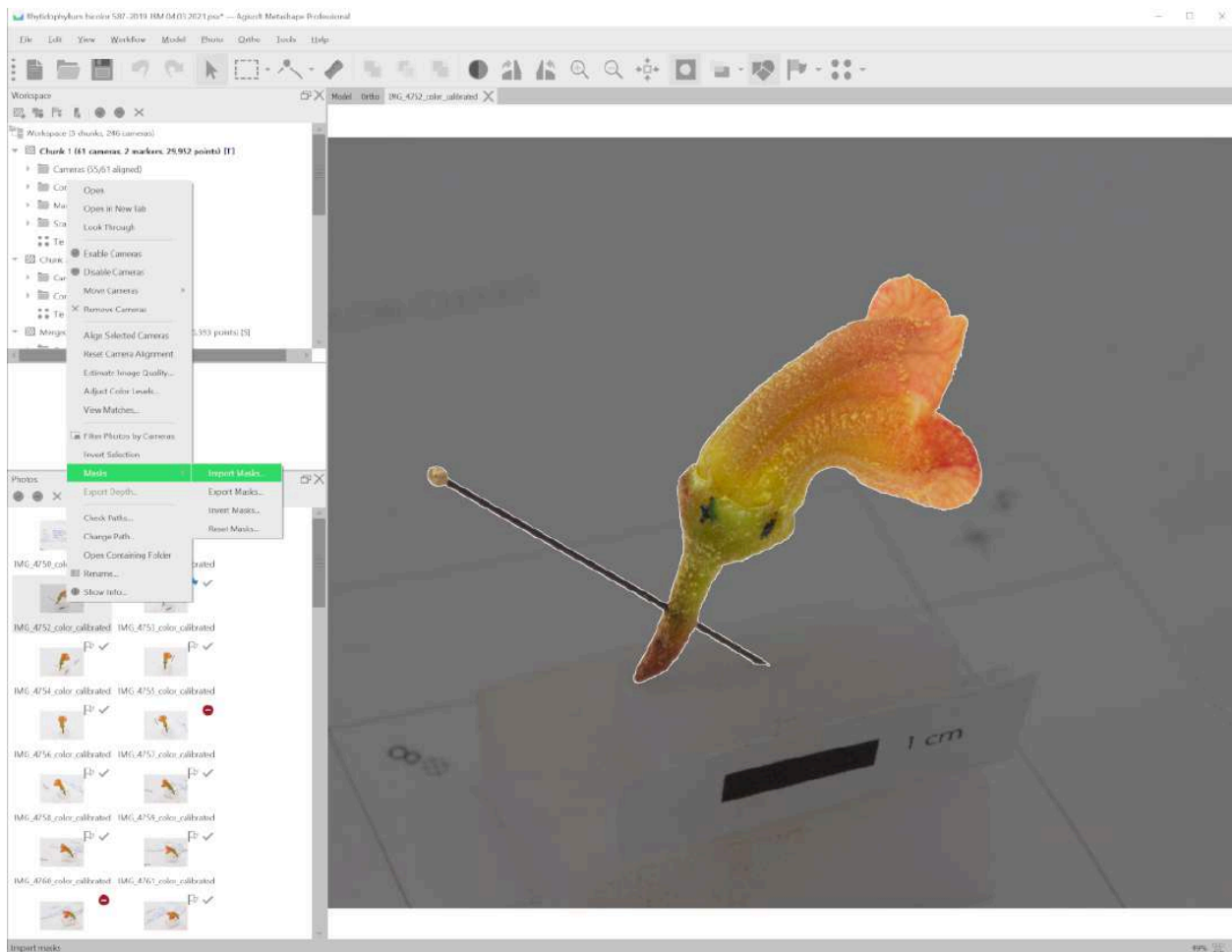
Figure 6.4: Right click on an image to select a mask to import.

235
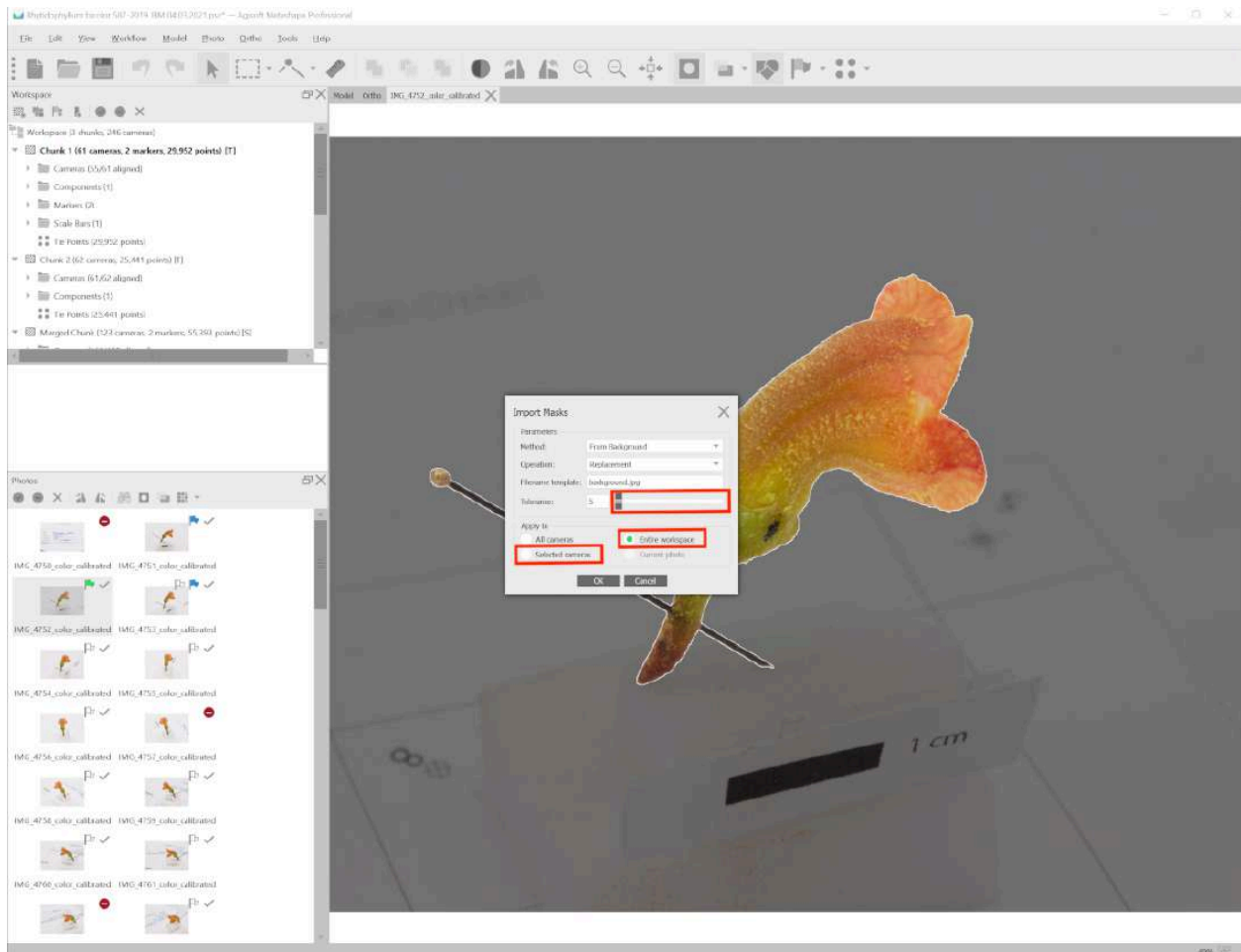
Figure 6.5: Import mask from a black image *background.jpg*, and select a tolerance value, to test on the selected camera (the image you right-clicked on). If the automatic mask is automatically well adjusted around the flower shape (darker gray around the flower), then apply to entire workspace (all the images).

Alternative masking method using Adobe Photoshop. It is also possible to use Adobe Photoshop to apply masks. We did not find particular improvements compared to the Agisoft Metashape approach.

1. Go to the file containing the pictures of chunk 1. Copy and paste this file, naming it accordingly (e.g. *Chunk1-Background*).

2. Go to Adobe Photoshop version 19.1 and up.

3. Make a copy of all of the photos you'll be using and place them in a new folder labeled *Chunk1-masks*.

4. Then, you will need to create ONCE a Photoshop action, that will be subsequently reused (see Figures 6.6 to 6.9 below) :
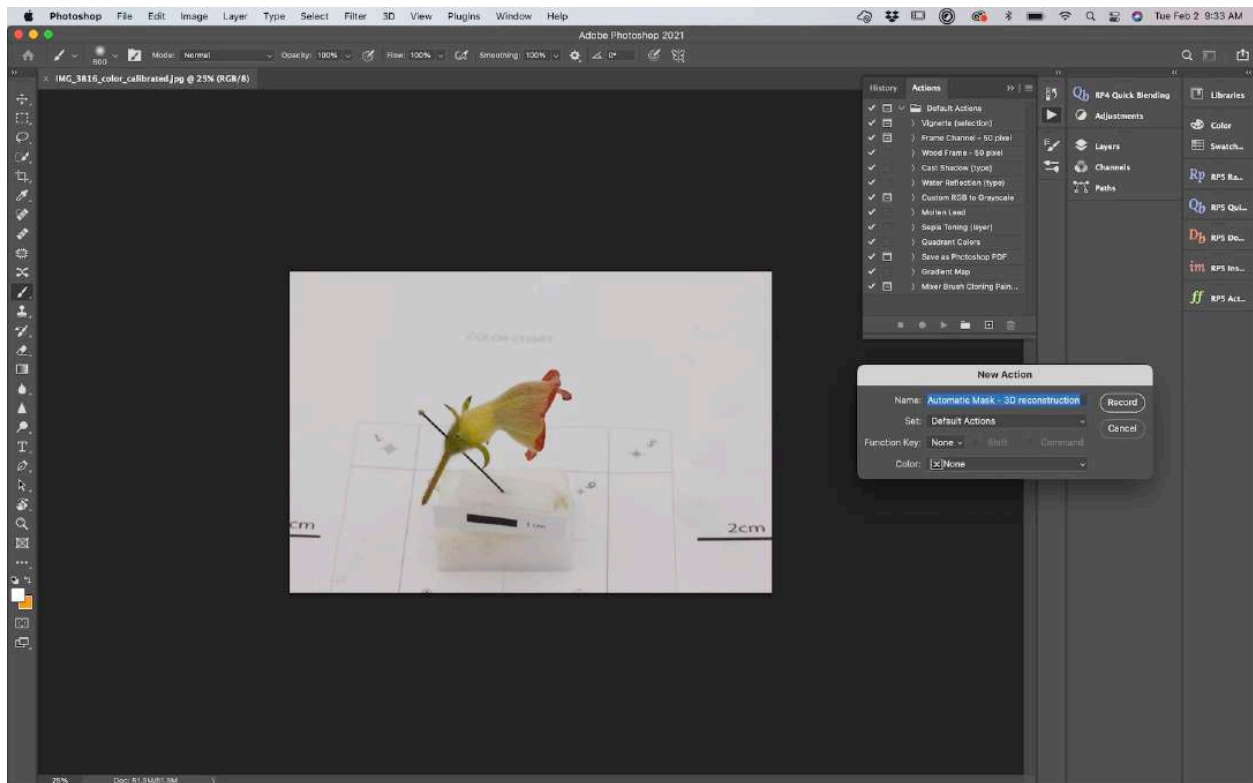
Figure 6.6: Record a new action called *Automatic Mask - 3D reconstruction*.
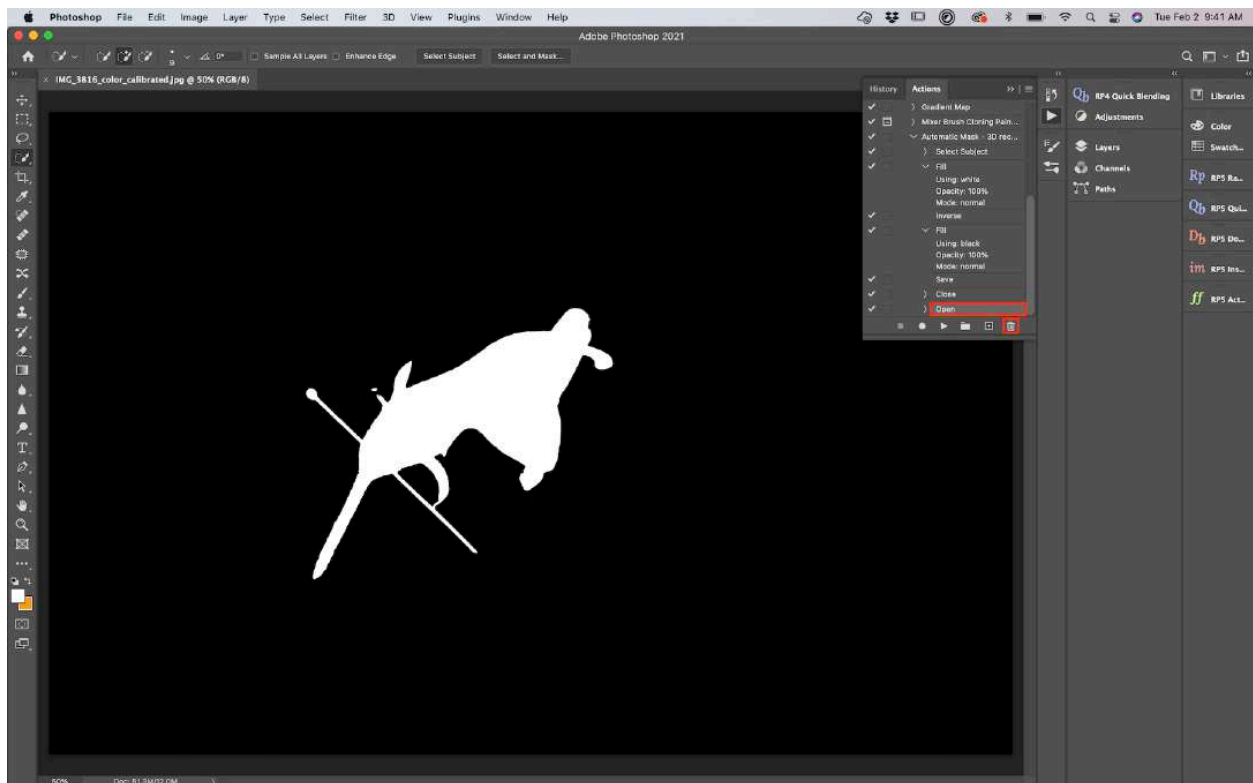
Figure 6.7: When you reopen your photo, don't forget to remove this extra task in your action.
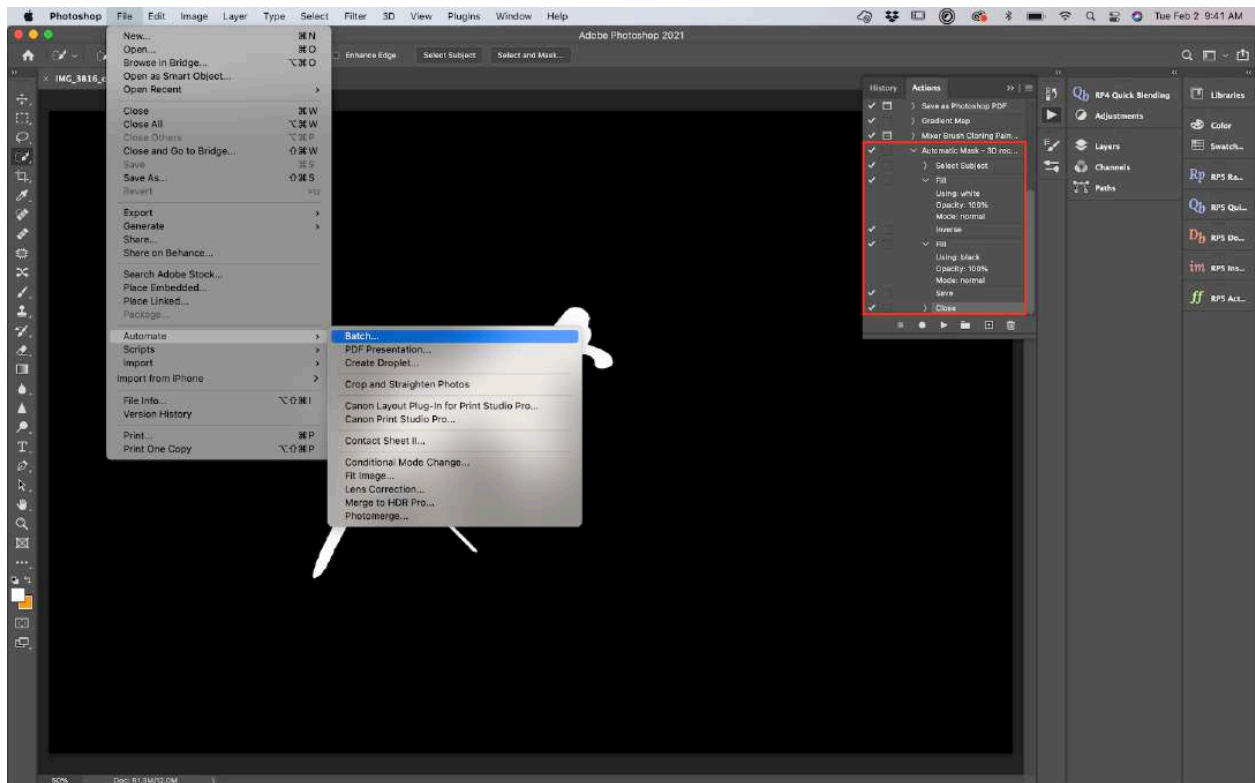
Figure 6.8: The action should include *Select Subject, Fill, Inverse, Fill, Save, Close*, and you can batch process this action to a specific folder of copied photos to create masks.
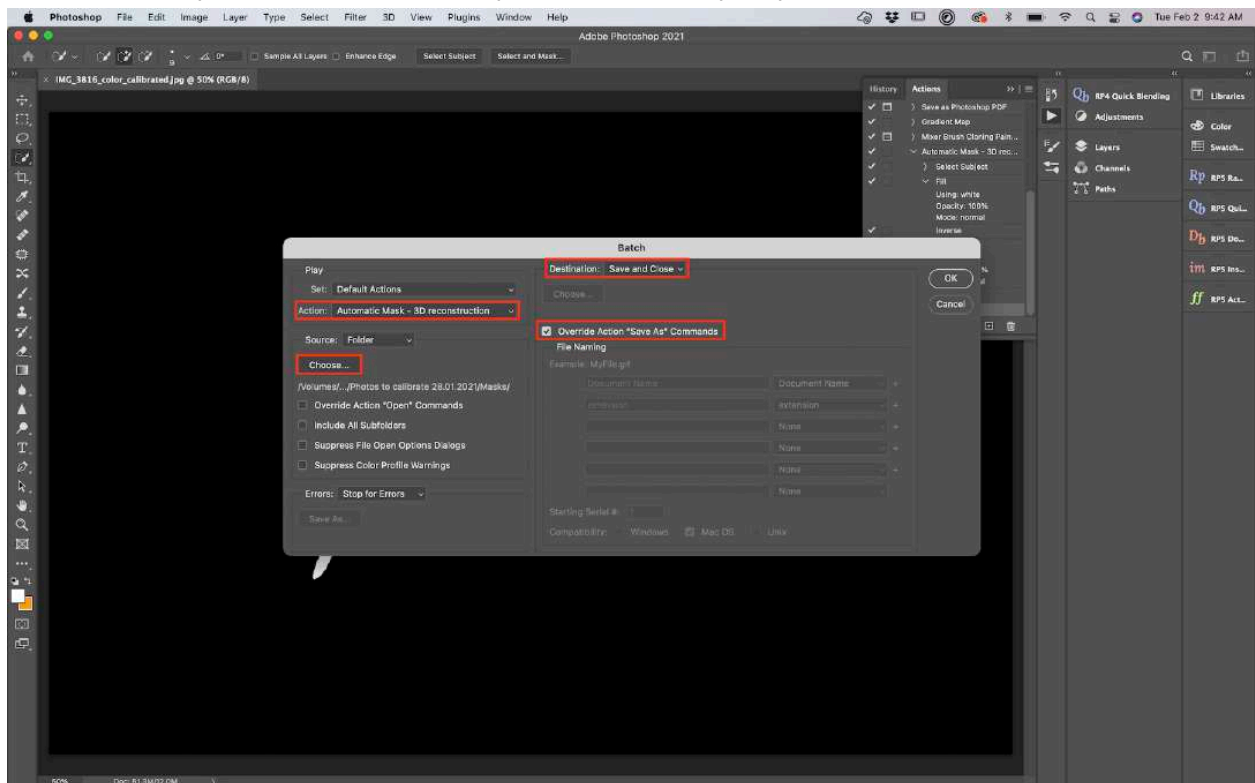
Figure 6.9: Apply the action to the folder of copied photos called *Chunk1-masks*.

5. Now you should have tranformed all your copied photos into masks, with the foreground object in white, and the background in black.

6. Go to Agisoft Metashape and right click on the first camera (photo) of chunk 1. Click on *Masks > Import Masks* and in the box that appears select method *From file*, operation *Replacement*. In *Filename Template* use *filename.jpg*. Select *Apply to all cameras* and then click *OK*.

7. Check the masks for touch ups.

6.6 Masks touch ups

The automatic application of masks at the previous steps is sometimes not entirely satisfactory for all photos. To add parts to the mask (i.e., remove them from the model) such as the foam block and the entomological pin, it is possible to select them using the selection tools and then add them using the respective *Add Selection* button (Figure 6.10). Similarly, you can remove or invert the selection with the buttons to the right of the *Add Selection* button.

Figure 6.10: Selection tools and add selection to mask tool.

6.7 Image alignment

1. Click on the chunk you want to align, which could comprise several image/camera groups.

2. Make sure to disable photos you don't want (e.g., the label photo, and blurry photos) and that the masks are clean.

3. Go to *Workflow > Align Photos* and put the accuracy on *High* or *Very high* (do not select the latter if you did focus stacking). To save some time, you can check *Generic preselection* in the section *Advanced*. Select *Apply masks* to *Key points* and click *OK*. Note that if you have applied the masks to only some photos, select *Apply masks* to *tie points*.

4. If you are aligning several chunks of photos, it is possible to run this job in batch for each chunk in *Workflow > Batch Process > Add* and select the *Job type* as *Align Photos* to apply to *All Chunks* or select specific ones (Figure 6.11).

Add Job   ✕

Job type: Align Photos   ▾
Apply to: All Chunks   ▾

✓ ▢ Chunk 1 (62 cameras)
✓ ▢ Chunk 2 (64 cameras)

Parameters:

Property	Value
▼ General	
Accuracy	High
Generic preselection	Yes
Reference preselection	Source
Reset current alignment	No
▼ Advanced	
Key point limit	40,000
Tie point limit	15,000
Apply masks to	Key points
Exclude stationary tie points	Yes
Guided image matching	No
Adaptive camera model fitting	No

OK   Cancel

Figure 6.11: Align photos in multiple chunks.

5. **Optional: Align using markers.** If the images cannot align properly, it is possible to place homologous markers on the flower, defined as remarkable points (e.g., distinguishable pattern such as color dots on the corolla), or little pen marks at the surface of the flower when homologous markers lack. These points need to be clearly identifiable on all chunks. You will need at least 5 markers, ideally located at different areas of the flower (e.g., near the pedicel, sepal tips, petals). Do not use points from the background to align chunks as they are independent from the flower (the flower changes position relative to the background).

   1. With the *Navigation* button selected (i.e., the "cursor" tool at the top), right click on the point you want to add a marker on.

   2. Click on *Place Marker > New Marker*.

   3. In the left panel, rename the marker accordingly. Make sure to use the same nomenclature on each chunk to be able to merge them according to their names.

6. To help the software recognize the markers, spread them on photos throughout the chunk (it is normally sufficient to manually place them on 2-3 photos and the software normally places them properly on the others, but make sure the markers are all properly placed).

7. If a marker is not visible in some photos, the flag of this marker should be white or the marker should be blocked on those specific photos. You can do that by right-clicking on the marker on these photos and select *Remove Projection* or *Block Marker*.

8. Repeat these step for each marker.

9. Go to *Workflow > Align Photos* and put the accuracy on *High* or *Very high* (the latter only for project without focus stacking). To save some time, you can check *Generic preselection* in the section *Advanced*. Select *Apply masks* to *Key points* and click *OK*. Note that if you have applied the masks to only some photos, select *Apply masks* to *Tie points*.

10. **Optional: Alignment optimization using gradual selection and camera positions.** If the camera alignment is not satisfactory, it is possible to clean the tie points obtained and try to re-align the cameras. For instance, in the tie points generated by the alignment, you can delete outlier and imprecise points (Figure 6.12 and 6.13):

    1. In the top menu, click on *Model* and then *Gradual Selection*. Select *Reconstruction uncertainty* on *Criterion* and play with the *Level* value to remove the uncertain points. The higher the value, the worst is the point placed. Values between 30 and 10 generally give good results. Then *OK*. Press *Delete* (or *fn + Backspace* in Mac) on your keyboard to delete the selected points in red. You don't need much more than 10,000 points for good photo alignments.

    2. After removing uncertain points, go to *View* and click on *Reference* to make the reference panel visible if it is not already.

    3. Click on the *Optimize Cameras* button (star icon) in the reference panel and in the *Optimize Camera Alignment* window, check all of the cameras in the *General* box and then click *OK* to optimize the camera posistions.

    4. In *Model > Gradual Selection*, ensure that *Reprojection error* parameter is below 1. If it is not, check if the alignment runs well by clicking on the *Show Cameras* button (camera icon) on the top (the cameras needs to form a full circle around the flower). If the alignment fails, try to re-align photos by following step 3 (don't forget to check the box *Reset Current Alignment*). If the alignment didn't fail, go to *Model > Gradual Selection > Reproduction error*, and set the level to 1 and click OK. Then press *Delete* (or *fn + Backspace* in Mac).

    5. Manually remove remaining outlier points using the selection tools.

11. Repeat these steps for each chunk.
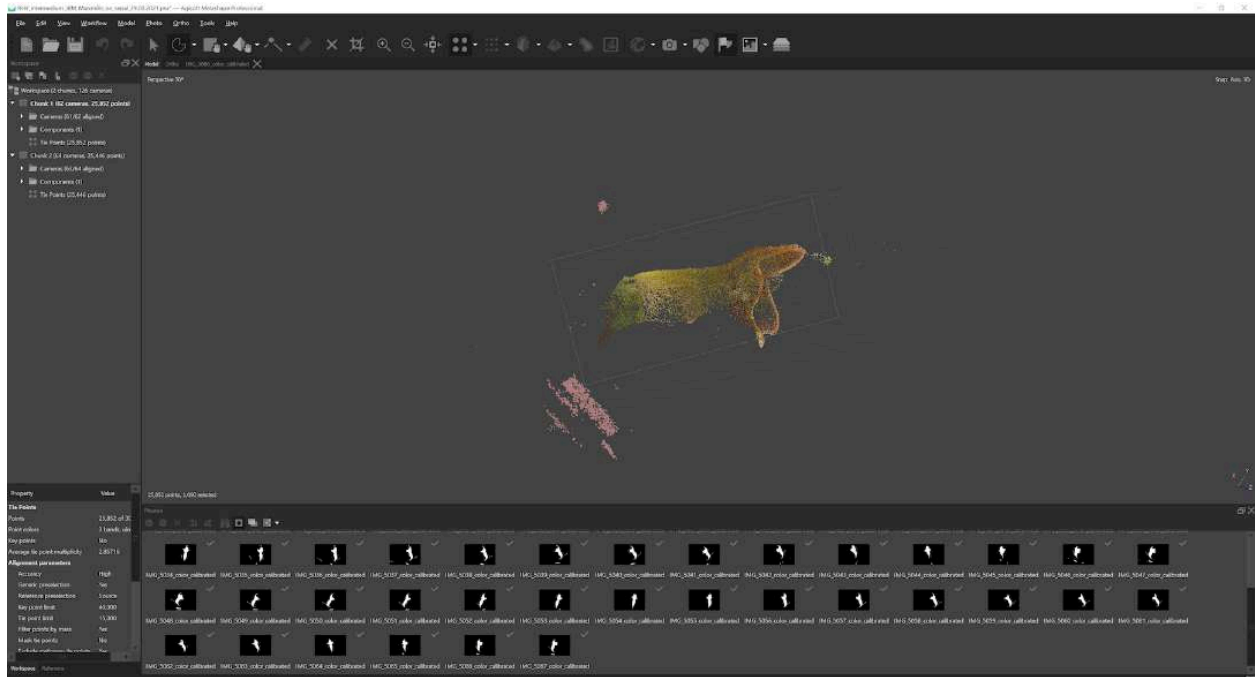
Figure 6.12: Use the selection tool to remove background points.
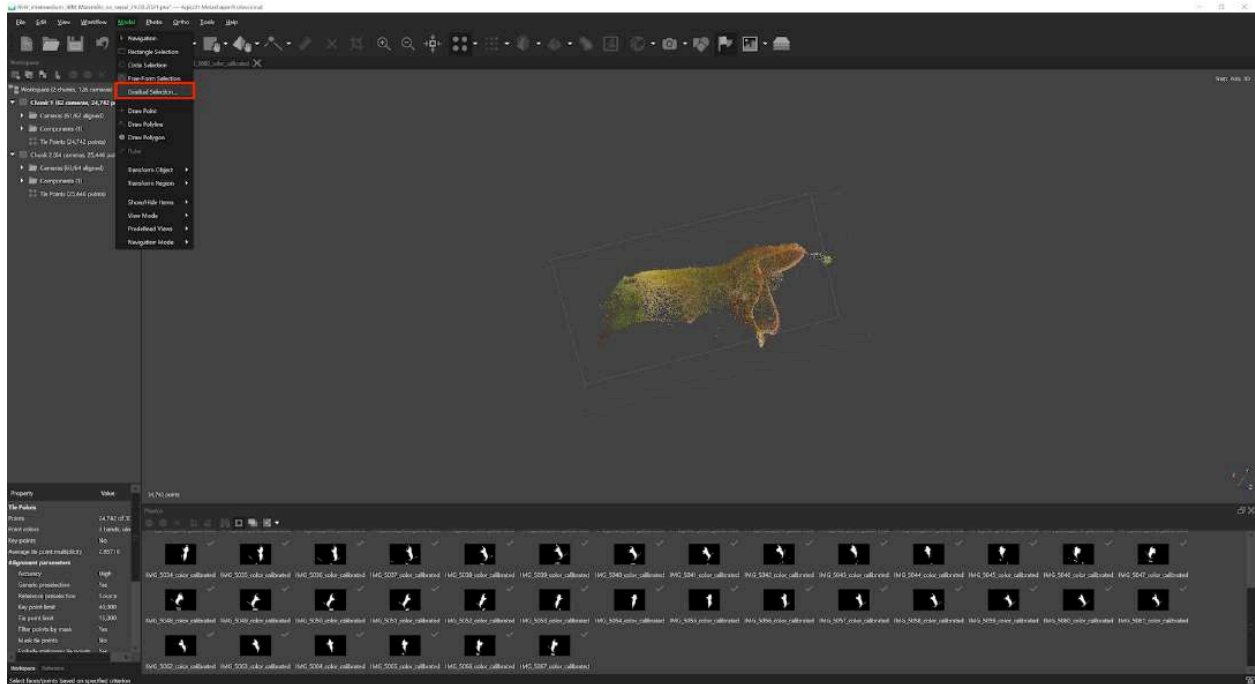
Figure 6.13: Use the gradual selection tool to remove additional mis-calculated points.

*Note: If the alignment fails using only one chunk and two or more camera groups, then it will be necessary to divide your job into several chunks. Each chunk should then contain photos from one flower position. Once the chunks are ready, you can proceed with the alignment following the previous steps.

6.8 Align chunks together

Note: This step is only necessary if your project is divided into several chunks.

At this step, it is important to align the different chunks with each other before they can be combined in a complete model. There are two ways to do this: using tie points (does not work every time) or using markers.

- To align using tie points:

1. Select one of the chunks that you would like to align.

2. Go to *Workflow > Align Chunks*, select all the chunks you want to align together and set the method as *Point based* (Figure 6.14).

3. Restrict the key points with masks.

4. Click on *OK*.

- To align using markers:

1. Place homologous markers on the flower, defined as remarkable points (e.g., distinguishable pattern such as color dots on the corolla), or little pen marks at the surface of the flower when homologous markers lack. These points need to be clearly identifiable on all chunks. You will need at least 5 markers, ideally located at different areas of the flower (e.g., near the pedicel, sepal tips, petals). Do not use points from the background to align chunks as they are independent from the flower (the flower changes position relative to the background).

    1. With the *Navigation* button selected (i.e., the cursor icon tool), right click on the point you want to add a marker on.

    2. Click on *Place Marker > New Marker*.

    3. In the left panel, rename the marker accordingly. Make sure to use the same nomenclature on each chunk to be able to merge them according to their names.

2. To help the software recognize the markers, spread them on photos throughout the chunk (it is normally sufficient to manually place them on 2-3 photos and the software normally places them properly on the others, but make sure the markers are all properly placed).

3. If a marker is not visible in some photos, the flag of this marker should be white or the marker should be blocked on those specific photos. You can do that by right-clicking on the marker on these photos and select *Remove Projection* or *Block Marker*.

4. Repeat these step for each marker and each chunk.

5. Select one chunk. Go to *Workflow* > *Align Chunks*, select the chunks you want to align, set the method as *Marker based* and then click *OK*.

When the chunks are aligned, a [T] is put at the end of your chunk name to notify that it is transformed. You can check the alignment using the icon to show aligned chunks (i.e., the icon of layers on top of each others, Figure 6.15). The different chunks should be well aligned over the whole flower. If the alignment of your chunks is unsatisfactory, try to place more markers on recognizable features and spread across the whole flower. Additionally, you can manually align chunks using the tools to move the models in the space, but this is highly not recommended.
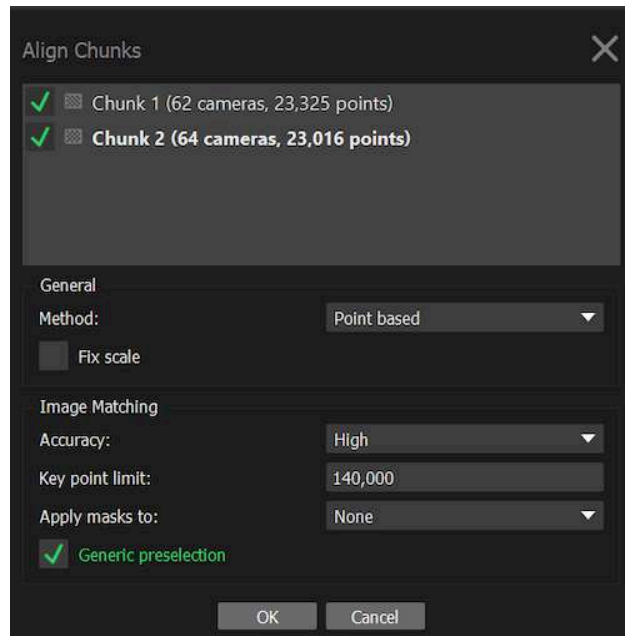
Figure 6.14: Align chunks.
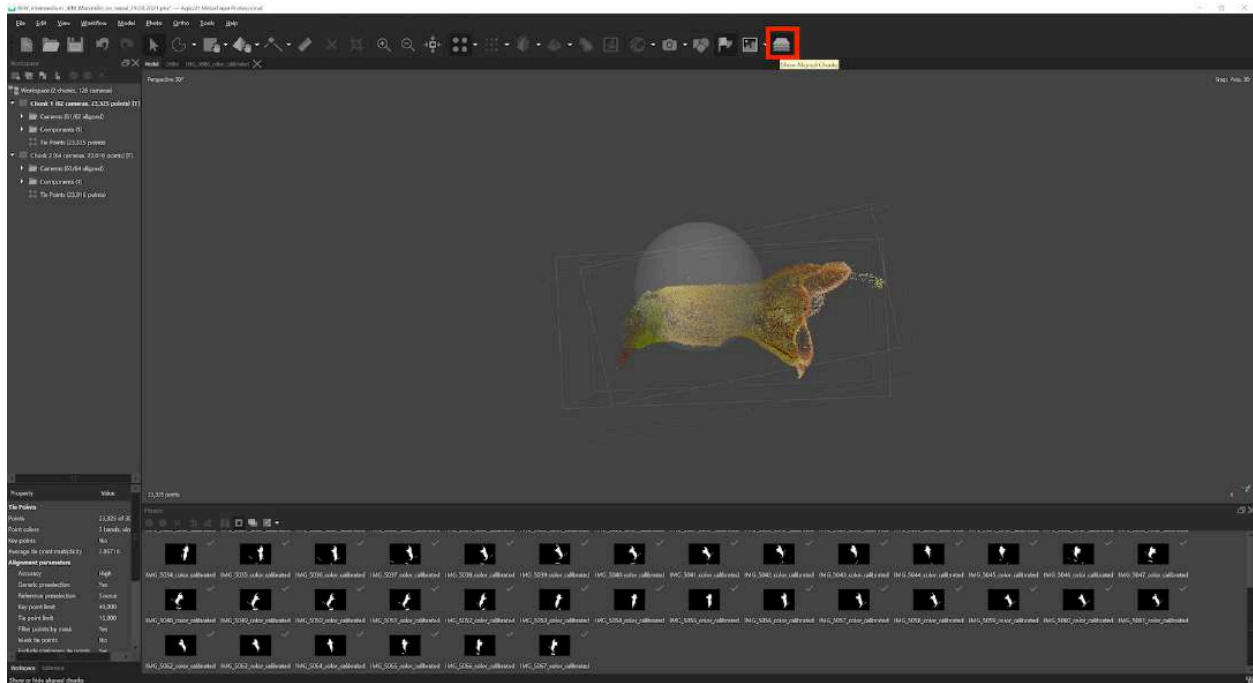
Figure 6.15: Show aligned chunks to verify their positions.

6.9 Merge chunks

Note: This step is only necessary if your project is divided into several chunks.

The next step is to merge chunks together when they are well aligned. Click on *Workflow > Merge chunks*, and merge using either the tie point method or the marker method depending on the option selected above.

6.10 Build 3D mesh

1. Select the chunk or the merged chunks for which you want to build a 3D mesh (model).

2. Go to *Workflow > Build Mesh*.

3. In the dialog box, make sure that *Source Data* is on *Depth maps*, *Quality* and *Face Count* on *High* (Figure 6.16). Note that although it is also possible to generate a mesh from a dense point cloud (which has to be built separately), the depth maps provide better results for objects with a high number of minor details.

4. Then go to *Advanced*, check *Calculate vertex colors* and click *OK*.

5. Once the mesh is produced, you should remove the pin and extra floating background parts using the selection tool. This will highlight the selection in red.

6. Verify your selection and press *Delete* (or *fn + Backspace*) to remove them.
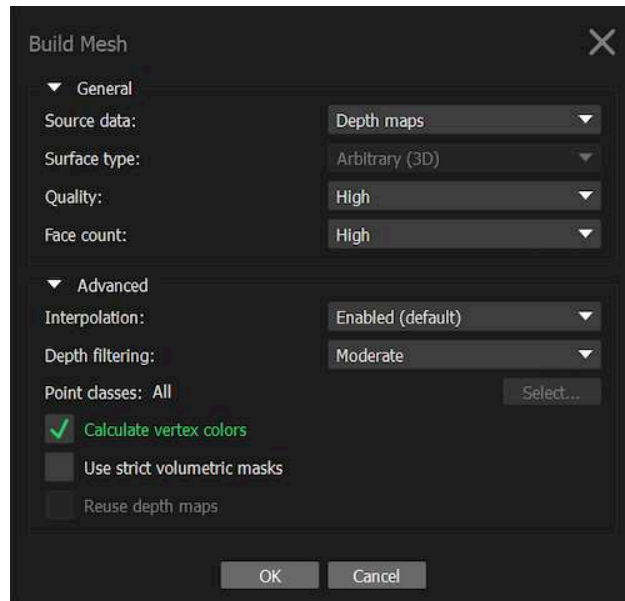
Figure 6.16: Build 3D mesh.

> Our protocol merges the chunks to build a tie point model of all chunks before constructing a model for the merge chunk. We found that this is the best approach, although it is also possible to build models for each chunk separately and then merge these models to obtain a full model.

6.11 3D mesh touch ups

1. You can smooth the mesh by clicking on *Tools*, *Mesh*, *Smooth Mesh*. You can also duplicate a 3D model to save one intact (right click on it and un-check *Use as default* to keep it as an archived model). If you smooth a mesh, you can't undo it.

2. You can fill holes in your mesh by clicking on *Tools > Mesh > Close Holes*. Note that if your holes are too big, the closing function can create unwanted structures. Similarly to smoothing, you cannot undo closing holes in the mesh. **HOWEVER**, this will remove the vertex colors in version 1.7.2, which we will need to place landmarks when doing the morphometrics.

6.12 Build texture

To build the texture go to *Workflow > Build Texture*, use the preset values and click *OK*.

6.13 Scaling

To scale the model, go to the pictures of your merged chunk and follow these steps:

1. On a picture displaying the scale bar, add new markers at each end of the scale bar and on a couple of additional photos.

2. In the left panel, select both markers, right click on them and select *Create Scale Bar*.

3. If the reference panel is not already visible on the left, go to *View* and click on *Reference*. Go to the reference panel, select the scale under *Scale Bars* and write 0.01 in the *Distance (m)* column (except if your scale bar has a different length, in which case, add the respective value of its length in meters).

4. Click on the *Update Transform* button in the reference panel (icon of two rotating arrows). This is an important step, because otherwise the scale will not be incorporated to your model.

5. To verify if the scale is taken into account, you can use the *Ruler* tool and select two points on your mesh to measure the distance between them.
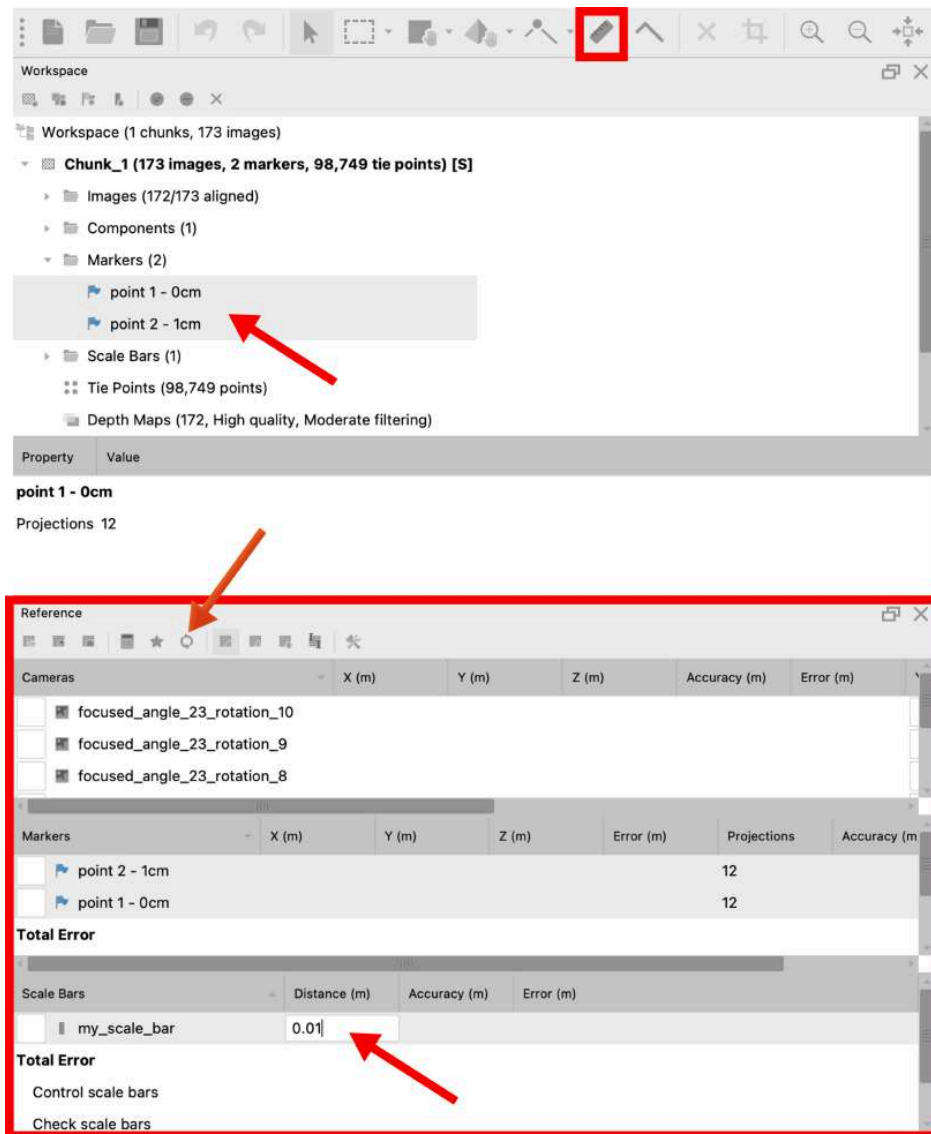
Figure 6.17: Scaling. Top arrow: Markers added at each end of the scale bar (i.e., at the 0 cm and 1 cm points). Middle Arrow: *Update Transform* button. Bottom arrow: Input of scale bar length in meters. Small red box (top): Ruler tool. Large red box (bottom): Reference panel.

6.14 Model orientation

1. In Metashape, be sure that *Show Info* and *Show Grid* in *Model > Show/Hide Items* are checked. You should see at the bottom right of the model panel the 3D axes.

2. Make sure that the scale is correct because changing it will affect the coordinates of the 3D model and you will need to re-orient it. You can verify the scale using the *Ruler* tool.

3. Use the *Navigation* tool to orient these 3D axes (x should be at 0° and y should be at 90°; Figure 6.18).

4. Once you orient the 3D axes in the wanted direction, you can then use the tool *Move Object* to put the flower in the center of the grid (the cross in the center point of the grid should be hidden in the central point of the 3D model; Figure 6.18 and Figure 6.19).

5. To orient the model, use the *Rotate Object*. The model should be facing the right side of the grid (the direction of the x axis; Figure 6.18 and Figure 6.19).

6. Orient the binding box as well, using the *Move Region*, *Resize Region* and *Rotate Region* tools. The side with the cross on the box should be on the ventral side of the flower, and the side with the two dashes should be facing the opening of the flower. Note that depending on the software you use to open the model, the first view orientation may change when you open the final object file (Figure 6.20).
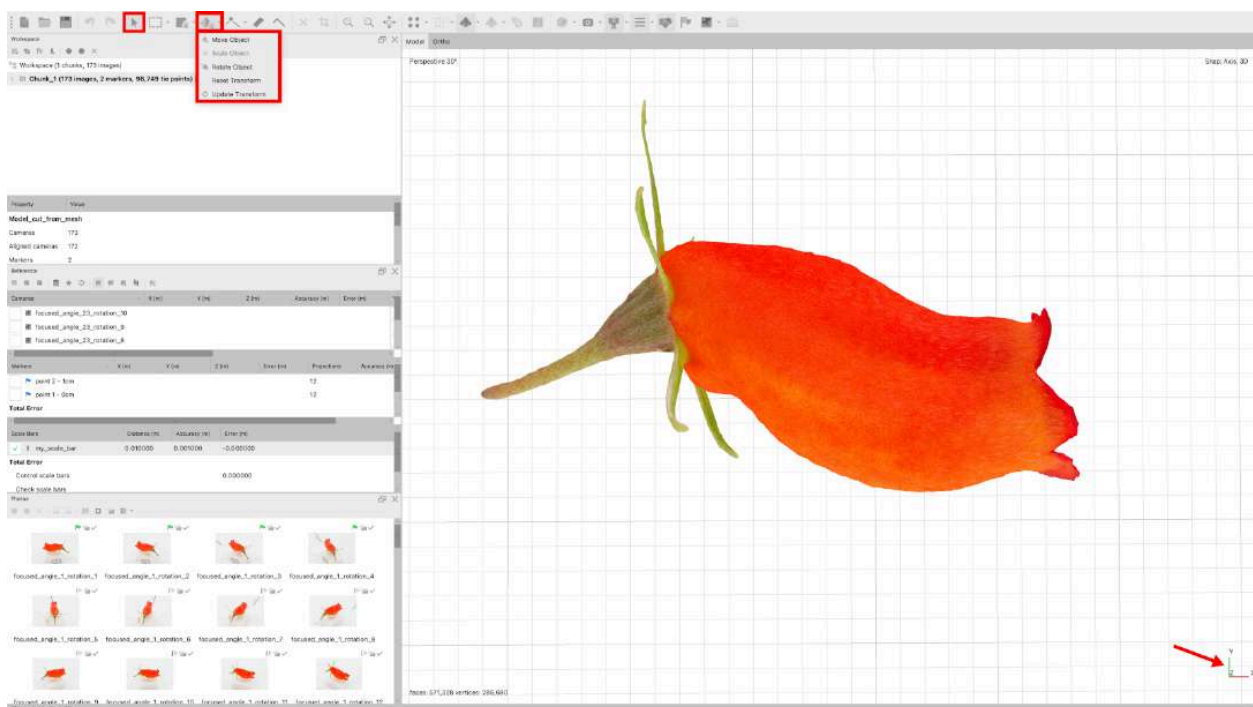
Figure 6.18: Object (model) orientation tools. Left box: *Navigation* tool. Left box group: Object orientation tools. Arrow: Desired 3D axes orientation.
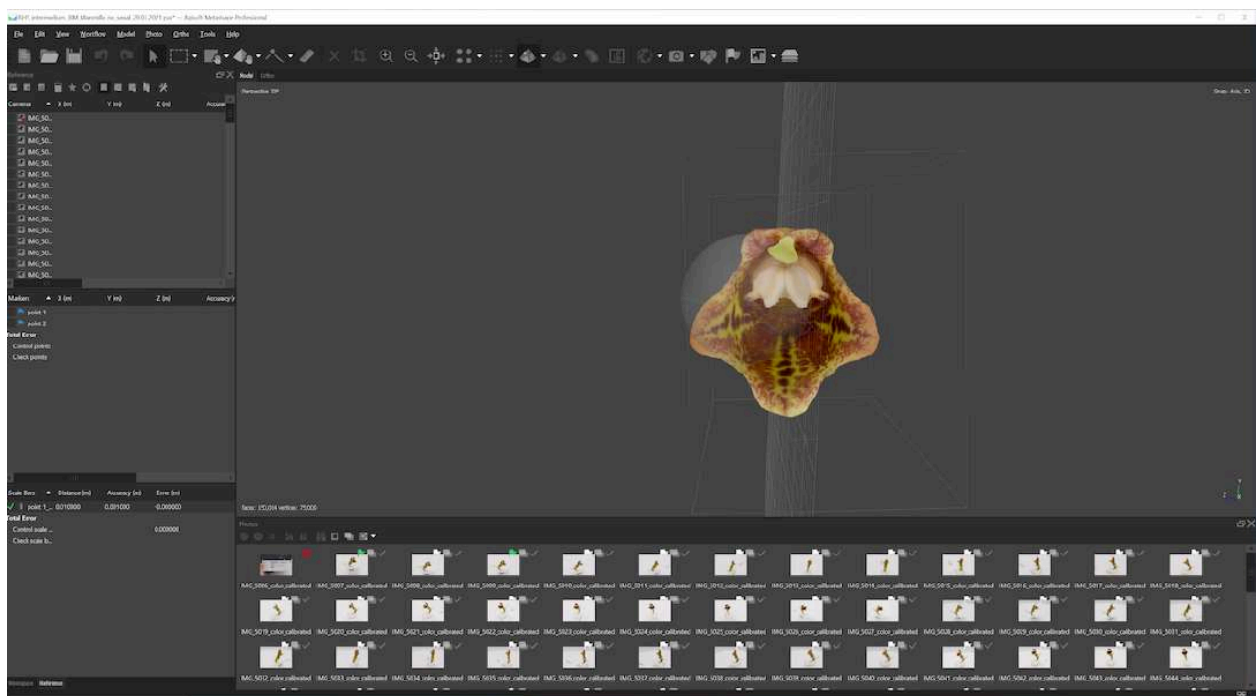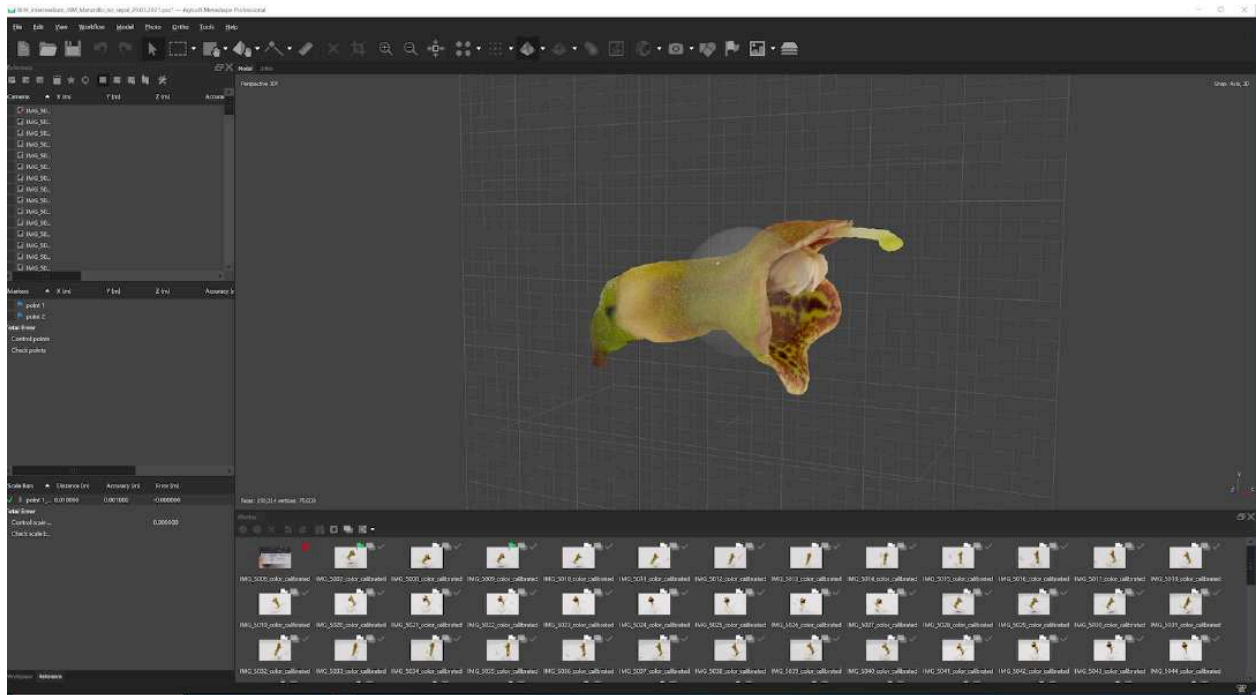
Figure 6.19: Desired model orientation on the grid.
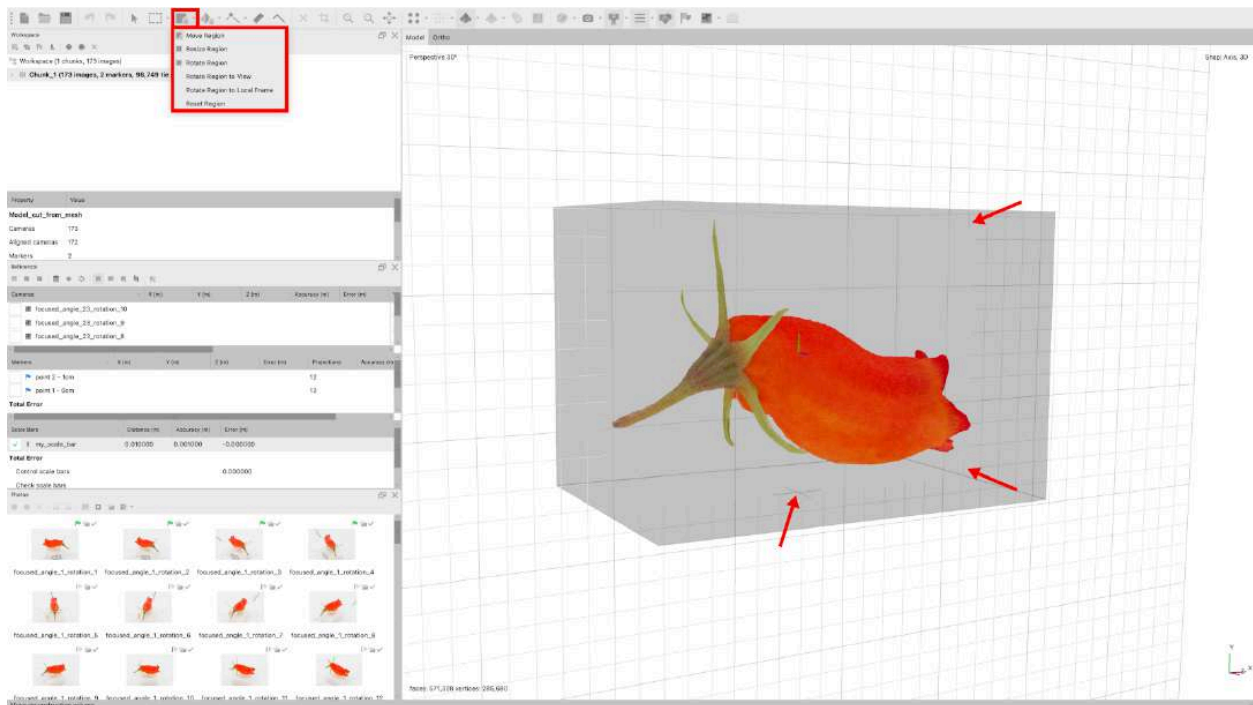
Figure 6.20: Binding box orientation tools. Box group: Binding box orientation tools. Arrows: The cross and the two dashes on two different sides of the binding box.

6.15 Export model and texture

1. You can export your 3D model by clicking on *File > Export > Export Model*.

2. Name your model.

3. Choose *.ply* as the extension.

4. In the dialog box, tick the *Vertex colors*. This option will allow you to get color on the actual 3D model.

5. Select *Export texture* as PNG.

6. Make sure to export the texture with transparency, by ticking the *Write alpha channel* or *Save alpha channel* option (depending on the Agisoft Metashape version). The texture is a separate file with detailed color information that is wrapped on the model.

7. Click on *OK*.

References

Adobe Systems Incorporated. 2012. "Digital Negative (DNG) Specification, Version 1.4.0.0." Adobe Systems Incorporated: San Jose, CA, USA, 2012.

Troscianko, Jolyon, and Martin Stevens. 2015. "Image Calibration and Analysis Toolbox–a Free Software Suite for Objectively Measuring Reflectance, Colour and Pattern." *Methods in Ecology and Evolution* 6 (11): 1320–31.

Annexe - Troisième chapitre

Supporting Information

Article title : Impact of pollination syndromes on diversification rates in a neotropical insular system.

Authors : Leménager, Marion ; Clark, John L. ; Martén-Rodríguez, Silvana ; Joly, Simon

Article acceptance date : in preparation.

The following Supporting Information is available for this article :

Tableau S12. Parameter settings for iPyrad assembly

Parameter name	Parameter setting
Assembly method	denovo
Reference sequence	none
Datatype	pairddrad
Restriction overhang	('TGCAGG', 'CGG')
max_low_qual_bases	5
Phred_Qscore_offset	33
mindepth_statistical	6
mindepth_majrule	6
maxdepth	100000
clust_threshold	0.9
max_barcode_mismatch	0
filter_adapters	2
filter_min_trim_len	35
max_alleles_consens	2
max_Ns_consens	0.05
max_Hs_consens	0.05
min_samples_locus	20
max_SNPs_locus	0.2
max_Indels_locus	5
max_shared_Hs_locus	0.25

Tableau S13. Assembly details of all the sequenced samples before manually removing samples. In pink samples were removed due to a lack of loci, and in green because of low sample coverage (below 10).

Sample name	Reads raw	Reads passed filter	Clusters total	Clusters hidepth	Heterozygotie estimation	Error estimation	Reads consensus
Bellonia_spinosa_10573	21976796	21966870	292539	103151	1.127e-02	1.087e-03	92705
Bellonia_spinosa_G8	3823002	3822469	22196	2536	1.374e-02	2.814e-03	2037
Gesneria_acaulis_11303	1470518	1469220	17577	3211	1.929e-02	3.065e-03	2649
Gesneria_acaulis_1149	5197114	5165605	290736	68480	1.552e-02	1.638e-03	60474
Gesneria_aspera_2014-011	4899462	4897165	71594	23055	5.821e-03	1.051e-03	21446
Gesneria_aspera_US-321092-3517	4018827	3976611	165575	124380	1.664e-02	5.641e-04	116620
Gesneria_barahoensis_US-818245-1239	32839419	32577728	883880	611984	2.148e-02	8.676e-04	558097
Gesneria_barahoensis_US-818248-1242	99352425	98668857	1153849	552115	2.562e-02	9.752e-04	499562
Gesneria_bicolor_2014-002	82272900	82237587	837720	187539	1.159e-02	1.282e-03	162648
Gesneria_bicolor_32	1914944	1912698	54155	19830	5.034e-03	1.109e-03	18615
Gesneria_binghamii_US-1920725-1591	808736	803727	27405	20104	8.391e-03	3.305e-04	19426
Gesneria_bracteosa_10567	9148110	9144383	83861	18419	1.140e-02	1.253e-03	16059
Gesneria_bracteosa_NY-1164186	6237	6209	440	316	1.254e-03	1.806e-04	314
Gesneria_bracteosa_US-1302686-27544	14	14	9	0	NaN	NaN	0
Gesneria_calycosa_1190	1183456	1183025	11833	2267	8.528e-03	1.200e-03	2002
Gesneria_calycosa_US-8177181190-1190	22914668	22690927	389134	231264	2.193e-02	7.987e-04	212381
Gesneria_celsioides_11981	1187504	1181832	54247	12619	2.316e-02	1.890e-03	10753
Gesneria_christii_10025	776487	776242	12353	4335	5.441e-03	1.024e-03	4113
Gesneria_christii_G6-1	17179879	17176427	110841	7418	1.525e-02	3.412e-03	5179
Gesneria_christii_G6-2	4889050	4887913	31806	1803	2.325e-02	4.444e-03	1116
Gesneria_christii_NY-1401471	6776718	6689538	204321	145948	1.814e-02	6.644e-04	136842
Gesneria_citrina_10020	442885	442479	14965	4430	4.276e-03	9.865e-04	4208
Gesneria_citrina_NY-1113731	966	965	57	41	2.421e-04	1.982e-04	41
Gesneria_citrina_NY-1113838	46910	46626	2435	1902	3.443e-03	1.829e-04	1874
Gesneria_clandestina_US-817725-1197	11508921	11326250	315080	210642	2.430e-02	1.091e-03	189558
Gesneria_clarensis_10488	10039344	10031499	115994	9884	1.784e-02	6.026e-03	6838
Gesneria_clarensis_US-580537-60066	2786242	2739183	67268	44694	1.650e-02	8.071e-04	41827
Gesneria_cornuta_1110	15319772	15312481	209771	60018	9.584e-03	1.128e-03	53173
Gesneria_cornuta_1116	20670515	20637339	424372	104442	1.926e-02	1.742e-03	89907
Gesneria_cubensis_2014-008	1651273	1650431	39433	17046	4.073e-03	9.626e-04	16350
Gesneria_cuneifolia_JBM-976-2017-o	30957467	30910358	469082	76161	2.281e-02	3.317e-03	58643
Gesneria_cuneifolia_JBM-976-2017-r	25783025	25746596	375479	52498	2.842e-02	4.139e-03	40285
Gesneria_cuneifolia_NY-2330288	82	82	11	3	9.331e-04	5.908e-05	3

Sample name	Reads raw	Reads passed filter	Clusters total	Clusters hidepth	Heterozygotie estimation	Error estimation	Reads consensus
Gesneria_cuneifolia_US-3473341-5161	24142505	23990620	597307	418674	1.862e-02	7.027e-04	385660
Gesneria_decapleura_NY-1401504	4358854	4294721	187608	140525	1.974e-02	7.164e-04	130417
Gesneria_decapleura_US-818246-1240	6775700	6719162	189283	134004	1.886e-02	8.529e-04	123480
Gesneria_depressa_13070	7118031	7114610	72330	20127	9.815e-03	1.141e-03	18342
Gesneria_duchartreoides_14576	1417980	1416078	39678	12114	1.573e-02	1.845e-03	10787
Gesneria_duchartreoides_15477	4286931	4283028	55173	13415	1.453e-02	2.703e-03	11510
Gesneria_ekmanii_1118	20479011	20469614	227978	80931	9.215e-03	8.863e-04	73564
Gesneria_ekmanii_2014-018	20547520	20531721	395748	129244	5.876e-03	1.095e-03	119161
Gesneria_ekmanii_2014-024	45034208	44997621	556667	141046	1.208e-02	9.625e-04	123859
Gesneria_exserta_1150	2212831	2205589	93387	25351	1.259e-02	1.589e-03	22797
Gesneria_ferruginea_US-1920722-92	1748849	1745968	19368	14427	4.001e-03	4.711e-04	14148
Gesneria_flava_1119	11747863	11745167	103567	16594	1.254e-02	1.650e-03	14071
Gesneria_flava_1127	22503010	22494861	262317	81625	9.852e-03	1.045e-03	72648
Gesneria_flava_2014-007	23956415	23935677	522004	190489	5.901e-03	1.052e-03	177405
Gesneria_fruticosa_1227	13993979	13989179	119694	20745	1.220e-02	1.554e-03	18101
Gesneria_fruticosa_2014-012	21305490	21297685	331907	128410	7.365e-03	1.151e-03	118816
Gesneria_fruticosa_NY-2647385	90561957	89591076	1215280	587981	2.787e-02	1.271e-03	521033
Gesneria_fruticosa_NY-2647410	32279601	31988224	537490	301664	2.403e-02	8.333e-04	266718
Gesneria_glandulosa_12772	1401348	1399504	19114	3880	1.996e-02	3.139e-03	3184
Gesneria_glandulosa_14572	1093024	1091412	28696	9713	8.569e-03	1.251e-03	9010
Gesneria_haitiensis_14352	616626	616435	10365	4635	4.676e-03	8.867e-04	4417
Gesneria_heterochroa_14592	5613473	5609196	38685	5050	1.586e-02	4.075e-03	3598
Gesneria_humilis_10040	25176175	25163844	337004	131214	9.678e-03	9.249e-04	120646
Gesneria_humilis_10626	20571424	20527126	430701	85840	2.493e-02	2.607e-03	69882
Gesneria_hybocarpa_NY-1401596	18622	18445	1047	823	2.055e-03	1.982e-04	816
Gesneria_hybocarpa_US-321289-34875	364	360	25	18	8.178e-04	1.417e-04	18
Gesneria_hypoclada_NY-1401607	30511	30079	2294	1699	2.084e-03	1.538e-04	1681
Gesneria_hypoclada_NY-1401610	13032935	12912036	301089	203407	2.311e-02	9.214e-04	181637
Gesneria_hypoclada_US-321291-3500	469100	465073	15545	11725	8.814e-03	3.182e-04	10940
Gesneria_jamaicencis_US-817721-1193	83760239	83123229	1215707	632159	2.538e-02	9.335e-04	563438
Gesneria_jamaicensis_1193	8546627	8542759	115202	46828	8.281e-03	9.676e-04	43439
Gesneria_lanceolata_14524	10444779	10431537	184187	47247	1.720e-02	1.568e-03	41125
Gesneria_libanensis_10575	530577	528833	23236	6293	1.217e-02	1.332e-03	5678
Gesneria_odontophylla_14360	4714293	4712767	50577	12612	9.988e-03	1.079e-03	11143

Sample name	Reads raw	Reads passed filter	Clusters total	Clusters hidepth	Heterozygotie estimation	Error estimation	Reads consensus
Gesneria_onacaensis_US-993085-93258	13534255	13353110	275374	171218	1.996e-02	6.647e-04	157679
Gesneria_onychocalyx_1195	449316	448917	11078	3773	3.924e-03	9.081e-04	3589
Gesneria_onychocalyx_US-817723-1195	19632723	19480554	471777	314743	2.173e-02	8.631e-04	280426
Gesneria_onychocalyx_US-817724-1196	53097228	52716330	924074	554231	2.494e-02	1.078e-03	490225
Gesneria_pachyclada_US-1920774-2393	10558	10540	643	490	8.178e-04	1.417e-04	488
Gesneria_pedicellaris_10635	10375131	10354936	233515	47645	2.723e-02	2.245e-03	38703
Gesneria_pedicellaris_13117	351239	350612	4161	497	2.298e-02	2.419e-03	324
Gesneria_pedunculosa_10644	7678982	7671943	83958	11757	1.910e-02	4.791e-03	8983
Gesneria_pulverulenta_NY-1401665	510703	509378	18555	14430	7.144e-03	2.793e-04	13986
Gesneria_pulverulenta_US-3498527-1237	364	364	20	13	1.280e-04	1.111e-04	13
Gesneria_pumila_US-817722-1194	5685753	5645122	179170	131491	1.349e-02	5.017e-04	125249
Gesneria_purpurascens_10564	12751	12727	609	242	5.199e-03	1.443e-03	227
Gesneria_quisqueyana_ADN-1298	4113447	4111237	39468	8245	7.483e-03	1.371e-03	7175
Gesneria_quisqueyana_ADN-1299	10720734	10719274	48664	2604	2.125e-02	5.120e-03	1610
Gesneria_quisqueyana_JBM-891-2015	200886	200408	5232	962	1.510e-02	2.635e-03	670
Gesneria_reticulata_10558	15175072	15143500	397167	86976	2.570e-02	2.356e-03	71159
Gesneria_reticulata_15967	10953610	10934480	318059	85925	1.922e-02	1.827e-03	74808
Gesneria_salicifolia_10566	4993410	4991763	34034	7285	9.766e-03	1.817e-03	6388
Gesneria_salicifolia_10627	4455520	4453690	28640	1793	1.666e-02	4.149e-03	1047
Gesneria_scabra_NY-1401717	2909086	2867005	99032	69886	2.059e-02	8.424e-04	64377
Gesneria_scabra_NY-1401719	8803912	8729896	207839	130683	2.293e-02	8.776e-04	116425
Gesneria_sintenisii_1252	32717	32577	1961	518	7.100e-03	1.138e-03	483
Gesneria_sintenisii_13757	17613926	17605651	272251	120898	7.417e-03	9.151e-04	112629
Gesneria_sylvicola_1241	131066	130971	3333	1563	2.524e-03	7.283e-04	1521
Gesneria_sylvicola_2014-027	20035349	20024288	313475	100557	8.105e-03	1.099e-03	92065
Gesneria_sylvicola_447	6902116	6898830	110111	49244	8.697e-03	8.391e-04	45271
Gesneria_ventricosa_6545	5414047	5407292	125126	29898	1.816e-02	2.256e-03	25685
Gesneria_ventricosa_G4	12036146	12033938	77745	7250	2.325e-02	2.242e-03	5143
Gesneria_ventricosa_NY-866187	45598898	45259279	903334	581104	2.011e-02	8.212e-04	526696
Gesneria_ventricosa_NY-933655	10828875	10734426	204245	125125	2.229e-02	1.043e-03	112302
Gesneria_viridiflora_10041	4946207	4943472	89169	36187	7.770e-03	1.008e-03	33690
Gesneria_viridiflora_10561	13592098	13589555	82665	10750	1.177e-02	2.201e-03	9078
Gesneria_viridiflora_14467	171165	171138	3250	1477	3.542e-03	8.856e-04	1421
Henckelia_malayana_G11	894929	894230	10192	1241	9.394e-03	1.823e-03	898

Sample name	Reads raw	Reads passed filter	Clusters total	Clusters hidepth	Heterozygotie estimation	Error estimation	Reads consensus
Kohleria_trinidad_1102	646354	646202	6390	1002	1.866e-02	1.087e-03	727
Pheidonocarpa_corymbosa_15972	329007	328342	4761	493	1.439e-02	3.046e-03	333
Rhytidophyllum_acunae_15980	11445967	11433349	212484	48090	1.722e-02	1.769e-03	40926
Rhytidophyllum_acunae_NY-4243374	2317222	2308307	46855	32886	1.557e-02	4.011e-04	30839
Rhytidophyllum_asperum_NY-1401842	29408	29051	2100	1570	2.273e-03	4.766e-04	1548
Rhytidophyllum_asperum_US-1010645-12895	388	388	37	13	9.998e-04	8.423e-05	13
Rhytidophyllum_asperum_US-818241-1235	84	84	7	3	2.275e-04	9.570e-05	3
Rhytidophyllum_auriculatum_1112	3448398	3447414	31251	9758	8.549e-03	8.129e-04	8918
Rhytidophyllum_auriculatum_2014-025	8154004	8149388	101514	29672	7.710e-03	1.281e-03	27132
Rhytidophyllum_berteroanum_NY-1401930	61	61	14	2	9.331e-04	5.908e-05	2
Rhytidophyllum_berteroanum_NY-1401934	185951	184645	5796	4364	6.430e-03	2.451e-04	4133
Rhytidophyllum_bullatum_2014-016	46591353	46559267	548029	167324	7.661e-03	1.084e-03	152977
Rhytidophyllum_caribaeum_US-1864428-SC2477	1027183	1022019	29293	22118	9.380e-03	4.151e-04	21480
Rhytidophyllum_caribaeum_US-1864474-SC2525	16728919	16624863	245307	144415	2.356e-02	1.023e-03	127834
Rhytidophyllum_crenulatum_10042	6886911	6880154	115212	32457	1.636e-02	1.810e-03	28715
Rhytidophyllum_crenulatum_9531	1579749	1578401	18886	2882	2.094e-02	5.087e-03	2229
Rhytidophyllum_daisyanum_NY-1477540	3620875	3601189	109744	76898	1.791e-02	6.475e-04	70858
Rhytidophyllum_daisyanum_NY-1477541	1332997	1328238	43134	31245	1.779e-02	6.501e-04	28879
Rhytidophyllum_exsertum_10585	1193156	1192950	11126	2295	8.991e-03	1.604e-03	2023
Rhytidophyllum_exsertum_JBM-1073-2010	12731156	12722311	93869	4991	2.245e-02	1.141e-02	2378
Rhytidophyllum_exsertum_JBM-112-1991	6709833	6705089	60481	5894	2.570e-02	6.853e-03	3892
Rhytidophyllum_exsertum_JBM-392-2014	11575235	11566826	81772	5449	1.935e-02	7.661e-03	3186
Rhytidophyllum_grande_grande_US-598261-9651	800919	795042	24296	16822	1.505e-02	9.769e-04	15381
Rhytidophyllum_grande_laevigatum_US-600418-9551	86138	85816	3895	3169	2.179e-03	2.549e-04	3132
Rhytidophyllum_grandiflorum_NY-1402053	36	36	8	2	1.562e-05	5.914e-04	2
Rhytidophyllum_grandiflorum_NY-2422480	4667411	4641750	102895	71469	2.154e-02	8.410e-04	64038
Rhytidophyllum_grandiflorum_nuecense_NY-2422481	1673548	1667907	42381	30751	1.395e-02	6.151e-04	29245
Rhytidophyllum_intermedium_10549	11226081	11223365	105147	5881	1.900e-02	4.490e-03	3804
Rhytidophyllum_lanatum_NY-1402066	13	13	3	1	1.855e-05	7.594e-04	1
Rhytidophyllum_lanatum_NY-2687390	870295	869279	7233	4747	7.959e-03	4.479e-04	4571
Rhytidophyllum_leucomallon_14338	14055408	14044923	84760	12902	1.945e-02	2.945e-03	9983
Rhytidophyllum_leucomallon_14363	4400288	4396734	100946	40685	7.725e-03	1.027e-03	37598
Rhytidophyllum_lomense_10466	6126019	6114995	182098	52159	1.982e-02	1.728e-03	44765
Rhytidophyllum_lomense_10470	416767	415191	25466	8220	8.842e-03	1.297e-03	7568

| Sample name	Reads raw	Reads passed filter	Clusters total	Clusters hidepth	Heterozygotie estimation	Error estimation	Reads consensus
Rhytidophyllum_minus_10500	8655316	8653161	70232	17280	9.964e-03	1.438e-03	15531
Rhytidophyllum_minus_JBM-938-2017-a	7799287	7792178	87616	9117	4.343e-02	5.143e-03	5202
Rhytidophyllum_petiolare_NY-1402106	763214	756735	23128	16928	1.401e-02	8.059e-04	15562
Rhytidophyllum_rhodocalyx_10530	6311870	6301230	252761	82498	1.462e-02	1.552e-03	73271
Rhytidophyllum_rupincola_11957	4031905	4024450	102061	29634	1.935e-02	1.682e-03	25732
Rhytidophyllum_rupincola_G5	2253331	2252933	16439	1548	2.065e-02	2.318e-03	1204
Rhytidophyllum_sp_2014-017	22944816	22933544	323599	102357	7.133e-03	1.033e-03	92739
Rhytidophyllum_sp_2014-022	33628275	33620290	249098	58917	1.011e-02	1.226e-03	52382
Rhytidophyllum_tomentosum_G2	2641203	2638905	33528	4956	1.308e-02	1.874e-03	3816
Rhytidophyllum_tomentosum_JBM-1327-2021	4025292	4021695	52211	5282	3.360e-02	5.048e-03	3165
Rhytidophyllum_vernicosum_G3	905163	904770	7137	1097	1.001e-02	1.448e-03	899
Rhytidophyllum_villosulum_10557	44389971	44381340	245394	12408	2.249e-02	3.311e-03	7671
Rhytidophyllum_villosulum_10569	3273250	3271864	29599	8986	9.320e-03	1.047e-03	8121
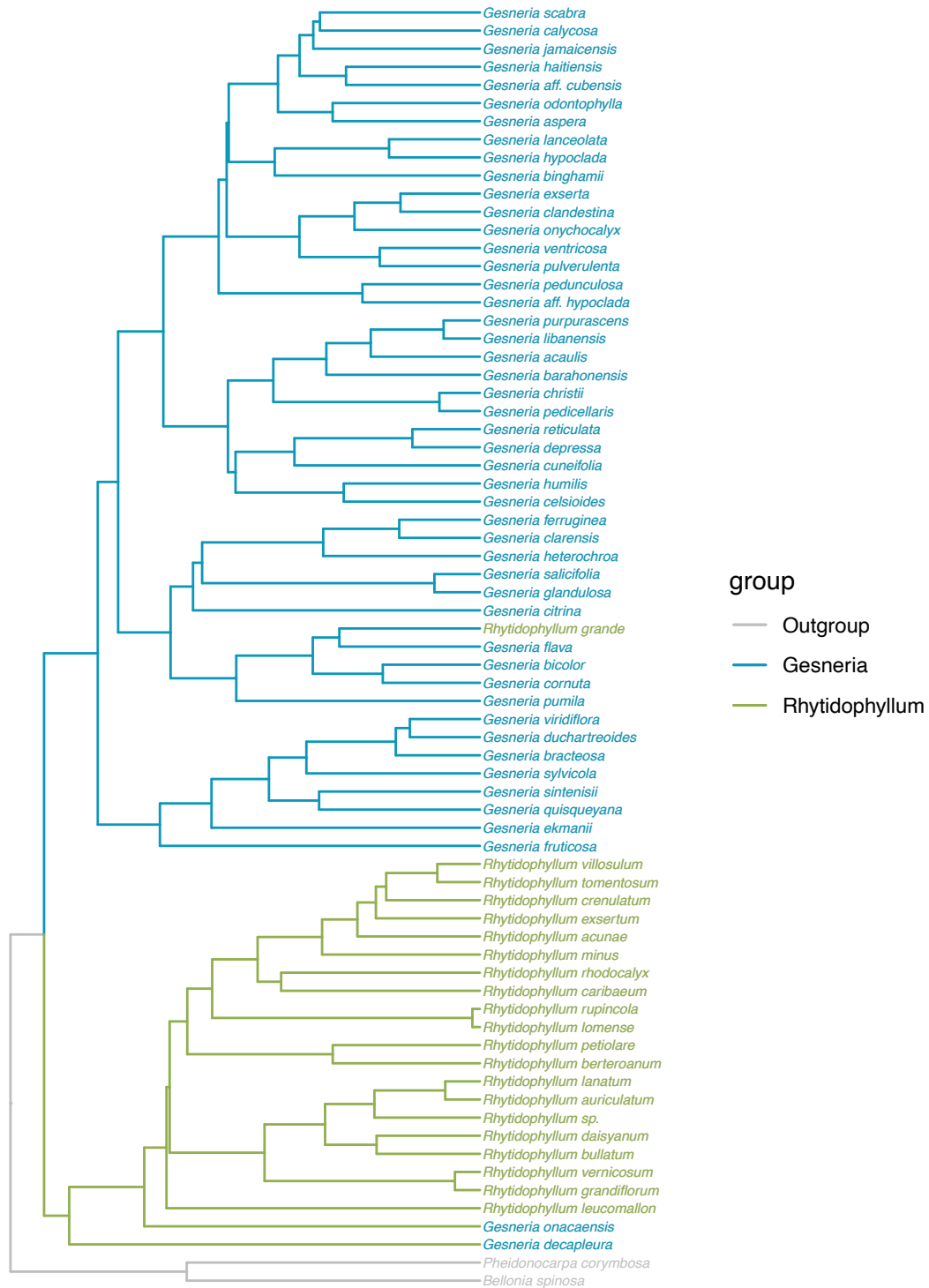
Figure S14. Species tree filtered from the MCC tree using specimens represented by the most genetic information for each species.
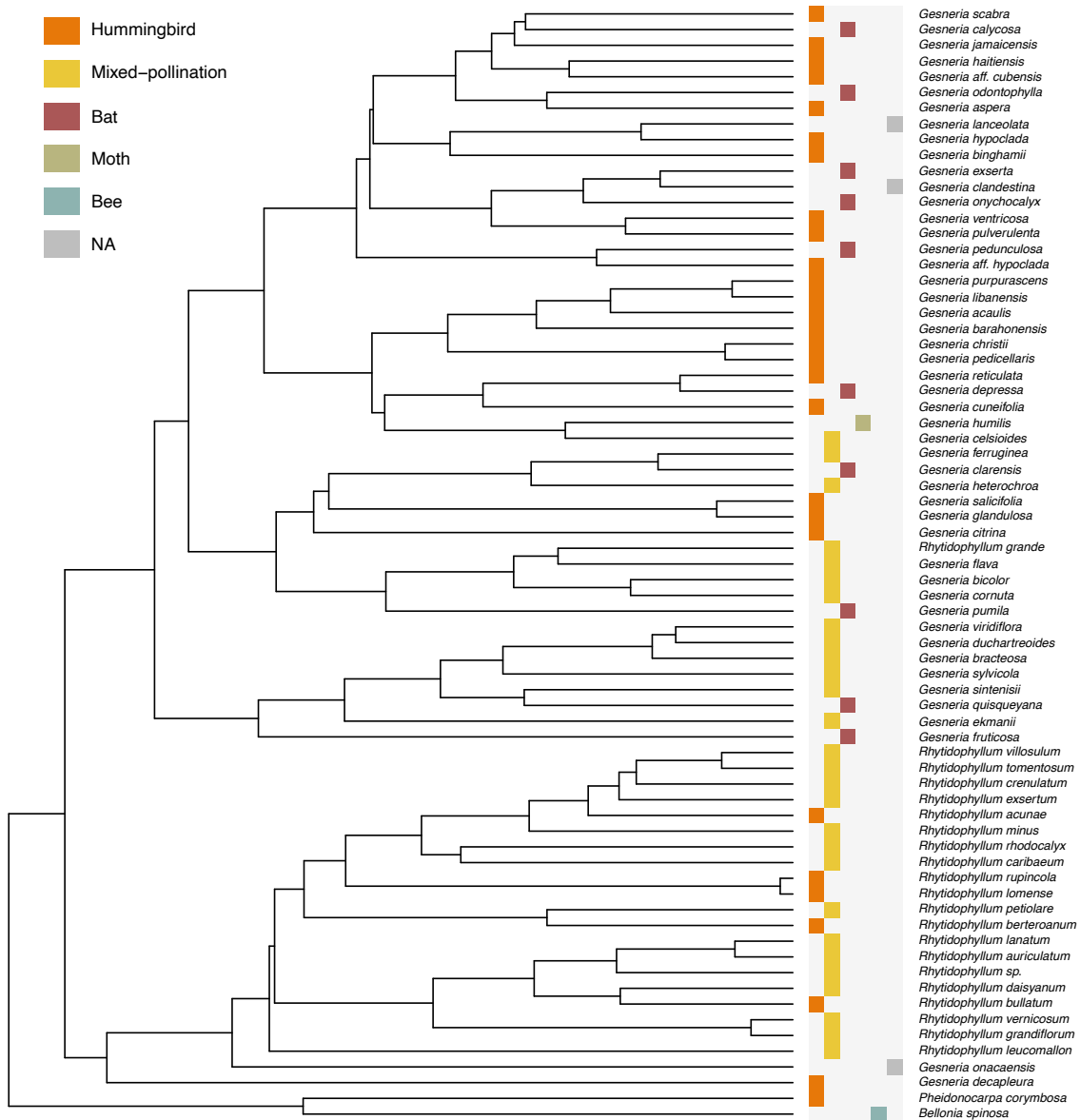
Figure S15. Pollination syndrome across Gesneriinae. Specialists for hummingbirds, bats, moths, bees, and mixed-pollinated species pollinated by hummingbirds, bats and insects. Syndromes without observations or enough information for pollination syndrome inference are noted as NA.

Figure S16. Lineage through time (LTT) plot of Antillean Gesneriaceae to illustrate patterns of lineage diversification through time. Under a pure-birth model on a semi-log scale, LTT plots follow a straight line on average.

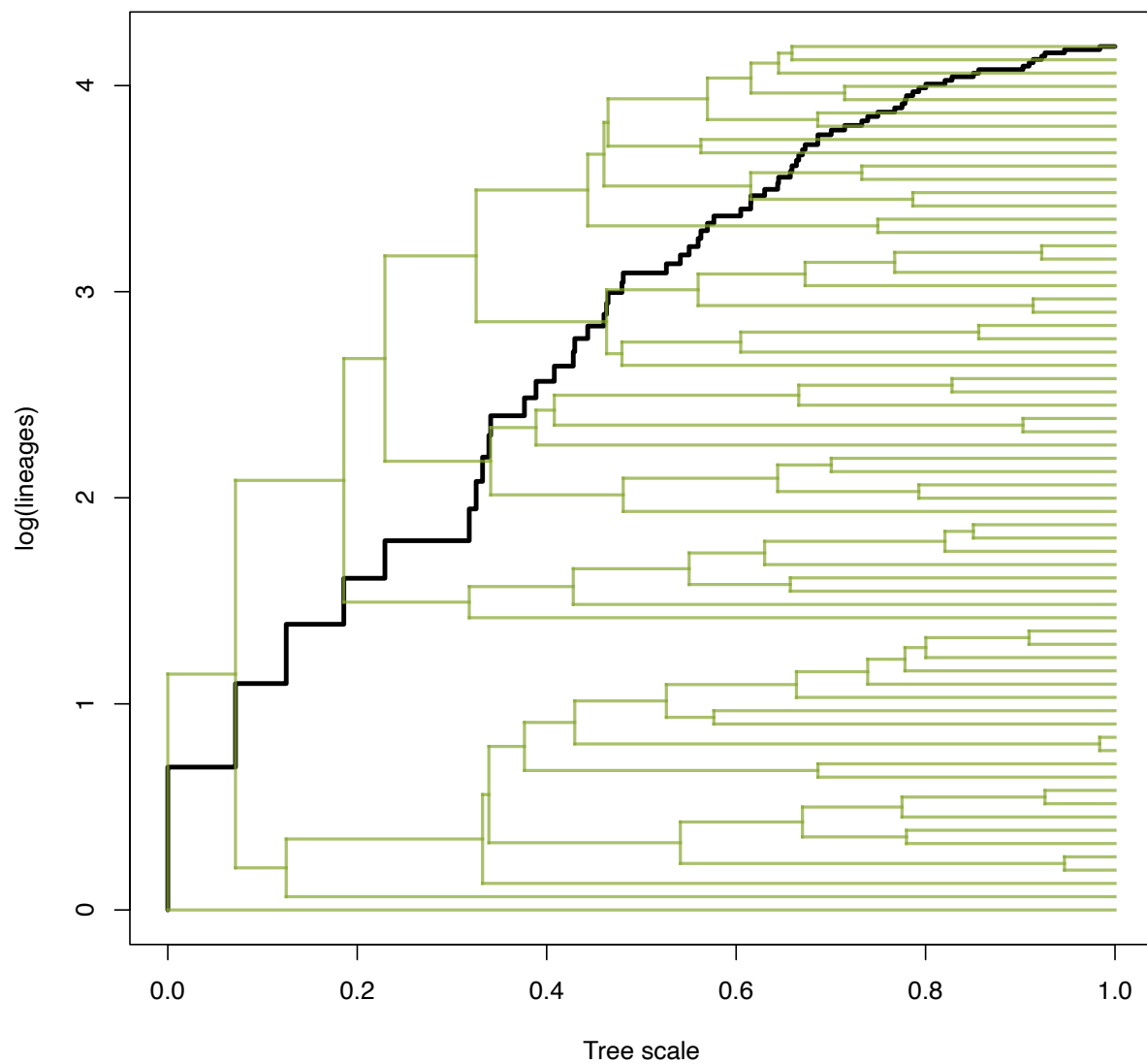**Figure S17.** Details of the SSE models parameters estimated for each state (specialist for bats, specialists for hummingbirds and generalists). Hidden states are indicated by the letters A, B and C. Although some models have the same pattern of model parameters through more than three hidden states (CID-4 and CID-6), they are not shown. Turnover ($\tau_i = \lambda_i + \mu_i$) parameter number refers to the number of parameters to estimate to be different during model calculation (i.e. if the same numbers are provided then the parameter estimates are considered identical). Extinction fraction ($\epsilon_i = \mu_i/\lambda_i$) is considered constant across states and hidden states. Transition rates matrices are also provided (last column).

Tableau S14. Detailed AICc weights for each of the series of SSE models depending on the parameters and input phylogeny (original, scaled to 1 or scaled to the crown age of Antillean Gesneriaceae 11.8Ma).

| Sampling fraction	Phylogeny scale	Bounds	null	MuSSE (2 pollination strategies)	MuSSE (3 pollination strategies)	CID2	CID3	MuHiSSE (2 pollination strategies)	MuHiSSE (3 pollination strategies)	CID4	CID6
Bat = 1 Hummingbird = 1 Generalist = 1	Original	bounded search	0.206	0.130	0.606	0.032	0.015	0.004	0.002	0.006	0.000
Bat = 1 Hummingbird = 1 Generalist = 1	Scaled to 1	unbounded search	0.189	0.120	0.314	0.216	0.098	0.021	0.005	0.036	0.002
Bat = 1 Hummingbird = 1 Generalist = 1	Scaled to 11.8Ma	bounded search	1.00	0.00	0.00	0.00	0.00	0.00	0.00	0.00	0.00
Bat = 0.55 Hummingbird = 0.71 Generalist = 0.82	Original	unbounded search	0.381	0.139	0.213	0.173	0.063	0.013	0.002	0.014	0.001
Bat = 0.55 Hummingbird = 0.71 Generalist = 0.82	Scaled to 1	unbounded search	0.379	0.138	0.212	0.172	0.063	0.013	0.002	0.021	0.001
Bat = 0.55 Hummingbird = 0.71 Generalist = 0.82	Scaled to 11.8Ma	unbounded search	0.717	0.187	0.046	0.047	0.000	0.000	0.000	0.003	0.000
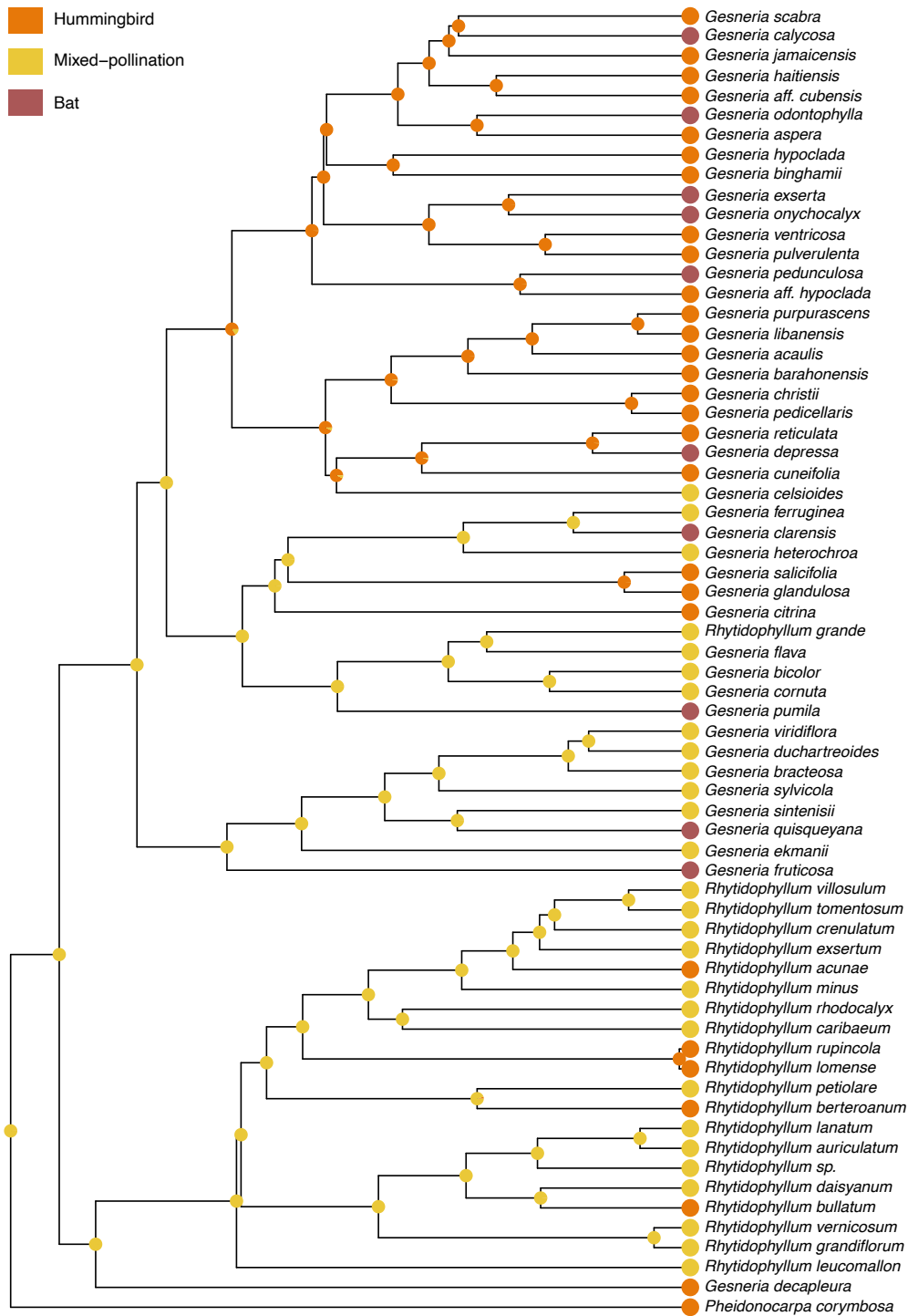
Figure S18. Ancestral state reconstruction of the three pollination syndromes (hummingbird specialist, bat specialist and generalist) according to the MuSSE model that attributes distinct rates of diversification for each pollination strategy.